
Electronic Thesis and Dissertation Repository

12-4-2018 2:30 PM

Suberin Biosynthesis and Deposition in the Wound-Healing Potato (*Solanum tuberosum* L.) Tuber Model

Kathlyn Natalie Woolfson
The University of Western Ontario

Supervisor
Bernards, Mark A.
The University of Western Ontario

Graduate Program in Biology
A thesis submitted in partial fulfillment of the requirements for the degree in Doctor of
Philosophy
© Kathlyn Natalie Woolfson 2018

Follow this and additional works at: <https://ir.lib.uwo.ca/etd>



Part of the [Plant Biology Commons](#)

Recommended Citation

Woolfson, Kathlyn Natalie, "Suberin Biosynthesis and Deposition in the Wound-Healing Potato (*Solanum tuberosum* L.) Tuber Model" (2018). *Electronic Thesis and Dissertation Repository*. 5935.
<https://ir.lib.uwo.ca/etd/5935>

This Dissertation/Thesis is brought to you for free and open access by Scholarship@Western. It has been accepted for inclusion in Electronic Thesis and Dissertation Repository by an authorized administrator of Scholarship@Western. For more information, please contact wlsadmin@uwo.ca.

Abstract

Suberin is a heteropolymer comprising a cell wall-bound poly(phenolic) domain (SPPD) covalently linked to a poly(aliphatic) domain (SPAD) that is deposited between the cell wall and plasma membrane. Potato tuber skin contains suberin to protect against water loss and microbial infection. Wounding triggers suberin biosynthesis in usually non-suberized tuber parenchyma, providing a model system to study suberin production. Spatial and temporal coordination of SPPD and SPAD-related metabolism are required for suberization, as the former is produced soon after wounding, and the latter is synthesized later into wound-healing. Many steps involved in suberin biosynthesis remain uncharacterized, and the mechanism(s) that regulate and coordinate SPPD and SPAD production and assembly are not understood. To explore the role of abscisic acid (ABA) in the differential regulation of SPPD and SPAD biosynthesis, I subjected wounded tubers to exogenous treatments including additional ABA, or the ABA biosynthesis inhibitor fluridone. Quantitative reverse transcription polymerase chain reaction (RT-qPCR) expression analysis of SPPD and SPAD biosynthetic genes, coupled with metabolite analyses, revealed that ABA positively influenced SPAD-, but not SPPD-associated, transcript and metabolite accumulation, indicating a role for ABA in the differential induction of wound-induced phenolic and aliphatic metabolism. I took an RNA-seq approach to study broader transcriptional changes that occur during wound-healing. The wound-healing transcriptome time-course illustrated that wounding leads to a substantial reconfiguration of transcription, followed by fine-tuning of responses dominated by suberization. Transcriptome analysis revealed that primary metabolic pathways demonstrate similar temporal expression patterns during wound-healing, but suberin-specific steps display distinct patterns at entire pathway and sub-branch levels. The observed transcriptional changes support a model in which wounding initially alters primary metabolism required to fuel SPPD, and subsequent SPAD, production. This investigation also provided support for uncharacterized biosynthetic steps, and highlighted putative transcription factors and suberin polymer assembly genes (*Casparian strip membrane domain proteins* and *GDSL lipase/esterases*) that may play

key roles in the regulation and coordination of SPPD and SPAD monomer biosynthesis, polymer assembly and deposition. Overall, my findings offer further insight into the coordination and timing of metabolic and regulatory events involved in wound-healing and associated suberization.

Keywords

Solanum tuberosum, wound-induced suberization, plant stress response, suberin poly(aliphatic) domain, suberin poly(phenolic) domain, abscisic acid, transcription factors, gene expression, RT-qPCR, RNA-seq, differential expression analysis, gene ontology, gene set analysis

Co-Authorship Statement

Chapter 2 was published as an open access article in *The Plant Journal* (Woolfson, K.N., Haggitt, M.L., Zhang, Y., Kachura, A., Bjelica, A., Rey Rincon, M.A., Kaberi, K.M. and Bernards, M.A. (2018) Differential induction of polar and non-polar metabolism during wound-induced suberization in potato (*Solanum tuberosum* L.) tubers. *The Plant Journal*, 93(5), 931-942). I am a co-first author with Meghan L. Haggitt (MLH), and Yanni Zhang (YZ), Alexandra Kachura (AK), Anica Bjelica (AB), M. Alejandra Rey Rincon (MARR), Karina M. Kaberi (KMK) and Mark A. Bernards (MAB) were co-authors. MLH, YZ and AB conducted preliminary studies on suberin metabolism and abscisic acid. I set up largescale experiments to include additional treatments and genes of interest. I conducted RT-qPCR and aided in polar metabolite extractions. AK, KMK and MARR helped with sample preparation, polar and non-polar metabolite extractions and analyses with MAB. MAB supervised the lab work, contributed to experimental conception and design. I drafted the first version of the published work, based on preliminary work in MLH's thesis, with contributions from MAB and other authors. The majority of data in the published article stems from my work, with 8-month old tuber data and some supplementary material from MLH's thesis.

Chapter 3 is being prepared for publication. I will be the first author, with MAB as co-author. MAB contributed to experimental conception, design, and supervision. I contributed to experimental conception and finalized experimental design, executed all experiments and analyses, and drafted the manuscript, with contributions from MAB. Biosynthetic pathway map figures were prepared by MAB; I identified the corresponding genes for each step and generated the heatmaps.

Dedication

This thesis is dedicated in loving memory to my late grandparents, Dora and Willie Woznica. They came to Canada after World War II in 1951 with nothing, and built a beautiful life here. They only had the chance to complete an elementary school education, but were both incredibly wise and I can only speculate what they could have achieved had they been granted the opportunity. Their inconceivable sacrifices made it possible for me to have the privilege to grow up in Canada and obtain a high level of education in a field that I am passionate about. I remember their emphasis on potatoes as an important food source in their unimaginable tales of survival, and the significance of my study organism is not lost on me. They imparted on me a love and appreciation for food and plants, and I often reflect on their optimistic outlook, resilience and joie de vivre to motivate me during challenging times.

Acknowledgments

Studying the “long and winding road to suberin production” seems like a fitting way to conclude the many years I have spent in school. It would not have been possible for me to reach this point without the support of my family, friends, and peers.

To my supervisor, Mark Bernards – I am incredibly fortunate to have pursued my PhD in your lab, and to have had the opportunity to learn so much from you during this time. I am particularly appreciative of your endless support and encouragement, which has driven me to achieve more than I initially thought was possible. Your mentorship has positively influenced my growth and self-confidence as a scientist. I would also like to thank my advisory committee members, Susanne Kohalmi and Frédéric Marsolais, for their constructive guidance along the way. I also appreciate Susanne letting me use her lab facilities and equipment.

So much of my thesis work was supported by the technical help and training provided by my peers. Thanks to Trish Tully for teaching me many important protocols, including the two-day long intensive RNA extractions that laid the foundation of my entire PhD thesis. Anica Bjelica – I am incredibly grateful for all of the times you made yourself available to give me technical advice and guidance. I especially acknowledge the invaluable help I received from Tian Wu and Vladimir Zhurov throughout my RNA-seq project – I would still be deep in the weeds if not for your insights and assistance. Thank you to the undergraduate students who worked with me – Alexandra Kachura, Alejandra Rey Rincon, and Karina Kaberi. My lab and office mates, including Dimitre Ivanov, Scarlett Puebla Barragan, Christine Dulal-Whiteway, Mali Mehdizadeh and Kevin Erratt, all provided me with moral support and made my time spent in NCB enjoyable.

To my first lab mate and lab mentor, my soulmate and husband, Brendan Walshe-Roussel – I am so grateful that our shared love of plants and mutual research pursuits put us on a path that led us to each other. Thank you for the lessons you have taught me throughout my academic experiences and your unwavering patience and calming influence. I am especially appreciative of the many times you helped me to realize my own growth, that

in turn allowed me to develop confidence in myself and my abilities as a scientist. You have supported and guided me in ways that are unique to our relationship as both lab mates and life mates. You have played such an integral role in so many aspects of my life that I cannot imagine doing any part of this without you.

To my parents, Frances and Ken Woolfson, thank you for your encouragement to explore my interests and pursue what I am most passionate about. You have always taught me that I could achieve my goals with hard work and perseverance, but there is no denying how privileged I am to have been born into such a loving and supportive family. I also want to acknowledge my sisters, Jess and Hayley Woolfson, who are the epitome of role models for a budding scientist, and who inspired me to pursue my BSc in Biology in the first place. My sisters and my brother-in-law Dave Dubiner have offered guidance and encouragement over the years as family and as fellow biologists. I am very excited to join the club as the fourth Dr. Woolfson! I am lucky to have grandparents, Molly and Sid Woolfson, who have always been excited to hear my work updates and share how proud they are. I am also fortunate to have become part of such a thoughtful and caring family – Wendy Walshe, Jimmy Roussel, Lauren Walshe-Roussel, Adrian and Felix Di Giovanni have collectively been a strong source of support, encouragement and motivation for me.

The challenges faced throughout my academic endeavours have been made easier over the years because of a special type of camaraderie – I would like to acknowledge my kindred spirit Kaitlin Merkowsky whose friendship has been invaluable throughout our many years of shared and paralleled experiences, as well as the wonderful friends I have made during my time at Western. Sarah McFarlane, Jackie Lebenzon, Kala Croft, Justin Croft, Tian Wu, John Ciancio, Carlie Muir, Tim Hain and many others – my time during grad school was so enjoyable and memorable because I shared it with all of you.

Table of Contents

Abstract.....	i
Co-Authorship Statement.....	iii
Dedication.....	iv
Acknowledgments.....	v
Table of Contents.....	vii
List of Tables.....	xiii
List of Figures.....	xiv
List of Abbreviations.....	xvi
Chapter 1.....	1
1 General introduction.....	1
1.1 The plant-environment interface.....	1
1.2 Structure, composition and spatial localization of the suberin macromolecule.....	2
1.3 Functional role of suberin as a physicochemical barrier to mitigate environmental stress.....	5
1.3.1 Role of root-localized suberin.....	5
1.3.2 Suberin role in cork cells.....	6
1.3.3 Suberin function in potato tubers.....	6
1.4 Suberin biosynthesis and assembly.....	7
1.4.1 Biosynthesis of phenolic domain components.....	8
1.4.2 Assembly of the suberin poly(phenolic) domain.....	9
1.4.3 Biosynthesis of suberin poly(aliphatic) domain monomers.....	11
1.4.3.1 Elongation.....	11
1.4.3.2 Oxidation.....	13

1.4.3.3	Reduction.....	15
1.4.4	Esterification, deposition and assembly of the suberin aliphatic domain components	16
1.4.4.1	Acyl-CoA-dependent aliphatic monomer esterification.....	16
1.4.4.2	ATP-binding cassette (ABC) transporters implicated in suberin deposition.....	17
1.4.4.3	Possible mechanism for aliphatic monomer polymerization.....	18
1.5	Regulation of suberization	20
1.5.1	Phytohormone roles in suberization.....	20
1.5.2	Transcription factors	22
1.6	The wound-healing potato tuber	25
1.6.1	Wound-induced signaling	25
1.6.2	Two major stages are involved in tuber wound-healing.....	26
1.6.3	Various biological events occur during the wound-healing time course ..	29
1.6.4	The wound-healing potato tuber as a model system for suberization studies	29
1.7	Dissertation overview	30
1.8	References.....	33
Chapter 2	46
2	Differential induction of polar and non-polar metabolism during wound-induced suberization in potato (<i>Solanum tuberosum</i> L.) tubers	46
2.1	Introduction.....	46
2.2	Materials and Methods.....	48
2.2.1	Tissue preparation.....	48
2.2.2	Polar metabolite analysis	49
2.2.3	Aliphatic suberin monomer biosynthesis.....	50
2.2.4	RNA isolation, cDNA synthesis and gene expression analysis	51

2.2.5	Data analysis	52
2.3	Results.....	53
2.3.1	Measurement of ABA in tubers post-wounding.....	53
2.3.2	Effect of ABA and FD treatment on suberin-related gene expression	54
2.3.3	Effect of ABA and FD treatment on polar metabolism	60
2.3.4	Effect of ABA and FD treatment on aliphatic suberin monomer composition.....	61
2.4	Discussion.....	64
2.4.1	ABA levels are dynamic during wound-healing.....	66
2.4.2	Polar metabolism is minimally affected by changes in ABA.....	67
2.4.3	Aliphatic suberin biosynthesis and deposition.....	68
2.5	References.....	69
Chapter 3	74
3	The wound-healing potato tuber: an RNA-seq approach.....	74
3.1	Introduction.....	74
3.2	Materials and Methods.....	77
3.2.1	Plant material and wounding experiment	77
3.2.2	RNA isolation	78
3.2.3	Strand-specific cDNA library construction and sequencing.....	78
3.2.4	Genome-guided transcriptome assembly	78
3.2.5	Differential expression (DE), gene ontology (GO), and gene set enrichment (GSEA) analyses	79
3.2.6	Targeted suberin-related biosynthetic gene analysis	80
3.2.7	Targeted candidate gene analysis via hierarchical clustering.....	81
3.2.8	cDNA synthesis and RT-qPCR validation of gene expression.....	81
3.3	Results.....	82

3.3.1	Genome-guided transcriptome assembly	82
3.3.2	Differential expression analysis in wound-healing tubers	83
3.3.3	Gene ontology (GO) analysis.....	86
3.3.4	Gene set enrichment analysis (GSEA).....	86
3.3.5	Wound-induced transcriptional changes: the long and winding road to suberin assembly	96
3.3.5.1	Starch degradation and carbohydrate metabolism.....	99
3.3.5.2	Shikimate pathway	101
3.3.5.3	Phenylpropanoid pathway	105
3.3.5.4	Phenolic suberin assembly	107
3.3.5.5	Tricarboxylic acid cycle	107
3.3.5.6	Fatty acid biosynthesis	108
3.3.5.7	Aliphatic metabolism.....	111
3.3.5.8	Aliphatic suberin assembly.....	113
3.3.6	Evaluation of suberin assembly candidates	113
3.3.7	Changes in abscisic acid metabolism after wounding	117
3.3.8	Temporal gene expression patterns of transcription factor candidates...	122
3.3.9	Validation of RNA-seq quantification by gene-specific RT-qPCR expression analysis.....	128
3.4	Discussion.....	130
3.4.1	Wound-healing is a dynamic process that leads to differential temporal patterns of transcription	131
3.4.2	Regulatory components of wound-healing and suberization.....	140
3.4.3	Targeting putative suberin biosynthesis and regulation genes in the wound-healing tuber transcriptome provides support for uncharacterized steps	147
3.4.4	Comparison of transcriptome findings with metabolite and protein based studies	149

3.4.5	Final considerations and conclusions.....	153
3.5	References.....	155
Chapter 4	165
4	General discussion	165
4.1	Thesis summary	165
4.1.1	The role of ABA in the differential temporal regulation of suberin-associated metabolism	165
4.1.2	The wound-healing tuber transcriptome	166
4.1.3	Summary	167
4.2	Wound-healing events during induced suberization and closing layer formation.....	167
4.2.1	Primary metabolism	169
4.2.2	Phenylpropanoid metabolism.....	169
4.2.3	Aliphatic metabolism	170
4.2.4	SPPD and SPAD assembly	171
4.2.4.1	Genes previously implicated in suberin assembly.....	171
4.2.4.2	Novel candidates and proposed mechanism for suberin assembly and its coordination	174
4.2.5	Regulators of differential induction of suberization processes.....	181
4.2.6	Other wound-healing processes involved in closing layer formation.....	183
4.3	Applications for crop improvement	184
4.4	Concluding remarks	185
4.5	References.....	187
Appendix A:	Reprint permission for Chapter 1	191
Appendix B:	Chapter 2 supplementary material.....	194
Appendix C:	Chapter 3 supplementary material.....	209

Curriculum Vitae 255

List of Tables

Table 2.1. Gene information and primer sequences used for RT-qPCR analyses of target genes involved in suberin biosynthesis and deposition.	57
Table 3.1 Summary of gene ontology information represented in biological process gene set enrichment analysis plot and change in terms over time.....	92
Table B1. Statistical analysis for gene expression data of four month old tubers.....	194
Table C1. TopGO analysis of top 50 gene ontology terms enriched within 5441 differentially expressed genes identified from the wound-healing tuber time course.	209
Table C2. Summary of gene ontology information represented in molecular function gene set enrichment analysis plot and change in terms over time.....	213
Table C3. Summary of gene ontology information represented in cellular component gene set enrichment analysis plot and change in terms over time.	217
Table C4. Suberin-related biosynthetic and assembly gene and encoded enzyme list. ..	225
Table C5. Casparian strip membrane protein (CASP) family in <i>Solanum tuberosum</i> . ..	244
Table C6. List of cutin synthase-like candidates screened in the wound-healing tuber RNA-seq data.....	246
Table C7. Abscisic acid-related biosynthetic gene information. Bolded numbers correspond to gene IDs used to generate heatmap figures.....	247
Table C8. Abscisic acid catabolism gene information.....	249
Table C9. Candidate transcription factors screened in the wound-healing transcriptome analysis.....	250
Table C10. Gene information and primer sequences used for RT-qPCR validation of RNA-seq expression values.	253
Table C11. Pearson correlation statistical output for RT-qPCR validation of RNA-seq transcript levels.	254

List of Figures

Figure 1.1. Proposed two-domain model for the macromolecular structure of suberin.	3
Figure 1.2. Spatial localization of the two-domain suberin macromolecule in periderm cells.	4
Figure 1.3. Wound-induced tuber suberization during two major stages of wound-healing.	28
Figure 2.1. Wound-induced changes in abscisic acid (ABA).....	54
Figure 2.2. Expression of suberin biosynthetic genes after wounding.	59
Figure 2.3. Polar metabolite analysis.....	61
Figure 2.4. Total aliphatic monomer accumulation in wounded potato tubers.	63
Figure 2.5. Wound induced potato suberin aliphatics by substance class.	64
Figure 3.1. Global overview of wound-healing transcriptome.	85
Figure 3.2. Gene set enrichment analysis (GSEA) of biological processes across differentially expressed genes (DEGs) identified in sequential wound-healing time point comparisons.	91
Figure 3.3. Roadmap to suberin biosynthesis and assembly.	98
Figure 3.4. Hierarchical clustering analysis of known and putative suberin assembly genes with newly identified candidate genes.....	116
Figure 3.5. Transcriptional changes in abscisic acid (ABA)-related metabolism during wound-healing.....	119
Figure 3.6. Hierarchical clustering analysis of transcription factor candidates with suberin-related biosynthetic and assembly genes across the tuber wound-healing time course.	124
Figure 3.7. Validation of gene expression by Pearson correlation of RNA-seq with RT-qPCR expression values.....	129
Figure 4.1. Temporal summary of biosynthetic and regulatory events during wound-healing and associated suberization.	168
Figure 4.2. Proposed mechanism for the suberization process in wound-healing tubers.	179

Figure B1. ABA verification by isotope dilution.....	197
Figure B2. Persistence of fluridone in potato tubers.....	198
Figure B3. Expression of suberin biosynthesis genes after wounding of eight month old tubers.....	199
Figure B4. PLS-DA analysis of polar metabolites isolated from eight month old tubers.	200
Figure B5. Accumulation of polar compounds in wound-healing tubers.	201
Figure B6. Chain length distribution of fatty acids isolated from suberizing potato tubers.	203
Figure B7. Chain length distribution of 1-alkanols isolated from suberizing potato tubers.	204
Figure B8. Chain length distribution of ω -hydroxy fatty acids isolated from suberizing potato tubers.....	206
Figure B9. Chain length distribution of α,ω -dioic acids (as methyl esters) isolated from suberizing potato tubers.	208
Figure C1. Gene set enrichment analysis (GSEA) of molecular function across differentially expressed genes (DEGs) identified in sequential wound-healing time point comparisons.	212
Figure C2. Gene set enrichment analysis (GSEA) of cellular components across differentially expressed genes (DEGs) identified in sequential wound-healing time point comparisons.	216
Figure C3. Transcriptional changes of known and putative genes encoding enzymes for suberin production over the wound-healing time course.....	218
Figure C4. Hierarchical clustering analysis of genes encoding putative Casparian membrane strip protein (CASP) and cutin esterase-like (GDSL) proteins to screen for candidate novel assembly genes.	243
Figure C5. Hierarchical clustering analysis of transcription factor candidates with characterized potato transcription factors <i>NAC103</i> and <i>WRKY1</i>	252

List of Abbreviations

4CL	4-coumarate-CoA ligase
ABA	Abscisic acid
ABCG	ATP-binding cassette (ABC) transporter, subfamily G
ACP	Acyl carrier protein
At	<i>Arabidopsis thaliana</i> (used as a prefix before gene or enzyme name)
BP	Biological process
C3H	<i>p</i> -coumarate 3-hydroxylase
C3'H	<i>p</i> -coumaroyl quinate/shikimate 3'-hydroxylase
C4H	Cinnamic acid 4-hydroxylase
CAD	Cinnamyl alcohol dehydrogenase
CASP	Casparian strip membrane domain protein
CC	Cellular component
CCoAOMT	Caffeoyl-CoA <i>O</i> -methyltransferase
CCR	Cinnamoyl-CoA reductase
CDS/CUS	Cutin deficient/cutin synthase
CER	ECERIFERUM
CoA	Coenzyme A
COMT	Caffeic acid <i>O</i> -methyltransferase
CPM	Counts per million
CYP	Cytochrome P450
CYP86A33	Cytochrome P450 gene family 86, subfamily A, gene 33
CYP86B12	Cytochrome P450 gene family 86, subfamily B, gene 12
CYTB ₅	Cytochrome P450 b ₅
DE	Differential expression
DEG	Differentially expressed genes
dpw	Days post-wounding
F5H	Ferulate 5-hydroxylase
FA	Fatty acid
FAE	Fatty acid elongase
FD	Fluridone
FPKM	Fragments per kilobase of transcript per million mapped reads
GDSL	Glycine-aspartic acid-serine-leucine motif lipase/esterase/hydrolase
Glycerol-3P	Glycerol-3-phosphate
GO	Gene ontology
GPAT5	Glycerol-3-phosphate acyltransferase 5
GPAT6	Glycerol-3-phosphate acyltransferase 6
GS(E)A	Gene set (enrichment) analysis
HCAA	Hydroxycinnamic acid amide
HCT	Hydroxycinnamate transferase
JA	Jasmonic acid

KAR	β -ketoacyl-ACP reductase
KCS	β -ketoacyl-CoA reductase
LACS	Long-chain acyl-CoA synthetase
MF	Molecular function
MYB	MYB family transcription factor
NAC	NAC domain transcription factor (NAM, no apical meristem, ATAF, Arabidopsis transcription activation factor, and CUC, cup-shaped cotyledon)
NOX	NADPH-dependent oxidase
PAL	Phenylalanine ammonia lyase
PGSC	Potato Genome Sequencing Consortium
PRX	Peroxidase
RT-qPCR	Quantitative reverse transcription polymerase chain reaction
RNA-seq	RNA sequencing
Sl	<i>Solanum lycopersicum</i> (used as a prefix before gene or protein name)
SOD	Superoxide dismutase
SPAD	Suberin poly(aliphatic) domain
SPPD	Suberin poly(phenolic) domain
St	<i>Solanum tuberosum</i> (used as a prefix before gene or protein name)
THT	Tyramine hydroxycinnamoyl transferase
VLCFA	Very long chain fatty acid
WBC	White/brown complex ABC transporter
WRKY	WRKY domain family transcription factor
XTH	Xyloglucan endotransglucosylase/hydrolase

Chapter 1

1 General introduction

1.1 The plant-environment interface

Plants have evolved various morphological and chemical mechanisms for protection against biotic and abiotic stresses. While different plants synthesize a range of specialized chemical defenses that are toxic or deterrent to microbial and insect pests, they can also produce defensive molecules that can be used to construct physical barriers. This integration of physical and chemical protection yields physicochemical barriers at plant-environment interfaces that occur across the extant plant kingdom, from bryophytes to angiosperms (reviewed by Yeats and Rose, 2013).

When plants transitioned from aquatic to terrestrial environments, they underwent important evolutionary adaptations to mitigate water loss: the formation of the cuticle, a cutin-based waxy coating of aerial plant organs including stems, leaves and fruits (e.g. reviewed by Waters, 2003; Samuels et al., 2008; Yeats and Rose, 2013), and the deposition of suberin, a phenolic- and fatty acid-derived polymer found in dermal tissues that do not form a cuticle (Esau, 1977; Matzke and Riederer, 1991). For example, suberin is deposited in the root epidermis and the entire perimeter of root endodermal and exodermal cells in association with the Casparian strip, a band of cell wall material comprising lignin-like phenolics and aliphatic suberin that is deposited in a ring around these inner cell layers (e.g. Schreiber et al., 1999; Thomas et al., 2007). These polymers act together as an apoplastic diffusion barrier to regulate water and ion transport through cell walls and act as a defense against pathogens (Schreiber, 2010; Nawrath et al., 2013).

Some plant defenses are innate, being produced during development, while others are induced in response to various stresses. Suberin is an especially interesting plant defense, as it is both deposited as part of normal growth and development, (e.g. roots and potato periderm) and its synthesis can also be induced by stresses such as wounding, drought and infection in tissues that usually produce suberin such as roots, as well as those that do

not, like potato tuber parenchyma (e.g. Kolattukudy and Soliday, 1985; Lulai, 2005; Vandeleur et al., 2009; Andreetta et al., 2013).

1.2 Structure, composition and spatial localization of the suberin macromolecule

Suberin is a large macromolecule that comprises two distinct, but covalently linked domains (Bernards, 2002). One domain is anchored in the primary cell wall and consists of polymerized phenolic compounds, mainly hydroxycinnamic acids and their derivatives, tyramine-derived hydroxycinnamic acid amides, and a small proportion of hydroxycinnamic alcohols (monolignols), and is referred to as the suberin poly(phenolic) domain (SPPD) (reviewed in Bernards et al., 1995; Bernards and Lewis, 1998; Bernards and Razem, 2001). The suberin poly(aliphatic) domain (SPAD) spans the space between the cell wall and plasma membrane, and is made up of fatty acid-derived aliphatic constituents including very long chain (C24 to C32) 1-alkanols, bifunctional ω -hydroxyalkanoic acids and α,ω -dioic acids, and mid-chain octadecanoates, as well as shorter C18 oxidized fatty acids, and non-polymerized (i.e. soluble) associated waxes that are largely alkyl hydroxycinnamate esters (Holloway, 1983; Graça and Pereira, 1997; Nawrath et al., 2013). Glycerol, ferulates and esterified hydroxycinnamic acids are also present in the SPAD (Riley and Kolattukudy, 1975; Cottle and Kolattukudy, 1982; Moire et al., 1999). The biopolymers suberin and cutin are similar, but can be differentiated by the characteristic presence of longer chain fatty acid derivatives (\geq C20) and the higher proportion of dicarboxylic acids found in suberin relative to cutin (Kolattukudy, 1981). The SPAD monomers are cross-linked by glycerol bridges to yield a three-dimensional polyester that is thought to promote its structural integrity. While monomers in the SPPD are also cross-linked, this is thought to be mediated via inter-unit C-C and ether linkages, rather than ester bonds (Bernards et al., 1995; Bernards, 2002). Glycerol also likely links the SPPD to the SPAD (Schmutz et al., 1994; Graça and Pereira 1999; Graça and Pereira, 2000). A proposed model for the two-domain macromolecular structure of suberin is depicted in **Figure 1.1** with its sub-cellular spatial localization shown in **Figure 1.2**.

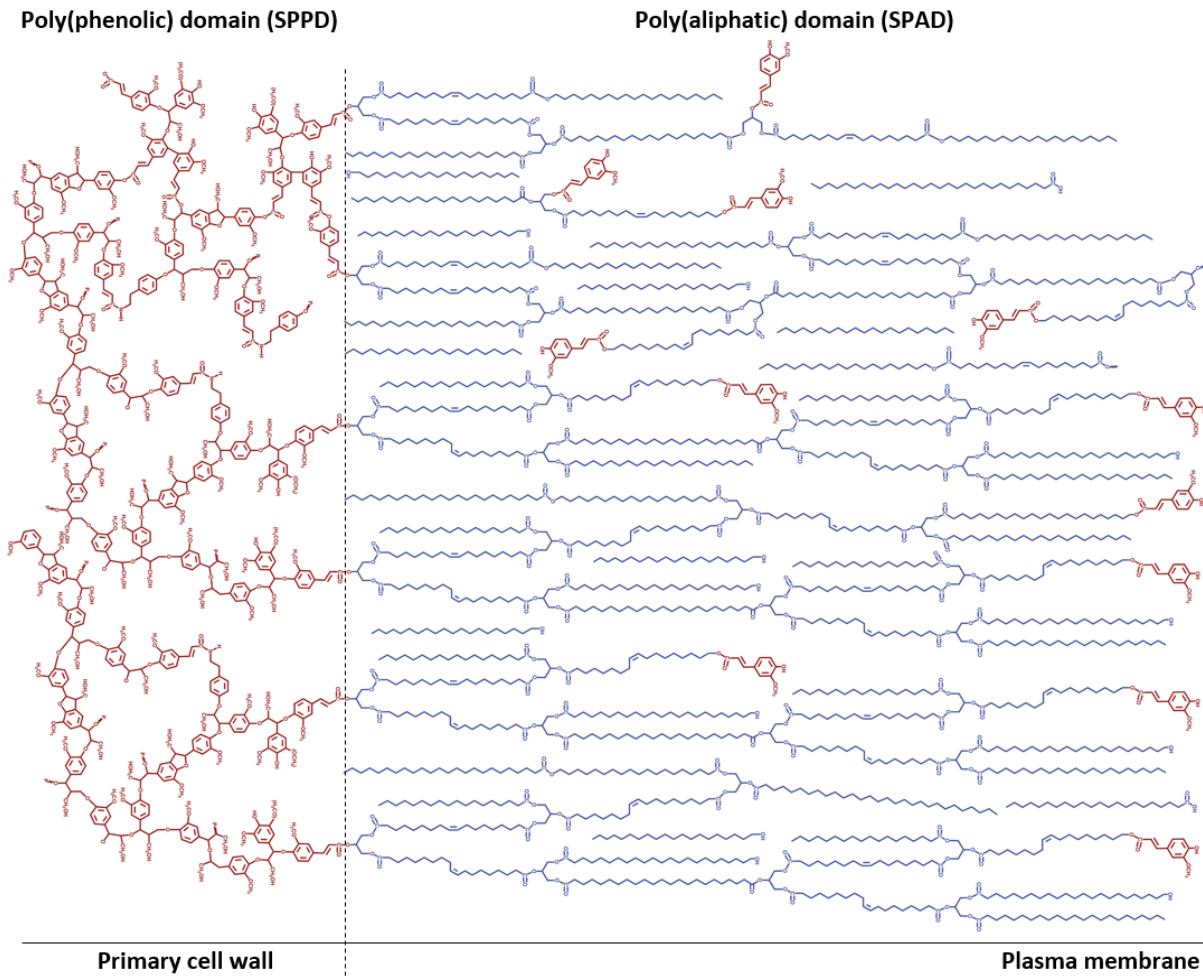


Figure 1.1. Proposed two-domain model for the macromolecular structure of suberin. Adapted from Bernards (2002). Phenolic compounds are highlighted in red, and aliphatic constituents are shown in blue.

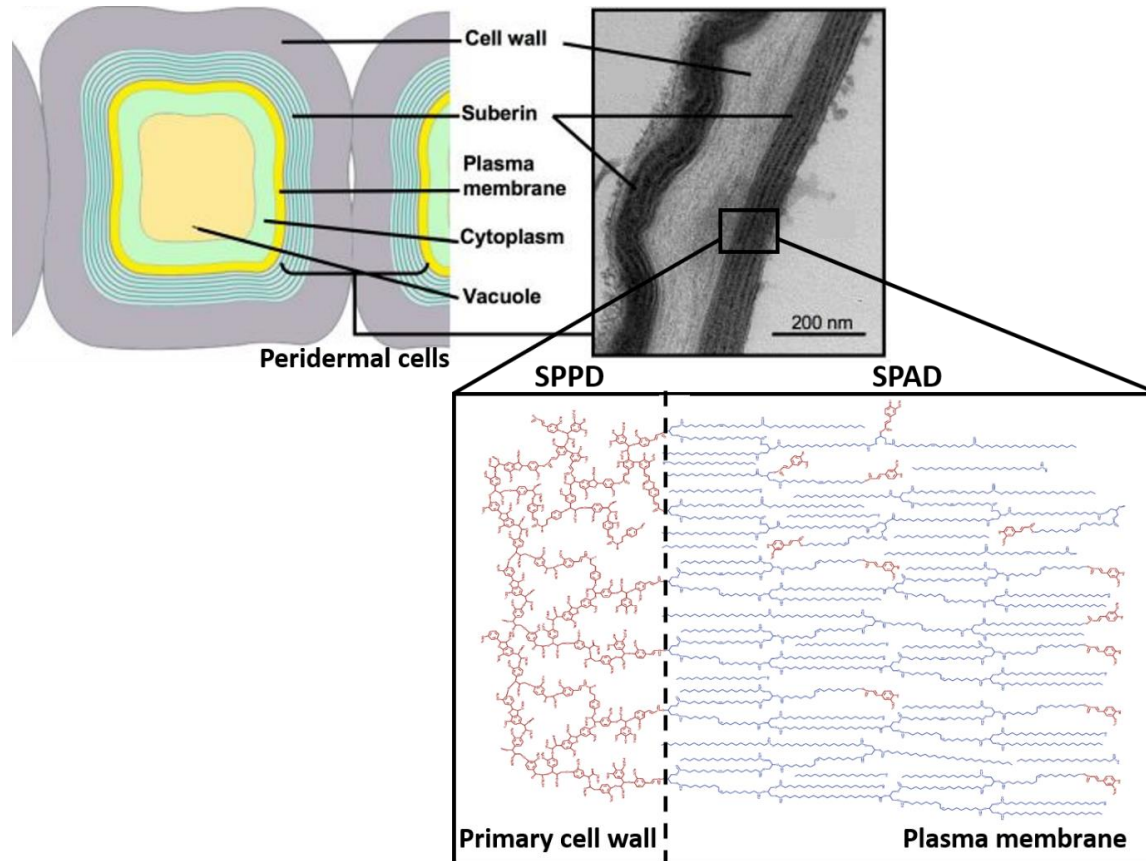


Figure 1.2. Spatial localization of the two-domain suberin macromolecule in periderm cells. The schematic is based on transmission electron microscopy imaging from suberized *Arabidopsis* secondary root cell periderm, in which the SPPD is anchored to the primary cell wall, and the SPAD can be seen as alternating light and dark bands that spans the space between the primary cell wall and the plasma membrane, around the entire cell. This figure has been adapted from figures by Molina (2010) and Bernards (2002).

1.3 Functional role of suberin as a physicochemical barrier to mitigate environmental stress

Suberin is present in different plant tissues and organs, where its physiological role is somewhat specialized to its localization, and its exact pattern of deposition and composition varies by developmental stage and species (Wilson and Peterson, 1983; Schreiber et al., 1999; Zeier et al., 1999). Generally, the role of suberin is to protect against water loss and infection, which is likely a product of its heteropolymeric composition.

1.3.1 Role of root-localized suberin

Suberin is deposited species-dependently in endodermal and/or exodermal layers of root cells. Arabidopsis mutant studies have demonstrated the requirement of properly formed endodermal suberin to appropriately control the uptake and transport of water and minerals. The *enhanced suberin 1* mutant has elevated endodermal root suberin content, and is connected to a reduction in transpiration and an increase in shoot solute accumulation (Baxter et al., 2009; Ranathunge and Schreiber, 2011). Additionally, loss of function *horst/cyp86a1* mutants that produce ca. 33% less aliphatic suberin monomers in roots than wild type plants demonstrate increased permeability to water and ions at the root level (Höfer et al., 2008; Ranathunge and Schreiber, 2011). That said, in spite of the enhanced level of aliphatic monomers in enhanced suberin mutants, hydraulic conductivity studies revealed that permeability was no lower than in wild type plants (Ranathunge and Schreiber, 2011). Suberin deposition can also be activated in roots by salt stress, and conversely, down-regulated under nitrate starvation conditions to facilitate soil nutrient uptake (Schreiber et al., 2005a). Comparisons of soybean (*Glycine max* L. Merr.) genotypes with varying degrees of root epidermal and endodermal suberization revealed that increased levels of root aliphatic suberin deposition were strongly correlated with improved resistance to a known root rot disease causing oomycete, *Phytophthora sojae* (Thomas et al., 2007).

1.3.2 Suberin role in cork cells

Bark is the protective layer outside of the vascular cambium of plant stems that undergo secondary thickening, and comprises different cell and tissue types that exhibit various functions. These physiological roles include protection against herbivory, microbial infection, and environmental stress, as well as wound-healing, and translocation and storage of soluble organic compounds (Lev-Yadun, 2011). Many protective properties can be attributed to the presence of cork, or suberized phellem cells, which derive from the meristematic secondary phloem (i.e.) phellogen layer, that is produced by the vascular cambium. The cork oak (*Quercus suber* L.) is a model woody species and representative of suberized phellem cells, due to its thick phellem layer that is commercially used for cork-derived products, and it is the namesake of this biopolymer (Graça and Pereira, 1997; Pereira et al., 1987). The hydrophobic and impermeable properties of cork are largely attributed to the presence of suberin and its associated waxes deposited in these bark cells, which prevents water loss and infection in trees (Marques and Pereira, 1987; Silva et al, 2005; Soler et al., 2007).

1.3.3 Suberin function in potato tubers

Potato tuber skin (i.e., periderm) contains suberin in its outermost layers. Proper formation and maturation of an intact, suberized tuber periderm yields a physical barrier against various environmental threats and stresses, including microbial infection, insects, water vapor loss (Lulai and Freeman, 2001; Serra et al., 2010), and skinning injury (Lulai, 2001; Lulai and Freeman, 2001; Schreiber et al., 2005b; Lulai, 2007). For example, studies focused on pathogen-resistant and susceptible potato cultivars have pointed to suberin as an important barrier to microbial infection of tubers (O'Brien and Leach, 1983; Vaughn and Lulai, 1991).

Suberization is also induced by wounding in potato tubers, where the deposition of suberin is one aspect of the overall wound-healing process that aids in sealing off damaged cells at the wound site (e.g., Lulai, 2007). Wound-associated suberin production has been well-studied in wounded potato model systems that allow for characterization of different suberization events over the course of wound-healing. A wound-healing potato

tuber study by Lulai and Corsini (1998) exploited the differential timing of SPPD and SPAD deposition to highlight the distinct physiological role of each suberin domain in resistance to pathogen infection. The immediately deposited SPPD was found to promote resistance to a bacterial cause of soft rot (*Erwinia carotovora* subsp. *carotovora*), but the phenolic matrix alone was not sufficient to prevent infection by a fungal pathogen, *Fusarium sambucinum*. Fungal resistance was only attained once the aliphatic portion of suberin was fully deposited later into the time course, ca. 5-7 days after wounding.

Suberin plays a critical role in protection against various abiotic and biotic stresses, and its production can be adjusted based on environmental signals. Due to its multitude of protective functions across the plant kingdom and in different plant organs and tissues, including those of agricultural and economic value, it is important to gain a fundamental understanding of how this complex polymer is synthesized.

1.4 Suberin biosynthesis and assembly

Decades of research that encompasses different species and employs several experimental approaches has led to the elucidation of many biosynthetic steps required for suberin production. Generally, characterization has focused on steps from two biosynthetic pathways implicated in phenolic and aliphatic monomer production required for the assembly of the respective poly(phenolic) and poly(aliphatic) suberin domains, while novel aspects of linkage and assembly have also been recently elucidated.

Total and relative suberin monomer composition varies between developmental stages, plant organs and species, but is similar enough that diverse plants express shared pathways required for suberin production (Matzke and Riederer, 1991; Zeier and Schreiber, 1998; Ranathunge et al., 2011). Many characterized suberin biosynthetic enzymes and their encoding genes exhibit conserved functionality across species, making many studies in different plant systems relevant and applicable to others.

Loss of function mutants have been used to characterize biosynthetic genes in *Arabidopsis* that translate well to putative potato orthologs in forward and reverse genetics experiments. For example, a key fatty acid ω -hydroxylase required to produce

predominant aliphatic suberin monomers, AtCYP86A1, was characterized using a *cyp86a1/horst* mutant system (Höfer et al., 2008), and subsequent reverse and forward genetics approaches in potato confirmed the function of its putative ortholog StCYP86A33 (Serra et al., 2009b; Bjelica et al., 2016). The wounded potato tuber has also been used as an effective model system to track temporal changes in metabolism and establish the timing of major biosynthetic events.

1.4.1 Biosynthesis of phenolic domain components

The SPPD is mostly made up of hydroxycinnamic acids and their derivatives, which are derived via the phenylpropanoid pathway. This biosynthetic pathway is highly conserved across the plant kingdom and is involved in preliminary steps that can be channeled towards the biosynthesis of different secondary metabolites, including monomers specific to lignin and the SPPD. The phenylpropanoid biosynthetic pathway is well-established in *Arabidopsis* due to its role in lignin biosynthesis, with many steps also characterized in potato.

Phenylalanine ammonia lyase (PAL) encodes the first committed step of the phenylpropanoid pathway, which converts the shikimate pathway-derived amino acid phenylalanine into cinnamate (Havir and Hanson, 1970). The next step towards phenolic production involves *para*-hydroxylation of cinnamic acid by cinnamic acid 4-hydroxylase (C4H) to yield 4-hydroxycinnamic acid, i.e. *p*-coumaric acid (Wang-Pruski and Cattle, 2004). Once formed, the hydroxycinnamate skeleton has several possible metabolic fates. Hydroxylation and methyl-transfer can be carried out by *p*-coumarate 3-hydroxylase (C3H), caffeic acid *O*-methyltransferase (COMT) and ferulate 5-hydroxylase (F5H) to synthesize other hydroxycinnamic acids (caffeic acid, ferulic acid, 5-OH-ferulic acid and sinapic acid), found in the final suberin poly(phenolic) domain (Meyer et al., 1996; Humphreys et al., 1999; Schoch et al., 2001). COMT can utilize both caffeate and 5-hydroxyferulate as substrates in this pathway (Humphreys et al., 1999).

Another phenylpropanoid route involves *p*-coumaric acid conversion into its acid-thiol derivative *p*-coumaroyl-CoA by 4-coumarate-CoA ligase (4CL) (Schneider et al., 2003), which can then be channeled toward three possible pathways for production of SPPD

monomers. One pathway leads to the production of hydroxycinnamoyl-CoA esters via hydroxycinnamoyl transferase (HCT)-mediated transfer of caffeoyl to CoA (Hoffmann et al., 2003), followed by *p*-coumaroyl-quininate/shikimate 3'-hydroxylase (C3'H) activity that can convert its two substrates *p*-coumaroyl shikimate and *p*-coumaroyl quininate to caffeoyl shikimate and caffeoyl quininate, respectively (Knollenberg et al., 2018). Caffeoyl-CoA, produced via C3H-hydroxylated *p*-coumaroyl-CoA or HCT-mediated conversion of caffeoyl quininate, can then undergo caffeoyl-CoA-*O*-methyltransferase (CCoAOMT)-catalyzed methylation of caffeoyl-CoA to yield feruloyl-CoA (Do et al., 2007).

Another metabolic pathway yields hydroxycinnamoyltyramines via tyramine hydroxycinnamoyl transferase (THT)-mediated conjugation of tyramine, derived from the decarboxylation of tyrosine (tyrosine decarboxylase; TyDC), with feruloyl-CoA, synthesized in the aforementioned pathway, to yield feruloyltyramine destined for the SPPD (Negrel et al. 1993). This pathway is also implicated in the wound- and pathogen-induced biosynthesis of hydroxycinnamic acid amides in leaves (e.g. Hagel and Facchini, 2005; Yogendra et al. 2014)

Additionally, hydroxycinnamoyl-CoA thioesters are converted by cinnamoyl-CoA reductase (CCR) into their corresponding hydroxycinnamaldehydes as a committed step towards monolignol biosynthesis (Larsen, 2004). Cinnamyl alcohol dehydrogenase (CAD) carries out the final NADPH-dependent reduction of hydroxycinnamaldehydes to their respective alcohols (i.e., monolignols). Since monolignols make up a small proportion of the SPPD (Bernards et al., 1995), and CCR enzyme activity is lower in suberizing potato tubers relative to lignifying *Pinus taeda* cells (Bernards et al., 2000), the monolignol biosynthetic pathway is considered the least significant metabolic route for hydroxycinnamoyl-CoAs (Bernards, 2002).

1.4.2 Assembly of the suberin poly(phenolic) domain

The poly(phenolic) domain of suberin can be considered “lignin-like” due to the presence of phenylpropanoid-derived monomers that include monolignols, cross linked to the cell wall (Kolattukudy, 1980; Kolattukudy, 1981). Lignin and the SPPD are distinguished by

their main monomer constituents (Bernards and Lewis, 1998; Bernards and Razem, 2001). The phenolic domain of suberin is thought to undergo polymerization mediated by peroxidase(s) and H₂O₂ (Espelie and Kolattukudy, 1985; Espelie et al., 1986), in a process akin to that described for lignification (Kolattukudy, 1980; Nawrath, 2002). A suberization-associated, H₂O₂-dependent anionic peroxidase from potato tuber is involved in the cross-linking of SPPD monomers via preferential oxidation of hydroxycinnamates with a greater number of methoxy groups (i.e. namely ferulic acid and its derivatives to a greater degree than caffeic acid, followed by coumaric acid and sinapic acid) over their corresponding alcohols, consistent with the greater proportion of polymerized hydroxycinnamates over monolignols in the wound-healing tuber SPPD (Bernards et al., 1999). The required H₂O₂ is likely generated by an NAD(P)H-dependent oxidase system, which is supported by evidence of reactive oxygen species production via oxidative bursts that occur upon tuber wounding (Bernards and Razem, 2001; Razem and Bernards, 2002; Razem and Bernards, 2003). Conversely, a salt stress-inducible cationic peroxidase, TPX1, has been described in tomato as playing a role in the polymerization of lignin and phenolic suberin monomers in roots (Quiroga et al., 2000, 2001). This highlights the differences in this process that may exist even in closely related solanaceous species.

Mediators that coordinate mechanisms required for the SPPD-specific polymerization processes have not been established, although this level of regulation has been elucidated in regards to Casparian strip formation. Casparian strip membrane domain proteins (CASPs) and CASP-like proteins (CASPLs) are involved in the precise localization of Casparian strip-specific cell wall modifications by acting as membrane scaffolds and mediating the recruitment of machinery involved in the polymerization of phenolics (Roppolo et al., 2011; Roppolo et al., 2014). Vulavala et al. (2017) demonstrated the expression of two *CASP* genes in developing potato tuber periderm cells, which produce suberin, but do not contain Casparian bands, and therefore may point to a role for CASP/CASPL family proteins in overseeing SPPD assembly.

1.4.3 Biosynthesis of suberin poly(aliphatic) domain monomers

The SPAD consists primarily of cross-linked modified fatty acids, primary alcohols and glycerol that are ultimately derived from glycolysis and the tricarboxylic acid cycle, which yield acetyl-CoA for plastid-localized fatty acid biosynthesis (Kolattukudy, 1981; Schreiber et al., 1999). Several downstream modifications of 16:0 and 18:0 fatty acid precursors yield final aliphatic suberin monomers characteristic of the SPAD. These include elongation long (C20) and very long chain fatty acids (VLCFA; mostly C24-C32), reduction of long and VLCFAs to primary alcohols, and ω -hydroxylation and further oxidation of ω -hydroxy fatty acids to α,ω -dioic acid. Several enzymes that catalyze these modification steps have been identified and characterized in Arabidopsis and/or potato systems (e.g. reviewed by Vishwanath et al., 2015).

Acyl activation is typically an initial requirement for downstream fatty acid metabolism and is carried out by long-chain acyl-CoA synthetase (LACS) family enzymes prior to cutin monomer biosynthesis (Schnurr et al. 2004; Lü et al. 2009), although no LACSs linked to suberin biosynthesis have been described. Additionally, acyl activation of final SPAD monomers may prelude linkage of modified aliphatic monomers with glycerol.

Chain elongation and oxidation represent two major fatty acid modification routes that yield the predominant aliphatic suberin monomers. Elongated chains can be reduced to form primary alcohols or decarboxylated to form alkanes, while a large proportion of oxidized fatty acids in the SPAD are short chains (especially C18) that have undergone desaturation instead of elongation. However, some elongated fatty acids are also oxidized to yield VLC ω -hydroxy and α,ω -dicarboxylic acids and are found in the SPAD.

1.4.3.1 Elongation

Fatty acid elongation is carried out by endoplasmic reticulum membrane-localized fatty acid elongase (FAE) complexes made up of four enzymes (reviewed by Samuels et al., 2008). β -ketoacyl-CoA synthases (KCS) are elongase complex enzymes that catalyze the condensation of acyl-CoA with fatty acyl-CoAs, and determine the chain length specificity for each reaction, although single condensing enzymes are able to participate in some consecutive elongation steps (Blacklock and Jaworski, 2006). Suberin-related

KCSs have been characterized in Arabidopsis and potato. *AtKCS2/DAISY* was first described by Franke et al. (2009) as a salt stress-inducible docosanoic acid synthase, since *daisy* mutants produced root suberin that exhibited a concomitant decrease in C22 and C24 VLCFA-based constituent accumulation, with increased C16, C18 and C20 amounts. *AtKCS20* was shown to be functionally redundant with *AtKCS2*, based on similar observations of C22 and C24 reductions in *kcs20* mutants, and a more substantial alteration to root suberin aliphatics in *kcs2 kcs20* double mutants (Lee et al., 2009). In potato, *StKCS6* is involved in aliphatic suberin and wax monomer synthesis (Serra et al., 2009a). *StKCS6* silencing led to a drop in C28 and greater chain lengths, and led to accumulation of C26 and shorter chains, indicating that *StKCS6* acts on C26 substrates but might elongate shorter chains as well.

The KCS-generated β -ketoacyl-CoA is then reduced by a β -ketoacyl-CoA reductase to hydroxyacyl-CoA. Beaudoin et al. (2009) described a β -ketoacyl-CoA reductase (*AtKCR1*) that catalyzes the first reduction step by the fatty acid elongase complex to yield chain lengths greater than C18 for incorporation into different aliphatic polymers including the SPAD. There have been no potato homologs characterized to date.

The next step involves a 3-hydroxyacyl-CoA dehydrogenase-mediated dehydration of 3-hydroxyacyl-CoA to yield trans-2,3-enoyl-CoA. In Arabidopsis, *AtPASTICCINO2* (*AtPAS2*) encodes the third elongase complex enzyme (Bach et al., 2008). While suberin-specific aliphatic analysis was not performed in *AtPAS2* characterization, it has demonstrated involvement in synthesizing VLCFA used as precursors for various lipidic compounds, including seed storage triacylglycerols, cuticular waxes and sphingolipids.

The final enzyme in the fatty acid elongase complex is an enoyl CoA reductase (ECR) that reduces its substrate into the elongated chain with two additional carbons. An enzyme has been characterized only in Arabidopsis, based on *cer10* mutants. *AtECR* was characterized by Zheng et al. (2005) in terms of its requirement for proper production of cuticular wax, seed triacylglycerols and sphingolipid production, but no suberin aliphatics were specifically analyzed.

1.4.3.2 Oxidation

Oxidation reactions yield modified fatty acids that comprise over half of the SPAD constituents in many plant species, including mid-chain epoxide and hydroxylated octadecanoates, and ω -hydroxyalkanoic acids and their further oxidized α,ω -dioic acid derivatives generated from saturated 16:0 to 24:0 chains as well as 18:1 unsaturated fatty acids. The presence of hydroxylated and dioic VLCFAs indicates that higher chain length products undergo elongation prior to oxidation (Kolattukudy and Agrawal, 1974; Agrawal and Kolattukudy, 1978a, 1978b; Bernardis, 2002). In potato suberin, ω -hydroxy acids and dicarboxylic acids are predominant and together constitute ca. 65% of the SPAD, with only trace quantities of mid-chain modified fatty acids, whereas in other species such as cork oak, mid chain epoxides and hydroxyalkanoic acids together comprise >70% of the SPAD (Holloway, 1983), and Arabidopsis root aliphatic suberin is made up of almost 70% ω -hydroxy acids and dioic acids (Franke et al., 2005).

Terminal carbon hydroxylations are carried out by cytochrome P450 enzymes belonging to the 86A, 86B, 94A and 704B subfamilies (Durst and Nelson, 1995), where most have been characterized in Arabidopsis and potato. An Arabidopsis CYP86A, *AtCYP86A1*, was first enzymatically characterized as a fatty acid ω -hydroxylase by Benveniste et al. (1998). Studies of loss-of-function *AtCYP86A1/HORST* and *AtCYP86B1/RALPH* mutants demonstrated the role of two monooxygenases with varying substrate specificities and functions, where the former yields shorter chain ω -hydroxy acids ($\leq C18$) and the latter is responsible for the formation of very long chain C22-C24 ω -hydroxylated fatty acids in root and seed suberin (Höfer et al., 2008; Compagnon et al., 2009). The *AtCYP86A1* ortholog *StCYP86A33* has been characterized in forward and reverse genetic studies, where its silencing led to a reduction in 18:1 and 20:0 ω -hydroxy acids and α,ω -dioic acids in tuber skin and concomitant increase in 22:0 and 24:0 monomers (Serra et al., 2009b), and it was found to complement the Arabidopsis *cyp86a1/horst-1* mutant by re-establishing production of oxidized monomers (Bjelica et al., 2016). Complementation of *horst-1* mutants with either *AtCYP86A1* or *StCYP86A33* resulted in an increase in longer chain distribution than the typically most abundant hydroxylated and dioic 18:1 monomers that is not consistent with RNAi-induced observations (Serra et al., 2009b;

Bjelica et al., 2016). This suggests these CYP86As could also use longer chains in addition to their demonstrated shorter chain (C12-C18) substrates, or this result could be a byproduct of the experimental system (Benveniste et al., 1998; Serra et al., 2009b; Bjelica et al., 2016).

Oxidation of the 16:1 ω -hydroxyhexadecanoic acid, into its corresponding α,ω -dioic acid is thought to be carried out by two NADP-dependent oxidoreductases in potato (Agrawal and Kolattukudy, 1977, 1978a). In the proposed sequence of events, an ω -hydroxy fatty acid dehydrogenase first oxidizes the ω -carbon of ω -hydroxy fatty acids to produce an ω -oxo fatty acid, which is further oxidized to a dicarboxylic acid by an ω -oxo acid dehydrogenase (Agrawal and Kolattukudy, 1978a, 1978b). Only the former appeared to be wound-induced in potato tubers, while the latter demonstrated higher activity than the first enzyme despite a lack of wound-induced change, suggesting that the rate-limiting step for dicarboxylic acid production is the conversion of ω -hydroxy to ω -oxo acid (Agrawal and Kolattukudy, 1978a). Since longer chain α,ω -dioic acids are present in the SPAD, this suggested pair of enzymes either may not have such a narrow chain length substrate specificity, or there may be other unidentified enzymes responsible for catalyzing these steps with longer chains (Bernards, 2002). Studies in other species suggest that these enzymatic activities are carried out successively by a single monooxygenase. That is, the CYP94 family of monooxygenases have been implicated in catalyzing the formation of cutin and suberin ω -hydroxy fatty acids and dioic acid monomers, by catalyzing ω -hydroxylation of fatty acids. Some enzymes have additionally demonstrated a role in subsequent dicarboxylic acid formation. In vetch, the phytohormone-responsive VsCYP94A1 oxidizes the terminal methyl of C10-C16, C18:1, C18:2 and C18:3 chains (Tijet et al., 1998; Benveniste et al., 2005). Tobacco NtCYP94A5 is capable of oxidizing the terminal methyl group of saturated and unsaturated C12-C18 fatty acids into ω -hydroxy fatty acids, except for the C18:0 stearic acid, and the recombinant protein appears to act on 9,10-epoxystearic acid with the highest efficiency. NtCYP94A5 was the first plant enzyme observed to further catalyze the successive oxidation of its preferred substrate into its alcohol, aldehyde and α,ω -diacid counterparts (Le Bouquin et al., 2001). The Arabidopsis CYP94C1 is a wound-

responsive enzyme that can hydroxylate saturated, unsaturated and C12-C18 chains, including epoxy-fatty acids. AtCYP94C1 activity exhibited a preference for C12 and C18 chains as substrates, with epoxystearic acid used most predominantly. Heterologous yeast microsome expression experiments demonstrated the ability of AtCYP94A1 to perform hydroxylations at ω -methyl group and in-chain positions, and to additionally catalyze α,ω -dioic acid formation (Kandel et al., 2007). While no CYP94s have been characterized to date in potato, Bjelica et al. (2016) demonstrated that the gene encoding a putative potato homolog of NtCYP94A5, *StCYP94A26*, is expressed in roots and wounded tubers.

1.4.3.3 Reduction

Fatty acyl-CoA reductases (FARs) catalyze the conversion of fatty acids to primary alkanols for incorporation in the SPAD. Domergue et al. (2010) used loss-of-function mutant lines to describe the role of three suberin-related FARs in Arabidopsis; AtFAR1, AtFAR4 and AtFAR5. All are involved in primary alcohol biosynthesis in root suberin and appear to have different saturated chain length substrate specificities. In *far1* mutants, C22 alcohols were reduced in quantity, *far4* mutants showed decreased C20 fatty alcohols and *far5* accumulated lower amounts of C18 alkanols, while heterologous expression in yeast demonstrated a range of chain length specificities from C18-C24. These fatty alcohol-forming enzymes also contribute toward formation of a large proportion of Arabidopsis root wax alkyl hydroxycinnamates (Kosma et al., 2012; Vishwanath et al., 2013).

Acyl-activated VLCFAs can also be routed towards synthesis of waxes that make up a soluble (i.e. unpolymerized) portion of the SPAD (Soliday et al., 1979). Decarboxylation reduces acyl-CoAs into intermediate aldehydes, and subsequent decarbonylation produces VLC-alkanes. In Arabidopsis, AtCER1 and AtCER3 are core components of a redox-dependent multi-enzyme complex, which interact with electron-transferring cytochrome B5 hemoproteins (CYTB_{5S}) as cofactors to perform these alkane forming reactions after activation by long-chain acyl CoA synthase, AtLACS1 (Lü et al., 2009; Bernard et al., 2012).

1.4.4 Esterification, deposition and assembly of the suberin aliphatic domain components

The SPAD contains modified fatty acid monomers linked to glycerol, and wax components such as alkyl ferulates that represent the convergence of the main suberin-associated phenolic and aliphatic monomer biosynthetic pathways. Aliphatic monomers such as ω -hydroxy acids and α,ω -dioic acids are linked together by esterification to glycerol (Moire et al., 1999; Graça and Pereira, 2000), where LACS-mediated acyl activation of modified products is likely required. The hydrophobic nature of aliphatic suberin constituents requires energetic export of these monomers from the plasma membrane into the lipophobic cell wall. Several plasma membrane-localized ATP-binding cassette (ABC) transporters have been characterized in associated with suberin assembly.

1.4.4.1 Acyl-CoA-dependent aliphatic monomer esterification

Glycerol 3-phosphate acyltransferases (GPATs) catalyze the transfer of acyl-CoAs to glycerols, to yield monoacylglycerols. GPATs exhibit different regiospecificity, where GPATs capable of catalyzing acylation of the *sn*-2 position of glycerol-3-phosphate represent a land plant-specific lineage of these enzymes (Yang et al., 2012). Arabidopsis AtGPAT5 loss-of-function mutants demonstrate substantial decreases in C20-C24 VLCFA and their ω -hydroxy and dicarboxylic acid derivatives in suberin found in roots and seed coats, and overexpression of *AtGPAT5* led to accumulation of *sn*-2 monoacylglycerols in the wax of Arabidopsis stems (Beisson et al., 2007; Li et al., 2007). These findings support a sequence of biosynthetic events in which monooxygenase-mediated oxidation of a fatty acyl-CoA occurs prior to its linkage with glycerol (Beisson et al., 2007; Yang et al., 2012). The wound-inducible AtGPAT7 is in the same clade as AtGPAT5, and its overexpression resulted in the accumulation of suberin monomers.

Feruloyl-CoA transferases are involved in the conjugation of the hydroxycinnamic acid, ferulic acid, with modified fatty acid suberin monomers. Feruloyl transferases have been characterized in Arabidopsis and potato, where feruloyl-CoA acts as an acyl donor in the reaction with an ω -hydroxy fatty acid acceptor to yield ferulate esters. The ferulate esters

represent a point of convergence between the two major suberin-related biosynthetic pathways and also may act as a point of connection between suberin domains, as they are proposed to promote linkage of the SPPD and SPAD, as well as between the SPPD and cell wall polysaccharides (e.g. Iiyama et al., 1990; reviewed by Graça and Santos, 2007; Pollard et al., 2008; Graça, 2009).

In potato periderm, feruloyl transferase StFHT is a wound-inducible fatty alcohol/fatty ω -hydroxyacid hydroxycinnamoyl acyltransferase that catalyzes the conjugation of ferulate to ω -hydroxyacids and primary alcohols in suberin, and primary alcohols in associated wax. StFHT may have a role in the synthesis of ω -feruloyloxy fatty acids that serve as precursors for ω -feruloyloxy fatty acid glycerol esters (Serra et al., 2010; Boher et al., 2013). In Arabidopsis, aliphatic suberin feruloyl transferase/ ω -hydroxyacid hydroxycinnamoyltransferase (AtASFT/HHT) transfers feruloyl-CoA to ω -hydroxy acids with an *in vitro* preference for 16-hydroxypalmitic acid and also demonstrates transferase activity toward primary fatty alcohols (Gou et al., 2009; Molina et al., 2009).

1.4.4.2 ATP-binding cassette (ABC) transporters implicated in suberin deposition

A rice transporter RCN1/OsABCG5 is required for root suberization (Shiono et al., 2014). That is, loss-of-function *reduced culm number 1 (rcn1)* mutant plants demonstrated lower quantities of C28 and C30 fatty acids, C16, C28 and C30 ω -hydroxy fatty acids and C16 and C18 dioic acids with a concomitant increase in C24 and C26 ω -hydroxy acids, relative to wild type plants.

A pathogen-inducible potato transporter StABCG1 is involved in the deposition of suberin in tuber skin (Landgraf et al., 2014). RNAi-mediated silencing of *StABCG1* led to the reduction of two major C18:1 aliphatic monomers, ω -hydroxy-octadec-9-eneoic acid and its corresponding α,ω -dioic acid along with longer (\geq C24) chain ω -hydroxy acids, dicarboxylic acids and fatty alcohols. Less ferulic acid was released in de-polymerized apolar extracts than in control plants, while feruloyloxy fatty acids and their glycerol esters, and other ferulic acid conjugates had accumulated in the soluble fraction of apolar extracts. These observations indicate that StABCG1 exports major aliphatic monomers

including those conjugated to ferulic acid and/or glycerol. StABCG11/WBC11 is the putative potato homolog of an Arabidopsis cuticle lipid exporter, AtABCG11/WBC11 (Bird et al., 2007). While StABCG11/WBC11 has not been functionally characterized in potato, its root and tuber-localized expression was shown to be regulated by the suberin-associated transcription factor StNAC103 (Verdaguer et al., 2016). Similarly, a putative ABC subfamily G, subgroup WBC/WHITE transporter is highly expressed in suberizing cork oak tissue (Soler et al., 2007).

Yadav et al. (2014) used single, double and triple *abcg2*, *abcg6* and *abcg20* loss-of-function mutant Arabidopsis lines to determine the role of these root and seed coat localized ABCG transporters. Aliphatic composition analysis of single mutants highlighted a role for each transporter in suberin production, although they did not have noticeable phenotypic changes. Triple mutants produced suberin with low levels of C20 and C22 saturated fatty acids, C22 alkanol, and C18:1 ω -hydroxyacid and also displayed altered suberin organization and higher water permeability properties in roots and seed coats. The deposition of a suberin polymer in triple mutants, albeit altered, suggests that additional transporters are involved, and highlights the likeliness of substrate specificity along with some redundancy across transporters. Lipid transfer proteins (LTPs) may be a possible supplementary mechanism of suberin monomer export, and while none have been directly linked to suberin deposition, several LTP-encoding genes were up-regulated along with known suberin biosynthetic genes and ABCG transporters in an overexpression system studying a transcriptional regulator of suberization (Legay et al., 2016).

1.4.4.3 Possible mechanism for aliphatic monomer polymerization

To date, no mechanism(s) has been described with respect to the assembly of SPAD monomers into a polyester macromolecule. In potato periderm suberin, Graça et al. (2015) proposed that two key acylglycerol building blocks provide the basis of the SPAD: glycerol- α,ω -diacid-glycerol as the core block, and glycerol- ω -hydroxyacid-ferulic acid to link the SPAD to the SPPD. Given the similarity of aliphatic suberin and cutin, it is possible that SPAD monomers undergo an assembly process analogous to that

of cutin. Cutin monomers include C16 and C18 ω -hydroxylated acids, mid-chains with epoxy and hydroxyl groups. Primary functional groups can be linked to glycerol at different positions to form 1- and 2-monoacylglycerol esters (Graça et al., 2002).

The glycine-aspartic acid-serine-leucine (GDSL) motif lipase/hydrolase family of cutin synthases are acyltransferases that mediate the transesterification of major cutin monomers esterified to glycerol (Yeats et al., 2012; Girard et al., 2012). Cutin synthases from tomato fruit (CD1/SICUS1) and Arabidopsis flowers (LTL1/AtCUS1) were shown to catalyze a two-step enzymatic polymerization reaction *in vitro* using a predominant cutin monomer as substrate (Yeats et al., 2012; Girard et al., 2012; Yeats et al., 2014; Philippe et al., 2016). First, cutin synthases act on a 2-mono-(10,16-dihydroxyhexadecanoyl)glycerol molecule to generate an acyl-enzyme intermediate while freeing the glycerol moiety, then the intermediate reacts with another cutin monomer to yield a dimer. The polymerization reaction proceeds with fatty acyl groups from more molecules of the same monomer and increasingly larger oligomers as substrates (Jiang et al., 2011; Yeats et al., 2012; Yeats et al., 2014). However, tomato cutin synthase SICD1/CUS1 produces only linear products from their acylglycerol substrates (Yeats et al., 2014), and suppression of *SICD1/CUS1* expression in RNAi knockdowns and mutants led to a change in esterification of *sn*-1,3 and *sn*-2 positions of glycerol, demonstrating that SICD1/CUS1 acts on primary and secondary hydroxyl groups of its cutin monomer substrates (Philippe et al., 2016). Together, these findings suggest that additional mechanisms are involved in cutin polymerization, including those responsible for branching and cross-linking of the polymer (Yeats et al., 2014; Philippe et al., 2016). Due to the compositional similarities between the cutin and suberin polymers, it is feasible that GDSL-esterase/lipase enzymes may be involved in aliphatic suberin assembly. While there is some overlap between cutin and aliphatic suberin monomers, there are several distinct monomers in each polymer, and therefore such enzymes would require the ability to use suberin-specific acylglycerols as substrates.

1.5 Regulation of suberization

The process of suberization must be highly coordinated to yield a complex, cross-linked heteropolymer that is specifically deposited in distinct subcellular locations and at different points in time. The differential timing of SPPD and SPAD monomer synthesis and deposition suggests that the enzymes involved in these biosynthetic pathways are controlled by different modes of regulation. The mechanistic details of this differential regulation are not understood, but some aspects regulating suberin biosynthesis have been described. A role for the phytohormone abscisic acid (ABA) has long been implicated as a regulator of suberization, and more recently, transcription factors in different species were demonstrated to control suberin biosynthetic genes.

1.5.1 Phytohormone roles in suberization

Abscisic acid is a carotenoid-derived signaling molecule involved in many developmental and stress-related processes in plants, which include mediating abiotic stress response to drought as well as biotic plant-pathogen interactions (e.g. reviewed by Mauch-Mani and Mauch, 2005; Tuteja, 2007). Abscisic acid has long been thought to play a regulatory role in potato tuber suberization. Given the established role of ABA in drought and pathogen stress responses, the involvement of ABA in suberization is consistent with the physiological function of suberin in protection against water loss and infection.

Soliday et al. (1978) first posited the likely role of this hormone in wound-induced tuber suberization after observing that ABA was released into a solution used to wash cut potatoes. Washing in the first two days after wounding was shown to prevent suberization and the exogenous addition of ABA back into washed tuber slices partially reversed this inhibition. This study proposed that in the early phase of wound-healing, ABA formation triggers some suberization-inducing factor that leads to the induction of enzymes for suberin biosynthesis. Follow-up work by Cottle and Kolattukudy (1982) determined that suberin and its associated waxes increased with ABA treatment. A slight enhancement of ω -hydroxy fatty acid dehydrogenase and phenylalanine ammonia-lyase activity, and a significant increase in suberization-associated peroxidase activity were observed after

ABA treatment, linking ABA to the induction of suberization enzymes (Cottle and Kolattukudy, 1982).

De novo ABA biosynthesis is triggered by tuber wounding as shown by an increase in ABA accumulation and the induction of ABA metabolism at the transcriptional level (Lulai et al., 2008; Lulai and Suttle, 2009; Kumar et al., 2010; Suttle et al., 2013). Lulai et al. (2008) provided further evidence of a role for ABA in wound-induced suberin deposition through the use of the biosynthetic inhibitor fluridone, which targets the phytoene desaturase enzyme involved in carotenoid biosynthesis (Sanderman and Boger, 1989), effectively diminishing substrate levels for *de novo* ABA production. While the impact of fluridone on suberization was only described using a fluorescence microscopy-based qualitative rating system, the impact of ABA inhibition and exogenous ABA application both appeared to be stronger on the SPAD relative to the SPPD. Endogenous ABA accumulation also promotes potato microtuber dormancy (Suttle and Hultstrand, 1994), and ABA levels decrease with age in resting tubers. The latter is linked to an age-associated increase in water permeability and loss of wound-healing ability (Kumar et al., 2010).

Overall, the involvement of ABA in wound-induced and native periderm suberization is evident, but knowledge of its targeted impact on recently characterized biosynthetic steps is limited. *In silico* analysis of the putative promoter region of the key suberin aliphatic gene *StCYP86A33* led to the identification of several ABA-linked response elements (Bjelica et al., 2016). Exogenous ABA application was shown to induce *StFHT* expression in wound-healing tubers in support of predicted *StFHT* *cis*-regulatory motifs for biotic and abiotic stress and ABA responsiveness, although the impact of ABA on *StFHT*-generated metabolites was not investigated (Boher et al., 2013). Further, ABA has been shown to up-regulate specific transcription factors associated with suberin deposition (see §1.5.2).

Other established wound-signaling hormones, such as jasmonic acid (JA) and ethylene (Hildmann et al., 1992; Léon et al., 2001), do not appear to be implicated in potato tuber suberization, although Barberon et al. (2016) observed that ethylene application led to the

degradation of suberin in Arabidopsis root endodermal cells. Ethylene evolution occurs after tuber wounding, and while it may play a role in other aspects of the wound response, inhibition of ethylene biosynthesis demonstrated that there is no apparent effect of ethylene on wound-induced suberin production in tubers (Lulai and Suttle, 2004; Lulai and Suttle, 2009). Jasmonic acid content also increases upon tuber wounding, and subsequently drops prior to the time at which ABA and ethylene reach their maximum levels (Lulai and Suttle, 2009), but its removal by tuber slice washing suggested its lack of requirement for suberization (Lulai et al., 2011). *StFHT* contains many putative hormone-responsive motifs including many associated with JA and salicylic (SA), but treatment with these hormones respectively demonstrated no change, or suppression, of *StFHT* expression (Boher et al., 2013).

1.5.2 Transcription factors

In the context of secondary metabolism, transcription factors (TFs) have been shown to regulate entire pathways including multiple branches (e.g. *Vitis vinifera* VvMYB5a that controls the phenylpropanoid pathway in grapevine, Deluc et al., 2006), or subgroups of pathway genes, and under stress-specific conditions (e.g. the wound-, pathogen- and UV-inducible poplar PtMYB134 that controls the proanthocyanidin branch of phenylpropanoid biosynthesis, Mellway et al., 2009). Transcription factors from Arabidopsis, potato, and apple have recently been implicated in suberin biosynthesis.

AtMYB41 was characterized as a salt stress- and ABA-induced regulator of aliphatic and, less definitively, phenolic suberin biosynthesis by Kosma et al. (2014). *AtMYB41* overexpression in Arabidopsis and its subsequent heterologous, transient expression in *Nicotiana benthamiana* resulted in ectopic accumulation of key suberin biosynthetic gene transcripts and characteristic metabolites in usually non-suberizing leaves, including *AtCYP86A1* and its ω -hydroxy fatty acid products as well as corresponding dicarboxylic acids (Kosma et al., 2014). While phenylpropanoid and lignin biosynthetic genes were also up-regulated, these were to a substantially lesser degree than suberin aliphatic biosynthetic genes, and mostly manifested as an increase in aliphatic suberin-associated ferulic acid. Remarkably, transmission electron microscopy revealed that the ectopic

deposition of suberin in leaf epidermal and mesophyll cells resembled the ultrastructural organization of suberin typical of *Arabidopsis* roots, which is also found in native and wound potato tuber periderm. The abundance of suberin synthesized in *AtMYB41*-overexpressing plants supports a role for this TF as an important regulator of suberization, and also suggests the role of additional regulatory mechanisms to control biosynthesis and deposition on a finer scale. The lesser degree of *AtMYB41* impact on phenolic suberin biosynthesis also suggests that further TFs and/or other mechanisms exist within a larger regulatory network.

StNAC103 was recently described by Verdagner et al. (2016) as a wound- and ABA-inducible negative regulator of aliphatic suberin and wax accumulation. Its promoter drove GUS expression in native and wound periderm phellem cells undergoing suberization, and also in tissues that do not produce suberin, namely lateral root primordia and root apical meristems. Its RNAi-mediated gene silencing led to the significant up-regulation of genes with predicted or known involvement in different branches of suberin-related metabolism: *StCYP86A33*, *StKAR*, *StFHT* and *StABCG11/WBC11*. Although TF binding activities were not investigated, the impact of *StNAC103*-silencing on these genes was consistent with an increase in their substrates, such as alkylferulate wax components, ω -hydroxyacids, primary alcohols, and alkanes. The observed transcriptional repression activities of *StNAC103* likely control suberin synthesis during wound-healing on a fine scale, and also probably function to prevent premature suberization in certain root localizations *in vivo*.

A transcriptomic comparison between russeted (i.e. suberized) and non-russeted apple varieties led to the identification of *Malus × domestica* MdMYB93, which displayed significantly higher expression in russeted skin, and correlated with the differential expression of putative homologs of other key suberin-related genes *CYP86A1*, *GPAT5* and *CYP86B1* (Legay et al., 2015). Using the same heterologous expression system as Kosma et al. (2014) in concert with metabolite and RNA-seq analysis, the apple MdMYB93 was characterized as a regulator of suberin biosynthesis and deposition (Legay et al., 2016). This TF was found to co-express with biosynthetic genes involved in lipid and phenylpropanoid metabolism, ABCG family transporters, and cell wall

development genes, and enhanced accumulation of key suberin monomers and building blocks. Although the phenolic composition was altered in the MdMYB93 overexpression system, these may reflect lignin-specific changes and the role of these compounds as SPPD monomers remains speculative (Legay et al., 2016).

A similar transcriptomic investigation of suberized tomato and russeted apple fruits led to the identification of genes associated with developmental suberin production, and yielded a suberization-related gene expression signature found to be highly conserved across angiosperms (Lashbrooke et al., 2016). Arabidopsis AtMYB107 and AtMYB9 were discovered through the study of suberin signature gene knockout mutants. Further TF loss-of-function mutants were indeed reduced in suberin phenolic and aliphatic components, and *AtMYB107* was up-regulated in *Atmyb9* mutants. These TFs therefore appear to act together to effectively regulate suberin-related phenylpropanoid and fatty acid biosynthesis. This work additionally identified putative orthologs in a suberin-related MYB clade through multi-species suberin signature co-expression analysis, including tomato SIMYB93, apple MdMYB53, grape VvMYB107, potato StMYB93 (currently annotated as StMYB102) and rice OsMYB93 (Lashbrooke et al., 2016).

In potato, StWRKY1 was not characterized in a suberin-specific context, but was shown to bind to promoter regions of phenylpropanoid genes encoding 4-coumarate-CoA ligase (4CL) and tyramine hydroxycinnamoyl transferase (THT) to mediate the deposition of protective hydroxycinnamic acid amides into cell walls of *Phytophthora infestans*-inoculated aerial tissues (Yogendra et al., 2015). *StWRKY1* silencing led to a drop in hydroxycinnamic acid amide abundance and rendered plants less resistant to the late blight-causing major crop pathogen (Yogendra et al., 2015), which is capable of directly infecting potato foliage as well as tubers (Lacey, 1967). These observations suggest that *StWRKY1* has a role in stress-induced phenylpropanoid metabolism, though a role in wound-induced suberization has not been demonstrated.

Among characterized TFs that regulate aspects of suberin-related metabolism, the aforementioned were either stress-induced TFs mostly affiliated with one suberin-associated metabolic pathway, or TFs with a demonstrated a role for both major suberin

biosynthetic pathways in a developmental context. Therefore, no clear regulators of SPPD-related metabolism have been defined with respect to potato tuber wound-healing or periderm suberization, or stress-induced accumulation of suberin in *Arabidopsis* roots. The regulatory oversight of differential pathway induction during the wound response, in terms of timing of biosynthesis and spatial organization of deposited suberin, remains unestablished.

1.6 The wound-healing potato tuber

Wounding induces a cascade of responses that lead to healing and protection of damaged tissue. In potato tubers, suberization is arguably the most important component of the overall wound-healing process, which occurs over a period of time and across two main phases after injury. The ability to rapidly suberize wounded parenchyma is imperative for tuber protection against damage incurred during growth, harvest, handling and cutting for seed production (reviewed by Lulai, 2007).

1.6.1 Wound-induced signaling

The changes that occur between initial cell damage, induction of suberization and final wound periderm maturation require wound-related signaling (e.g. Léon et al., 2001). The initial perception of physical damage may be mediated by an immediate shift in osmotic potential in wounded cells (Rosenstock and Kahl, 1978), or by molecules that are released by damaged cells and act as elicitors in intact cells adjacent to the wound site, such as cell wall components like oligogalacturonides (Bishop et al., 1981). Ion flux resulting in plasma membrane depolarization, cytosolic calcium concentration changes, the generation of active oxygen species, and protein phosphorylation are aspects of proposed signal transduction mechanisms, which in turn lead to phytohormone-mediated transcriptional changes of defensive and wound-healing related genes (reviewed by de Bruxelles and Roberts, 2001).

Many studies that have collectively led to the general characterization of wound signaling have been conducted in leaves. Signal(s) and mechanism(s) associated with suberization in potato tubers have not been fully elucidated (Lulai, 2007). Tubers produce reactive

oxygen species (ROS) within 30-60 minutes of wounding, in an event that is distinct from later oxidase-associated oxidative bursts thought to be involved in wound-healing and SPPD cross-linking (Razem and Bernardts, 2003). Therefore, the first ROS may be involved in the initial signal cascade (Razem and Bernardts, 2003). Wound-induced signal transduction that leads to suberization is likely mediated by ABA, but does not appear to require JA or ET, as described in §1.5.1. Aside from suberization, the subsequent wound response involves re-organization in overall metabolism to fuel and feed into suberin-specific biosynthetic reactions, and cell cycle activities to develop new cells that underscore the physical healing process. Signals and/or other mechanisms that coordinate and activate these additional processes required for wound-healing have not been described.

1.6.2 Two major stages are involved in tuber wound-healing

The first stage of wound-healing leads to the formation of a closing layer within ca. 5-6 days of wounding. Closing layer formation is considered a primary level of suberization and involves the reinforcement of 1-2 layers of existing parenchyma cells adjacent to the wound site via suberin deposition (Thomson et al., 1995; Lulai, 2007; Lulai and Neubauer, 2014). This initial response involves the induction of phenylpropanoid biosynthesis that yields suberin poly(phenolic) compounds. Once SPPD synthesis and deposition into parenchyma cell walls is completed, the SPAD monomers are synthesized, linked and deposited (Lulai and Corsini, 1998; Bernardts, 2002). The second stage leads to the production of the wound periderm, or secondary suberization, which is initiated ca. 7 days after wounding and is completed over the course of another ca. 21 days (28 days post-wounding) (Lulai and Neubauer, 2014). This process involves the generation of a new layer of meristematic progenitor cells called the wound phellogen, analogous to cork cambium. These mother cells give rise to phellem cells that undergo suberization and remain beneath the closing layer, and also produce phelloderm cells that reside below the phellogen (Lulai, 2007). The cessation of suberized phellem cells marks the maturation of the wound periderm (Lulai and Neubauer, 2014; **Figure 1.3**).

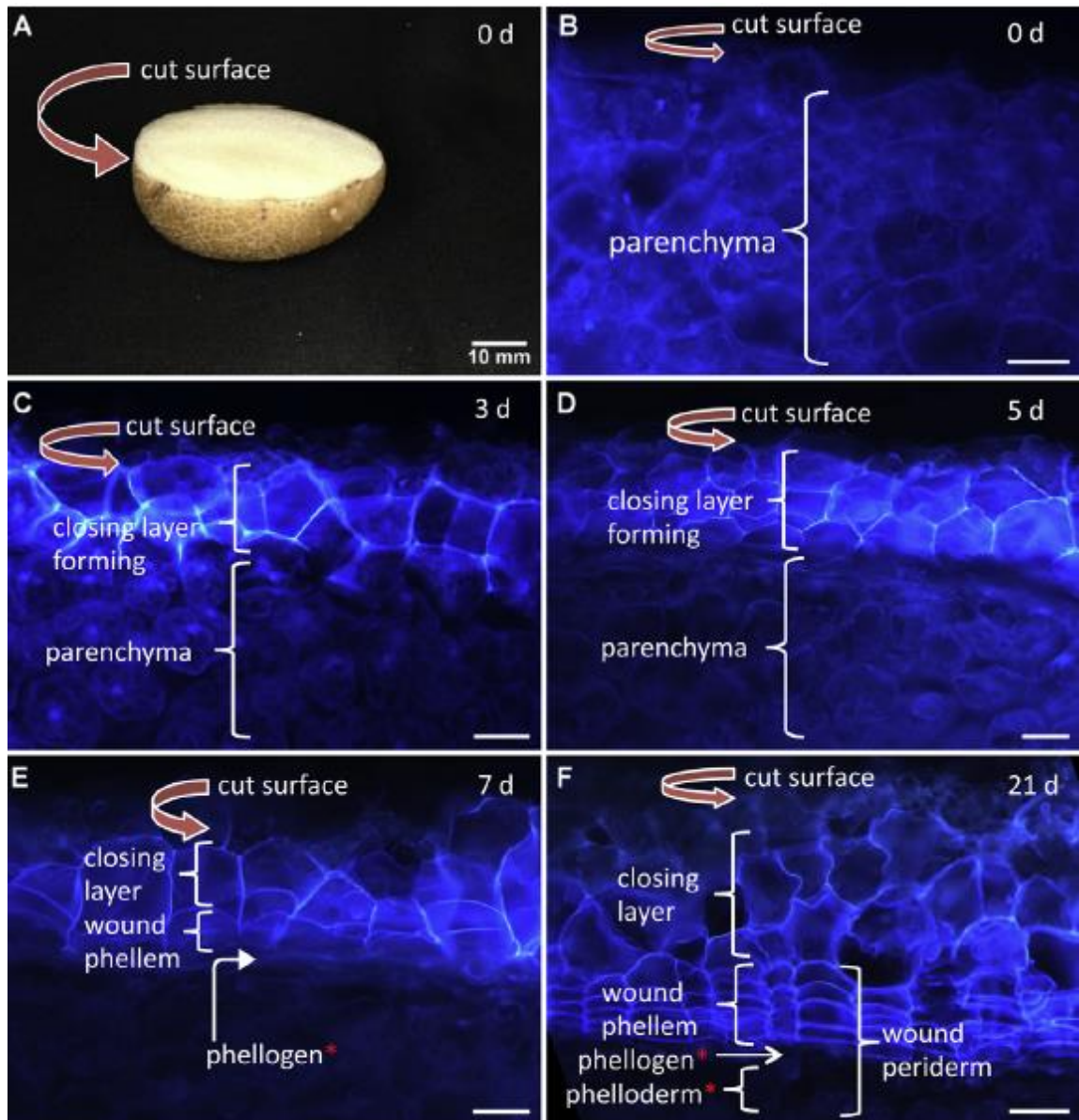


Figure 1.3. Wound-induced tuber suberization during two major stages of wound-healing. **A.** The cut tuber surface where closing layer formation occurs in response to wounding and **B-F.** Tuber wound-healing is shown as it progresses over time, visualized by epifluorescence microscopy to detect accumulation of cell-wall localized autofluorescent suberin poly(phenolic) (SPP) compounds over the course of closing layer and wound periderm formation, respectively. **B.** At 0 days post wounding (dpw), SPPs have not accumulated, but weak parenchyma cell wall autofluorescence is visible. **C.** By 3 dpw, SPPs are detectable in parenchyma cell walls adjacent to the wound site and represent a component of closing layer formation. **D.** At 5 dpw, SPP accumulation is present around entire walls of the outer cell layer; the suberin poly(aliphatic) (SPA) components do not autofluoresce and cannot be seen in this image, but accumulate by this point of wound-healing and closing layer formation. **E.** By 7 dpw, SPP deposition ceases within existing parenchyma cells, and active phellogen is present, as indicated by SPP autofluorescence on newly formed phellem cells beneath the closing layer, identified by their rectangular shape. The formation of newly suberizing phellem cells indicates that wound periderm formation has initiated. **F.** By 21 dpw, several layers of wound phellem cells have formed and undergone suberization during active wound periderm formation. The phellogen continues to generate phellem cells until 28 dpw. A limited number of non-fluorescent, parenchyma-like phelloderm cells form beneath the phellogen at this time. Bars = 5 μm . *Indicates cells that are not visibly autofluorescent. Figure copied directly and caption adapted from Lulai and Neubauer (2014).

1.6.3 Various biological events occur during the wound-healing time course

The same suite of suberization-related genes are up-regulated in the two temporal cycles that define the two phases of wound-healing (Lulai and Neubauer, 2014), and wounding also induces cell wall protein and pectin methyl esterase genes that may be important for strengthening phellogen cell walls during closing layer and wound periderm formation (Neubauer et al., 2012).

Interestingly, the cell cycle undergoes biphasic activation as well, in which DNA replication is induced and takes place without cell division during early closing layer formation, then cell division is evident during wound periderm formation (Lulai et al., 2016). DNA synthesis during the S-phase does not occur until after 12 hours post-wounding, and proceeds for ca. 30 hours, ending approximately 4 days before the closing layer is formed (Lulai et al., 2014).

Less is known about the early stages of wound-healing prior to closing layer formation, although it is clear that important processes are initialized within ca. 12 hours of wounding. Fairly recent research is still uncovering the nuances of the temporal changes across wound-healing, which are not well-established at finer timescales. There is a necessary requirement for initiation of primary metabolism in the tuber as it transitions from dormant to wound-healing, in order to supply metabolites and energy-rich molecules for various wound-healing processes, including, but not limited to, suberization. Wound-healing tubers differentially synthesize groups of metabolites and express relevant biosynthetic enzymes on a temporal scale, including those directly incorporated into the suberin polymer, as well as primary metabolites (Yang and Bernards, 2007; Chaves et al., 2009).

1.6.4 The wound-healing potato tuber as a model system for suberization studies

After wounding, *de novo* suberin synthesis in usually non-suberizing tuber parenchyma cells functions to seal off and heal the damaged area, which promotes post-injury survival (reviewed in Lulai, 2007). Since wounded tuber surfaces produce large amounts of

suberin (Kolattukudy and Dean, 1974), and are amenable to exogenous application of chemicals such as phytohormones and inhibitors (e.g. Soliday et al., 1978; Cottle and Kolattukudy, 1982; Lulai et al., 2008), the wounded tuber provides an ideal model system for studying the process of suberization over time. This experimental system also offers the opportunity to explore the regulatory mechanisms involved in this induced stress response, and other aspects of wound-healing.

Gaining a fundamental understanding of plant defenses and their regulation has important implications for the production of stress-tolerant crops, which could ultimately translate into enhanced crop yield and post-harvest stability. Suberin is ubiquitous to roots and stems that undergo secondary thickening (i.e. the cork layer of bark), and exhibits important physiological functions in the regulation of water and ion transport, as well as protection against pathogen infection (e.g. Kolattukudy and Dean, 1974; Lulai and Corsini, 1998; Silva et al., 2005; Baxter et al., 2009). The overall chemical composition and biosynthetic steps involved in wound-induced tuber suberin production are generally conserved in developmental tuber periderm suberization (Schreiber et al., 2005b), and in species that synthesize suberin localized to other plant organs (e.g. Arabidopsis roots and seeds, and tomato and apple fruit skins, e.g. Legay et al., 2015; Legay et al., 2016; Lashbrooke et al., 2016), and therefore the tuber model offers information that can be applied directly to this important crop species, but also to others.

1.7 Dissertation overview

I used a wound-healing potato tuber model system to explore the temporal dynamics of induced suberization and other associated wound-responsive processes at the levels of transcription and metabolite accumulation. The major objectives of this project were to establish mechanisms responsible for the differential temporal regulation of suberin-related metabolism, gain insight into global changes that occur during wound-healing including, but not limited to, suberization, to further understand coordination and timing of events, and to identify novel targets for downstream characterization that include regulatory components and biosynthetic genes.

In Chapter 2, wound-healing time course experiments were used to test the hypothesis that ABA plays a regulatory role in the differential induction of suberin-related metabolic pathways. The regulatory role of ABA was evaluated by subjecting wounded tubers to exogenous treatments including additional ABA and an ABA inhibitor, fluridone (FD). Gene expression and metabolite analyses were performed in concert to establish the regulatory role of ABA at the level of transcription and biosynthesis across the closing layer timeframe of the wound-healing response.

Abscisic acid is affiliated with the wound response, wound-healing and the suberization process (Cottle and Kolattukudy, 1982; Lulai et al., 2008; Kumar et al., 2010), but its impact on different branches of suberin-associated metabolism are not clear. The differential timing of the pathways involved in the production of SPPD and SPAD monomers has been established (Lulai and Corsini, 1998; Lulai and Neubauer, 2014), but no mechanisms regulating this varied induction had been specifically explored. The temporal patterns of expression for genes involved in linkage, assembly and transport of the polymer and their relationship to ABA are also not well-described in the wound-healing context. This study expands upon previous knowledge to present new insights into the differential regulatory role of ABA on suites of genes representative of suberin biosynthesis and assembly.

In Chapter 3, wound-healing tubers were used to construct a time-series transcriptome that was explored with both global and targeted approaches to address questions about the biological changes that occur during wound-healing generally, and suberization specifically. Time points were selected to gain insight into early stages of wound-healing prior to closing layer formation and capture initial regulatory events. Whereas many wound-healing tuber studies focus solely on suberization, I have considered other wound-activated processes that are less directly related to suberin production, including primary metabolism, and other wound-related responses or requirements for healing, especially at the transcriptional level. In completing the first transcriptomic analysis of the wound-healing potato tuber, it was possible to explore these different aspects of the overall wound response and test the hypothesis that tuber wounding leads to a largescale re-configuration of transcription including early initiation of primary metabolism.

Chapter 4 is presented as an integration of findings about events that relate to tuber wound-healing and suberization. This discussion offers an updated overview to the standard suberization biosynthetic scheme by including new information about primary metabolism, regulatory components, novel prospects for assembly genes, and associated physical healing events, all framed within the early wound-healing time course leading up to closing layer formation. Suggestions for future studies focus on aspects of the wound-healing process that warrant additional exploration and downstream characterization, such as further work on novel candidate genes.

1.8 References

- Agrawal, V.P. and Kolattukudy, P.E.** (1977). ω -Hydroxyacid oxidation in enzyme preparations from suberizing potato tuber disks. *Plant Physiology* **59**, 667-672.
- Agrawal, V.P. and Kolattukudy, P.E.** (1978a). Purification and characterization of a wound-induced omega-hydroxy fatty acid:NADP oxidoreductase from potato tuber disks (*Solanum tuberosum* L.). *Archives of Biochemistry and Biophysics* **191**, 452-465.
- Agrawal, V.P. and Kolattukudy, P.E.** (1978b). Mechanism of action of a wound-induced ω -hydroxy fatty acid:NADP oxidoreductase isolated from potato tubers (*Solanum tuberosum* L.) *Archives of Biochemistry and Biophysics* **191**, 466-478.
- Andreetta, A., Dignac, M. F., and Carnicelli, S.** (2013). Biological and physico-chemical processes influence cutin and suberin biomarker distribution in two Mediterranean forest soil profiles. *Biogeochemistry* **112**, 41-58.
- Bach, L., Michaelson, L.V., Haslam, R., Bellec, Y., Gissot, L., Marion, J., Da Costa, M., Boutin, J.P., Miquel, M., Tellier, F. and Domergue, F.** (2008). The very-long-chain hydroxy fatty acyl-CoA dehydratase PASTICCINO2 is essential and limiting for plant development. *Proceedings of the National Academy of Sciences of the United States of America* **105**(38), 14727-14731.
- Barberon, M., Vermeer, J.E.M., De Bellis, D., Wang, P., Naseer, S., Andersen, T.G., Humbel, B.M., Nawrath, C., Takano, J., Salt, D.E. and Geldner, N.** (2016). Adaptation of root function by nutrient-induced plasticity of endodermal differentiation. *Cell* **164**(3), 447-459.
- Baxter, I., Hosmani, P.S., Rus, A., Lahner, B., Borevitz, J.O., Muthukumar, B., Mickelbart, M.V., Schreiber, L., Franke, R.B. and Salt, D.E.** (2009). Root suberin forms an extracellular barrier that affects water relations and mineral nutrition in *Arabidopsis*. *PLoS Genetics*, **5**(5), p.e1000492.
- Beaudoin, F., Wu, X., Li, F., Haslam, R.P., Markham, J.E., Zheng, H., Napier, J.A. and Kunst, L.** (2009). Functional characterization of the *Arabidopsis* β -ketoacyl-coenzyme A reductase candidates of the fatty acid elongase. *Plant Physiology*, **150**(3), 1174-1191.
- Beisson, F., Li, Y., Bonaventure, G., Pollard, M. and Ohlrogge, J.B.** (2007). The acyltransferase GPAT5 is required for the synthesis of suberin in seed coat and root of *Arabidopsis*. *The Plant Cell*, **19**(1), 351-368.
- Benveniste, I., Tijet, N., Adas, F., Philipps, G., Salaun, J.P. and Durst, F.** (1998). *CYP86A1* from *Arabidopsis thaliana* encodes a cytochrome P450-dependent fatty acid omega-hydroxylase. *Biochemical and Biophysical Research Communications* **243**, 688-693.
- Benveniste, I., Bronner, R., Wang, Y., Compagnon, V., Michler, P., Schreiber, L., Salaun, J.P., Durst, F. and Pinot, F.** (2005) *CYP94A1*, a plant cytochrome

P450-catalyzing fatty acid omega-hydroxylase, is selectively induced by chemical stress in *Vicia sativa* seedlings. *Planta* **221**, 881-890.

- Bernard, A., Domergue, F., Pascal, S., Jetter, R., Renne, C., Faure, J.D., Haslam, R.P., Napier, J.A., Lessire, R. and Joubès, J.** (2012). Reconstitution of plant alkane biosynthesis in yeast demonstrates that *Arabidopsis* ECERIFERUM1 and ECERIFERUM3 are core components of a very-long-chain alkane synthesis complex. *The Plant Cell* **24**, 3106-3118.
- Bernards, M.A.** (2002). Demystifying suberin. *Canadian Journal of Botany* **80**(3), 227-240.
- Bernards, M.A., Fleming, W.D., Llewellyn, D.B., Priefer, R., Yang, X., Sabatino, A., and Plourde, G.L.** (1999). Biochemical characterization of the suberization-associated anionic peroxidase of potato. *Plant Physiology* **121**, 135-145.
- Bernards, M.A., Lopez, M.L., Zajicek, J. and Lewis, N.G.** (1995). Hydroxycinnamic acid-derived polymers constitute the polyaromatic domain of suberin. *Journal of Biological Chemistry* **270**(13), 7382-7386.
- Bernards, M.A., and Lewis, N.G.** (1998). The macromolecular aromatic domain in suberized tissue: a changing paradigm. *Phytochemistry* **47**(6), 915-933.
- Bernards, M.A., and Razem, F.A.** (2001). The poly(phenolic) domain of potato suberin: a non-lignin plant cell wall polymer. *Phytochemistry* **57**, 1115-1122.
- Bernards, M.A., Susag, L.M., Bedgar, D.L., Anterola, A.M. and Lewis, N.G.** (2000). Induced phenylpropanoid metabolism during suberization and lignification: a comparative analysis. *Journal of Plant Physiology* **157**(6), 601-607.
- Bird, D., Beisson, F., Brigham, A., Shin, J., Greer, S., Jetter, R., Kunst, L., Wu, X., Yephremov, A. and Samuels, L.** (2007). Characterization of *Arabidopsis* ABCG11/WBC11, an ATP binding cassette (ABC) transporter that is required for cuticular lipid secretion. *The Plant Journal* **52**(3), 485-498.
- Bishop, P.D., Makus, D.J., Pearce, G. and Ryan, C.A.** (1981). Proteinase inhibitor-inducing factor activity in tomato leaves resides in oligosaccharides enzymically released from cell walls. *Proceedings of the National Academy of Sciences of the United States of America* **78**, 3536-3540.
- Bjelica, A., Haggitt, M.L., Woolfson, K.N., Lee, D.P., Makhzoum, A.B. and Bernards, M.A.** (2016). Fatty acid ω -hydroxylases from *Solanum tuberosum*. *Plant Cell Reports* **35**(12), 2435-2448.
- Blacklock, B.J. and Jaworski, J.G.** (2006). Substrate specificity of *Arabidopsis* 3-ketoacyl-CoA synthases. *Biochemical and Biophysical Research Communication* **346**, 583-590.
- Boher, P., Serra, O., Soler, M., Molinas, M. and Figueras, M.** (2013). The potato suberin feruloyl transferase FHT which accumulates in the phellogen is induced by wounding and regulated by abscisic and salicylic acids. *Journal of Experimental Botany*, **64**(11), 3225-3236.

- Chaves, I., Pinheiro, C., Paiva, J.A., Planchon, S., Sergeant, K., Renaut, J., Graça, J.A., Costa, G., Coelho, A.V. and Ricardo, C.P.P.** (2009). Proteomic evaluation of wound-healing processes in potato (*Solanum tuberosum* L.) tuber tissue. *Proteomics* **9**(17), 4154-4175.
- Compagnon, V., Diehl, P., Benveniste, I., Meyer, D., Schaller, H., Schreiber, L., Franke, R., and Pinot, F.** (2009). CYP86B1 is required for very long chain ω -hydroxyacid and α , ω -dicarboxylic acid synthesis in root and seed suberin polyester. *Plant Physiology* **150**, 1831-1843.
- Cottle, W. and Kolattukudy, P.E.** (1982). Abscisic acid stimulation of suberization: induction of enzymes and deposition of polymeric components and associated waxes in tissue cultures of potato tuber. *Plant Physiology* **70**(3), 775-780.
- de Bruxelles, G.L. and Roberts, M.R.** (2001). Signals regulating multiple responses to wounding and herbivores. *Critical Reviews in Plant Sciences* **20**(5), 487-521.
- Deluc, L., Barrieu, F., Marchive, C., Lauvergeat, V., Decendit, A., Richard, T., Carde, J.P., Mérillon, J.M. and Hamdi, S.** (2006). Characterization of a grapevine R2R3-MYB transcription factor that regulates the phenylpropanoid pathway. *Plant Physiology* **140**(2), 499-511.
- Do, C.-T., Pollet B., Thévenin J., Sibout R., Denoue D., Barrière Y., Lapierre C., and Jouanin L.** (2007). Both caffeoyl coenzyme A 3-*O*-methyltransferase 1 and caffeic acid *O*-methyltransferase 1 are involved in redundant functions for lignin, flavonoids and sinapoyl malate biosynthesis in *Arabidopsis*. *Planta* **226**, 1117-1129.
- Domergue, F., Vishwanath, S.J., Joubès, J., Ono, J., Lee, J.A., Bourdon, M., Alhattab, R., Lowe, C., Pascal, S., Lessire, R. and Rowland, O.** (2010). Three *Arabidopsis* fatty acyl-CoA reductases, FAR1, FAR4, and FAR5, generate primary fatty alcohols associated with suberin deposition. *Plant Physiology* **153**, 1539-1554.
- Durst, F. and Nelson, D.R.** (1995). Diversity and evolution of plant P450 and P450-reductases. *Drug Metabolism and Drug Interactions*, **12**(3-4), 189-206.
- Esau, K.** (1977). *Anatomy of Seed Plants*, 2nd Edition (pp. 183-197). New York, NY: Wiley & Sons.
- Espelie, K.E., Franceschi, V.R. and Kolattukudy, P.E.** (1986). Immunocytochemical localization and time course of appearance of an anionic peroxidase associated with suberization in wound-healing potato tuber tissue. *Plant Physiology* **81**(2), 487-492.
- Espelie, K.E. and Kolattukudy, P.E.** (1985). Purification and characterization of an abscisic acid-inducible anionic peroxidase associated with suberization in potato (*Solanum tuberosum*). *Archives of Biochemistry and Biophysics* **240**, 539-545.
- Franke, R., Briesen, I., Wojciechowski, T., Faust, A., Yephremov, A., Nawrath, C., and Schreiber, L.** (2005). Apoplastic polyesters in *Arabidopsis* surface tissues—A typical suberin and a particular cutin. *Phytochemistry* **66**, 2643-2658.

- Franke, R., Höfer, R., Briesen, I., Emsermann, M., Efremova, N., Yephremov, A. and Schreiber, L.** (2009). The DAISY gene from *Arabidopsis* encodes a fatty acid elongase condensing enzyme involved in the biosynthesis of aliphatic suberin in roots and the chalaza-micropyle region of seeds. *The Plant Journal* **57**, 80-95.
- Girard, A.L., Mounet, F., Lemaire-Chamley, M., Gaillard, C., Elmorjani, K., Vivancos, J., Runavot, J.L., Quemener, B., Petit, J., Germain, V. and Rothan, C.** (2012). Tomato GDSL1 is required for cutin deposition in the fruit cuticle. *The Plant Cell* **24**(7), 3119-3134.
- Graça, J.** (2009) Hydroxycinnamates in suberin formation. *Phytochemistry Reviews* **9**(1), 85-91.
- Graça, J., Cabral, V., Santos, S., Lamosa, P., Serra, O., Molinas, M., Schreiber, L., Kauder, F. and Franke, R.** (2015). Partial depolymerization of genetically modified potato tuber periderm reveals intermolecular linkages in suberin polyester. *Phytochemistry* **117**, 209-219.
- Graça, J. and Pereira, H.** (1997). Cork suberin: a glyceryl based polyester. *Holzforschung: International Journal of the Biology, Chemistry, Physics and Technology of Wood* **51**(3), 225-234.
- Graça, J. and Pereira, H.** (1999). Glyceryl-acyl and aryl-acyl dimers in *Pseudotsuga menziesii* bark suberin. *Holzforschung: International Journal of the Biology, Chemistry, Physics and Technology of Wood*, **53**(4), 397-402.
- Graça, J., and Pereira, H.** (2000). Diglycerol alkendioates in suberin: building units of a poly(acylglycerol) polyester. *Biomacromolecules* **1**, 519-522.
- Graça, J. and Santos, S.** (2007). Suberin: a biopolyester of plants' skin. *Macromolecular Bioscience*, **7**(2), 128-135.
- Graça, J., Schreiber, L., Rodrigues, J. and Pereira, H.** (2002). Glycerol and glyceryl esters of ω -hydroxyacids in cutins. *Phytochemistry* **61**(2), 205-215.
- Gou, J.Y., Yu, X.H. and Liu, C.J.** (2009). A hydroxycinnamoyltransferase responsible for synthesizing suberin aromatics in *Arabidopsis*. *Proceedings of the National Academy of Sciences of the United States of America* **106**(44), 8855-18860.
- Hagel, J.M. and Facchini, P.J.** (2005). Elevated tyrosine decarboxylase and tyramine hydroxycinnamoyltransferase levels increase wound-induced tyramine-derived hydroxycinnamic acid amide accumulation in transgenic tobacco leaves. *Planta*, **221**(6), 904-914.
- Havir, E.A. and Hanson, K.R.** (1970). [72a] L-phenylalanine ammonia-lyase (potato tubers). In *Methods in Enzymology* (Vol. 17, pp. 575-581). Academic Press.
- Hildmann, T., Ebnet, M., Peña-Cortés, H., Sánchez-Serrano, J.J., Willmitzer, L. and Prat, S.** (1992). General roles of abscisic and jasmonic acids in gene activation as a result of mechanical wounding. *The Plant Cell* **4**(9), 1157-1170.
- Höfer, R., Briesen, I., Beck, M., Pinot, F., Schreiber, L., and Franke, R.** (2008). The *Arabidopsis* cytochrome P450 *CYP86A1* encodes a fatty acid omega-hydroxylase

- involved in suberin monomer biosynthesis. *Journal of Experimental Botany* **59**, 2347-2360.
- Holloway, P.J.** (1983). Some variations in the composition of suberin from the cork layers of higher plants. *Phytochemistry* **22**, 495-502.
- Hoffmann, L., Maury, S., Martz, F., Geoffroy, P., and Legrand, M.** (2003). Purification, cloning, and properties of an acyltransferase controlling shikimate and quinate ester intermediates in phenylpropanoid metabolism. *Journal of Biological Chemistry* **278**, 95-103.
- Humphreys, J.M., Hemm, M.R., and Chappie, C.** (1999). New routes for lignin biosynthesis defined by biochemical characterization of recombinant ferulate 5-hydroxylase, a multifunctional cytochrome P450-dependent monooxygenase. *Proceedings of the National Academy of Sciences of the United States of America* **96**, 10045-10050.
- Iiyama, K., Lam, T.B.T. and Stone, B.A.** (1990) Phenolic acid bridges between polysaccharides and lignin in wheat internodes. *Phytochemistry* **29**, 733-737.
- Jiang, Y., Morley, K.L., Schrag, J.D., and Kazlauskas, R.J.** (2011). Different active-site loop orientation in serine hydrolases versus acyltransferases. *ChemBioChem* **12**(5), 768-776.
- Kandel, S., Sauveplane, V., Compagnon, V., Franke, R., Millet, Y., Schreiber, L., Werck-Reichhart, D., and Pinot, F.** (2007). Characterization of a methyl jasmonate and wounding responsive cytochrome P450 of *Arabidopsis thaliana* catalyzing dicarboxylic fatty acid formation in vitro. *The FEBS Journal* **274**, 5116-5127.
- Kolattukudy, P.E.** (1980). Biopolyester membranes of plants: cutin and suberin. *Science* **208**, 990-1000.
- Kolattukudy, P.E.** (1981). Structure, biosynthesis, and biodegradation of cutin and suberin. *Annual Review of Plant Physiology* **32**, 539-567.
- Kolattukudy, P.E. and Agrawal, V.P.** (1974). Structure and composition of aliphatic constituents of potato tuber skin (suberin). *Lipids* **9**(9), 682-691.
- Kolattukudy, P.E., and Dean, B.B.** (1974) Structure, gas chromatographic measurement, and function of suberin synthesized by potato tuber tissue slices. *Plant Physiology* **54**(1), 116-121.
- Kolattukudy, P.E. and Soliday, C.L.** (1985). Effects of stress on the defensive barriers of plants. In *UCLA symposia on molecular and cellular biology (USA)*.
- Kosma, D.K., Molina, I., Ohlrogge, J.B. and Pollard, M.** (2012). Identification of an *Arabidopsis* fatty alcohol:caffeoyl-Coenzyme A acyltransferase required for the synthesis of alkyl hydroxycinnamates in root waxes. *Plant Physiology* **160**, 237-248.
- Kosma, D.K., Murmu, J., Razeq, F.M., Santos, P., Bourgault, R., Molina, I. and Rowland, O.** (2014). AtMYB41 activates ectopic suberin synthesis and assembly in multiple plant species and cell types. *The Plant Journal* **80**(2), 216-229.

- Knollenberg, B.J., Liu, J., Yu, S., Lin, H. and Tian, L.** (2018). Cloning and functional characterization of a p-coumaroyl quinate/shikimate 3'-hydroxylase from potato (*Solanum tuberosum*). *Biochemical and Biophysical Research Communications* **496**(2), 462-467.
- Kumar, G.N.M., Lulai, E.C., Suttle, J.C., and Knowles, N.R.** (2010). Age-induced loss of wound-healing ability in potato tuber is partly regulated by ABA. *Planta* **232**, 1433-1445.
- Lacey, J.** (1967). Susceptibility of potato tubers to infection by *Phytophthora infestans*. *Annals of Applied Biology* **59**, 257-264.
- Landgraf, R., Smolka, U., Altmann, S., Eschen-Lippold, L., Senning, M., Sonnewald, S., Weigel, B., Frolova, N., Strehmel, N., Hause, G. and Scheel, D.** (2014). The ABC transporter ABCG1 is required for suberin formation in potato tuber periderm. *The Plant Cell* **26**, 3403–3415.
- Larsen, K.** (2004). Molecular cloning and characterization of cDNAs encoding cinnamoyl CoA reductase (CCR) from barley (*Hordeum vulgare*) and potato (*Solanum tuberosum*). *Journal of Plant Physiology* **161**, 105-112.
- Lashbrooke, J.G., Cohen, H., Levy-Samocho, D., Tzfadia, O., Panizel, I., Zeisler, V., Massalha, H., Stern, A., Trainotti, L., Schreiber, L. and Costa, F.** (2016). MYB107 and MYB9 homologs regulate suberin deposition in angiosperms. *The Plant Cell* **28**, 2097-2116.
- Le Bouquin, R., Skrabs, M., Kahn, R., Benveniste, I., Salaün, J.P., Schreiber, L., Durst, F. and Pinot, F.** (2001). CYP94A5, a new cytochrome P450 from *Nicotiana tabacum* is able to catalyze the oxidation of fatty acids to the ω -alcohol and to the corresponding diacid. *European Journal of Biochemistry*, **268**(10), 3083-3090.
- Lee, S.B., Jung, S.J., Go, Y.S., Kim, H.U., Kim, J.K., Cho, H.J., Park, O.K., and Suh, M.C.** (2009). Two *Arabidopsis* 3-ketoacyl CoA synthase genes, *KCS20* and *KCS2/DAISY*, are functionally redundant in cuticular wax and root suberin Biosynthesis, but differentially controlled by osmotic stress. *The Plant Journal* **60**, 462-475.
- Legay, S., Guerriero, G., Deleruelle, A., Lateur, M., Evers, D., André, C.M. and Hausman, J.F.** (2015). Apple russetting as seen through the RNA-seq lens: strong alterations in the exocarp cell wall. *Plant Molecular Biology* **88**(1-2), 21-40.
- Legay, S., Guerriero, G., André, C., Guignard, C., Cocco, E., Charton, S., Boutry, M., Rowland, O. and Hausman, J.F.** (2016). MdMyb93 is a regulator of suberin deposition in russeted apple fruit skins. *New Phytologist*, **212**(4), 977-991.
- Léon, J., Rojo, E., and Sánchez-Serrano, J.J.** (2001). Wound signaling in plants. *Journal of Experimental Botany* **52**, 1-9.
- Lev-Yadun, S.** (2011) Bark in *Encyclopedia of Life Sciences* (London: Nature Publishing Group). Published in print in: 2007. Handbook of Plant Science **1**, ed. K. Roberts (Chichester: John Wiley & Sons, Ltd.), 153-156.

- Li, Y., Beisson, F., Koo, A.J., Molina, I., Pollard, M. and Ohlrogge, J.** (2007). Identification of acyltransferases required for cutin biosynthesis and production of cutin with suberin-like monomers. *Proceedings of the National Academy of Sciences of the United States of America* **104**(46), 18339-18344.
- Lü, S., Song, T., Kosma, D.K., Parsons, E.P., Rowland, O., and Jenks, M.A.** (2009). *Arabidopsis CER8* encodes LONG-CHAIN ACYL-COA SYNTHETASE 1 (LACS1) that has overlapping functions with LACS2 in plant wax and cutin synthesis. *The Plant Journal* **59**, 553-564.
- Lulai, E.C.** (2001). Tuber periderm and disease resistance. In W.R. Stevenson, R. Loria, G.D. Franc and D.P. Weingartner (Eds.), *Compendium of Potato Diseases*, (p. 3). St. Paul, MN, USA: APS Press.
- Lulai, E.C.** (2005). Non-wound-induced suberization of tuber parenchyma cells: A physiological response to the wilt disease pathogen *Verticillium dahliae*. *American Journal of Potato Research*, **82**(6), 433-440.
- Lulai, E.C.** (2007). Skin-set, wound healing, and related defects. In D. Vreugenhill (Ed.), *Potato Biology and Biotechnology* (pp. 471-500). Oxford, UK: Elsevier.
- Lulai, E.C., Campbell, L.G., Fugate, K.K. and McCue, K.F.** (2016). Biological differences that distinguish the 2 major stages of wound healing in potato tubers. *Plant Signaling & Behavior*, **11**(12), p.e1256531.
- Lulai, E.C. and Corsini, D.L.** (1998). Differential deposition of suberin phenolic and aliphatic domains and their roles in resistance to infection during potato tuber (*Solanum tuberosum* L.) wound-healing. *Physiological and Molecular Plant Pathology*, **53**(4), 209-222.
- Lulai, E.C. and Freeman, T.P.** (2001). The importance of phellogen cells and their structural characteristics in susceptibility and resistance to excoriation in immature and mature potato tuber (*Solanum tuberosum* L.) periderm. *Annals of Botany* **88**, 555-561.
- Lulai, E.C., Huckle, L., Neubauer, J.D. and Suttle, J.C.** (2011) Coordinate expression of AOS genes and JA accumulation: JA is not required for initiation of closing layer in wound healing tubers. *Journal of Plant Physiology* **168**, 976-982.
- Lulai, E.C. and Neubauer, J.D.** (2014). Wound-induced suberization genes are differentially expressed, spatially and temporally, during closing layer and wound periderm formation. *Postharvest Biology and Technology* **90**, 24-33.
- Lulai, E.C., Neubauer, J.D. and Suttle, J.C.** (2014). Kinetics and localization of wound-induced DNA biosynthesis in potato tuber. *Journal of plant physiology*, **171**(17), 1571-1575.
- Lulai, E.C., and Suttle, J.C.** (2004). The involvement of ethylene in wound induced suberization of potato tuber (*Solanum tuberosum* L.): a critical assessment. *Postharvest Biology and Technology* **34**, 105-112.
- Lulai, E.C. and Suttle, J.C.** (2009). Signals involved in tuber wound-healing. *Plant Signaling & Behavior*, **4**(7), 620-622.

- Lulai, E.C., Suttle, J.C., and Pederson, S.M.** (2008). Regulatory involvement of abscisic acid in potato tuber wound-healing. *Journal of Experimental Botany* **59**(6), 1175-1186.
- Matzke, K., and Riederer, M.** (1991). A comparative study into the chemical constitution of cutins and suberins from *Picea abies* (L.) Karst., *Quercus robur* L., and *Fagus sylvatica* L. *Planta*, **185**: 233–245.
- Marques, A., and Pereira, H.** (1987). On the determination of suberin and other structural components in cork from *Quercus suber* L. *Anais do Instituto Superior de Agronomia* **42**, 321-335.
- Mauch-Mani, B. and Mauch, F.** (2005). The role of abscisic acid in plant–pathogen interactions. *Current Opinion in Plant Biology* **8**(4), 409-414.
- Meyer, K., Cusumano, J.C., Somerville, C. and Chapple, C.C.** (1996). Ferulate-5-hydroxylase from *Arabidopsis thaliana* defines a new family of cytochrome P450-dependent monooxygenases. *Proceedings of the National Academy of Sciences of the United States of America* **93**(14), 6869-6874.
- Mellway, R.D., Tran, L.T., Prouse, M.B., Campbell, M.M. and Constabel, C.P.** (2009). The wound-, pathogen-, and ultraviolet B-responsive MYB134 gene encodes an R2R3 MYB transcription factor that regulates proanthocyanidin synthesis in poplar. *Plant Physiology*, **150**(2), 924-941.
- Moire, L., Schmutz, A., Buchala, A., Yan, B., Stark, R.E., and Ryser, U.** (1999). Glycerol is a suberin monomer. New experimental evidence for an old hypothesis. *Plant Physiology* **119**, 1137-1146.
- Molina, I., Li-Beisson, Y., Beisson, F., Ohlrogge, J.B. and Pollard, M.** (2009). Identification of an *Arabidopsis* feruloyl-coenzyme A transferase required for suberin synthesis. *Plant Physiology*, **151**(3), 1317-1328.
- Molina, I.** (2010) Biosynthesis of plant lipid polyesters. In *AOCS Lipid Library* (<https://lipidlibrary.aocs.org/Biochemistry/content.cfm?ItemNumber=40311>).
- Nawrath, C.** (2002). The biopolymers cutin and suberin. *The Arabidopsis Book* **1**, e0021.
- Nawrath, C., Schreiber, L., Franke, R.B., Geldner, N., Reina-Pinto, J.J., and Kunst, L.** (2013). Apoplastic diffusion barriers in *Arabidopsis*. *The Arabidopsis Book* **11**, e0167.
- Negrel, J., Javelle, F., and Paynot, M.** (1993). Wound-induced tyramine hydroxycinnamoyl transferase in potato (*Solanum tuberosum*) tuber discs. *Journal of Plant Physiology* **142**, 518-524.
- Neubauer, J.D., Lulai, E.C., Thompson, A.L., Suttle, J.C. and Bolton, M.D.** (2012). Wounding coordinately induces cell wall protein, cell cycle and pectin methyl esterase genes involved in tuber closing layer and wound periderm development. *Journal of Plant Physiology*, **169**(6), 586-595.
- O'Brien, V.J. and Leach, S.S.** (1983). Investigations into the mode of resistance of potato tubers to *Fusarium roseum* 'Sambucinum'. *American Potato Journal*, **60**(4), 227-233.

- Pereira, H., Rosa, M., and Fortes, M.** (1987). The cellular structure of cork from *Quercus suber* L. *IAWA Journal* **8**(3), 213-213.
- Philippe, G., Gaillard, C., Petit, J., Geneix, N., Dalgalarrodo, M., Bres, C., Mauxion, J.P., Franke, R., Rothan, C., Schreiber, L. and Marion, D.** (2016). Ester-crosslink profiling of the cutin polymer of wild type and cutin synthase tomato (*Solanum lycopersicum* L.) mutants highlights different mechanisms of polymerization. *Plant Physiology* **170**, 807-820.
- Pollard, M., Beisson, F., Li, Y. and Ohlrogge, J.B.** (2008). Building lipid barriers: biosynthesis of cutin and suberin. *Trends in Plant Science* **13**, 236-246.
- Quiroga, M., Guerrero, C., Botella, M.A., Barcelo, A., Amaga, I., Medina, M.I., Alfonso, F.J., de Forchetti, S.M., Tigier, H. and Valpuesta, V.** (2000). A tomato peroxidase involved in the synthesis of lignin and suberin. *Plant Physiology* **122**, 1119-1127.
- Quiroga, M., de Forchetti, S.M., Taleisnik, E. and Tigier, H.A.** (2001). Tomato root peroxidase isoforms: Kinetic studies of the coniferyl alcohol peroxidase activity, immunological properties and role in salt stress. *Journal of Plant Physiology* **158**, 1007-1013.
- Ranathunge, K. and Schreiber, L.** (2011). Water and solute permeabilities of *Arabidopsis* roots in relation to the amount and composition of aliphatic suberin. *Journal of Experimental Botany* **62**(6), 1961-1974.
- Ranathunge, K., Schreiber, L. and Franke, R.** (2011). Suberin research in the genomics era—new interest for an old polymer. *Plant Science* **180**(3), 399-413.
- Razem, F.A., and Bernards, M.A.** (2002). Hydrogen peroxide is required for poly(phenolic) domain formation during wound induced suberization. *Journal of Agricultural and Food Chemistry* **50**, 1009-1015.
- Razem, F.A. and Bernards, M.A.** (2003). Reactive oxygen species production in association with suberization: Evidence for an NADPH-dependent oxidase. *Journal of Experimental Botany* **54**, 935-941.
- Riley, R.G. and Kolattukudy, P.** (1975). Evidence for covalently attached p-coumaric acid and ferulic acid in cutins and suberins. *Plant Physiology* **56**(5), 650-654.
- Roppolo, D., De Rybel, B., Tendon, V.D., Pfister, A., Alassimone, J., Vermeer, J.E., Yamazaki, M., Stierhof, Y.D., Beeckman, T. and Geldner, N.** (2011) A novel protein family mediates Casparian strip formation in the endodermis. *Nature* **473**(7347), 380-383.
- Roppolo, D., Boeckmann, B., Pfister, A., Boutet, E., Rubio, M.C., Dénervaud-Tendon, V., Vermeer, J.E., Gheyselinck, J., Xenarios, I. and Geldner, N.** (2014). Functional and evolutionary analysis of the CASPARIAN STRIP MEMBRANE DOMAIN PROTEIN family. *Plant Physiology* **165**(4), 1709-1722.
- Rosenstock, G. and Kahl, G.** (1978). In G. Kahl (Ed.), *Biochemistry of Wounded Plant Tissues* (p. 623), Berlin, New York: Walter de Gruyter & Co.

- Samuels, L., Kunst, L., and Jetter, R.** (2008). Sealing plant surfaces: cuticular wax formation by epidermal cells. *Annual Review of Plant Biology* **59**, 683-707.
- Sanderman, G., Boger, P.** (1989). Inhibition of carotenoid biosynthesis by herbicides. In P. Boger, G. Sanderman (Eds.), *Target Sites of Herbicide Action* (pp. 25-44). Boca Raton, FL: CRC Press.
- Schmutz, A., Jenny, T. and Ryser, U.** (1994). A caffeoyl-fatty acid-glycerol ester from wax associated with green cotton fibre suberin. *Phytochemistry*, **36**(6), 1343-1346.
- Schneider, K., Hövel, K., Witzel, K., Hamberger, B., Schomburg, D., Kombrink, E. and Stuible, H.-P.** (2003). The substrate specificity-determining amino acid code of 4-coumarate:CoA ligase. *Proceedings of the National Academy of Sciences of the United States of America* **100**, 8601-8606.
- Schnurr, J., Shockey, J., Browse, J.** (2004). The acyl-CoA synthetase encoded by *LACS2* is essential for normal cuticle development in *Arabidopsis*. *Plant Cell* **16**, 629-642.
- Schoch, G., Goepfert, S., Morant, M., Hehn, A., Meyer, D., Ullmann, P. and Werck-Reichhart, D.** (2001). CYP98A3 from *Arabidopsis thaliana* is a 3'-hydroxylase of phenolic esters, a missing link in the phenylpropanoid pathway. *Journal of Biological Chemistry* **276**(39), 36566-36574.
- Schreiber, L.** (2010) Transport barriers made of cutin, suberin and associated waxes. *Trends in Plant Science* **15**, 546-553.
- Schreiber, L., Franke, R., and Hartmann, K.** (2005a) Effects of NO₃ deficiency and NaCl stress on suberin deposition in rhizo- and hypodermal (RHCW) and endodermal cell walls (ECW) of castor bean (*Ricinus communis* L.) roots. *Plant Soil* **269**, 333-339.
- Schreiber, L., Franke, R., and Hartmann, K.** (2005b) Wax and suberin development of native and wound periderm of potato (*Solanum tuberosum* L.) and its relation to peridermal transpiration. *Planta* **220**, 520-530.
- Schreiber, L., Hartmann, K., Skabs, M., and Zeier, J.** (1999). Apoplastic barriers in roots: chemical composition of endodermal and hypodermal cell walls. *Journal of Experimental Botany* **50**, 1267-1280.
- Serra, O., Soler, M., Hohn, C., Franke, R., Schreiber, L., Prat, S., Molinas, M., and Figueras, M.** (2009a). Silencing of StKCS6 in potato periderm leads to reduced chain lengths of suberin and wax compounds and increased peridermal transpiration. *Journal of Experimental Botany* **60**, 697-707.
- Serra, O., Soler, M., Hohn, C., Sauveplane, V., Pinot, F., Franke, R., Schreiber, L., Prat, S., Molinas, M., and Figueras, M.** (2009b). *CYP86A33*-targeted gene silencing in potato tuber alters suberin composition, distorts suberin lamellae, and impairs the periderm's water barrier function. *Plant Physiology* **149**, 1050-1060.
- Serra, O., Hohn, C., Franke, R., Prat, S., Molinas, M., and Figueras, M.** (2010). A feruloyl transferase involved in the biosynthesis of suberin and suberin-associated

wax is required for maturation and sealing properties of potato periderm. *The Plant Journal* **62**, 277-290.

- Shiono, K., Ando, M., Nishiuchi, S., Takahashi, H., Watanabe, K., Nakamura, M., Matsuo, Y., Yasuno, N., Yamanouchi, U., Fujimoto, M. and Takanashi, H.** (2014). RCN1/OsABCG5, an ATP-binding cassette (ABC) transporter, is required for hypodermal suberization of roots in rice (*Oryza sativa*). *The Plant Journal* **80**(1), 40-51.
- Silva, S., Sabino, M., Fernandes, E., Correlo, V., Boesel, L., and Reis, R.** (2005). Cork: properties, capabilities and applications. *International Materials Reviews* **50**, 345-365
- Soler, M., Serra, O., Molinas, M., Huguet, G., Fluch, S. and Figueras, M.** (2007). A genomic approach to suberin biosynthesis and cork differentiation. *Plant Physiology*, **144**(1), 419-431.
- Soliday, C.L., Dean, B.B., and Kolattukudy, P.E.** (1978). Suberization: inhibition by washing and stimulation by abscisic acid in potato disks and tissue culture. *Plant Physiology* **61**, 170-174.
- Soliday, C.L., Kolattukudy, P.E., and Davis, R.W.** (1979). Chemical and ultrastructural evidence that waxes associated with the suberin polymer constitute the major diffusion barrier to water vapor in potato tuber (*Solanum tuberosum* L.). *Planta* **146**, 607-614.
- Suttle, J.C., and Hultstrand, J.F.** (1994). Role of endogenous abscisic acid in potato microtuber dormancy. *Plant Physiology* **105**, 891-896.
- Suttle, J.C., Lulai, E.C., Huckle, L.L. and Neubauer, J.C.** (2013). Wounding of potato tubers induces increases in ABA biosynthesis and catabolism and alters expression of ABA metabolic genes. *Journal of Plant Physiology* **170**, 560-566.
- Thomas, R., Fang, X., Ranathunge, K., Anderson, T.R., Peterson, C.A. and Bernards, M.A.** (2007). Soybean root suberin: Anatomical distribution, chemical composition and relationship to partial resistance to *Phytophthora sojae*. *Plant Physiology* **144**(1), 299-311.
- Thomson, N., Evert, R.F. and Kelman, A.** (1995). Wound-healing in whole potato tubers: a cytochemical, fluorescence, and ultrastructural analysis of cut and bruise wounds. *Canadian Journal of Botany* **73**(9), 1436-1450.
- Tijet, N., Helvig, C., Pinot, F., Le Bouquin, R., Lesot, A., Durst, F., Salaün, J.P. and Benveniste, I.** (1998). Functional expression in yeast and characterization of a clofibrate-inducible plant cytochrome P-450 (CYP94A1) involved in cutin monomers synthesis. *Biochemical Journal*, **332**(2), 583-589.
- Tuteja, N.** (2007). Abscisic acid and abiotic stress signaling. *Plant Signaling & Behavior* **2**(3), 135-138.
- Vandeleur, R.K., Mayo, G., Sheldon, M.C., Gillham, M., Kaiser, B.N., and Tyerman, S.D.** (2009). The role of plasma membrane intrinsic protein aquaporins in water transport through roots: diurnal and drought stress responses reveal different

- strategies between isohydric and anisohydric cultivars of grapevine. *Plant Physiology* **149**, 445-460.
- Vaughn, S.F., and Lulai, E.C.** (1991). The involvement of mechanical barriers in the resistance response of a field-resistant and a field-susceptible potato cultivar to *Verticillium dahliae*. *Physiological and Molecular Plant Pathology* **38**, 455-465.
- Verdager, R., Soler, M., Serra, O., Garrote, A., Fernández, S., Company-Arumí, D., Anticó, E., Molinas, M. and Figueras, M.** (2016). Silencing of the potato *StNAC103* gene enhances the accumulation of suberin polyester and associated wax in tuber skin. *Journal of Experimental Botany* **67**(18), 5415-5427.
- Vishwanath, S.J., Delude, C., Domergue, F. and Rowland, O.** (2015). Suberin: biosynthesis, regulation, and polymer assembly of a protective extracellular barrier. *Plant Cell Reports* **34**, 573-586.
- Vishwanath, S.J., Kosma, D.K., Pulsifer, I.P., Scandola, S., Pascal, S., Joubes, J., Dittrich-Domergue, F., Lessire, R., Rowland, O., and Domergue, F.** (2013). Suberin-associated fatty alcohols in *Arabidopsis thaliana*: distributions in roots and contributions to seed coat barrier properties. *Plant Physiology* **163**, 1118-1132.
- Vulavala, V.K., Fogelman, E., Rozenal, L., Faigenboim, A., Tanami, Z., Shoseyov, O. and Ginzberg, I.** (2017). Identification of genes related to skin development in potato. *Plant Molecular Biology* **94**(4-5), 481-494.
- Wang-Pruski, G. and Cantle, S.E.** (2004) Cloning and expression of cinnamic acid 4-hydroxylase in potato, a gene related to after-cooking darkening. *Acta Physiologiae Plantarum* **26**, 60-61.
- Waters, E.R.** (2003). Molecular adaptation and the origin of land plants. *Molecular Phylogenetics and Evolution* **29**, 456-463.
- Wilson, C.A. and Peterson, C.A.** (1983). Chemical composition of the epidermal, hypodermal, endodermal and intervening cortical cells walls of various plant roots. *Annals of Botany* **51**, 759-769.
- Yadav, V., Molina, I., Ranathunge, K., Castillo, I.Q., Rothstein, S.J. and Reed, J.W.** (2014). ABCG transporters are required for suberin and pollen wall extracellular barriers in *Arabidopsis*. *The Plant Cell* **26**(9), 3569-3588.
- Yang, W.L. and Bernards, M.A.** (2007). Metabolite profiling of potato (*Solanum tuberosum* L.) tubers during wound-induced suberization. *Metabolomics* **3**(2), 147-159.
- Yang, W., Simpson, J.P., Li-Beisson, Y., Beisson, F., Pollard, M.R. and Ohlrogge, J.B.** (2012). A land-plant-specific glycerol-3-phosphate acyltransferase family in *Arabidopsis*: substrate specificity, sn-2 preference and evolution. *Plant Physiology* **160**(2), 638-652.
- Yeats, T.H., Huang, W., Chatterjee, S., Viart, H.M.F., Clausen, M.H., Stark, R.E. and Rose, J.K.** (2014). Tomato Cutin Deficient 1 (CD1) and putative orthologs

comprise an ancient family of cutin synthase-like (CUS) proteins that are conserved among land plants. *The Plant Journal* **77**(5), 667-675.

- Yeats, T.H., Martin, L.B.B., Viart, H.M.F., Isaacson, T., He, Y., Zhao, L., Matas, A.J., Buda, G.J., Domozych, D.S., Clausen, M.H. and Rose, J.K.C.** (2012). The identification of cutin synthase: formation of the plant polyester cutin. *Nature Chemical Biology* **8**(7), 609-611.
- Yeats, T.H. and Rose, J.K.C.** (2013). The formation and function of plant cuticles. *Plant Physiology* **163**(1), 5-20.
- Yogendra, K.N., Kumar, A., Sarkar, K., Li, Y., Pushpa, D., Mosa, K.A., Duggavathi, R., and Kushalappa, A.C.** (2015). Transcription factor *StWRKY1* regulates phenylpropanoid metabolites conferring late blight resistance in potato. *Journal of Experimental Botany* **66**(22), 7377-7389.
- Yogendra, K.N., Pushpa, D., Mosa, K.A., Kushalappa, A.C., Murphy, A., and Mosquera, T.** (2014). Quantitative resistance in potato leaves to late blight associated with induced hydroxycinnamic acid amides. *Functional & Integrative Genomics* **14**, 285-298.
- Zeier, J., Ruel, K., Ryser, U., and Schreiber, L.** (1999). Chemical analysis and immunolocalization of lignin and suberin in the endodermal and hypodermal/rhizodermal cell walls of developing maize (*Zea mays* L.) primary roots. *Planta* **209**, 1-21.
- Zeier, J. and Schreiber, L.** (1998). Comparative investigation of primary and tertiary endodermal cell walls isolated from the roots of five monocotyledoneous species: chemical composition in relation to fine structure. *Planta* **206**(3), 349-361.
- Zheng, H., Rowland, O. and Kunst, L.** (2005). Disruptions of the *Arabidopsis* enoyl-CoA reductase gene reveal an essential role for very-long-chain fatty acid synthesis in cell expansion during plant morphogenesis. *The Plant Cell* **17**(5), 1467-1481.

Chapter 2

2 Differential induction of polar and non-polar metabolism during wound-induced suberization in potato (*Solanum tuberosum* L.) tubers

A version of this chapter was published in *The Plant Journal* (Woolfson, K.N., Haggitt, M.L., Zhang, Y., Kachura, A., Bjelica, A., Rey Rincon, M.A., Kaberi, K.M. and Bernards, M.A. (2018) Differential induction of polar and non-polar metabolism during wound-induced suberization in potato (*Solanum tuberosum* L.) tubers. *The Plant Journal*, 93(5), 931-942).

2.1 Introduction

In response to a wounding event, the cells surrounding a wound site synthesize and deposit the biopolymer suberin. The main functions of suberin are to seal the tissue at the wound site, and provide protection from water loss and invading pathogens (e.g., Esau, 1977). The regulation of wound-induced suberin biosynthesis and deposition has been difficult to investigate due to the complexity of the biopolymer itself and the variety of physiological and metabolic processes activated upon wounding. Nevertheless, it is clear that suberization requires the coordination of two major plant metabolic pathways: phenylpropanoid biosynthesis and fatty acid biosynthesis, which yield phenolic and aliphatic monomers, respectively. These are polymerized *in situ* to form a poly aliphatic polymer (suberin) and its associated poly(phenolic) domain (reviewed in Bernards, 2002; Graça and Santos, 2007; Ranathunge et al., 2011; Beisson et al., 2012; Vishwanath et al., 2015; Graça, 2015). In potato, the phenolic monomers include hydroxycinnamyl alcohols (monolignols), hydroxycinnamic acids, amides and esters, while the aliphatic monomers consist of very long chain fatty acids, 1-alkanols, ω -hydroxy fatty acids and α,ω -dioic acids. Once at the site of incorporation, phenolics are thought to be cross-linked within the cell wall via an oxidative free-radical coupling process (Razem and Bernards, 2002; Arrieta-Baez and Stark, 2006), while aliphatic monomers may be esterified together or through glycerol linkers to create an insoluble matrix (insolubles) (Beisson et al., 2007; Yang et al., 2010, 2012, 2016), or remain as un-linked waxes (solubles) associated with

the polymer (reviewed in Li-Beisson et al., 2013; Graça et al., 2015; Vishwanath et al., 2015). While the precise macromolecular structure of suberin is not known, one common feature of suberized tissues is the presence of both phenolic and aliphatic polymeric domains within the same cells. There is considerable evidence that the poly(phenolic) and poly(aliphatic) domains are distinct (e.g., Mattinen et al., 2009), but cross-linked (Stark and Garbow, 1992; Yan and Stark, 1998).

Wound-induced suberization involves two stages, progressing through the formation of a “closing layer” to the development of the wound periderm (Lulai and Neubauer, 2014). The closing layer is formed during the first seven days post-wounding in parenchyma cells surrounding the wound site. Over the next 40 days, the wound periderm is formed from newly developed meristematic tissue (the phellogen), resulting in ordered files of suberized phellem cells that provide a more substantial and long-term protective barrier (Lulai and Neubauer, 2014). Throughout this process, suberin biosynthesis and deposition requires both spatial and temporal regulation of individual genes as well as entire biosynthetic pathways.

In the context of potato aliphatic suberin biosynthesis, exogenous ABA has been shown to play a role in the up-regulation of 18:1 ω -hydroxy fatty acid and α,ω -dioic acid biosynthesis, as well as impact the function of the suberin barrier in potato tubers as measured by the resistance of water vapour diffusion through wound-healed surface tissue (Soliday et al., 1978; Cottle and Kolattukudy, 1982). More recently, Lulai et al., (2008) treated wound-healing potato tubers with ABA as well as fluridone (FD), a phytoene desaturase inhibitor (Gamble and Mullet, 1986) that blocks the production of precursors of ABA biosynthesis. Using qualitative measures (intensity of histochemical staining), FD inhibition of ABA biosynthesis was shown to result in a decrease in the accumulation of aliphatic components as well as an increase in the amount of water loss post-wounding (Lulai et al., 2008). However, the impact on phenolic metabolism was less clear, and resulted in only a relatively small attenuation in the induction of phenylalanine ammonia-lyase (StPAL1) enzyme activity (Lulai et al., 2008; Kumar et al., 2010). *In silico* analysis of the approx. 1.7 kb upstream promoter region of *StCYP86A33*, which encodes a fatty acid ω -hydroxylase required for aliphatic metabolism (Serra et al., 2009a;

Bjelica et al., 2016), uncovered 41 putative ABA-like responsive elements relative to only a few other hormone-related promoter motifs (Bjelica et al., 2016). The prevalence of ABA-related motifs in the *StCYP86A33* promoter further supports the role of ABA in regulating aliphatic suberin monomer biosynthesis. Similarly, a recent investigation into the interplay between ABA and salicylic acid on the expression of feruloyl transferase (FHT) in potato also supported a role for ABA in the regulation of aliphatic suberin biosynthesis (Boher et al., 2013). In Arabidopsis, ABA has also been shown to affect suberin biosynthesis and deposition. For example, Efetova et al. (2007) demonstrated a role for ABA in drought-induced stress protection. Similarly, Barberon et al. (2016) demonstrated a role for ABA in the developmental deposition of Arabidopsis root suberin, and provided evidence for interference in the process by ethylene.

The recently sequenced *Solanum tuberosum* (group Phureja) genome (Xu et al., 2011), has facilitated the identification of many key suberin-associated genes in potato, some of which have now been functionally characterized (reviewed in Vishwanath et al., 2015). Coupled with the ability to accurately identify and quantify aliphatic suberin monomers, the goals of the present research were two-fold: (1) to investigate the involvement of ABA in the expression of a broad range of suberin-associated genes in potato and (2) to relate gene expression to changes in phenolic and aliphatic metabolism, during wound-induced suberin biosynthesis and deposition.

2.2 Materials and Methods

2.2.1 Tissue preparation

Four and eight month old potato (*Solanum tuberosum* cv. Russet Burbank) tubers were washed, surface sterilized with 20% v/v bleach for 20 minutes, transferred to a laminar flow cabinet, and left to air dry overnight. Tubers were sectioned into 1-2 cm thick slices, and subdivided into four treatments: (1) dH₂O-washed control, (2) 10⁻⁴ M FD, (3) 10⁻⁴ M ABA (four month old tubers only) and (4) 10⁻⁴ M FD with 10⁻⁴ M ABA. Treatment concentrations were the same as reported previously (Soliday et al., 1978; Cottle and

Kolattukudy, 1982; Lulai et al., 2008). Tuber slices were incubated for 4 hours in 1 L of treatment solution, with occasional mixing, at room temperature in a laminar flow cabinet. FD and ABA (each at 100 mM) were dissolved in dimethyl sulfoxide (DMSO) and diluted with dH₂O to the final concentration (10⁻⁴ M). DMSO was added to 0.1% v/v in the dH₂O treatment. Tuber slices were subsequently rinsed with sterile dH₂O and placed upright in sterile Magenta® boxes on an elevated mesh platform covering a wetted No.1 Whatman paper (to maintain a high humidity environment). All treatments were incubated in the dark at 28°C for one to six days; with day zero samples collected immediately after treatment (at four hours post-wounding).

To harvest tissue, tuber slices were sampled perpendicular to the cut faces with a No. 9 copper cork borer (VWR International) to yield cylinders. Using a razor blade, the top and bottom tissue of the resulting tuber cylinders were quickly excised to create approx. 1 mm thick tuber discs. For each time-point, tuber discs from the same Magenta® box were pooled to create one sample. All harvested tissue was quickly flash frozen and ground by mortar and pestle into a fine powder in liquid N₂, then stored at -80°C (for RNA analysis) or -20°C (for metabolite and suberin analysis). Frozen tissue (for each treatment and timepoint) was subdivided for polar metabolite analysis, aliphatic suberin monomer composition analysis and RNA extraction. The entire time course experiment was independently replicated three times using four month old tubers (n=3), with three technical replicates per experiment for RT-qPCR, and twice with eight-month old tubers (n=2) with three technical replicates per experiment for chemical analysis, but pooled tissue (1 technical replicate per experiment) used for RT-qPCR.

2.2.2 Polar metabolite analysis

Approximately 100 mg of each sample was extracted using MeOH-methyltertbutyl ether-water (1:3:1), with a modified protocol adapted from Giavalisco et al. (2011). Briefly, with sample tubes kept on ice, 500 µL of cold (-20°C) 50% v/v MeOH containing 0.05 mg/mL anthracene-9-COOH (C₁₅H₁₀O₂; Exact Mass= 222.068085; [M+H]⁺ = 223.0685 m/z) as a polar phase internal standard (Cuthbertson et al., 2013) was added to each sample, followed by the addition of 750 µL of cold (-20°C) methyltertbutyl ether

(MtBE). Tubes were thoroughly vortexed then placed on a rotating mixer in the cold room (5°C) for 30 minutes. Samples were subsequently placed in a sonicating bath for 15 minutes in the cold room prior to their centrifugation in a bench top microcentrifuge for 10 minutes. In order to recover polar compounds, 400 µL of the MeOH-H₂O phase was transferred to a clean microcentrifuge tube, diluted with 800 µL dH₂O and re-centrifuged. The supernatant from each sample was then transferred to a screw cap chromatography vial and analyzed by LCMS in positive ion mode using a protocol based on Landgraf et al. (2014).

Chromatographic separations were performed on an Agilent 1260 LC system (Agilent Technologies) equipped with a C-18 column (Eclipse Plus RRHT, 2.1 x 50 mm, 1.8 µm; Agilent Technologies) by applying the following gradient at a flow rate of 0.25 mL min⁻¹, after a sample injection of 2 µL: 0 to 2 minutes, 100% A (0.1% v/v formic acid in Milli-Q H₂O); 12 minutes, 70% A, 30% B (0.1% v/v formic acid in acetonitrile- H₂O [9:1]); 17 minutes, 100% B; hold at 100% B for 4 minutes. A 9 minute post-run equilibration was completed at 100% A. ESI-TOF parameters: drying gas at 350°C, 10 mL/min; nebulizer at 45 PSI; Vcap at 4000 V; Fragmentor at 130 V. Spectra were collected at 1.03/sec (9729 transients/spectrum) in the 100-1700 m/z range. Reference mass solution (121.050873 m/z and 922.009798 m/z) was infused constantly via a second nebulizer at 15 psi. ABA and fluridone were measured by mining the data for the appropriate ABA and FD mass ([M+H]⁺) signals at 265.1539 and 330.1121 m/z, respectively. Peak areas were obtained using Agilent Mass Hunter Qualitative Analysis software (VB05) (Agilent Technologies, USA).

2.2.3 Aliphatic suberin monomer biosynthesis

Samples were ground to a fine powder in liquid N₂ with a mortar and pestle, transferred to pre-weighed cellulose filter paper squares (Whatman Ltd., England), rolled into cylinders and extracted in a micro-soxhlet extractor using 50 mL of 2:1 chloroform:MeOH over 3 hours (twice), followed by an overnight extraction using 50 mL of chloroform. Soluble extracts were retained, pooled and dried under vacuum in a round-bottom flask using a rotary evaporator (Büchi, Switzerland). Extractive-free

residues were dried at room temperature and weighed into sub-samples ranging from 5-15 mg of tissue. Soluble extractives and extractive-free residues were prepared for GC analysis as described (Meyer et al., 2011).

2.2.4 RNA isolation, cDNA synthesis and gene expression analysis

Total RNA was isolated as described by Chang et al. (1993) from the flash-frozen tuber tissue. RNA was quantified spectrophotometrically using a NanoDrop model ND-2000c Spectrophotometer set for RNA determination (Thermo-Scientific). The quality of total RNA was determined by the ratio of absorbance at 260/280 nm (>1.8). Qualitative assessment of RNA was performed with an Agilent 2100 Bioanalyzer (RIN \geq 7). RNA (0.5 $\mu\text{g}/\mu\text{L}$) was treated with DNase I (Invitrogen), and cDNA synthesis performed with SuperScript II/RNaseOUT (Invitrogen) according to the manufacturer's instructions. RNA from three independent tuber-wounding experiments was used to produce three replicates of 24 cDNA templates (tissue collection on days 0, 1, 2, 3, 4 & 6 from the 4 treatments). Quantitative reverse transcription PCR (RT-qPCR) was performed using a Bio-Rad CFX Connect system. Amplification of genes of interest and endogenous controls *EF1- α* and *APRT* (Nicot et al., 2005) from 47.6 ng cDNA template were performed using sequence-specific primers (**Table 2.1**) and iTaq Universal SYBR Green Supermix (Bio-Rad), according to the manufacturer's protocol. A standard curve was performed in duplicate using pooled cDNA templates, with a dilution range from 381 to 0.61 ng, to determine PCR reaction efficiency. The reaction efficiency (E) of each primer pair was calculated from the slope of the standard curve linear regression where $E = 10(-1/\text{slope})$ and percent efficiency, $E\% = (E - 1) \times 100\%$ (Pfaffl, 2001). Expected RT-qPCR product lengths of all 14 genes were visualized by agarose gel electrophoresis. Each product's corresponding gel band was extracted and its nucleotide sequence confirmed (Robarts Research Institute DNA Sequencing, London, ON). RT-qPCR specificity was confirmed by melt curve analysis and gene expression data were processed using Bio-Rad CFX manager version 3.1 software according to the manufacturer's directions to yield $\Delta\Delta\text{Cq}$ values, based on the Pfaffl (2001) and Vandesompele et al. (2002) methods. Each set of 24 cDNA templates was used for RT-qPCR reactions with each primer pair,

using *EF1- α* and *APRT* as endogenous references (Nicot et al., 2005) for normalization of relative expression (Vandesompele et al., 2002). The calculated expression levels were corrected for PCR reaction efficiency.

2.2.5 Data analysis

Polar metabolite data (Agilent *.d files) were exported as *.mzData files for import into mzMine (V 2.14.2) (Pluskal et al., 2010) and molecular feature extraction and alignment. Broad molecular feature tolerance parameters ($m/z \pm 0.005$; $RT \pm 0.5$ min) were used to compensate for potential retention time and m/z drift across samples. After chromatogram deconvolution and alignment, data were normalized to the internal standard (anthracene-9-carboxylic acid), and exported as a *.csv aligned peak list. The data for each replicate were aligned separately, combined into one dataset, and manually re-aligned to retain features found consistently within treatments across all three replicates. After further normalization based on the mass of tissue extracted, the data were imported into SIMCA-P V14.0 (Umetrics). PLS-DA analyses were performed in SIMCA-P using default parameter settings.

Data analysis of aliphatic suberin monomers combined GC-MS for aliphatic monomer identification and GC-FID to quantify the compounds of interest. Data were normalized to the internal standard (triacontane), and subsequently, tissue surface area. Statistical analysis of soluble and insoluble aliphatic suberin monomer datasets was done using R. A two-way Analysis of Variance (ANOVA) for total aliphatics was performed using treatment (water, FD, ABA, FD + ABA) and time (days: 0, 1, 2, 3, 4, 6) as factors, with a Tukey HSD post-hoc test. P-values less than 0.05 were reported as statistically significant. Statistical significance between water and other treatments are denoted by different symbols: *, FD; ^, ABA; +, FD + ABA.

For RT-qPCR data, one plate of RT-qPCR reactions used 24 cDNA templates from one experimental replicate in technical triplicates along with no-template controls (to ensure no contamination), and inter-run calibrator samples for each target gene (to detect and correct for variation between targets from different experimental replicates assayed in separate RT-qPCR runs). This was repeated for all three biological replicates of cDNA

templates obtained from tissue from 3 independent experiments. Data were combined across the three replicate plates per gene and adjusted via inter-run calibration to yield means, and endogenous reference genes (*StEF1- α* and *StAPRT*) were used to normalize expression of each target gene as described in §2.2.4.

Gene expression data was log₂-transformed to meet required assumptions for statistical testing before it was plotted and subjected to statistical analyses. Two-way ANOVAs were performed using R for each target gene. If there was a significant interaction between treatment and time, one-way ANOVAs for treatment and/or time were performed as appropriate to isolate the effects of each factor on mRNA levels. Where there was a significant treatment effect, one-way ANOVAs were performed to identify significant differences in log₂ gene expression ($p \leq 0.05$; $|\log_2\text{-fold change}| \geq 1$) between treatments at each time-point. Where there was a significant time effect, one-way ANOVAs were performed using sequential time-point contrasts, followed by Benjamini-Hochberg post-hoc tests. Only cases where $p \leq 0.05$ and the magnitude of change between the compared data points exceeded a 2-fold threshold were considered to be of biological significance (Karlen et al., 2007) (**Table B1**).

2.3 Results

2.3.1 Measurement of ABA in tubers post-wounding

To ensure that FD treatment effectively inhibited *de novo* ABA biosynthesis in tubers, as well as to determine the duration of efficacy, ABA levels were measured in wounded potato tuber tissue collected from each treatment/time point, by extracting the [M+H]⁺ signal at m/z 265.1539 from polar metabolite profiles (**Figure 2.1**). The identification of ABA was verified using a targeted, isotope dilution method (**Figure B1**). In water-treated controls, ABA began to accumulate within two days post wounding, reaching a maximum, sustained level by three days post wounding. By contrast, ABA accumulated significantly slower in FD-treated tissue, remaining less than 50% of control levels until late in the time course (**Figure 2.1**). Exogenous ABA, whether in combination with FD

or not, was readily taken up by the wounded tuber tissue, reaching levels >200% of control four days post-wounding. Importantly, FD was only present in the polar extracts of tissues treated with FD, at all time points, confirming that the compound persisted throughout the analysis period (**Figure B2**).

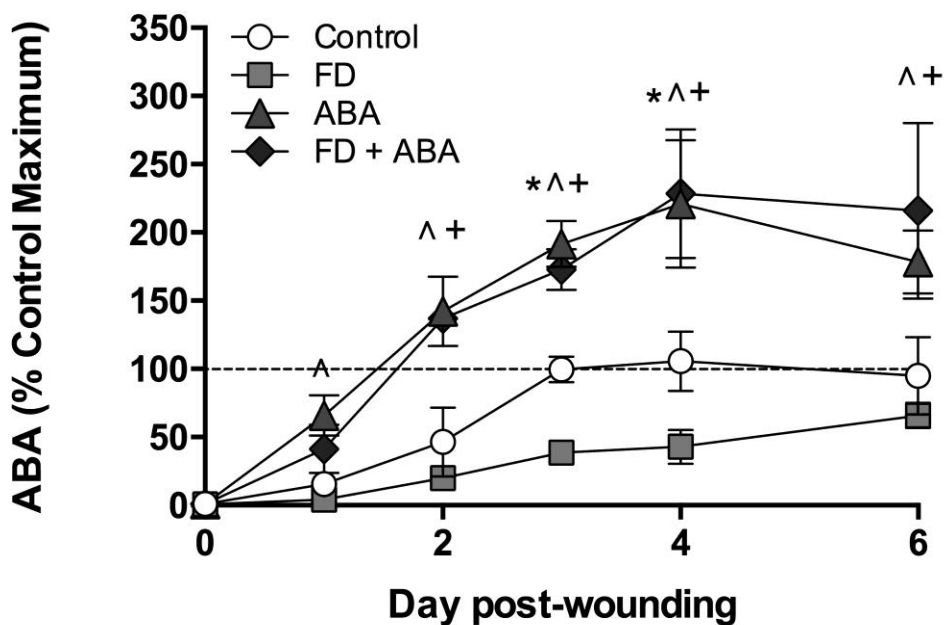


Figure 2.1. Wound-induced changes in abscisic acid (ABA). ABA amounts were estimated from polar extracts prepared from tissue treated with water, fluridone (FD), ABA or FD + ABA by mining the data for the appropriate mass ($[M + H]^+$) signal at 265.1539. Peak areas were obtained using Agilent Mass Hunter Qualitative Analysis software (VB05; Agilent Technologies, USA), and converted into percent values by setting the maximum peak area for control extracts to 100%. Data points marked with different symbols indicate statistically significant differences ($P < 0.05$) between water and FD (*), water and ABA (^), and water and FD + ABA (+). Data points represent the sample mean \pm SD ($n = 3$).

2.3.2 Effect of ABA and FD treatment on suberin-related gene expression

The wound-induced expression of a suite of genes involved in suberin biosynthesis was tracked in independent time course experiments using tubers of two different ages (four months and eight months post-harvest) with similar results. Tubers were treated with water (control), FD, ABA (4 month old tubers only) or FD + ABA. Genes were chosen on the basis of their involvement in phenolic metabolism (phenylalanine ammonia-lyase,

StPAL1; cinnamate-4-hydroxylase, *StC4H*; cinnamoyl-CoA reductase, *StCCR*; and tyramine:hydroxycinnamoyl-CoA hydroxycinnamoyl transferase, *StTHT*), aliphatic metabolism (two fatty acid ω -hydroxylases, *StCYP86A33*, *StCYP86B12*; fatty acyl-CoA reductase, *StFAR3*; and keto-acyl synthase, *StKCS6*), as well as convergent metabolism; i.e., that linking phenolic and aliphatic monomers (fatty acyl:hydroxycinnamoyl-CoA hydroxycinnamoyl transferase, *StFHT*), acyl chains and glycerol (glycerol-3-phosphate acyl transferases, *StGPAT5*, *StGPAT6*), and in the delivery of aliphatic monomers to the site of suberization (ATP-binding cassette transporter, *StABCG1*) (**Table 2.1**).

Representative data from four month old tubers (three replicate experiments) are presented (**Figure 2.2**). Gene expression data for the older tubers is presented as supplemental data (**Figure B3**).

Phenylalanine ammonia-lyase is the entry point enzyme into phenolic metabolism. Treatment of tuber tissue with FD, ABA or a combination of FD + ABA did not alter *StPAL1* gene expression patterns relative to water-treated controls (**Figure 2.2**). That is, *StPAL1* expression was induced within one day of wounding and remained relatively high throughout the time course, and treatment of tissue with FD, ABA or the combination of FD + ABA had no significant effect on this pattern of expression. In contrast, *StC4H*, which encodes the cinnamate-4-hydroxylase that inserts a hydroxyl group in the *para* position of cinnamic acid to form the characteristic “phenolic” functional group, did not show a clear pattern of induced expression, and neither FD, ABA nor FD + ABA treatments altered this result. While neither of these two genes encode enzymes unique to suberin-related poly(phenolic) domain formation, they represent general markers for the induction of phenolic metabolism.

CCR, the gene encoding a cinnamoyl-CoA reductase that is responsible in part for reducing hydroxycinnamic acids to their corresponding alcohols (monolignols), showed an induced expression pattern similar to that of *StPAL1*, in response to wounding (**Figure 2.2**). Monolignols are known to form part of the suberin poly(phenolic) domain (Bernards et al., 1995; Negrel et al., 1996). While FD-treatment did not affect *StCCR* expression, exogenous ABA (whether alone or in combination with FD) led to a significantly earlier expression of this gene. Expression of *StTHT*, the gene that encodes a

tyramine:hydroxycinnamoyl-CoA hydroxycinnamoyl transferase, was significantly up-regulated soon after wounding in both control and FD-treated tubers, but not by ABA or FD + ABA treatments (**Figure 2.2, Table B1**).

In water-treated controls, genes associated with aliphatic metabolism, including *StCYP86A33* (fatty acid ω -hydroxylase), *StCYP86B12* (fatty acid ω -hydroxylase), *StFAR3* (involved in 1-alkanol formation) and *StKCS6* (involved in acyl chain elongation), were induced by two days post-wounding (**Figure 2.2**). FD treatment of tubers resulted in a clear, significant delay in the induction of *StCYP86A33*, *StCYP86B12*, *StFAR3*, and *StKCS6* gene expression, though differences in expression levels between water and FD treatments were non-significant by the end of the time course. By contrast, the application of ABA (with or without FD) to wounded tubers resulted in significantly earlier *StCYP86A33*, *StCYP86B12* and *StFAR3* gene expression relative to water-treated tubers (**Figure 2.2; Table B1**).

Genes involved in convergent metabolism linking phenolic and aliphatic monomers (*StFHT*), acyl chains to glycerol (*StGPAT5*, *StGPAT6*), or in the delivery of aliphatic monomers to the site of suberization (*StABCG1*) all shared the same temporal expression patterns as genes involved in aliphatic metabolism, in response to wounding (**Figure 2.2; water controls**). The application of FD resulted in a significant delay in induced expression of all four of these genes, while the application of ABA (with or without FD) to wounded tubers resulted in significantly earlier *StFHT*, *StGPAT5*, *StGPAT6* and *StABCG1* gene expression relative to water-treated tubers (**Table B1**).

Table 2.1. Gene information and primer sequences used for RT-qPCR analyses of target genes involved in suberin biosynthesis and deposition. Genes were selected due to previous identification and/or characterization in *Solanum tuberosum*, or based on amino acid sequence identity to *Arabidopsis thaliana** or *Solanum lycopersicum** proteins.

Gene	GenBank Accession No.	Predicted function	Primer sequences	Product length (bp)	Efficiency (%)
StPAL1 ^a	X63103.1	Phenylalanine ammonia-lyase	F: CAAACTTGACGCTGATGAAGC R: ACAGGACAATTGATGCCATAACC	131	104.6
StC4H ^b	DQ341174.1	Cinnamic acid 4-hydroxylase	F: ACCAAGAGCATGGACAGCAA R: ATCCTCGTTGATCTCTCCCTTCT	84	101.8
StCCR ^c	AY149608.1	Cinnamoyl CoA reductase	F: GAGCCAGCGGTTATAGGGAC R: TCCACAACCTTTATCCGGGGC	131	110.4
StTHT ^d	AB061243.1	Tyramine hydroxycinnamoyl transferase	F: AGGTATGGCAAATTGCATGGTG R: TGTCTCTTCCTCAATTTTCCCCT	69	109.9
StCYP86A33 ^e	NM_001288290.1	Cytochrome P450 fatty acid ω -hydroxylase	F: GACACGTGGCTCATGCAAAG R: TTGTCGTAGTGTCCGGGTTG	63	99.0
StCYP86B12 ^{f*}	XM_006354906.2	Cytochrome P450 fatty acid ω -hydroxylase	F: TCCACCCCTCACTACCCCAA R: CGTGGGAGTGACAAACCGTA	86	104.6
StFAR3 ^{g*}	XM_006347176.2	Fatty acyl-CoA reductase	F: CCAGTAACGTTTCGCATGTCC R: ACGAAGGGCCATGTATCTGC	147	102.1
StKCS6 ^h	EU616538.1	3-Ketoacyl-CoA synthase	F: AACCGCACAAATCAAGACACCA R: TCTCTGGGATGAACACTGGGT	76	100.8
StGPAT5 ^{i*}	XM_006346646.2	Glycerol-3-phosphate acyltransferase	F: ACCGAACCCTACTTGACCCT R: GCGTCCACTTCTCGAATCCT	142	102.8
StGPAT6 ^{j*}	XM_006362983.2	Glycerol-3-phosphate 2-O-acyltransferase	F: TGGCCAACGTGGTGTACTTT R: CAGCAGTAACAACGGGGTCT	65	109.2
StFHT ^k	NM_001288261.1	Feruloyl transferase	F: TGTGAAGCAAGGAGTGCCAA R: ACCGGCACGGCTATATTCTG	99	107.7
StABCG1 ^l	XM_006345853.2	ATP-binding cassette subfamily G transporter	F: GCTGTAGGCCCTTGTAGGTGG R: CCGGAGAGGAACGTGACAAA	101	108.1
StEF1- α ^m	AB061263.1	Elongation factor 1- α	F: TGGTCGTGTTGAGACTGGTG R: AACATTGTACCCGGGGAGTG	133	100.9
StAPRT ^m	XM_006361995.2	Adenine phosphoribosyltransferase	F: GAACCGGAGCAGGTGAAGAA R: GAAGCAATCCCAGCGATACG	121	99.2

Initial identification and/or functional characterization of potato, tomato and/or Arabidopsis genes by: ^aWang et al. (2008); ^bWang-Pruski & Cante (2004); ^cLarsen (2004); ^dNakane et al. (2003); ^eSerra et al. (2009a); ^f*Compagnon et al. (2009); ^g*Domergue et al. (2010); ^hSerra et al. (2009b); ⁱ*Beisson et al. (2007) and sequence used by ^lLulai & Neubauer (2014); ^j*Li-Beisson et al. (2009); ^kBoher et al. (2013); ^lLandgraf et al. (2014). ^mReference genes selected based on Nicot et al. (2005) analysis.

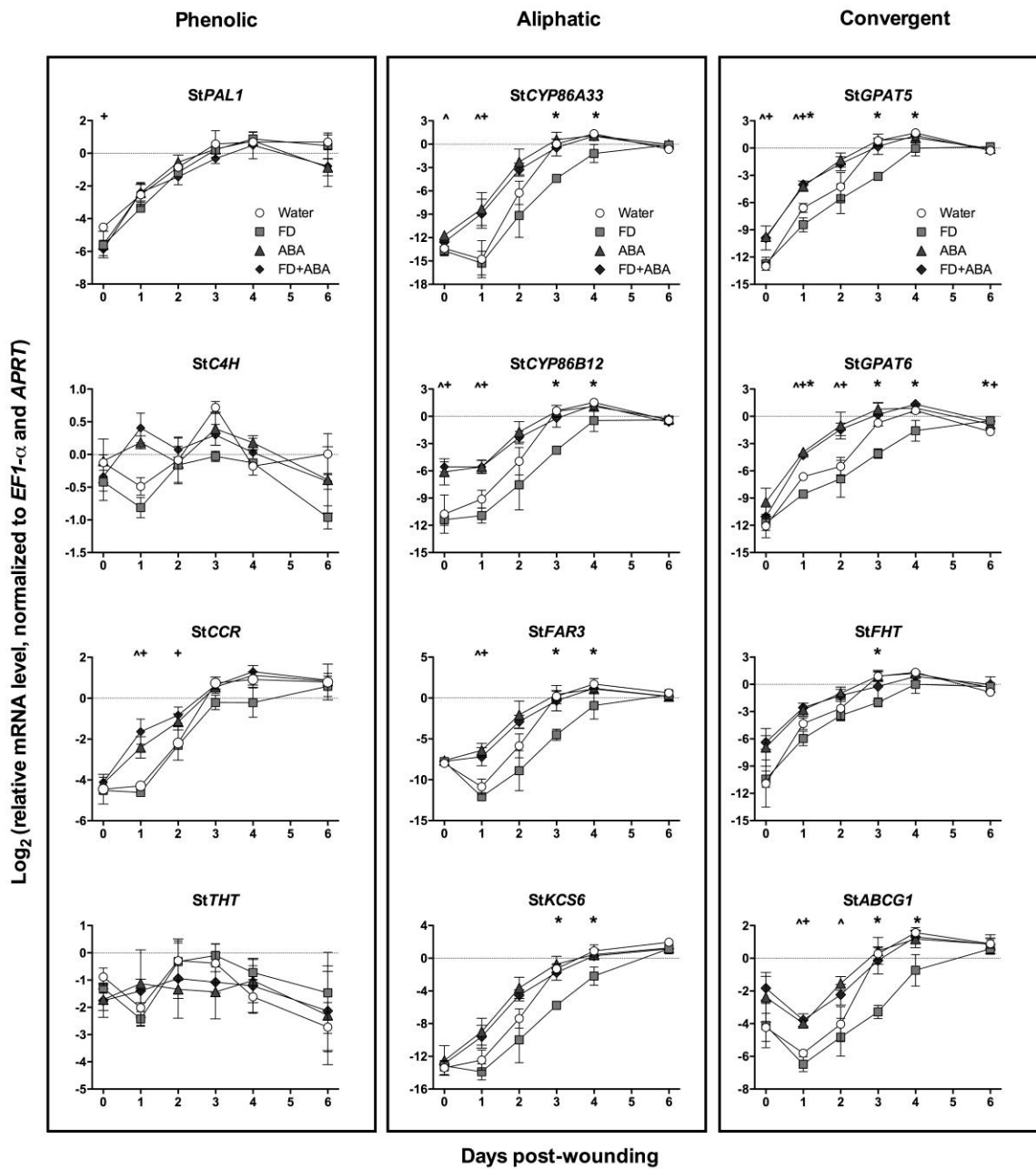


Figure 2.2. Expression of suberin biosynthetic genes after wounding. mRNA levels of phenolic suberin biosynthetic genes (*StPAL1*, *StC4H*, *StCCR* and *StTHT*), aliphatic suberin biosynthetic genes (*StCYP86A33*, *StKCS6*, *StCYP86B12* and *StFAR3*) and genes involved in linkage and deposition (i.e., convergent; *StGPAT5*, *StGPAT6*, *StFHT* and *StABCG1*) (see **Table 2.1**) were measured by RT-qPCR. Gene expression values were normalized to the endogenous reference genes *StEF1- α* and *StAPRT*. One-way ANOVAs were performed to determine significant differences in \log_2 gene expression ($p \leq 0.05$; $|\log_2\text{-fold change}| \geq 1$) at each time-point. Data points marked with different symbols indicate statistically significant differences ($p < 0.05$, and exceeding a 2-fold change) between water and FD (*), water and ABA (^) and, water and FD + ABA (+). Data points represent the sample mean \pm SD (n = 3).

2.3.3 Effect of ABA and FD treatment on polar metabolism

Non-targeted profiling of polar metabolites allowed a direct measure of the impact of FD, ABA and the combined FD + ABA treatments on polar metabolism during wound-healing. Within one day of wounding, there was a clear shift in polar metabolite profiles, regardless of tuber age, which continued until a new steady state profile was achieved by four days post-wounding (**Figure 2.3, Figure B4**). Within these temporal changes there was only a small apparent treatment effect, as the water-, FD-, ABA- and FD + ABA-treated sample profiles clustered together until later time points (e.g., day four, day six) post-wounding, where samples from both ABA-treatments began to separate from the water- and FD-treated ones (**Figure 2.3, Figure B4**). The minimal treatment effect was also evident at the individual compound level, with no clear difference in the profiles of compounds such as L-phe, L-tyr, L-trp, caffeoyl putrescine, dihydrocaffeoyl putrescine, feruloyl putrescine, dihydroferuloyl putrescine, feruloyl octopamine (FO), feruloyl tyramine (FT), chlorogenic acid, FT-FT dimer, FT-FO dimer, α -chaconine, or α -solanine, which could be tentatively identified amongst the polar metabolites, based on their retention time and exact mass (Landgraf et al., 2014; **Figure B5**). Of these, FT, FO and the FT-FT and FT-FO dimers are likely to be destined for the poly(phenolic) domain of suberin (e.g., Negrel et al., 1996), while the other compounds are known soluble compounds from potato.

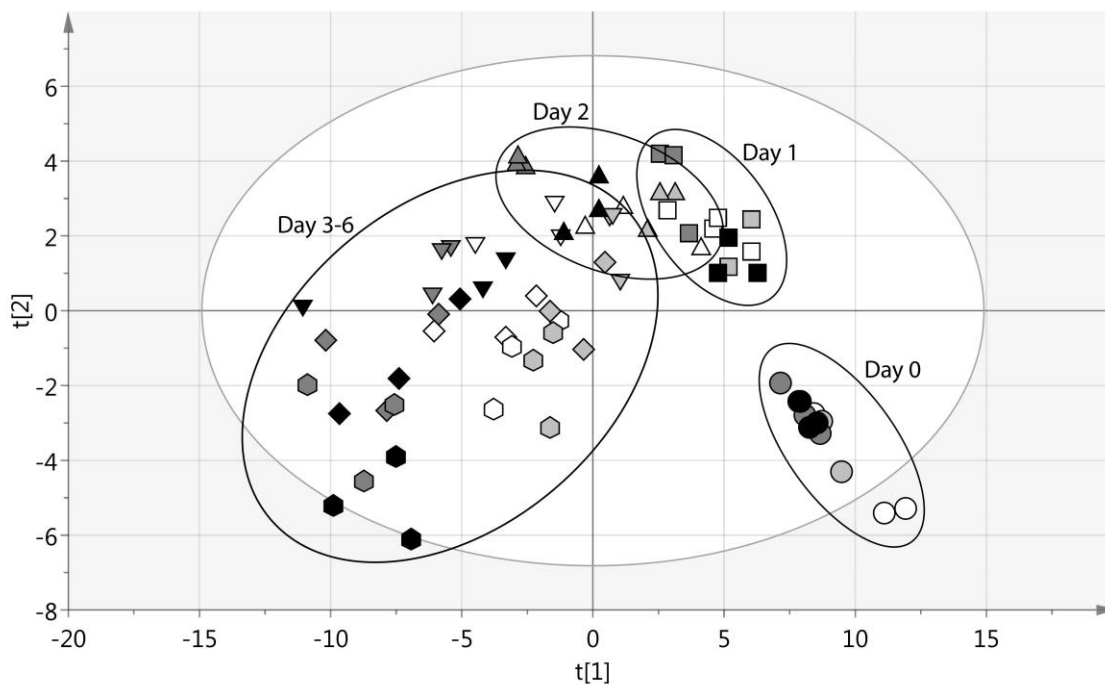


Figure 2.3. Polar metabolite analysis. Polar metabolites were extracted from wound-induced potato tuber discs after treatment with water (open symbols), FD (light grey symbols), ABA (dark grey symbols) or FD + ABA (black symbols) and analyzed by LC-MS. After molecular feature extraction, alignment and normalization, the data were analyzed using SIMCA-P (Umetrics) software. The PLS-DA plot was generated using treatment and time groupings as discriminant factors to help maximize separation between treatments and time points. Each symbol represents a single polar metabolite profile prepared from tissue at 0 days post-wounding (dpw) (circles), 1 dpw (squares), 2 dpw (triangles), 3 dpw (inverted triangles), 4 dpw (diamonds) or 6 dpw (hexagons).

2.3.4 Effect of ABA and FD treatment on aliphatic suberin monomer composition

In the water-treated control tissues, the amount of total soluble aliphatic monomers that could be extracted remained relatively constant across all six days post-wounding regardless of tuber age (**Figure 2.4**). As suberization progressed, insoluble aliphatic monomers continued to accumulate in control tissue, with more total aliphatic suberin being deposited in younger tubers, compared to older ones. These same patterns were observed when total aliphatics were broken down by chain length within each substance class (**Figures B6-9**). FD treatment differentially impacted suberizing tubers, depending on age. In younger tubers, the soluble pools of aliphatic compounds were not significantly different in the FD treatment, relative to the water controls, except for the

day three time point. However, the accumulation of aliphatic monomers in the insoluble (polymerized) fraction in FD-treated tissues was consistently lower than that of water-treated controls, especially after six days, albeit not statistically significant (**Figure 2.4**). This same pattern was evident, and statistically significant, when older tubers were used (**Figure 2.4**).

Treatment of four month old tubers with exogenous ABA, with or without FD, had little effect on the soluble pools of suberin aliphatics (**Figure 2.4**), while treatment of eight month old tubers with a combination of FD and ABA led to a significantly greater accumulation of monomers (**Figure 2.4**). Regardless of tissue age, exogenous ABA, when added in combination with FD, completely “rescued” the tissue from the FD treatment-related effects (i.e., reduced or no poly(aliphatic) suberin deposition) and led to an enhanced aliphatic suberin deposition, especially at later time points (**Figure 2.4**).

Analysis of individual compound classes (fatty acids, 1-alkanols, ω -hydroxy fatty acids, α,ω -dioic acids) (**Figure 2.5**), revealed a similar pattern of soluble aliphatic accumulation in response to the FD and ABA treatments as for the total aliphatics. The FD effect was more pronounced in older tubers (**Figure 2.5**). Remarkably, there was very little accumulation of α,ω -dioic acids in the soluble pools in any treatment group (**Figure 2.5**), despite these compounds accounting for almost half of total aliphatic suberin monomers released upon transesterification (**Figure 2.5**). Overall, FD treatment resulted in little or no accumulation of polymerized aliphatics, especially in older tubers. This reduced accumulation of aliphatic suberin was rescued by exogenous ABA (with or without FD). Importantly, the application of ABA did not alter the timing of suberin aliphatic monomer accumulation relative to water-treated controls.

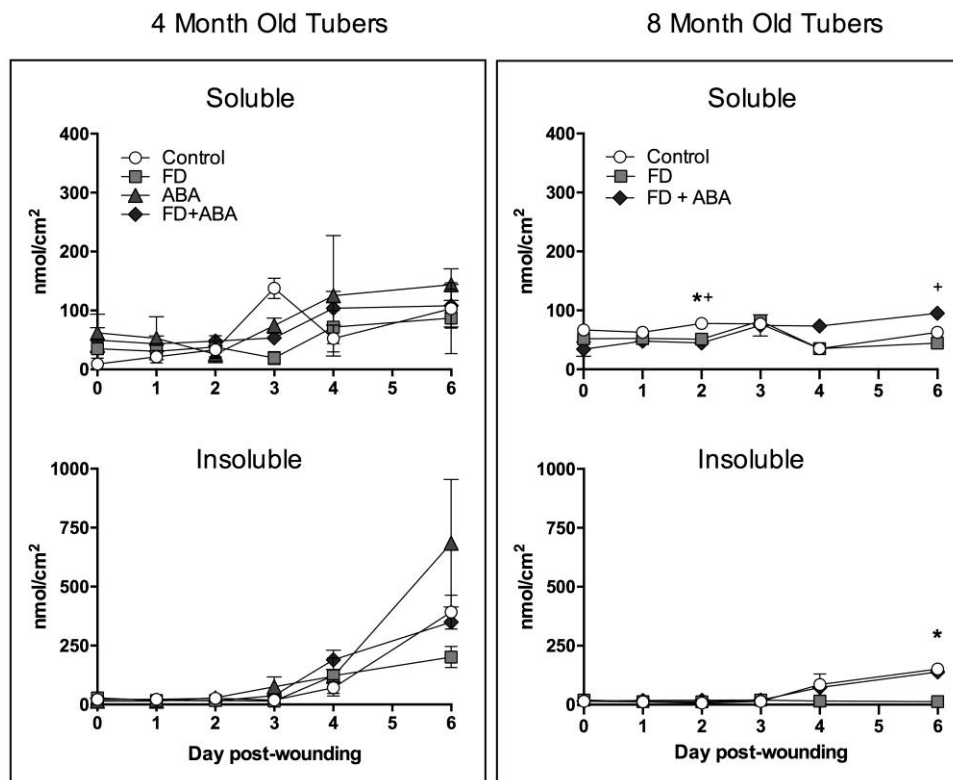


Figure 2.4. Total aliphatic monomer accumulation in wounded potato tubers. Total soluble and insoluble aliphatic suberin monomers (sum of fatty acids, fatty alcohols, ω -OH fatty acids and α,ω -dioic acids) were extracted from four and eight month old tuber tissue following wounding and an initial treatment with water, fluridone (FD), abscisic acid (ABA; four month old tubers only) or FD + ABA. Data points marked with different symbols indicate statistically significant differences ($p \leq 0.05$) between water and FD (*), water and ABA (^) and, water and FD + ABA (+). Data points represent the sample mean \pm SD ($n = 3$).

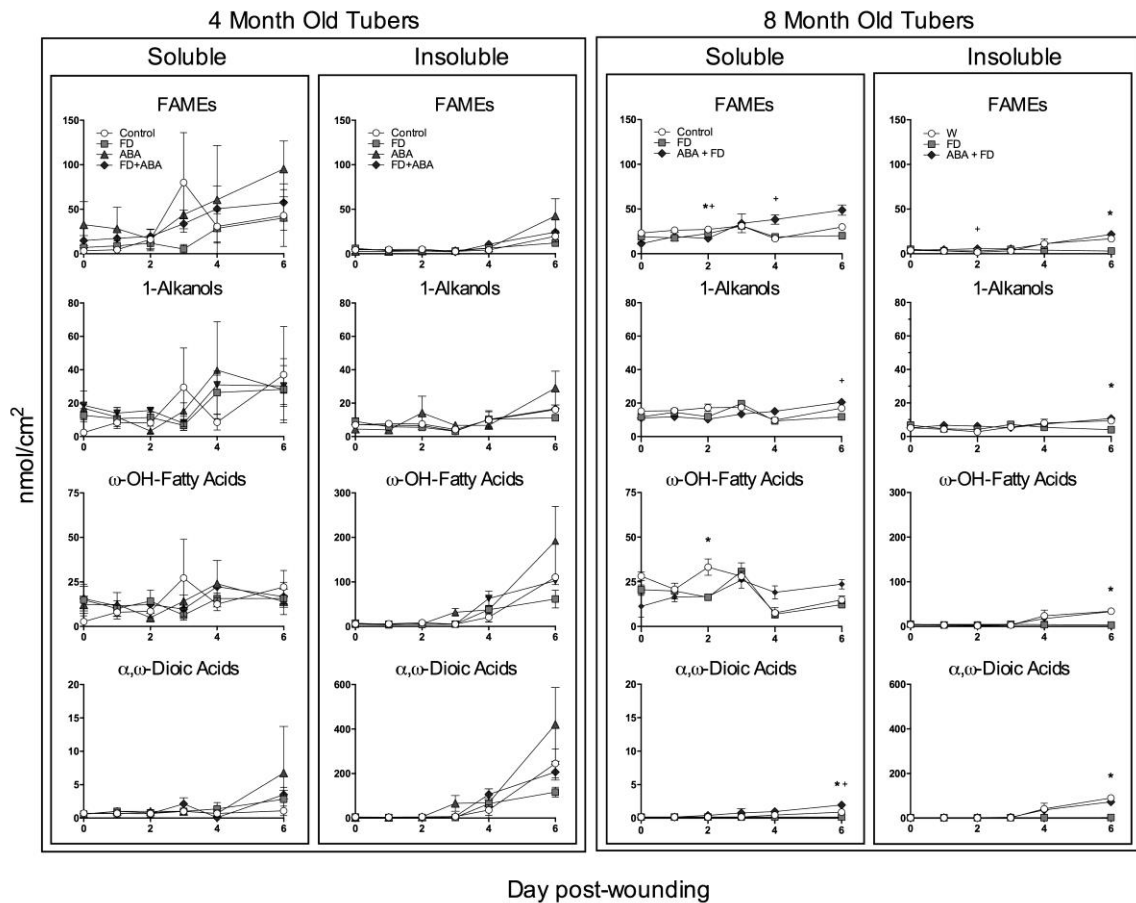


Figure 2.5. Wound induced potato suberin aliphatics by substance class. Total soluble and insoluble fatty acids, fatty alcohols, ω -OH fatty acids and α,ω -dioic acids were analyzed for four- and eight-month old, wound healing tuber tissue following initial treatment with water, FD, ABA or FD + ABA. Data points marked with different symbols indicate statistical significance ($p \leq 0.05$) between water and FD (*), water and ABA (^) and, water and FD + ABA (+). Data points represent the sample mean \pm SD ($n = 3$).

2.4 Discussion

The biosynthesis of suberin requires the coordinated synthesis and deposition of two distinct biopolymers or domains. One domain, thought to be deposited first in the primary cell wall, is poly(phenolic) and comprises hydroxycinnamyl alcohols (monolignols), hydroxycinnamic acids, amides and esters (Bernards et al., 1995; Negrel et al., 1996). The other, which is poly(aliphatic), is deposited between the cell wall and plasma

membrane (with a characteristic lamellar pattern), consists of fatty acids, 1-alkanols, ω -hydroxy fatty acids and α,ω -dioic acids (e.g., Holloway, 1983) and glycerol (Graça et al., 2000a, 2000b, 2000c). While there are phenolic acids (principally ferulic acid, but also caffeic and coumaric acids, depending on species) esterified within the poly(aliphatic) domain, these are low in abundance, and their removal via transesterification yields a more recalcitrant phenolic polymer core (Graça, 2015). Accordingly, the regulation of both phenolic and aliphatic metabolism must be coordinated to ensure the delivery of the appropriate monomers to the cell wall in a temporally correct manner. This is especially true for wound-induced suberin biosynthesis, wherein a rapid and highly organized deposition of suberin occurs in the cells immediately adjacent to the wound site. In recent years, a number of genes associated with suberin biosynthesis have been identified, and some characterized, using *Arabidopsis*, tomato and potato as model systems. In potato, these include genes with confirmed or putative roles in phenolic metabolism (*StPAL1*, *StC4H*, *StCCR*, *StTHT*) and aliphatic metabolism (*StCYP86A33*, *StCYP86B12*, *StFAR3*, *StKCS6*), as well as genes involved in convergent metabolism linking phenolic and aliphatic monomers (*StFHT*), acyl chains to glycerol (*StGPAT5*, *StGPAT6*), or in the delivery of aliphatic monomers to the site of suberization (*StABCG1*) (Table 1). In addition, transcription factors that function as regulators of stress-induced suberin biosynthesis have been identified in *Arabidopsis* and potato (e.g., *AtMYB41*; Kosma et al., 2014; *StNAC103*; Verdaguer et al., 2016). The discovery of suberin-associated genes allows for exploration of their underlying function and regulation. For example, three transgenic potato lines with “engineered” suberin have been developed and characterized (Serra et al., 2009a, 2009b; Serra et al., 2010), based on the RNAi knockdown of *StCYP86A33*, *StKCS6* and *StFHT*, respectively. All three have an altered aliphatic suberin phenotype and reduced function. By contrast, there are no potato mutants defective in phenolic metabolism; however, earlier work in which *StPAL1* activity was inhibited using 2-aminoindane-phosphonic acid suggests a critical role for functional phenolic metabolism in the establishment of an effective suberin barrier to pathogen infection of stored tubers (Hammerschmidt, 1984).

The sequencing of the potato genome (Xu et al., 2011) has opened the door to discovery of putative regulatory elements of known suberin biosynthesis genes, providing clues to potential mechanisms that govern their expression. For example, we recently demonstrated that the 1.7 kb region upstream of the *StCYP86A33* open reading frame contains over 40 ABA-response or ABA-response like motifs, supporting a role for ABA in the regulation of this important aliphatic suberin biosynthesis gene (Bjelica et al., 2016). While the general involvement of ABA in suberin deposition in potato tubers in response to wounding has already been demonstrated (Soliday et al., 1978; Cottle and Kolattukudy, 1982; Lulai et al., 2008; Kumar et al., 2010), whether both phenolic and aliphatic metabolism are affected by this plant hormone remains unclear. Here we established that the wound-induced metabolism leading to monomers of aliphatic suberin is impaired when *de novo* biosynthesis of ABA is impaired, but that polar metabolism leading to phenolic monomers is not greatly affected.

2.4.1 ABA levels are dynamic during wound-healing

Resting tubers contain high levels of ABA (e.g., 80-120 ng/g FW), though this declines with age post-harvest (Lulai et al., 2008; Kumar et al., 2010). Indeed, the timing of tuber response to wounding correlates with tuber age and ABA levels (Kumar et al., 2010), which partly explains the temporal differences we observed between our experiments using tubers of different age. Extensive washing of freshly cut tuber tissue leads to the loss of endogenous ABA (Soliday et al., 1978; Cottle and Kolattukudy, 1982), which helps explain why we observed low levels of ABA in our tissue immediately post-harvest. Regardless of tuber age, however, wounding triggered the *de novo* synthesis of ABA (Figure 1; Kumar et al., 2010) and wound-induced expression of aliphatic metabolism genes, as well as the deposition of aliphatic suberin, followed the same temporal pattern as ABA biosynthesis. This is clearly evident in temporal aliphatic gene expression patterns in our time course experiments, regardless of tuber age. That is, aliphatic gene expression appeared to track *de novo* ABA biosynthesis. Overall, the inhibition of *de novo* ABA biosynthesis resulting from the application of FD delayed the induction of aliphatic suberin biosynthesis genes, without impacting phenolic metabolism genes. The application of FD + ABA, or ABA alone, resulted in aliphatic metabolism

gene expression patterns similar to those of water-treated tubers. That is, exogenous ABA compensated for the reduced level of *de novo* ABA biosynthesis in FD-treated tissue. However, there must be other factors involved in regulation of the wound-healing response since exogenous ABA did not affect phenolic metabolism or the timing of aliphatic metabolism downstream of gene expression.

The role of other phytohormones, including jasmonates, salicylic acid and ethylene, in wound-induced suberization in potato remains speculative (Lulai and Suttle, 2004, 2009; Lulai et al., 2008). That is, the application of inhibitors of ethylene synthesis had no impact on suberin deposition, and while jasmonate levels changed transiently, no specific role in suberization was identified (Lulai et al., 2011). More recently, Barberon et al., (2016) demonstrated a role for ABA in the developmental deposition of Arabidopsis root suberin, and provided evidence for interference in the process by ethylene. However, it remains unclear how these two plant hormones interact to affect suberin deposition.

2.4.2 Polar metabolism is minimally affected by changes in ABA

Wounding of potato tubers induces the accumulation of a number of phenolic metabolites, some of which are destined for polymerization into the poly(phenolic) domain associate with suberin (e.g., monolignols, hydroxycinnamic acids, feruloyl octopamine, feruloyl tyramine) while others accumulate as soluble metabolites (e.g., caffeoyl putrescine, dihydrocaffeoyl putrescine, feruloyl putrescine, dihydroferuloyl putrescine, chlorogenic acid). Treatment of wounded tubers with FD did not affect the accumulation of any of these compounds, consistent with the minimal effect observed on the expression of genes associated with phenolic metabolism. For example, the induction of *StPAL1* was reflected in a rapid decline in soluble pools of L-phe in all treatments (**Figure B5**), while the induction of *StTHT*, which encodes tyramine:hydroxycinnamoyl-CoA hydroxycinnamoyl transferase and links hydroxycinnamic acids with tyramine, was reflected by increased levels of feruloyl tyramine derivatives. Of particular importance to the present study, the treatment of tissues with either FD, ABA or the combination of FD + ABA did not alter phenolic gene expression (**Figure 2.2**) or polar compound

accumulation patterns (**Figure 2.3**) to the extent observed in aliphatic gene (**Figure 2.2**) and metabolite analyses (**Figures 2.4-2.5, B6-9**).

2.4.3 Aliphatic suberin biosynthesis and deposition

The application of FD to wound-healing potato tubers resulted in both delayed expression of aliphatic metabolism genes and reduced accumulation of aliphatic suberin monomers, though this was somewhat age-dependent. For example, delayed expression of *StCYP86A33*, which functions as a fatty acid ω -hydroxylase in potato suberin formation (Serra et al., 2009a; Bjelica et al., 2016) resulted in a significant reduction in the accumulation of 18-OH-octadec-9-eneoic acid and 1,18-octadec-9-ene dioic acid, the two major aliphatic suberin monomers in potato, especially in older tubers. A similar reduction in the accumulation of 1-alkanols and very long chain aliphatics was coincident with reduction in *StFAR3* and *StKCS6* expression, respectively. Interestingly, FD treatment also resulted in the delayed expression of *StFHT*, which codes for a fatty acyl-CoA:hydroxycinnamate hydroxycinnamoyl transferase and functions to link phenolic and aliphatic monomers together into ferulate conjugates. Ferulate compounds accumulate late in the potato wound-healing process (Bernards and Lewis, 1992), so overall the delayed *StFHT* expression would not likely impact the overall suberization process.

Overall, ABA was shown to play a role in the processes leading to suberization in a wound-healing tuber model. The main impact was at the transcriptional level of key aliphatic suberin monomer biosynthesis genes that resulted in the reduced accumulation of soluble aliphatic compounds and incorporation into the insoluble aliphatic suberin matrix. The *de novo* biosynthesis of ABA appears to play a role in aliphatic suberin biosynthesis; indeed, the accumulation of wound-induced ABA (around day 3 post-wounding), was coincident with the onset of aliphatic metabolism. Abscisic acid itself, however, is not the only regulatory compound involved in suberization, since reduction of ABA in the FD treatment neither abolished soluble monomer accumulation nor impacted polar metabolism. While ABA is a major factor affecting suberin-associated gene expression and downstream insoluble aliphatic monomer accumulation, other unknown factors must also participate in the regulation of soluble aliphatic accumulation.

2.5 References

- Arrieta-Baez, D. and Stark, R.E.** (2006). Modeling suberization with peroxidase-catalyzed polymerization of hydroxycinnamic acids: Cross-coupling and dimerization reactions. *Phytochemistry* **67**, 743-753.
- Barberon, M., Vermeer, J.E.M., De Bellis, D., Wang, P., Naseer, S., Andersen, T.G., Humbel, B.M., Nawrath, C., Takano, J., Salt, D.E. and Geldner, N.** (2016). Adaptation of root function by nutrient-induced plasticity of endodermal differentiation. *Cell* **164**, 447-459.
- Beisson, F., Li, Y., Bonaventure, G., Pollard, M. and Ohlrogge, J.B.** (2007). The acyltransferase GPAT5 is required for the synthesis of suberin in seed coat and root of *Arabidopsis*. *The Plant Cell* **19**, 351-368.
- Beisson, F., Li-Beisson, Y., and Pollard, M.** (2012). Solving the puzzles of cutin and suberin polymer biosynthesis. *Current Opinion in Plant Biology* **15**, 1-9.
- Bernards, M.A.** (2002). Demystifying suberin. *Canadian Journal of Botany* **80**, 227-240.
- Bernards, M.A. and Lewis, N.G.** (1992). Alkyl ferulates in wound healing potato tubers. *Phytochemistry* **31**, 3409-3412.
- Bernards, M.A., Lopez, M.L., Zajicek, J. and Lewis, N.G.** (1995). Hydroxycinnamic acid-derived polymers constitute the polyaromatic domain of suberin. *The Journal of Biological Chemistry* **270**, 7382-7386.
- Bjelica, A., Haggitt, M.L., Woolfson, K.N., Lee, D.N.P., Makhzoum, A.B. and Bernards, M.A.** (2016). Fatty acid ω -hydroxylases from *Solanum tuberosum*. *Plant Cell Reports* **35**, 2435-2448.
- Boher, P., Serra, O., Soler, M., Molinas, M., and Figueras, M.** (2013). The potato suberin feruloyl transferase FHT which accumulates in the phellogen is induced by wounding and regulated by abscisic and salicylic Acids. *Journal of Experimental Botany* **64**, 3225-3236.
- Chang, S., Puryear, J. and Cairney, J.** (1993). A simple and efficient method for isolating RNA from pine trees. *Plant Molecular Biology Reporter* **11**, 113-116.
- Compagnon, V., Diehl, P., Benveniste, I., Meyer, D., Schaller, H., Schreiber, L., Franke, R., and Pinot, F.** (2009). CYP86B1 is required for very long chain ω -hydroxyacid and α,ω -dicarboxylic acid synthesis in root and seed suberin polyester. *Plant Physiology* **150**, 1831-1843.
- Cottle, W. and Kolattukudy, P.E.** (1982). Abscisic acid simulation of suberization. *Plant Physiology* **70**, 775-780.
- Cuthbertson, D.J., Johnson, S.R., Piljac-Zegarac, J., Kappel, J., Schafer, S., Wust, M., Ketchum, R.E.B., Croteau, R.B., Marques, J.V., Davin, L.B., Lewis, N.G., Rolf, M., Kutchan, T.M., Soejarto, D.D. and Lange, B.M.** (2013).

Accurate mass-time tag library for LC/MS-based metabolite profiling of medicinal plants. *Phytochemistry* **91**, 187-197.

- Domergue, F., Vishwanath, S. J., Joubès, J., Ono, J., Lee, J. A., Bourdon, M., Alhattab, R., Lowe, C., Pascal, S., Lessire, R. and Rowland, O.** (2010). Three *Arabidopsis* fatty acyl-coenzyme A reductases, FAR1, FAR4, and FAR5, generate primary fatty alcohols associated with suberin deposition. *Plant Physiology* **153**, 1539-1554.
- Esau, K.** (1977). Anatomy of Seed Plants, 2nd Edition (pp. 183-197). New York, NY: Wiley & Sons.
- Efetova, M., Zeier, J., Riederer, M., Lee, C.W., Stingl, N., Mueller, M., Hartung, W., Hedrich, R. and Deeken, R.** (2007). A central role of abscisic acid in drought stress protection of *Agrobacterium*-induced tumors on *Arabidopsis*. *Plant Physiology* **145**, 853-862
- Gamble, P.E. and Mullet, J.E.** (1986). Inhibition of carotenoid accumulation and abscisic acid biosynthesis in fluridone-treated dark-grown barley. *European Journal of Biochemistry* **160**, 117-121.
- Giavalisco, P., Matthes, Y.L.A., Eckhardt, A., Hubberten, H., Hesse, H., Segu, S. and Willmitzer, L.** (2011). Elemental formula annotation of polar and lipophilic metabolites using ¹³C, ¹⁵N and ³⁴S isotope labeling, in combination with high resolution mass spectrometry. *The Plant Journal* **68**, 364-376.
- Graça, J., Cabral, V., Santos, S., Lamosa, P., Serra, O., Molinas, M., Schreiber, L., Kauder, F. and Franke, R.** (2015). Partial depolymerization of genetically modified potato tuber periderm reveals intermolecular linkages in suberin polyester. *Phytochemistry* **117**, 209-219.
- Graça, J.** (2015). Suberin: the biopolyester at the frontier of plants. *Frontiers in Chemistry* **3**(62), doi:10.3389/fchem.2015.00062.
- Graça, J. and Pereira, H.** (2000a). Methanolysis of bark suberins: analysis of glycerol and acid monomers. *Phytochemical Analysis* **11**, 45-51.
- Graça, J. and Pereira, H.** (2000b). Diglycerol alkendioates in suberin: building units of a poly(acylglycerol) polyester. *Biomacromolecules* **1**, 519-522.
- Graça, J. and Pereira, H.** (2000c). Suberin structure in potato periderm: glycerol, longchain monomers, and glyceryl and feruloyl dimers. *Journal of Agricultural and Food Chemistry* **48**, 5476-5483.
- Graça, J. and Santos, S.** (2007). Suberin: A biopolyester of plants' skin. *Macromolecular Bioscience* **7**, 128-135.
- Hammerschmidt, R.** (1984). Rapid deposition of lignin in potato tuber tissue as a response to fungi nonpathogenic on potato. *Physiological Plant Pathology* **24**, 33-42.
- Holloway, P.J.** (1983). Some variations in the composition of suberin from the cork layers of higher-plants. *Phytochemistry* **22**, 495-502.

- Karlen, Y., McNair, A., Perseguers, S., Mazza, C. and Mermoud, N.** (2007). Statistical significance of quantitative PCR. *BMC Bioinformatics* **20**(8), 131-146.
- Kosma, D.K., Murmu, J., Razeq, F.M., Santos, P., Bourgault, R., Molina, I. and Rowland, O.** (2014). AtMYB41 activates ectopic suberin synthesis and assembly in multiple plant species and cell types. *The Plant Journal* **80**, 216-229.
- Kumar, G.N., Lulai, E.C., Suttle, J.C. and Knowles, N.R.** (2010). Age-induced loss of wound-healing ability in potato tubers is partly regulated by ABA. *Planta* **232**, 1433-1445.
- Landgraf, R., Smolka, U., Altmann, S., Eschen-Lippold, L., Senning, M., Sonnewald, S. and Rosahl, S.** (2014). The ABC transporter ABCG1 is required for suberin formation in potato tuber periderm. *The Plant Cell* **26**, 3403-3415.
- Larsen, K.** (2004). Molecular cloning and characterization of cDNAs encoding cinnamoyl CoA reductase (CCR) from barley (*Hordeum vulgare*) and potato (*Solanum tuberosum*). *Journal of Plant Physiology* **161**, 105-112.
- Li-Beisson, Y., Pollard, M., Sauveplane, V., Pinot, F., Ohlrogge, J. and Beisson, F.** (2009). Nanoridges that characterize the surface morphology of flowers require the synthesis of cutin polyester. *Proceedings of the National Academy of Sciences of the United States of America* **106**, 22008-22913.
- Li-Beisson, Y., Shorrosh, B., Beisson, F., Andersson, M.X., Arondel, V., Bates, P.D., Baud, S., Bird, D., Debono, A., Durrett, T.P., Franke, R.B., Graham, I.A., Katayama, K., Kelly, A.A., Larson, T., Markham, J.E., Miquel, M., Molina, I., Nishida, I., Rowland, O., Samuels, L., Schmid, K.M., Wada, H., Welti, R., Xu, C., Zallot, R. and Ohlrogge, J.** (2013). Acyl-Lipid Metabolism. *The Arabidopsis Book* **11**: e0161.
- Lulai, E.C., Huckle, L., Neubauer, J.D. and Suttle, J.C.** (2011). Coordinate expression of AOS genes and JA accumulation: JA is not required for initiation of closing layer in wound healing tubers. *Journal of Plant Physiology* **168**, 976-982.
- Lulai, E.C. and Neubauer, J.D.** (2014). Wound-induced suberization genes are differentially expressed, spatially and temporally, during closing layer and wound periderm formation. *Postharvest Biology and Technology* **90**, 24-33.
- Lulai, E.C. and Suttle, J.C.** (2004). The involvement of ethylene in wound induced suberization of potato tuber (*Solanum tuberosum* L.): A critical assessment. *Postharvest Biology and Technology* **34**, 105-112.
- Lulai, E.C. and Suttle, J.C.** (2009). Signals involved in tuber wound-healing. *Plant Signaling & Behavior* **4**, 620-622.
- Lulai, E.C., Suttle, J.C. and Pederson, S.M.** (2008). Regulatory involvement of abscisic acid in potato tuber wound-healing. *Journal of Experimental Botany* **59**, 1175-1186.
- Mattinen, M.L., Filpponen, I., Järvinen, R., Li, B., Kallio, H., Lehtinen, P. and Argyropoulos, D.** (2009). Structure of the polyphenolic component of suberin

- isolated from potato (*Solanum tuberosum* var. Nikola). *Journal of Agricultural and Food Chemistry* **57**, 9747-9753.
- Meyer, C.J., Peterson, C.A. and Bernard, M.A.** (2011). A comparison of suberin monomers from the multiseriate exodermis of *Iris germanica* during maturation under differing growth conditions. *Planta* **233**, 773-786.
- Nakane, E., Kawakita, K., Doke, N., and Hirofumi, Y.** (2003). Elicitation of primary and secondary metabolism during defense in the potato. *Journal of General Plant Pathology* **69**, 378-384.
- Negrel, J., Pollet, B. and Lapierre, C.** (1996). Ether-linked ferulic acid amides in natural and wound periderms of potato tuber. *Phytochemistry* **43**, 1195-1199.
- Nicot, N., Hausman, J.-F., Hoffmann, L. and Evers, D.** (2005). Housekeeping gene selection for real-time RT-PCR normalization in potato during biotic and abiotic stress. *Journal of Experimental Biology* **56**, 2907-2914.
- Pfaffl, M.W.** (2001). A new mathematical model for relative quantification in real-time RT-PCR. *Nucleic Acids Research* **29**, 2002-2007.
- Pluskal, T., Castillo, S., Villar-Briones, A. and Oresic, M.** (2010). MZmine 2: Modular framework for processing, visualizing, and analyzing mass spectrometry-based molecular profile data. *BMC Bioinformatics* **11**, 395-405.
- Ranathunge, K., Schreiber, L. and Franke, R.** (2011). Suberin research in the genomics era – New interest for an old polymer. *Plant Science* **180**, 399-413.
- Razem, F.A. and Bernard, M.A.** (2002). Hydrogen peroxide is required for poly(phenolic) domain formation during wound-induced suberization. *Journal of Agricultural and Food Chemistry* **50**, 1009-1015.
- Serra, O., Hohn, C., Franke, R., Prat, S., Molinas, M. and Figueras, M.** (2010). A feruloyl transferase involved in the biosynthesis of suberin and suberin-associated wax is required for maturation and sealing properties of potato periderm. *The Plant Journal* **62**, 277-290.
- Serra, O., Soler, M., Hohn, C., Sauveplane, V., Pinot, F., Franke, R., Schreiber, L., Prat, S., Molinas, M. and Figueras, M.** (2009a). *CYP86A33*-targeted gene silencing in potato tuber alters suberin composition, distorts suberin lamellae, and impairs the periderm's water barrier function. *Plant Physiology* **149**, 1050-1060.
- Serra, O., Soler, M., Hohn, C., Franke, R., Schreiber, L., Prat, S., Molinas, M. and Figueras, M.** (2009b). Silencing of *StKCS6* in potato periderm leads to reduced chain lengths of suberin and wax compounds and increased peridermal transpiration. *Journal of Experimental Botany* **60**, 697-707.
- Soliday, C.L., Dean, B.B. and Kolattukudy, P.E.** (1978). Suberization: Inhibition by washing and stimulation by abscisic acid in potato disks and tissue culture. *Plant Physiology* **61**, 170-174.
- Stark, R.E. and Garbow, J.R.** (1992). Nuclear magnetic resonance relaxation studies of plant polyester dynamics. 2. Suberized potato cell wall. *Macromolecules* **25**, 149-154.

- Vandesompele, J., De Preter, K., Pattyn, F., Poppe, B., Van Roy, N., De Paepe, A. and Speleman, F.** (2002). Accurate normalization of real-time quantitative RT-PCR data by geometric averaging of multiple internal control genes. *Genome Biology* **3**(7), research0034.1-research003411.
- Verdaguer, R., Soler, M., Serra, O., Garrote, A., Fernandez, S., Company-Arumi, D., Antico, E., Molinas, M. and Figueras, M.** (2016). Silencing of the potato *StNAC103* gene enhances the accumulation of suberin polyester and associated wax in tuber skin. *Journal of Experimental Botany* **67**(18), 5415-5427.
- Vishwanath, S.J., Kosma, D.K., Pulsifer, I.P., Scandola, S., Pascal, S., Joubès, J., Dittrich-Domergue, F., Lessire, R., Rowland, O. and Domergue, F.** (2013). Suberin-associated fatty alcohols in *Arabidopsis*: Distributions in roots and contributions to seed coat barrier properties. *Plant Physiology* **163**, 1118-1132.
- Vishwanath, S.J., Delude, C., Domergue, F. and Rowland, O.** (2015). Suberin: biosynthesis, regulation, and polymer assembly of a protective extracellular barrier. *Plant Cell Reports* **34**, 573-586.
- Wang, X., El Hadrami, A., Adam, L.R. and Daayf, E.** (2008). Differential activation and suppression of potato defence responses by *Phytophthora infestans* isolates representing US-1 and US-8 genotypes. *Plant Pathology* **57**, 1027-1037.
- Wang-Pruski, G. and Cattle, S.E.** (2004). Cloning and expression of cinnamic acid 4-hydroxylase in potato, a gene related to after-cooking darkening. *Acta Physiologiae Plantarum* **26**, 60-61.
- Xu, X., et al; Potato Genome Sequencing Consortium (PGSC)** (2011). Genome sequence and analysis of the tuber crop potato. *Nature* **475**, 189-195.
- Yan, B. and Stark, R.E.** (1998). A WISE NMR approach to heterogeneous biopolymer mixtures: dynamics and domains in wounded potato tissues. *Macromolecules* **31**, 2600-2605.
- Yang, W.L., Pollard, M., Li-Beisson, Y., Beisson, F., Feig, M. and Ohlrogge, J.B.** (2010). A distinct type of glycerol-3-phosphate acyltransferase with sn-2 preference and phosphatase activity producing 2-monoacylglycerol. *Proceedings of the National Academy of Sciences of the United States of America* **107**, 12040-12045.
- Yang, W.L., Pollard, M., Li-Beisson, Y., and Ohlrogge, J.B.** (2016). Quantitative analysis of glycerol in dicarboxylic acid-rich cutins provides insights into *Arabidopsis* cutin structure. *Phytochemistry* **130**, 159-169.
- Yang, W., Simpson, J.P., Li-Beisson, Y., Beisson, F., Pollard, M., and Ohlrogge, J.B.** (2012). A land-plant-specific glycerol-3-phosphate acyltransferase family in *Arabidopsis*: substrate specificity, sn-2 preference, and evolution. *Plant Physiology* **160**, 638-652.

Chapter 3

3 The wound-healing potato tuber: an RNA-seq approach

3.1 Introduction

Potato (*Solanum tuberosum* L.) is the most important non-grain staple crop in the world. Crop losses are largely attributed to pathogen infection and dehydration during both growth and post-harvest storage (Guenther, 1995; Guenther et al., 2001). The heteropolymer suberin comprises a poly(phenolic) domain covalently linked to a spatially distinct poly(aliphatic) domain (reviewed in Bernards, 2002; Graça and Santos, 2007; Ranathunge et al., 2011; Beisson et al., 2012; Vishwanath et al., 2015; Graça, 2015), and is deposited in both native and wound periderm cells, where it acts as a physicochemical barrier against various abiotic and biotic stresses (Kolattukudy, 1987; Lyon 1989; Lulai and Orr, 1994; Lulai and Corsini, 1998). Suberin is deposited in periderm cell walls during tuber development and maturation, i.e. its synthesis and deposition allows for skin-set after harvest (Lulai and Freeman, 2001; Lulai, 2007). Suberin production is also triggered in response to mechanical wounding in potato tubers (Esau, 1977), where it plays a role in resistance to water loss and microbial infection by sealing off the wound site (Lulai and Corsini, 1998).

Wound-healing is a complex component of plant protection against different stresses, and encompasses many processes, including suberization. A variety of physiological and metabolic events are activated upon wounding that lead to the biosynthesis and deposition of the highly organized suberin heteropolymer. This level of coordination requires spatial and temporal regulation of genes individually, but also as subsets that constitute entire biosynthetic pathways.

At the cellular level, wound-induced suberization involves two stages: a suberized closing layer is first formed within 5-7 days of wounding in existing parenchyma cells that surround the wound site, and then layers of suberized phellem cells develop over the next 40 days from new meristematic tissue (the phellogen) to produce a final wound periderm (Neubauer et al., 2012; Lulai and Neubauer, 2014). Rapid wound-healing is

essential for protection against desiccation and infection (Lulai, 2007), making the processes involved in initial closing layer formation of particular importance.

Some aspects of the differential spatial organization and temporal induction of the two major metabolic pathways required for phenolic and aliphatic monomer production have been described (Yang and Bernards, 2006; Woolfson et al., 2018). For example, the poly(phenolic) domain monomers, which include hydroxycinnamyl alcohols (monolignols), hydroxycinnamic acids, amides and esters produced via phenylpropanoid metabolism (Bernards et al., 1995; Negrel et al., 1996), accumulate within 1 day of wounding (Yang and Bernards, 2006) and are deposited into the cell wall (Lulai and Neubauer, 2014). Genes characteristic of phenolic metabolism (e.g., *PAL*, *C4H*, *CCR*, *THT*) are induced rapidly, post wounding (Woolfson et al., 2018). By contrast, the poly(aliphatic) suberin domain spans the space between the cell wall and plasma membrane in tuber periderm cells, and consists of fatty acids (FAs), modified FAs such as fatty alcohols, ω -hydroxy FAs, and α,ω -dioic acids, and glycerol (Holloway, 1983; Graça and Pereira, 2000a, 2000b, 2000c; Lulai and Neubauer, 2014) that are produced within 3 days of wounding (Yang and Bernards, 2006). Genes characteristic of aliphatic metabolism (e.g., *KCS6*, *FAR3*, *CYP86A33*, *CYP86B12*) are induced after *ca.* 2 days post wounding (Woolfson et al., 2018). Genes involved in aliphatic polymer assembly (*FHT*, *GPATs*) and transport (*ABCG1*) are highly expressed by 3-4 days into wound-healing (Woolfson et al., 2018).

The temporal regulation of phenolic and aliphatic metabolism remains unresolved. Recently, the transcription factor NAC103 was characterized as a negative regulator of some key aliphatic suberin and wax genes (Verdaguer et al., 2016), while abscisic acid (ABA) was shown to play a role in the differential induction of polar and non-polar metabolism by impacting only aliphatic suberin biosynthetic genes in potato tubers (Woolfson et al., 2018). Regardless, many aspects of the regulation of induced suberization remain uncharacterized, including that of the poly(phenolic) domain. Moreover, in a dormant potato tuber, many components of primary metabolism must be initiated upon wounding, to generate metabolic precursors for targeted, suberin-specific steps and the energy-rich molecules required to fuel enzyme-catalyzed biosynthetic

reactions. Therefore, I hypothesize that the wound-induced suberization and associated wound-healing processes must require the initial and sustained conversion of starch into usable carbon, ATP and NADPH to fuel all subsequent reactions, including the enhanced production and activation of any regulatory components such as ABA or other stress-induced hormones. I predict the involvement of several regulatory components required for suberization, including transcription factors and mediators of suberin assembly.

In the presented work, I address knowledge gaps in suberin biosynthesis by taking an RNA-seq approach to studying the wound-healing potato tuber. This approach has been greatly facilitated by the publishing of the potato genome sequence (PGSC, 2011). Our transcriptomic investigation expands upon and explores implicated pathways including, but not limited to, suberin monomer biosynthesis, to establish a greater overview of the molecular activities that underlie the overall wound-healing process. Further understanding of metabolic processes leading up to and directly required for suberization, the timing of biosynthetic and assembly events, and elucidation of regulatory components are all of fundamental importance and may offer potential targets for crop improvement applications related to improved suberization, especially in the context of tuber post-harvest storage. Past potato RNA-seq experiments have focused on the response and resistance to different abiotic and biotic stress-related conditions in different organs and across developmental stages (Massa et al., 2011; Gao et al., 2013; Gong et al., 2015; Goyer et al., 2015; Gálvez et al., 2016), but to our knowledge, this is the first time that RNA-seq has been employed to address the mechanisms involved in tuber wound-healing. Metabolite profiling (Yang and Bernards, 2007) and proteomic studies (Chaves et al., 2009) have been conducted in wound-healing tubers to track changes pertaining to primary and secondary metabolism at both the chemical and protein accumulation levels. This transcriptomic study provides the first global gene expression overview during wound-healing and acts to bridge previous metabolite and protein-focused studies, and offers new insights into the timing of transcriptional regulation of processes previously explored from different perspectives.

The goals of this project were to further establish the temporal changes in gene expression that occur during the wound-healing process, identify novel candidate genes

required for different branches of the broader suberin-related pathway as they relate to its biosynthesis, assembly or regulation, and to integrate this information and update the current framework by generating a more comprehensive “roadmap” to suberin biosynthesis in the wound-healing potato tuber.

The integration of gene expression data with the biochemical pathway towards suberin biosynthesis and assembly expands widely upon the sets of previously analyzed genes. This analysis thus provides a comprehensive overview that improves upon a well-substantiated foundation (Bernards, 2002), by removing unsupported hypothetical steps and incorporating more recently characterized steps (e.g. Beisson et al., 2007; Li et al., 2007; Landgraf et al., 2014; Serra et al., 2009b; Serra et al., 2010; Bjelica et al., 2016).

3.2 Materials and Methods

3.2.1 Plant material and wounding experiment

Four to five month old potato (*Solanum tuberosum* cv. Russet Burbank) tubers were removed from cold storage (5°C), washed with tap water, surface sterilized with 20% v/v bleach for 20 minutes, transferred to a laminar flow cabinet, and left to air dry overnight. Tubers were sectioned into approx. 1 cm thick slices, rinsed briefly with sterile dH₂O and placed upright in sterile Magenta® boxes on an elevated mesh platform atop a moistened No. 1 Whatman paper to maintain high humidity. Boxes of tuber slices were incubated in the dark at 28°C for up to three days. Samples collected within 1 hour of wounding and rinsing were considered “0” days post-wounding (dpw).

To harvest tissue, wound surfaces were excised from the cut tuber faces with razor blades. For each time point, tissue collected from tuber material in one Magenta® box was pooled to represent one sample replicate. All harvested tissue was immediately flash frozen and ground into a fine powder in liquid N₂ by mortar and pestle, and then stored at -80°C for future RNA extraction. The entire time course experiment was independently replicated three times (n=3).

3.2.2 RNA isolation

Total RNA was isolated from flash-frozen tuber material as described by Chang et al. (1993). RNA was quantified with a NanoDrop model ND-2000c Spectrophotometer set for RNA determination (Thermo-Scientific), and total RNA quality was determined by absorbance ratios at 260/280 nm (>1.8). RNA was qualitatively assessed with an Agilent 2100 Bioanalyzer, and samples with $RIN \geq 7$ were used for sequencing and to produce cDNA for RT-qPCR validation.

3.2.3 Strand-specific cDNA library construction and sequencing

cDNA library construction and sequencing were performed by Genome Quebec (Montreal QC, Canada). Total RNA was used to produce 15 strand-specific cDNA libraries to represent 5 time-points (0, 0.5, 1, 2 and 3 days post-wounding) with $n=3$ biological replicates, which were then multiplexed and sequenced on four lanes using the Illumina HiSeq2500 platform (Illumina, San Diego, CA) to generate 125-bp paired-end reads.

3.2.4 Genome-guided transcriptome assembly

Raw reads were processed using Trimmomatic version 0.36 (Bolger et al., 2014). Clean reads were obtained by removing Illumina adapter sequences, low quality or N bases, and reads less than 36 bases long after the completion of quality trimming steps. FastQC was used to confirm the quality of processed data (Andrews, 2010).

Bowtie2 v2.2.9 (Trapnell et al., 2012) was used to build an index for the reference genome using PGSC v4.03 (PGSC 2011; Sharma et al., 2013). Clean paired-end reads were aligned to the reference genome using TopHat v2.1.1 and parameters were adjusted to suit the potato genome as described by the PGSC (e.g. “-i 10 -I 15000” options to set minimum to maximum intron size of 10-15000bp as represented in the PGSC v4.03 GFF) (Trapnell et al., 2012). Alignment files (.bam) were filtered to remove discordant pairs and multiple-mapped reads, then used to assemble and merge transcripts using the Cufflinks v2.2.1 package (Trapnell et al., 2012). HTSeq v0.8.0 was used to count the number of reads that mapped to each gene (Anders et al., 2015).

Limma (Ritchie et al., 2015) and edgeR (Robinson et al., 2010) Bioconductor packages were used in R v3.3.3 (R Core Team, 2018) for count trimmed mean of M-values (TMM)-normalization and transformation (e.g. counts per million; CPM, \log_2 CPM, fragments per kilobase of transcript per million mapped reads; FPKM, \log_2 FPKM) for downstream analysis and visualization, including differential expression analysis (Law et al., 2014; Smyth, 2005; Ritchie et al., 2015). For analyses, only those genes with at least 1 CPM in at least 3 of 15 libraries being compared were retained (Robinson et al., 2010). Filtering yielded 17,906 expressed loci.

3.2.5 Differential expression (DE), gene ontology (GO), and gene set enrichment (GSEA) analyses

Differentially expressed genes (DEGs) were identified across time points using pairwise comparisons. Genes were considered significantly up- or down-regulated between two sequential time points if they met $p \leq 0.01$ and absolute \log_2 fold change $|(LFC)| \geq 2$ significance cut-offs. Lists of significant DEGs for sequential time points were generated using the voom function with quality weighting (voomWithQualityWeights) (Law et al., 2014) in the limma Bioconductor package (Ritchie et al., 2015) to estimate the mean-variance relationship of log-transformed TMM-normalized HTSeq count data, which were then entered into the limma empirical Bayes analysis pipeline using the aforementioned significance cut-off parameters with the Benjamini-Hochberg (BH) procedure (Benjamini and Hochberg, 1995).

Gene Ontology (GO) annotation information was retrieved from the Ensembl Plants *Solanum tuberosum* BiomaRt (Kinsella et al., 2011). Additional GO annotations were determined via peptide BLAST (blastp) between potato and its close relative tomato (*Solanum lycopersicum*). For blastp, representative potato peptide sequences were queried against tomato ITAG 3.2 peptide database where a single top matching locus was reported with an e-value cut-off of 0.001. Missing GO terms were retrieved by mapping to GO ID using the Bioconductor packages AnnotationDbi and GO.db (Carlson, 2018; Pagès et al., 2018). TopGO was used with the Fisher's test statistic and "weight01" algorithm filtered with a weighted p value < 0.05 cut-off (Alexa and Rahnenfuhrer, 2016)

to generate a list of the top 50 Biological Process GO annotations associated with 5441 identified DEGs.

Gene set enrichment analysis (GSEA) was performed using a custom version of the Bioconductor package, Piano (Väremo et al., 2013) called tunedPiano, as described by Martel et al. (2015). Voom-generated $\log_2(\text{fold change})$, p and t values were used as gene level statistics input for the GSEA, using gene lists generated from the original $p \leq 0.01$ and $|\text{LFC}| \geq 2$ cutoffs. Parametric analysis of gene set enrichment (PAGE algorithm, Kim and Volsky, 2005) was selected following comparison with other methods. Genes were grouped into sets using GO annotation information, where biological process (BP), molecular function (MF) and cellular component (CC) categories were each analyzed individually. Gene sets were limited to those containing a minimum of five genes and a BH-adjusted p value < 0.05 was used to determine significance of distinct up- or down-regulation of a gene set.

3.2.6 Targeted suberin-related biosynthetic gene analysis

A comprehensive list of known and putative suberin-related genes was generated based on predicted enzymatic functions required for each step of various pathway branches. Predicted functions were used in combination with information from the Potato Genome Sequencing Consortium (PGSC) and NCBI databases to identify likely candidates. Where genes could not be found in the PGSC database via functional annotated name search, they were identified based on blastp with potato sequences found on NCBI wherever possible. If the potato sequence could also not be found on NCBI, blastp was used with known proteins from Arabidopsis found on NCBI or The Arabidopsis Information Resource (TAIR; Berardini et al., 2015), or tomato proteins identified via the Sol Genomics Network (SGN; Fernandez-Pozo et al., 2015) or NCBI, to identify putative potato homologs.

Heatmaps were generated with pheatmap (Kolde, 2012) using $\log_2(\text{FPKM})$ values to visualize temporal changes in suberin-related target gene expression. Heatmap figures that appear in the main text (**Figure 3.3A-I**) utilized a maximum of three representatives of known and candidate genes from complete candidate lists found in **Appendix C**

(**Figure C3A-G; Table C4**). These representatives were selected based on expression level and overall pattern; i.e. genes that showed the highest FPKM levels and appeared to be wound-induced were included, wherever possible.

3.2.7 Targeted candidate gene analysis via hierarchical clustering

Euclidean distance heatmaps were constructed with $\log_2(\text{FPKM})$ using the ward.D2 option to implement Ward's method of hierarchical clustering, to determine similarities between transcription factor or assembly gene candidates and suberization-related gene expression profiles (Ward, 1963; Murtagh and Legendre, 2014).

3.2.8 cDNA synthesis and RT-qPCR validation of gene expression

A portion of total RNA used for the RNA-seq experiment (see **Methods 3.2.1-3.2.2**) was also reverse transcribed and used for gene expression validation. RNA (0.5 $\mu\text{g}/\mu\text{L}$) was treated with DNase I (Invitrogen), and cDNA was synthesized with SuperScript II/RNaseOUT (Invitrogen) following the manufacturer's instructions. RNA samples obtained from each time point with three biological replicates were used to yield 15 cDNA templates (5 time points from 3 biological replicates). Quantitative reverse transcription PCR (RT-qPCR) was performed using a Bio-Rad CFX Connect system. Amplification of genes of interest from 47.6 ng cDNA template was performed in technical triplicate using sequence-specific primers and iTaq Universal SYBR Green Supermix (Bio-Rad), following the manufacturer's protocol. PCR reaction efficiency was determined by standard curves performed in duplicate using pooled cDNA templates at a dilution range from 381 to 0.61 ng (Pfaffl, 2001). Primer sequences and amplification efficiencies can be found in **Table C10**.

One plate of RT-qPCR reactions for four genes, including the endogenous reference, used 5 cDNA templates, with each template representing one sample time point from one experimental replicate performed in technical triplicates. No-template controls were used to ensure no contamination occurred, and inter-run calibrator samples were included to allow for detection and correction of plate-to-plate variation. This was repeated for all three biological replicates of cDNA templates obtained from wound tissue derived from three independent experiments. Data were combined across the three replicate plates per

gene and adjusted via inter-run calibration to yield means ($n=3$), and endogenous reference gene *EF1- α* values were used to normalize expression of each target gene. RT-qPCR specificity was confirmed by melt curve analysis and gene expression data were processed using Bio-Rad CFX manager version 3.1 software according to the manufacturer's directions, based on the Pfaffl (2001) method. Gene expression data from a separate time course experiment, published in Woolfson et al. (2018), was used for additional validation (see **Methods §2.2.1, 2.2.4-2.2.5**). *EF1- α* and *APRT* (Nicot et al., 2005) were used as endogenous references for normalization (Vandesompele et al., 2002). The calculated expression levels were corrected for PCR reaction efficiency.

Gene expression values for 14 genes from RT-qPCR ($\Delta\Delta Cq$) and RNA-seq (CPM) analyses were normalized to 0 dpw values, then \log_2 -transformed to generate \log_2 (fold change) values. Pearson's correlation coefficients were calculated for \log_2 (fold change) values from the two experimental procedures, with $\alpha = 0.05$. The 95% confidence interval was calculated and plotted as 95% confidence bands.

3.3 Results

3.3.1 Genome-guided transcriptome assembly

Potato tuber tissue was collected at 0, 0.5, 1, 2 and 3 days post-wounding (dpw) in order to capture different stages of the early wound-healing process at the transcriptional level. On average, libraries yielded over 65 million raw 125-bp reads that were trimmed to produce more than 51 million clean read pairs. High quality, clean reads had a 70% concordant pair alignment rate, and of these concordant pairs, over 87% mapped to annotated gene features in the potato genome. The numbers of concordant pairs that aligned to multiple locations (4.16%), or mapped to ambiguous regions in the genome (1.9%), were low, and were filtered out prior to quantification. Of the 39,031 predicted protein-coding genes in the potato genome (PGSC, 2011), 38,986 had corresponding gene identification names, of which 17,906 demonstrated some level of expression in this study (46%). Principal component analysis of normalized counts per million (CPM)

demonstrated that libraries representing biological replicates clustered together, and were well separated on the basis of time (**Figure 3.1A**).

3.3.2 Differential expression analysis in wound-healing tubers

To characterize transcriptional changes that occur during wound-healing, pairwise comparisons were made between sequential time points (0-0.5, 0.5-1, 1-2, and 2-3 dpw) for differential expression analysis. Changes in mRNA abundance as a proxy for differential gene expression over time were analyzed to identify genes that significantly change between successive time points. This analysis identified 5441 differentially expressed genes (DEGs) across all time point comparisons, with the largest number DEGs detected (2547 up-regulated; 1956 down-regulated) between 0 and 0.5 dpw. Later time point comparisons revealed decreasing numbers of DEGs as wound-healing progressed, where the majority of DEGs were up-regulated (0.5-1 dpw: 669 up-regulated and 169 down-regulated; 1-2 dpw: 621 up-regulated and 104 down-regulated; 2-3 dpw: 266 up-regulated and 81 down-regulated; **Figure 3.1B**). Most of the identified DEGs were unique to each time point comparison, and no single gene continued to change significantly across all time points (**Figure 3.1C**).

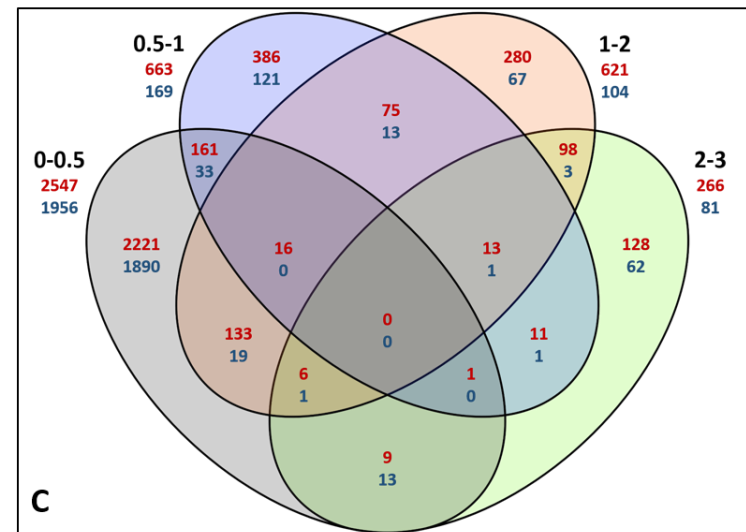
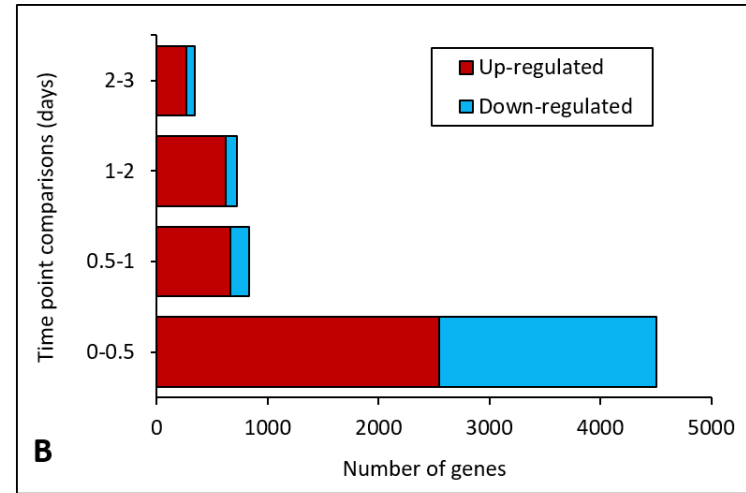
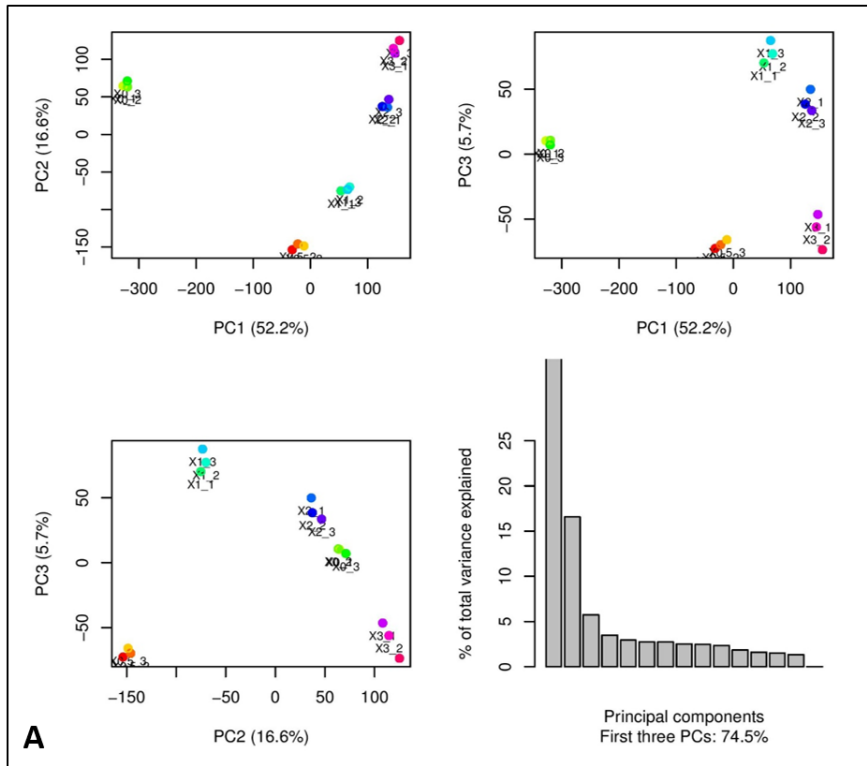


Figure 3.1. Global overview of wound-healing transcriptome. A. Principle component analysis (PCA) of RNA-seq libraries. Colours represent biological replicate libraries generated from the same time point (gene $\log_2(\text{CPM})$ space without scaling). **B. Differentially expressed genes (DEGs) across time point comparisons.** Genes were considered significantly up- or down-regulated if they met $p \leq 0.01$ and $|\log_2(\text{fold change})| (|\text{LFC}|) \geq 2$ significance cut-offs. Lists of significantly DEGs were generated using voom by applying these parameters with the Benjamini-Hochberg procedure to TMM-normalized HT-Seq count data. **C. Venn diagram of DEGs significantly up- (red) or down-regulated (blue) over the wound-healing time course.** Genes were considered significantly up- or down-regulated if they met $p \leq 0.01$ and $|\text{LFC}| \geq 2$ significance cut-offs. Lists of significantly DEGs were generated using voom by applying these parameters with the Benjamini-Hochberg procedure to TMM-normalized HT-Seq count data.

3.3.3 Gene ontology (GO) analysis

Gene ontology (GO) analysis was performed to characterize DEGs by biological role. Available GO annotation information accessed through BiomaRt covered 19,096 genes (49% of the genome). Additional GO information based on peptide BLAST between tomato and potato increased the number of annotated genes to 26,217 (67% of the genome). Of the 17,906 genes found to be expressed in this study, 90% were represented in this annotated gene list.

TopGO analysis of the biological processes (BP) GO category demonstrated that within the list of 5441 total DEGs identified throughout the time course, the top 50 categories were reflective of biotic and abiotic stress response genes (e.g. response to stress, response to biotic stimulus, response to bacterium, chitin catabolic process, and response to heat), signaling and regulatory processes (e.g. “histone phosphorylation”, “dephosphorylation”), a range of biosynthetic pathways and metabolic processes that pertain to primary and secondary metabolism (e.g. “amino acid biosynthesis”, “sterol biosynthesis”, “carbohydrate metabolism”, “acetyl-CoA metabolism”, “lipid metabolism”, “oxidation-reduction process”, “brassinosteroid biosynthesis”, “indoleacetic acid biosynthesis” and “isoprenoid biosynthesis”), and various processes pertaining to the cell cycle and cell wall (e.g. “xyloglucan metabolic process”, “DNA replication”, “cell wall biogenesis”, “regulation of cell cycle”) (**Table C1**). Overall, this TopGO analysis highlighted several wound-related biological processes in terms of stress responses, metabolic changes, and physical alterations at the cellular level.

3.3.4 Gene set enrichment analysis (GSEA)

Generally, differential expression analyses pointed to large, immediate transcriptional changes followed by a decline in the number of DEGs, and TopGO analysis highlighted several biological processes associated with stress and wound-healing. Together, these findings raised the hypothesis that during early time points after wounding, transcriptional re-organization occurs on a large scale and is followed by a plateau and fine-tuning of specialized responses for suberization and physical aspects of healing. To

test this idea and further visualize changes in groups of genes between time points during wound-healing, a parametric analysis of gene set enrichment (PAGE) algorithm was used for gene set analysis of the 5441 DEGs identified across the entire time course, via sequential time point comparisons (Kim and Volsky, 2005; Våremo et al., 2013). GO annotation terms were used to group genes into sets, where each respective ontology category was employed for separate analyses (biological process, BP; molecular function, MF; cellular component, CC). Limma-generated gene level statistics, including \log_2 (fold change), adjusted p -value, and the directional t -statistic, were used as input for the analyses.

In total, 96 BP term gene sets were significantly up- or down-regulated during wound-healing, where 2331 of the total 5441 DEGs were represented in enriched terms. These sequential time comparisons were used to demonstrate how implicated processes change over time (**Figure 3.2, Table 3.1**). In the first 0.5 dpw, gene sets involved in amino acid biosynthesis (nodes 13, 63, 70, 73) such as tryptophan (69), L-phenylalanine (95) and glycine (62), and GO terms related to primary metabolic pathways such as “glycolytic process” (7) and “tricarboxylic acid cycle” (48), were up-regulated along with protein synthesis related terms such as “translation” (21) and “ribosome biogenesis” (33). Genes included in the “L-phenylalanine biosynthesis” and “tricarboxylic acid cycle” terms encode enzymes involved in the synthesis of precursors required for the two major suberin biosynthetic pathways. Some regulatory terms were down-regulated, such as “protein dephosphorylation” (35) and “calcium ion transmembrane transport” (50), while others, including “histone H3-K9 methylation” (57) and “RNA methylation” (32), were up-regulated. Surprisingly, many stress response terms were down-regulated between 0-0.5 dpw, including the general GO term “response to stress” (39), and more specific stress terms for response to: cold (6), chitin (17), light intensity (18), heat (66), hydrogen peroxide (79), fungus (86), bacterium (92), as well as “jasmonic acid mediated signaling pathway” (24). Many terms that were significantly up- or down-regulated within 0.5 dpw did not change further across the time course and were therefore maintained at steady expression levels after their initial substantial change.

From 0.5 to 1 dpw, “carbohydrate metabolism” (20), “cell wall organization” (10) and “cell wall biogenesis” (22), for which the latter two terms include many genes encoding xyloglucan endotransglucosylase/hydrolases, cellulose synthases, pectinesterases and glycosyltransferases, and several terms associated with the cell cycle that mainly reflect processes involved in mitosis (54, 56, 59, 77, 82, 83, 94) were up-regulated, while terms associated with protein production (21, 33, 61) were down-regulated. Regulatory terms including “histone phosphorylation” (55), which is associated with mitosis and linked to transcriptional activation, “histone H3-K9 methylation” (57), which is associated with transcriptional repression, and “activation of protein kinase activity” (93), were up-regulated. Catabolic process terms differed across this time point comparison; “lignin catabolic process” (60) decreased while “cell wall macromolecule catabolic process” (49) was up-regulated.

Interestingly, only two nodes represented significantly enriched up-regulated terms between 1 and 2 dpw, where one gene set represented “response to abscisic acid” (ABA) (38) and the other term encompassed genes involved in nucleosome assembly (31). The “response to ABA” term includes several transcription factors, such as *MYB102*, the potato ortholog of a regulator of suberin production from Arabidopsis and tomato, as well as the osmotic stress-responsive gene *Asg1*. This time period during wound-healing marks a point at which many processes initially up-regulated quickly after wounding reach a plateau, or subsequently decline in expression. For example, the primary metabolism terms “carbohydrate metabolism” (20) and “tricarboxylic acid cycle” (48), along with many processes related to the mitotic cell cycle and protein synthesis that had been up-regulated at earlier time points, were significantly down-regulated between 1-2 dpw.

Subsequently, the final time point comparison from 2-3 dpw shows the up-regulation of 5 nodes that were not previously enriched during the time course, except for a prior significant down-regulation of “oxidation-reduction process” (5) between 0.5-1 dpw. Three of the up-regulated terms were “fatty acid biosynthesis” (1), “oxidation-reduction process” (5) and “lipid metabolism” (9), where many genes within these terms encode

key aliphatic suberin biosynthetic enzymes, along with genes annotated as acyltransferases, lipases and peroxidases. Among these genes, some are involved in final steps of fatty acid biosynthesis (e.g. ketoacyl-ACP reductase, *KAR*, and β -hydroxyacyl-ACP dehydratase), subsequent elongation (e.g. several ketoacyl-CoA synthases including *KCS6*, fatty acyl-CoA reductases including *FAR3*, and very long chain β -hydroxyacyl-CoA dehydratase), and modification (e.g. fatty acid hydroxylases like the ω -hydroxylase *CYP86A33*) reactions, as well as the final step of glycerol production (glycerol-3-phosphate dehydrogenase (*GPDH*)).

Several genes found up-regulated in the GO term “oxidation-reduction process” are involved in phenylpropanoid metabolism, where some are required for early, general pathway steps (e.g. *p*-coumarate 3-hydroxylase (*C3H*) and *p*-coumaroyl quinate/shikimate 3'-hydroxylase (*C3'H*)), and others encode three consecutive steps towards monolignol biosynthesis (ferulate-5-hydroxylase (*F5H*), cinnamoyl-CoA reductase (*CCR*), and cinnamyl alcohol dehydrogenase (*CAD*)). The presence of these genes within this term is mostly due to significant up-regulation at earlier time point comparisons, but their categorization as up-regulated from 2-3 dpw reflects an increase in these transcripts at the end of the time course, albeit changes are not necessarily of statistical significance.

The other two GO terms up-regulated between 2-3 dpw were “secondary cell wall biogenesis” (40) and “protein phosphorylation” (11). Down-regulated terms included those related to mitosis and the cell cycle that were previously up-regulated (54, 56, 81-83, 91), DNA replication (28, 42, 51, 52, 84), protein translation (21, 33), and post-translational modifications (55, 57). Terms involved in transcriptional repression such as “gene silencing” (44) and “DNA methylation” (53) also decreased in this later stage of wound-healing. GO terms related to the catabolism of: polysaccharides (27), pectin (34), cell wall macromolecules (49), chitin (78) and cellulose (89) were all significantly down-regulated.

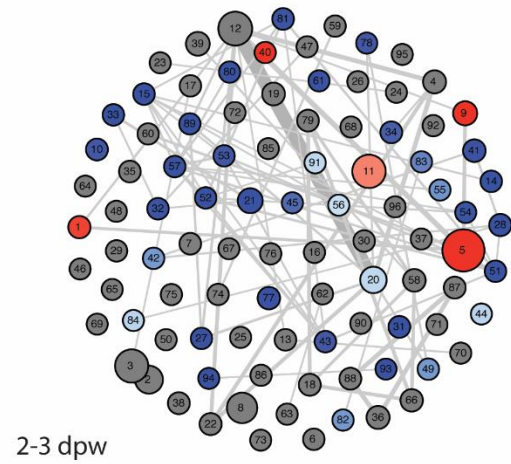
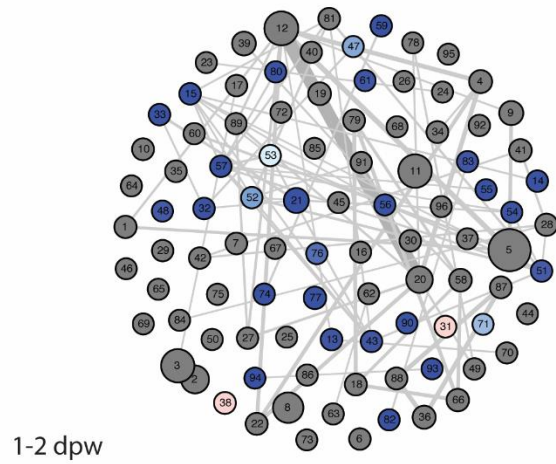
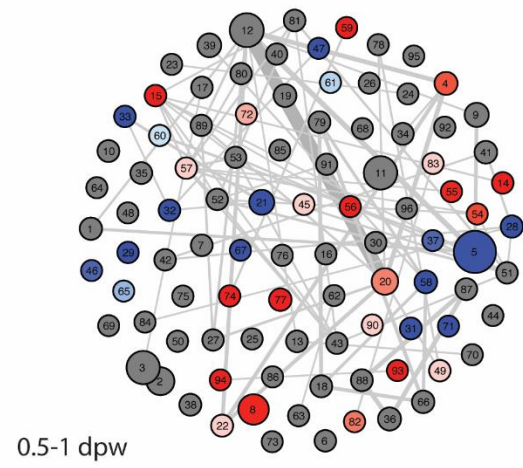
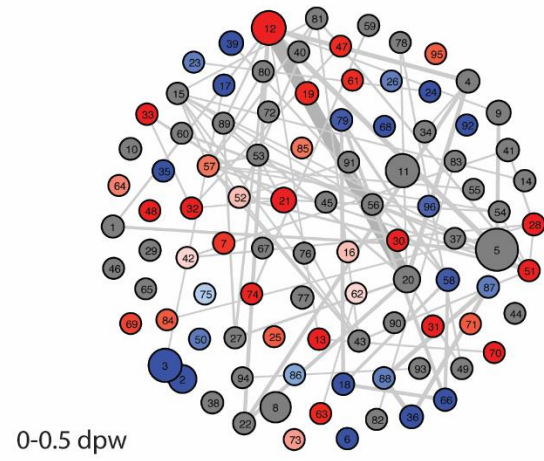
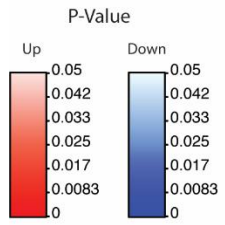


Figure 3.2. Gene set enrichment analysis (GSEA) of biological processes across differentially expressed genes (DEGs) identified in sequential wound-healing time point comparisons. Together, time point comparison panels represent a union parametric analysis of gene set enrichment (PAGE) of biological process (BP) categorized gene ontology (GO) terms. Nodes represent gene sets and their size represents a range from 5-464 genes, and edges show overlapping genes between sets, with width representing ranges from 5-149 genes. Blue sets are down-regulated, red are up-regulated, and grey nodes denote terms that were not detected as significantly differentially regulated (i.e. enriched) at that time point comparison. Labels denote assigned node numbers that correspond to **Table 3.1** with associated GO ID, GO term and regulation overview.

Table 3.1 Summary of gene ontology information represented in biological process gene set enrichment analysis plot and change in terms over time.

Node	GO ID	GO Term	Time point comparison (days post-wounding)			
			0-0.5	0.5-1	1-2	2-3
1	GO:0006633	fatty acid biosynthetic process	-	-	-	↑
2	GO:0006351	transcription, DNA-templated	↓	-	-	-
3	GO:0006355	regulation of transcription, DNA-templated	↓	-	-	-
4	GO:0071555	cell wall organization	-	↑	-	-
5	GO:0055114	oxidation-reduction process	-	↓	-	↑
6	GO:0009409	response to cold	↓	-	-	-
7	GO:0006096	glycolytic process	↑	-	-	-
8	GO:0008150	biological_process	-	↑	-	-
9	GO:0006629	lipid metabolic process	-	-	-	↑
10	GO:0009664	plant-type cell wall organization	-	-	-	↓
11	GO:0006468	protein phosphorylation	-	-	-	↑
12	GO:0008152	metabolic process	↑	-	-	-
13	GO:0008652	cellular amino acid biosynthetic process	↑	-	↓	-
14	GO:0000226	microtubule cytoskeleton organization	-	↑	↓	↓
15	GO:0000911	cytokinesis by cell plate formation	-	↑	↓	↓
16	GO:0010090	trichome morphogenesis	↑	-	-	-
17	GO:0010200	response to chitin	↓	-	-	-
18	GO:0009644	response to high light intensity	↓	-	-	-
19	GO:0032259	methylation	↑	-	-	-
20	GO:0005975	carbohydrate metabolic process	-	↑	-	↓
21	GO:0006412	translation	↑	↓	↓	↓
22	GO:0042546	cell wall biogenesis	-	↑	-	-
23	GO:0006612	protein targeting to membrane	↓	-	-	-
24	GO:0009867	jasmonic acid mediated signaling pathway	↓	-	-	-
25	GO:0016036	cellular response to phosphate starvation	↑	-	-	-
26	GO:0030968	endoplasmic reticulum unfolded protein response	↓	-	-	-
27	GO:0000272	polysaccharide catabolic process	-	-	-	↓
28	GO:0006260	DNA replication	↑	↓	-	↓
29	GO:0006364	rRNA processing	-	↓	-	-
30	GO:0006511	ubiquitin-dependent protein catabolic process	↑	-	-	-
31	GO:0006334	nucleosome assembly	↑	↓	↑	↓
32	GO:0001510	RNA methylation	↑	↓	↓	↓
33	GO:0042254	ribosome biogenesis	↑	↓	↓	↓
34	GO:0045490	pectin catabolic process	-	-	-	↓
35	GO:0006470	protein dephosphorylation	↓	-	-	-
36	GO:0015979	photosynthesis	↓	-	-	-
37	GO:0006541	glutamine metabolic process	-	↓	-	-

38	GO:0009737	response to abscisic acid	-	-	↑	-
39	GO:0006950	response to stress	↓	-	-	-
40	GO:0009834	plant-type secondary cell wall biogenesis	-	-	-	↑
41	GO:0006281	DNA repair	-	-	-	↓
42	GO:0006310	DNA recombination	↑	-	-	↓
43	GO:0009909	regulation of flower development	-	-	↓	↓
44	GO:0016458	gene silencing	-	-	-	↓
45	GO:0048449	floral organ formation	-	↑	-	↓
46	GO:0006333	chromatin assembly or disassembly	-	↓	-	-
47	GO:0006606	protein import into nucleus	↑	↓	↓	-
48	GO:0006099	tricarboxylic acid cycle	↑	-	↓	-
49	GO:0016998	cell wall macromolecule catabolic process	-	↑	-	↓
50	GO:0070588	calcium ion transmembrane transport	↓	-	-	-
51	GO:0006270	DNA replication initiation	↑	-	↓	↓
52	GO:0006275	regulation of DNA replication	↑	-	↓	↓
53	GO:0006306	DNA methylation	-	-	↓	↓
54	GO:0010389	regulation of G2/M transition of mitotic cell cycle	-	↑	↓	↓
55	GO:0016572	histone phosphorylation	-	↑	↓	↓
56	GO:0051225	spindle assembly	-	↑	↓	↓
57	GO:0051567	histone H3-K9 methylation	↑	↑	↓	↓
58	GO:0006457	protein folding	↓	↓	-	-
59	GO:0007010	cytoskeleton organization	-	↑	↓	-
60	GO:0046274	lignin catabolic process	-	↓	-	-
61	GO:0006414	translational elongation	↑	↓	↓	↓
62	GO:0006545	glycine biosynthetic process	↑	-	-	-
63	GO:0006730	one-carbon metabolic process	↑	-	-	-
64	GO:1903959	regulation of anion transmembrane transport	↑	-	-	-
65	GO:0000413	protein peptidyl-prolyl isomerization	-	↓	-	-
66	GO:0009408	response to heat	↓	-	-	-
67	GO:0009553	embryo sac development	-	↓	-	-
68	GO:0030154	cell differentiation	↓	-	-	-
69	GO:0000162	tryptophan biosynthetic process	↑	-	-	-
70	GO:0009073	aromatic amino acid family biosynthetic process	↑	-	-	-
71	GO:0006626	protein targeting to mitochondrion	↑	↓	↓	-
72	GO:0048438	floral whorl development	-	↑	-	-
73	GO:0006807	nitrogen compound metabolic process	↑	-	-	-
74	GO:0007017	microtubule-based process	↑	↑	↓	-
75	GO:0007623	circadian rhythm	↓	-	-	-
76	GO:0007059	chromosome segregation	-	-	↓	-
77	GO:0007018	microtubule-based movement	-	↑	↓	↓
78	GO:0006032	chitin catabolic process	-	-	-	↓
79	GO:0042542	response to hydrogen peroxide	↓	-	-	-

80	GO:0006342	chromatin silencing	-	-	↓	↓
81	GO:0008283	cell proliferation	-	-	-	↓
82	GO:0000278	mitotic cell cycle	-	↑	↓	↓
83	GO:0007049	cell cycle	-	↑	↓	↓
84	GO:0032508	DNA duplex unwinding	↑	-	-	↓
85	GO:0035999	tetrahydrofolate interconversion	↑	-	-	-
86	GO:0009620	response to fungus	↓	-	-	-
87	GO:0009765	photosynthesis, light harvesting	↓	-	-	-
88	GO:0018298	protein-chromophore linkage	↓	-	-	-
89	GO:0030245	cellulose catabolic process	-	-	-	↓
90	GO:0030048	actin filament-based movement	-	↑	↓	-
91	GO:0051726	regulation of cell cycle	-	-	-	↓
92	GO:0009617	response to bacterium	↓	-	-	-
93	GO:0032147	activation of protein kinase activity	-	↑	↓	↓
94	GO:0060236	regulation of mitotic spindle organization	-	↑	↓	↓
95	GO:0009094	L-phenylalanine biosynthetic process	↑	-	-	-
96	GO:0048317	seed morphogenesis	↓	-	-	-

Biological process (BP) terms offer insights relevant to wound-healing and associated suberization events largely reflected by metabolic pathway, signaling and regulatory terms. Molecular function (MF) and cellular component (CC) GO term analyses were also conducted to further supplement BP findings by providing information about mechanisms relating to molecular interactions, and the sub-cellular localization of these events, respectively.

In the MF term analysis, 67 gene sets comprising 2648 genes from the DEG list changed significantly over time (**Figure C1, Table C2**). Between 0-0.5 dpw, up-regulated terms included those involved in enzyme-mediated catalytic activities (e.g. ligase, 12; isomerase 22; *O*-methyltransferase, 36; oxidoreductase, 41; and general catalytic activities, 21), while many binding functions (i.e. selective and non-covalent interactions) were down-regulated (4, 44, 58, 60, 62), except for “protein heterodimerization” (19) and “RNA binding” (20), which increased. Most of these initially up-regulated enzyme activity terms decreased by 0.5-1 dpw except for “*O*-methyltransferase activity” (36), which did not change again until further up-regulation between 2-3 dpw, and “protein heterodimerization” (19), a term that alternated between up- and down-regulation for each successive time point comparison. The majority of changing genes in this term that are initially up-regulated encode all four core histones and some variants, and their expression drives the overall node directional statistic. Other genes within this term act mostly in an opposite temporal pattern and encode transcription factors such as CCAAT-binding proteins. Some terms related to oxidoreductase activities were down-regulated between 0.5-1 dpw, did not change further between 1-2 dpw, then were significantly up-regulated 2-3 dpw (9, 29, 41, 48), as observed for the BP oxidation-reduction term. Several general transferase activity terms (7, 8, 34) as well as “*O*-methyltransferase activity” (36) and “acyltransferase activity” (39) were significantly up-regulated during late stages of the time course, along with “peroxidase activity” (43), which also overlap with genes comprising BP terms enriched in the 2-3 dpw time point comparison.

In the CC term analysis, 38 significantly regulated gene sets changed over the time course, with 2641 DEGs represented by enriched terms (**Figure C2, Table C3**). Many

initially up-regulated GO terms reflected cellular machinery involved in protein synthesis (“ribosome”, 13, and “small ribosomal subunit”, 30) and cell cycle components (e.g. “nucleolus”, 15, “cytoskeleton”, 23, “microtubule”, 29), while these terms were down-regulated across later points of the time course. The cell wall term was up-regulated between 0.5-1 dpw, maintained between 1-2 dpw, then significantly down-regulated between 2-3 dpw, which is similar in trend for cell wall-related BP terms, except for the secondary cell wall-specific BP term. “Golgi apparatus” (5), “membrane” (1) and “integral membrane” (2) were the only cellular components that were up-regulated between days 2-3 post-wounding. The latter term is made up of hundreds of genes, of which those up-regulated at this time point comparison include known and putative suberin-deposition related ABC subfamily G transporters, *ABCG1*, *ABCG6* and *ABCG11*, as well as other uncharacterized ABC and MDR family transporters, and genes encoding Casparian strip membrane (CASP) or CASP-like (CASPL) proteins, including *CASP8* and *CASP9*. Other genes up-regulated between 2-d dpw with involvement in esterification of aliphatic suberin monomers to glycerol (*GPAT5* and *GPAT6*) or to feruloyl-CoA (*FHT*) were also included in this term.

3.3.5 Wound-induced transcriptional changes: the long and winding road to suberin assembly

A broad roadmap to suberin production was generated with associated transcriptome data to provide a comprehensive overview of the expression patterns for all characterized and putative potato suberin-related metabolic events throughout the wound-healing time course (<https://www.uwo.ca/biology/faculty/bernards/research/index.html> under “Suberin Roadmap”; **Figure 3.3**). This scheme was constructed using a previous model (Bernards, 2002) as a basis for pathway steps, but updated to incorporate current knowledge and recent advances in our understanding of suberin biosynthesis. This hypothetical framework was used to probe RNA-seq data for expression of relevant steps, and by incorporating transcriptomic data into the overview, gene expression information helped to guide the formation of the new roadmap.

Roadmap to Suberin

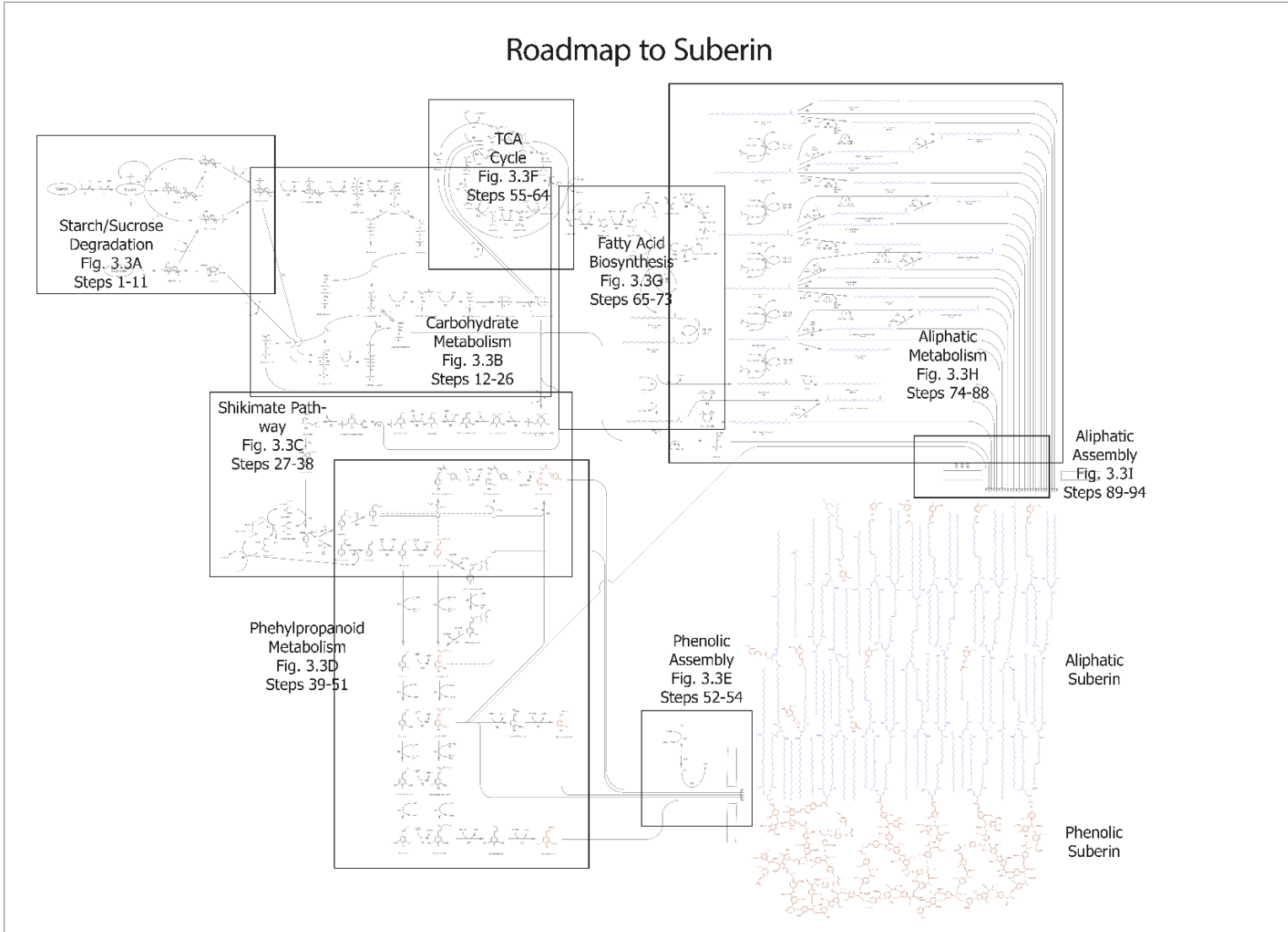


Figure 3.3. Roadmap to suberin biosynthesis and assembly. **A.** Starch and sucrose degradation. **B.** Carbohydrate metabolism **C.** Shikimate pathway **D.** Phenylpropanoid metabolism **E.** Phenolic suberin assembly **F.** Tricarboxylic acid (TCA) cycle **G.** Fatty acid biosynthesis **H.** Aliphatic metabolism **I.** Aliphatic suberin assembly. Panels comprise detailed pathway branch figures, in which final monomers destined for SPPD incorporation are red and SPAD components are blue, and corresponding heatmaps to demonstrate changes in transcript accumulation of known and putative genes that encode pathway steps involved in suberin biosynthesis and assembly over the wound-healing time course. Log₂FPKM means for n=3 biological replicates are presented for each time point. Numbered pathway steps correspond to numbers on heatmaps, and to numbers in the associated supplemental screening figure and table that include gene ID information (**Figure C3; Table C4**).

Our previous work, which integrated gene expression and metabolite accumulation data, demonstrated the differential temporal regulation of aliphatic and phenolic suberin biosynthesis and assembly (Woolfson et al., 2018). The generation of this transcriptomic dataset made it possible to explore an extensive, targeted list of wound-healing and suberin-related genes of interest and observe how they change during the time course at an individual level, but also in conjunction with other genes from shared pathways. This approach was also used to provide support for hypothesized steps towards suberization and to identify candidates for further investigation.

$\text{Log}_2(\text{FPKM})$ values for each target gene at each time point were used for heatmap visualization of changes for each target gene throughout wound-healing. Each gene corresponds to a known or predicted enzyme involved in the pathway towards suberin biosynthesis and assembly. This pathway comprises various branches of metabolism required for suberin production. The earliest steps involve primary metabolic processes for starch and sucrose degradation (steps 1-11, **Figure 3.3A**), carbohydrate metabolism (steps 12-26, **Figure 3.3B**), the shikimate pathway (steps 27-38, **Figure 3.3C**), the tricarboxylic acid cycle (steps 55-64, **Figure 3.3F**) and fatty acid biosynthesis (steps 65-73, **Figure 3.3G**), which yield energy and precursor molecules that fuel and feed into downstream, suberin-specific metabolism. Phenylpropanoid metabolism (steps 39-51, **Figure 3.3D**) and aliphatic metabolism (steps 74-88, **Figure 3.3H**) produce final suberin monomers that then undergo transport and linkage via respective phenolic (steps 52-54, **Figure 3.3E**) and aliphatic suberin assembly steps (steps 89-94, **Figure 3.3I**) to build and deposit the heteropolymer. Genes presented in **Figure 3.3** were selected from a larger pool of candidates (**Figure C3, Table C4**), from which a maximum of three representative genes were selected per enzymatic step based on expression levels and wound-induction profiles, wherever possible.

3.3.5.1 Starch degradation and carbohydrate metabolism

Starch and sucrose degradation and carbohydrate metabolism pathways comprise genes involved in starch breakdown (steps 1-11; **Figure 3.3A**) that mostly yield glucose and its phosphorylated products, mainly glucose-6-phosphate (G6P), used as a precursor for the

ATP-, NADH- and pyruvate-generating glycolytic pathway (7, 12, 19-26), and its parallel pentose phosphate pathway (13-18), which yields 5-carbon sugars and NADPH (**Figure 3.3B**).

Most de-branching steps of starch metabolism (1-6) were already expressed at 0 dpw and either decreased or increased slightly by 0.5 dpw, then exhibited consistent levels of transcript accumulation for the duration of the time course. Here β -amylase (5.1) exhibited the highest expression levels that were maintained over time. The two types of phosphorylases that yield G6P (hexokinase, step 7) and G1P (α -1,4 glucan phosphorylase, step 8) displayed different patterns after wounding, where hexokinase expression slightly increased after wounding, but α -1,4 glucan phosphorylases dropped to lower mRNA levels between 0 and 0.5 dpw, then did not change further. One gene encoding a glycosyltransferase for sucrose synthesis (10.1) demonstrated a down-regulation from 0-0.5 dpw, followed by a gradual increase over the time course, achieving its peak expression at 3 dpw. The expression levels of G6P-forming phosphoglucomutase (9) and the UTP-glucose generating uridylyltransferase (11) did not appear to be altered by wounding, as they remained consistent over all time points.

Generally, at least one gene encoding each enzymatic step of the glycolytic pathway was up-regulated from 0 to 0.5 dpw, and retained consistent expression until 3 dpw, where several achieve their highest FPKM levels by 1 dpw. The rate-limiting phosphofructokinase-catalyzed step and one enolase-encoding gene were exceptions, since their transcript levels did not change between the first two time points. That is, phosphofructokinase expression remained steady until 3 dpw, while enolase expression dropped slightly at 2 dpw. The final step for pyruvate biosynthesis, encoded by pyruvate kinase (26), was up-regulated between 0 and 0.5 dpw, and mostly present at consistent transcript levels over time.

The pentose phosphate sub-branch of carbohydrate metabolism showed similar patterns of expression over time (i.e. an initial increase in FKPM by 0.5 dpw), although slightly lower levels relative to glycolysis genes. The most highly expressed genes within this pathway shared the aforementioned pattern of expression, which includes at least one

gene encoding each NADPH-yielding dehydrogenase step (13.1 and 15.1) in the oxidative ribulose-5-phosphate producing pathway, as well as the transketolase (18.1) responsible for non-oxidative synthesis of sugars including fructose-6-phosphate.

Among all sub-pathways within carbohydrate metabolism, the steps required for starch degradation and the pentose phosphate pathway generally had lower log₂FPKM values than genes involved in glycolysis, and within sub-branches, different expression patterns were also observed.

3.3.5.2 Shikimate pathway

The shikimate pathway bridges carbohydrate and phenylpropanoid metabolism via the production of aromatic amino acids phenylalanine, tyrosine and tryptophan, where the former two are required for SPPD monomer biosynthesis. These products are synthesized using the phospho*enol*-pyruvate-derived intermediate prephenate (via steps 27-33) and glutamate as a nitrogen source (steps 34-36) that yields arogenate, followed by either dehydratase (37) or dehydrogenase (38) conversion into phenylalanine, or tyrosine, respectively (**Figure 3.3C**). Most genes in this pathway were expressed at 0 dpw, except for three genes with undetectable transcripts at this time point (3-dehydroquinase dehydratase/shikimate dehydrogenase, 29.1; 3-phosphoshikimate 1-carboxyvinyltransferase, 31.2; glutamine synthetase, 35.3), then were subsequently up-regulated between 0 and 0.5 dpw. The most highly expressed genes within this pathway include the first committed pathway step, DAHP synthase (27.1), and glutamine synthetase (GS, 35.1), a key nitrogen metabolism enzyme that makes the transamination of prephenate possible.

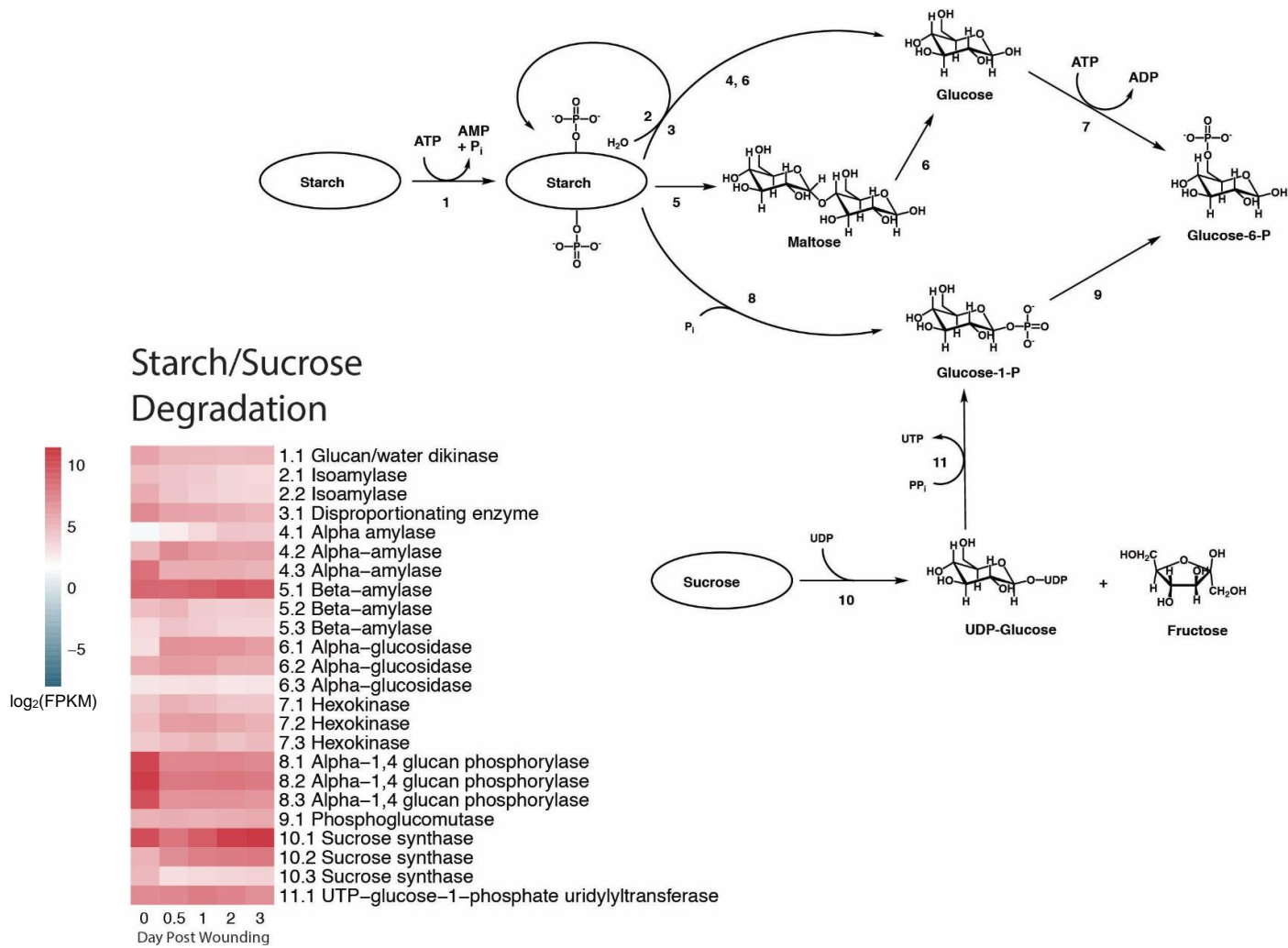


Figure 3.3A. Starch and sucrose degradation.

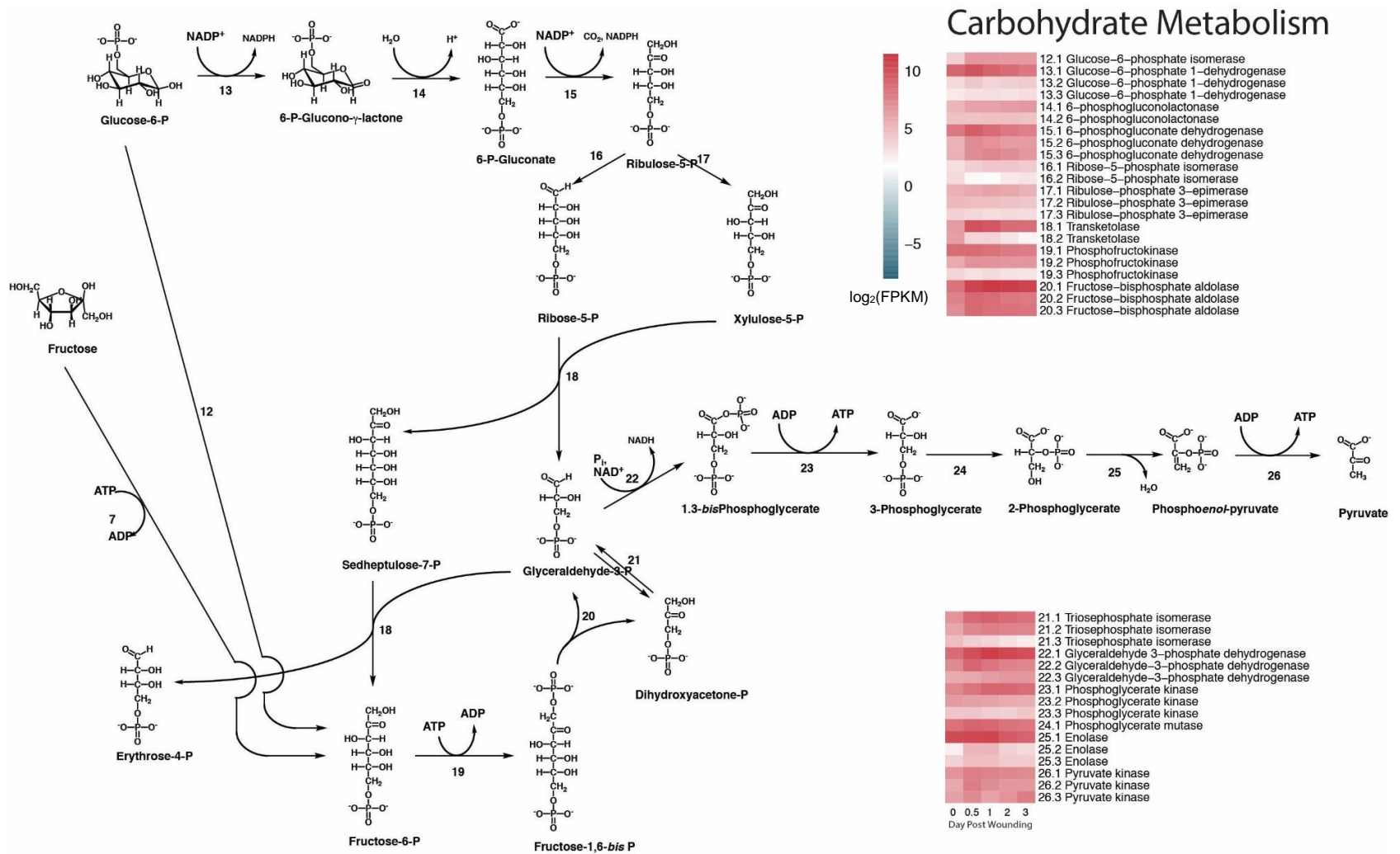


Figure 3.3B. Carbohydrate metabolism.

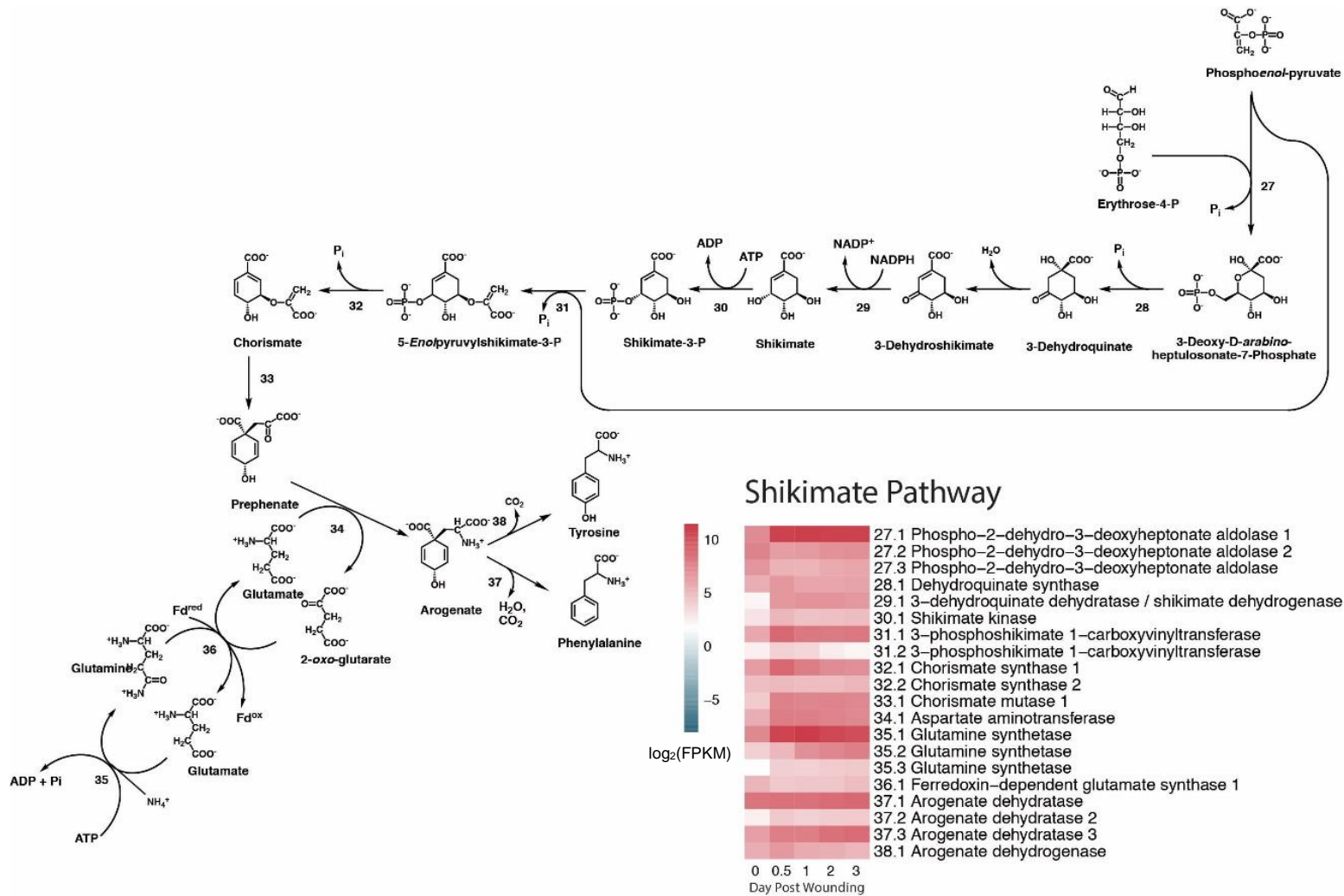


Figure 3.3C. Shikimate pathway.

3.3.5.3 Phenylpropanoid pathway

Different sub-branches of genes implicated in phenylpropanoid metabolism that yield polar suberin monomers, monolignols and hydroxycinnamic acid amides, were up-regulated at different points during wound-healing and demonstrated varied expression patterns over time (**Figure 3.3D**). Generally, most genes were expressed at 0 dpw, except for some *O*-methyltransferases (46.1, 47.2 and 47.3) and the monolignol biosynthetic genes cinnamoyl CoA reductase (49.1) and cinnamyl alcohol dehydrogenase (50.2), which exhibited very little to no expression at 0 dpw.

Genes encoding steps required for synthesis of hydroxycinnamates and their thioesters (steps 40-48) were up-regulated by 0.5 dpw, and were maintained at high levels throughout the duration of the time course. The main exception was p-coumaroyl quinate/shikimate 3'-hydroxylase (45.1), which was present at its highest levels on 0 dpw, then decreased over time.

Tyrosine decarboxylase (39.1) catalyzes the conversion of tyrosine to tyramine as a precursor for hydroxycinnamic acid amide (HCAA) synthesis, and its transcripts were very low and did not exceed log₂FPKM value over 2 until 3 dpw. The only gene in this pathway that utilizes tyramine as substrate, tyramine hydroxycinnamoyl transferase (THT, 51.1), was expressed throughout the time course, albeit at lower levels than those required for synthesis of other SPPD monomers like feruloyl-CoA, which is required for HCAA and also a known substrate of THT. Monolignol-specific biosynthetic genes (49-50) also showed different patterns than the majority of genes in this branch, where expression levels gradually increased over time and peaked at 3 dpw.

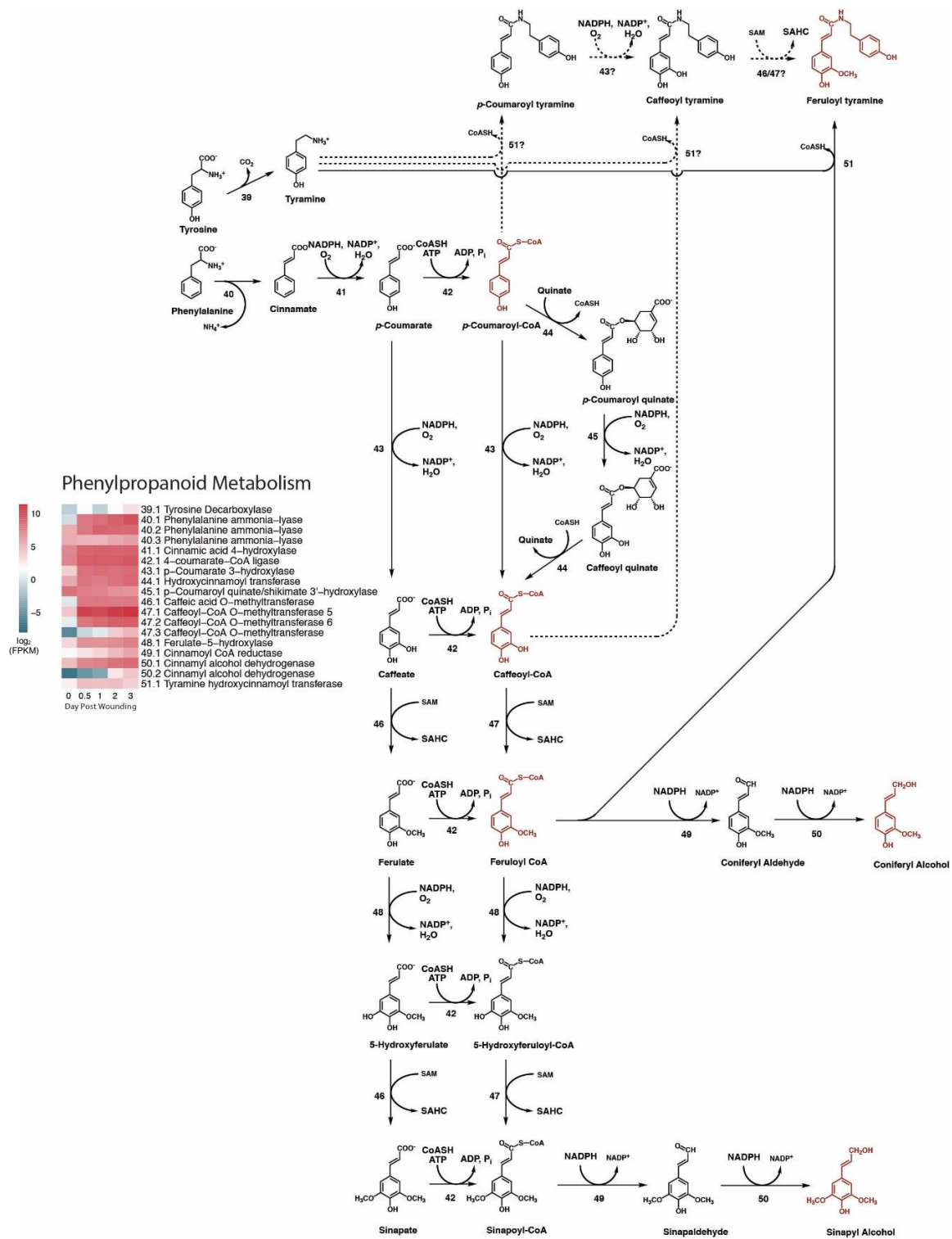


Figure 3.3D. Phenylpropanoid pathway.

3.3.5.4 Phenolic suberin assembly

Most phenolic suberin assembly genes demonstrated similarly consistent FPKM levels over time, but generally at lower levels than the biosynthetic branch (**Figure 3.3E**). NADPH-dependent oxidases were generally expressed throughout the time course, although one encoding gene (52.1) was at its peak expression at 0 dpw, whereas another (52.2) was not expressed until 0.5 dpw and reached its highest expression at 3 dpw. Two superoxide dismutases (53.1-53.2) were expressed consistently over time, but levels of the former were ca. 3.5 log₂-fold greater than the latter, and the third gene (53.3) was not expressed from 0.5-3 dpw. The suberization-associated anionic peroxidases (54.1-54.2) demonstrated different temporal patterns than other assembly genes since they increased gradually in expression over time, in which the induction of one (54.1) preceded the other (54.2) by as much as 12 hours.

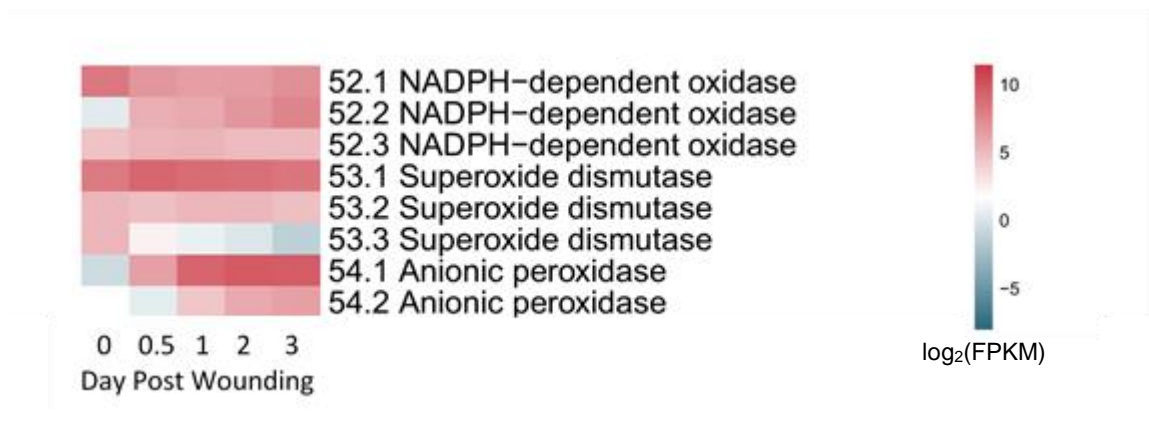


Figure 3.3E. Phenolic suberin assembly.

3.3.5.5 Tricarboxylic acid cycle

Another metabolic fate for phosphoenolpyruvate is conversion to pyruvate and entry into the tricarboxylic acid (TCA) cycle, which yields acetyl-CoA required for fatty acid biosynthesis, and NADH that is used in the electron transport chain to generate ATP (**Figure 3.3F**). Most genes encoding TCA cycle enzymes and complex components were expressed at 0 dpw, except for one citrate synthase gene (57.3). Two pyruvate dehydrogenase complex subunits (55.1 and 55.3) involved in the initial production of

acetyl-CoA, and citrate synthase (57.1) that yields citrate from pyruvate-derived oxaloacetate and acetyl-CoA, continued to increase in transcript abundance, reaching their maximum expression levels on 3 dpw, and phosphoenolpyruvate carboxylases (56.1-56.2) that synthesize oxaloacetate decreased after 0 dpw. The remaining genes that encode subsequent pathway steps (58-64) were up-regulated to their maximal levels at 0.5 dpw, and remained at similar transcript abundances through to 3 dpw. Fumarase (step 63) transcript abundance could not be assessed as it did not have an associated PGSC-based gene ID.

3.3.5.6 Fatty acid biosynthesis

Fatty acid biosynthesis requires acetyl-CoA, generated by citrate lyase (step 65), acting on citrate exported from mitochondria. This step was up-regulated between 0-0.5 dpw (**Figure 3.3G**). The subsequent steps involved in acetyl-CoA carboxylation (step 66) to form malonyl-CoA and transfer of activated malonyl-CoA to the acyl carrier protein (ACP, step 67) and all subsequent elongation steps by the fatty acid synthase complex (FAS, steps 68-71) followed similar induction patterns and maintained fairly consistent expression levels between 0.5-3 dpw. The steroyl-ACP (18:0) product of the FAS is then either released as 18:0 stearic acid (step 72), or desaturated to 18:1 oleic acid (step 73). The transcript abundance of the desaturase (73.1) was higher than that of the thioesterase (72.1), especially at 0 dpw. Otherwise, they shared similar profiles with all other genes in this pathway.

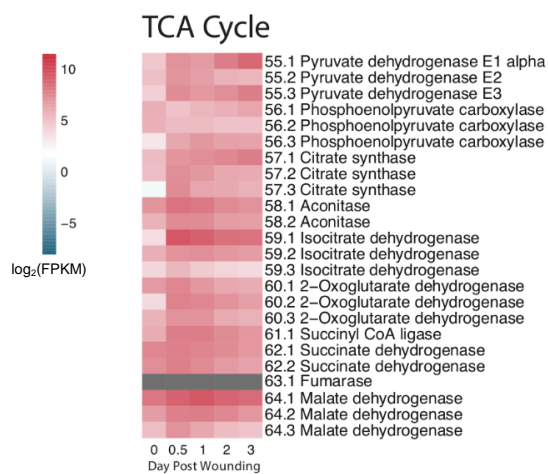
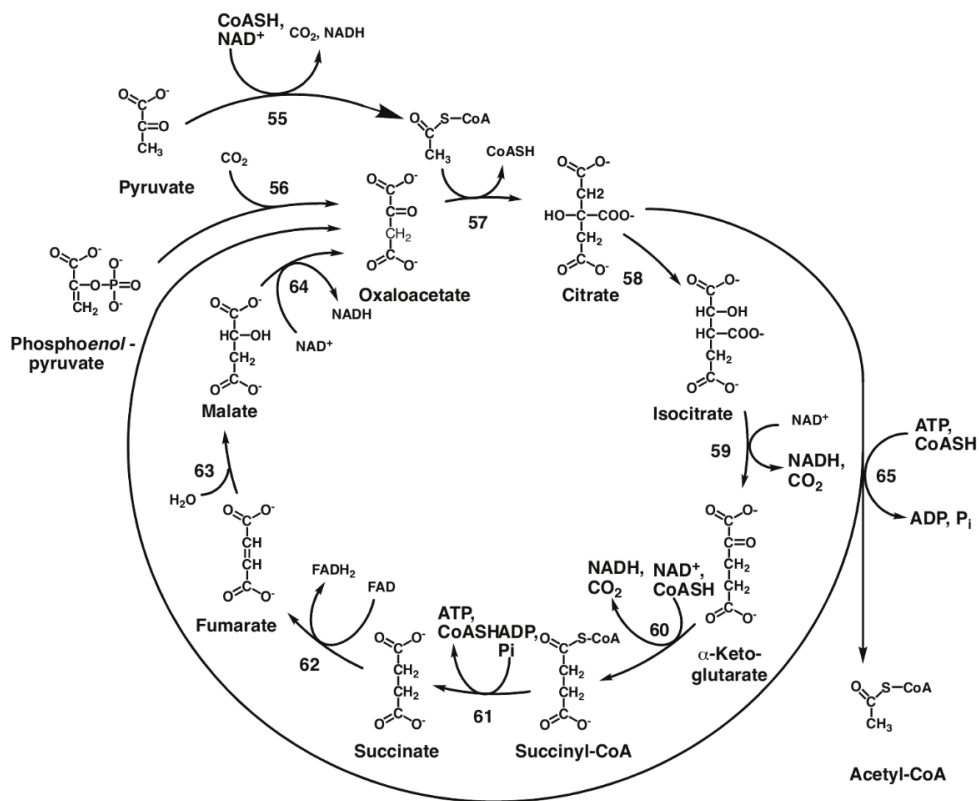


Figure 3.3F. Tricarboxylic acid cycle. Fumarase (step 63) is included as a step in the pathway, but is shown in grey because its sequence did not have a corresponding PGSC gene identification number, and therefore transcript abundance could not be estimated in this study.

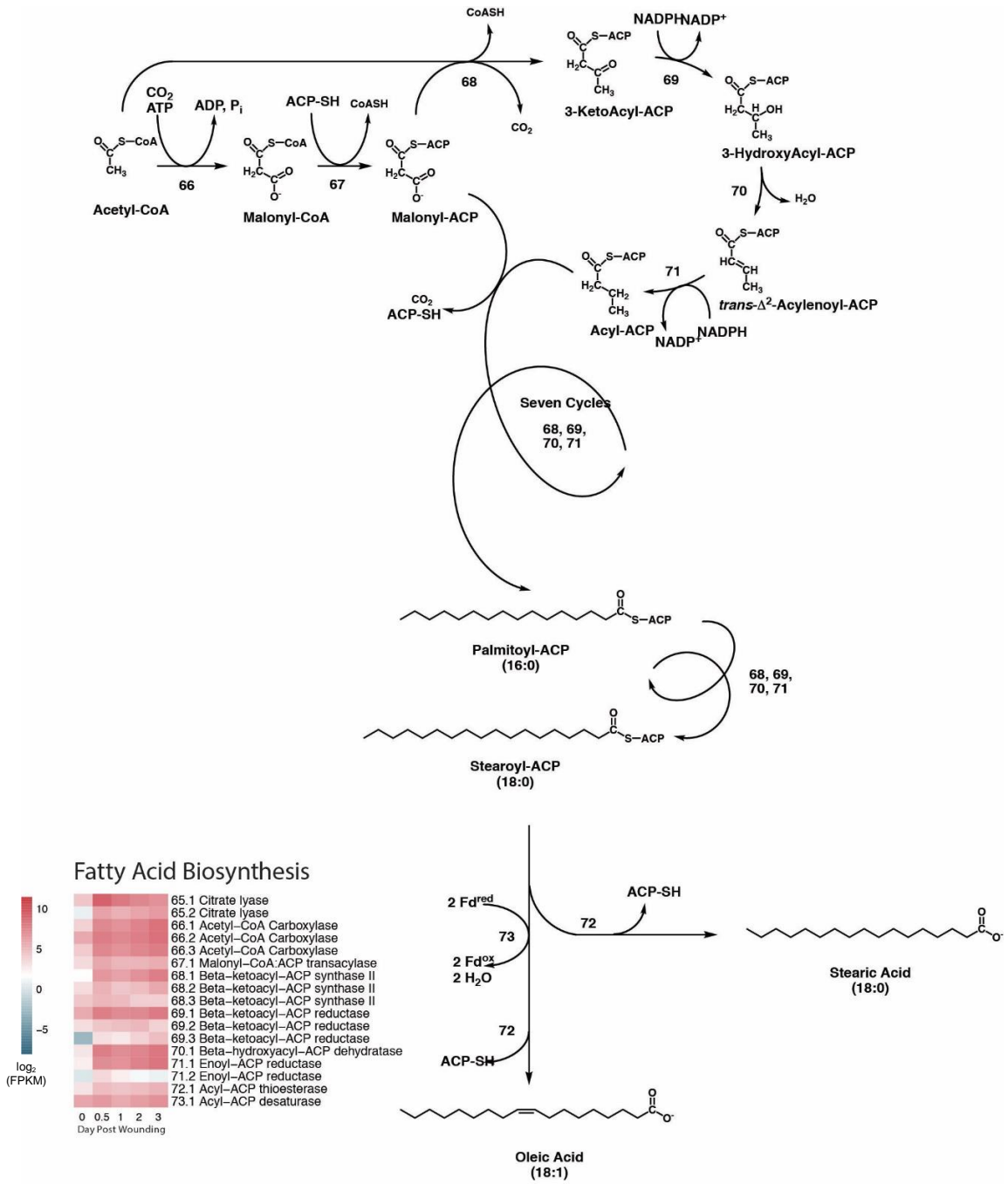


Figure 3.3G. Fatty acid biosynthesis.

3.3.5.7 Aliphatic metabolism

Stearic acid (18:0) and oleic acid (18:1) from the fatty acid biosynthesis pathway are used as substrates for further modifications to yield aliphatic suberin monomers, including chain elongation (74-77), hydroxylation (79-82), acyl reduction (83), acyl chain activation (84) and decarboxylation (85-86) (**Figure 3.3H**). Some modifying enzymes act directly on 18C fatty acids from the previous pathway (steps 78-81), and others use VLCFA substrates after elongation steps (steps 82-87).

In contrast to other pathways that yield precursors or phenolic monomers, genes related to specialized and more final aliphatic monomer biosynthesis were not up-regulated until later time points (days 1 or 2 post-wounding), and typically increased gradually over time, until reaching their highest log₂FPKM levels on day 3 of wound-healing. Temporal patterns were also observed within these pathways branches. For example, other than the gene encoding the first subunit of the FAS complex (74), the transcripts of most chain elongation steps (75-77) accumulated by 0 or 0.5 dpw, which is up to two days earlier than other fatty acid modification genes such hydroxylation (79-82), reduction (83), acyl chain activation (84) and decarboxylation steps (85-86), which encode enzymes that use long chain fatty acids as substrates. An exception to this general pattern is the putative α,ω -dioic acid forming hydroxylase, CYP94A26 (81.3), which is highest at 0 dpw. Other sub-branches within this pathway expressed different patterns than most modification genes, but showed temporal patterns consistent with elongation genes, including CER-interacting cytochrome b_{5s} (step 87) and glycerol-forming dehydrogenases (step 88).

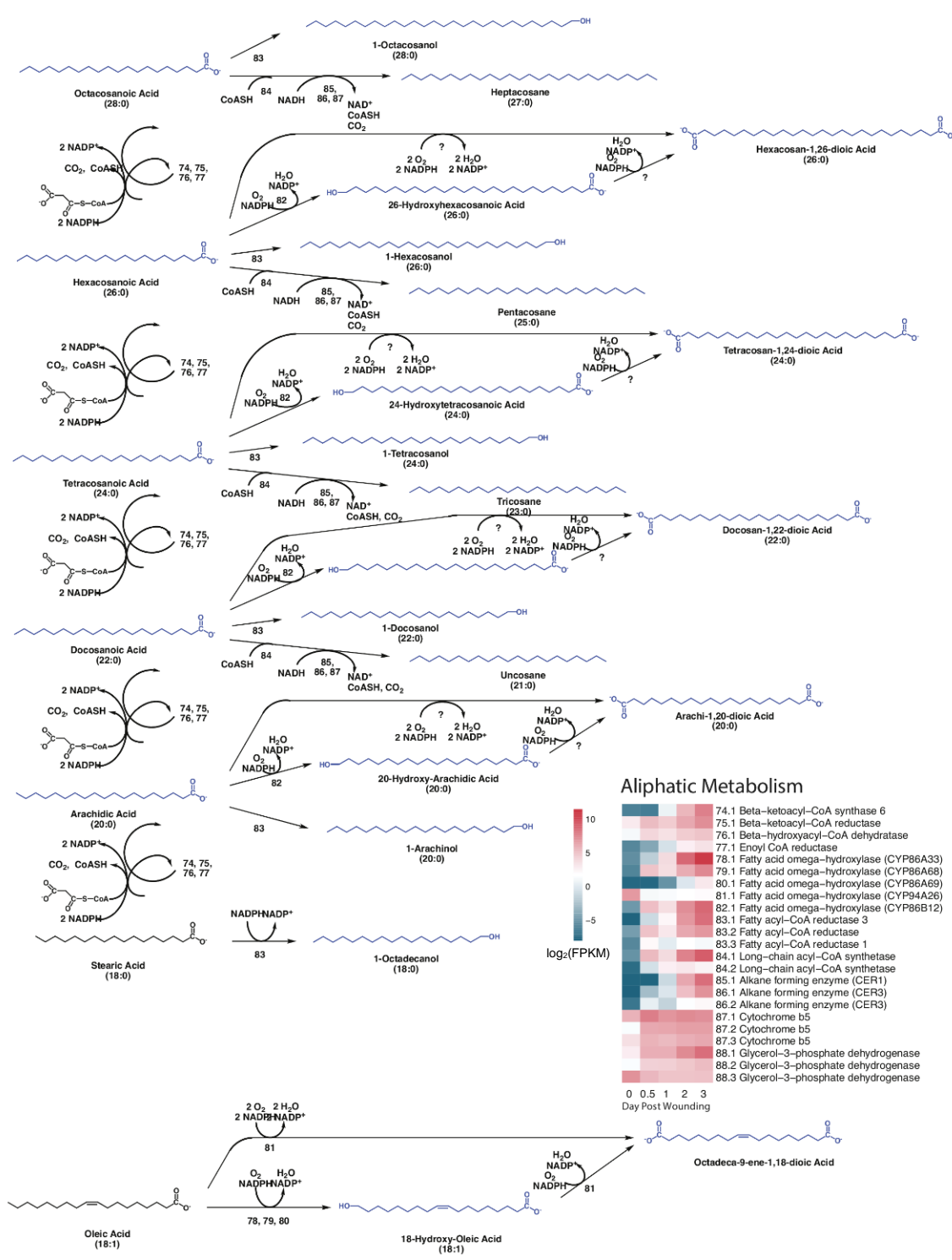


Figure 3.3H. Aliphatic metabolism.

3.3.5.8 Aliphatic suberin assembly

Genes that encode enzymatic steps involved in aliphatic suberin linkage (e.g. to feruloyl-CoA, step 89, or to glycerol, step 90) and deposition by ABC transporters (92-94) demonstrated clear wound-induction profiles as seen for many fatty acid modification genes (**Figure 3.3I**). For example, *FHT* (89.1) was strongly up-regulated more than 10 \log_2 -fold between 0 to 0.5 dpw, and the *GPATs* (90.1-91.1) were up-regulated 8 and 9 \log_2 -fold, respectively. *ABCG1* (92.1) increased 3 \log_2 -fold by 0.5 dpw, and two ABC transporters (93.1-93.4) did not have detectable transcript accumulation until 2 dpw, following greater than 4 \log_2 -fold up-regulation from 1 dpw.

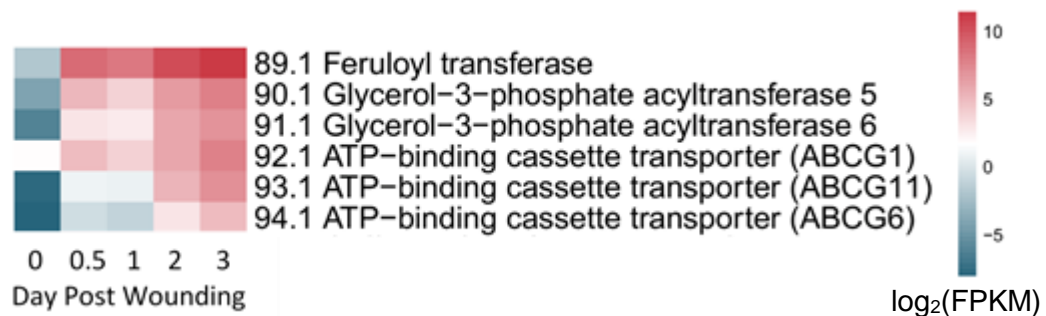


Figure 3.3I. Aliphatic suberin assembly.

3.3.6 Evaluation of suberin assembly candidates

Many biochemical steps for suberin monomer synthesis are known or can be predicted, but aside from the participation of peroxidase in SPPD production, and enzymatic esterification and deposition steps involved in SPAD assembly, no mechanisms have been established for the overall polymerization, assembly and organization of either domain. Since proposed mechanisms are analogous to those known for cutin polymerization and lignin-based Casparian strip assembly, putative potato homologs and/or protein family members of characterized cutin synthases and Casparian strip membrane (CASP) and CASP-like (CASPL) proteins were identified and evaluated for potential involvement in wound-induced tuber suberization. All annotated potato CASPs

were included in this analysis, of which *CASP8* (C.12) and *CASP9* (C.13) are expressed during periderm maturation (**Figure C4, Table C5**).

The putative potato homolog of tomato cutin synthase (SlCDS1/CUS1), *StCDS1* (G.1) along with many similar proteins that were either annotated as putative members of the GDSL-esterase/lipase family, or annotated as zinc finger domain-containing proteins and are homologs of Arabidopsis and tomato GDSL or CUS proteins (G.2-G.8), were incorporated in this analysis to investigate a possible role for these in the wound-healing suberin biosynthetic process (**Figure C4, Table C6**).

Preliminary screening in which putative *CASP* and *GDSL* genes were clustered demonstrated that over half of genes encoding *CASP*/*CASPL* and *GDSL* family proteins were not expressed in the time course (**Figure C4, Table C5-C6**). Of those *CASP*-encoding genes that were expressed, *CASP8* (C.12) and *CASP9* (C.13) and *CASP GSVIVT00013434001* (C.14) displayed the highest \log_2 FPKM values and clustered together, with 18 others demonstrating some level of expression during the time course. Only two of eight genes encoding *GDSL*-type proteins were expressed (G.6 and G.7), which did not include the SlCDS1 likely ortholog, *StCDS1* (G.1).

The 21 expressed *CASP* and two *GDSL* candidates were included in another clustering analysis with previously outlined suberin phenolic and aliphatic assembly genes to generate hypotheses about their potential involvement in certain pathways (**Figure 3.4**). Five of the most highly expressed candidates (*CASP8*, C.12; *CASP9* C.13; *CASP GSVIVT00013434001*, C.14; and *GDSL*, G.7) followed similar temporal patterns, in which no transcripts were detected until 0.5 dpw, and continued to increase until 3 dpw. These genes clustered together with a phenolic assembly branch peroxidase (54.1), GPATs involved in glycerol linkage to aliphatic monomers (90.1 and 90.2), and a gene that represents a point of convergence between the phenolic and aliphatic pathways, feruloyl transferase (FHT, 89.1), that esterifies aliphatic monomers to phenylpropanoid pathway-derived feruloyl-CoA. Another highly expressed *GDSL* candidate, G.7, exhibited a similar profile, but was not initially up-regulated until 1 dpw, and another *CASP* candidate (C.17) followed the same temporal pattern, but with lower overall

expression levels. These genes clustered with two putative ABC transporters, ABCG6 (94.1) and ABCG11 (93.1) with hypothetical involvement in aliphatic suberin deposition.

Two *CASP* candidates, C.33 and C.34, were not expressed at 0 dpw, initially up-regulated at 0.5 dpw, and then decreased in expression, and closely followed expression patterns of the known assembly genes that they clustered with, including the aliphatic transporter *ABCG1* (92.1), *NADPH-dependent oxidase* (52.2) and *anionic oxidase* (54.2). Other *CASP* candidates that were expressed more consistently over time grouped together with genes that are implicated in phenolic suberin assembly, including two NADPH-dependent oxidases (52.1, 52.3) and two superoxide dismutase genes (53.1, 53.2). Several candidate *CASPs* clustered with another superoxide dismutase gene (53.3), and all shared very low, consistent expression levels.

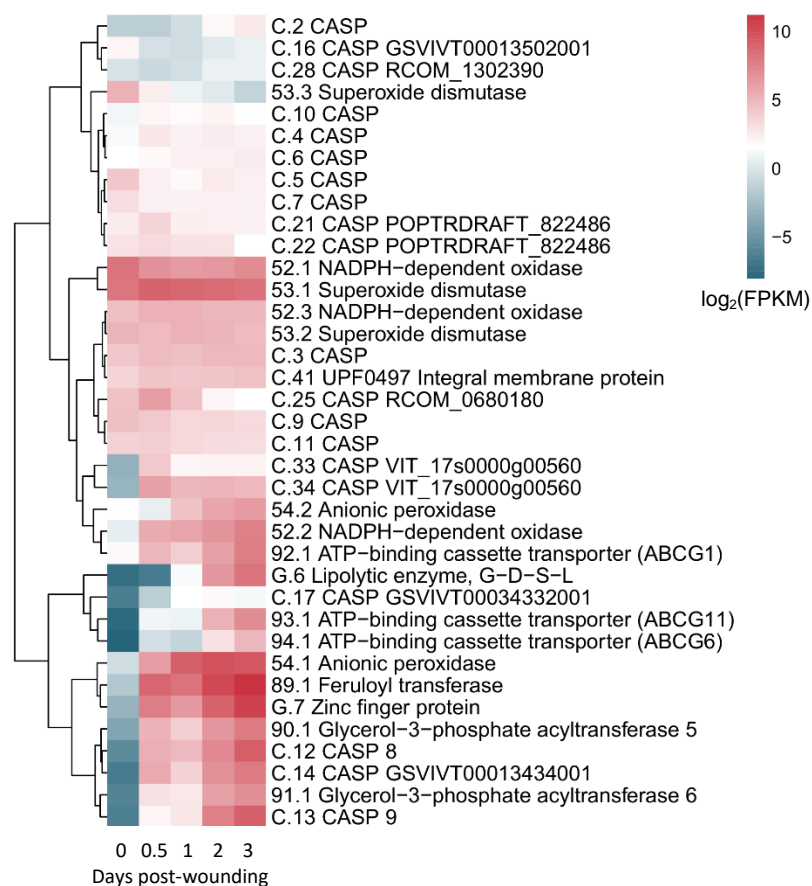


Figure 3.4. Hierarchical clustering analysis of known and putative suberin assembly genes with newly identified candidate genes. Genes included have putative predicted roles in aliphatic monomer polymerization (GDSLs, denoted by G), and recruitment and organization of machinery for assembly of the suberin polymer (CASPs, denoted by C) over the wound-healing time course. Biological replicate means of $n=3$ log₂FPKM values are presented for each time point.

3.3.7 Changes in abscisic acid metabolism after wounding

A role for abscisic acid (ABA) was previously implicated in the regulation of aliphatic suberin biosynthesis, linkage and deposition genes during wound-induced suberization. Genes involved in ABA synthesis and degradation were therefore targeted for analysis to better characterize the timing of ABA metabolism during the wound response and gain insight into its regulatory role. ABA is derived from β -carotene, therefore early isoprenoid and carotenoid biosynthetic genes were included in our analysis to establish expression patterns for pathways that provide the required precursors (**Figure 3.5, Table C7**). For the isoprenoid pathway (steps 1-11), all genes showed some level of expression at 0 dpw, and most were up-regulated to their highest levels (e.g. steps 2, 5-8, 10-11) by 0.5 dpw. The most clear exception to this pattern is that of geranyl diphosphate synthase (step 9), which was down-regulated to nearly undetectable levels by 0.5 dpw.

Interestingly, the gene encoding the enzyme for the following step that utilizes geranyl diphosphate as substrate, farnesyl diphosphate synthase, displayed the highest level of expression across all isoprenoid genes at 0.5 dpw. Genes for later steps of the pathway that yield the intermediate geranylgeranyl pyrophosphate, which is a precursor for carotenoid synthesis, remained consistently expressed throughout the time course (**Figure 3.5A**)

Carotenoid pathway genes (steps 12-14) mostly exhibited their highest expression levels at 0 dpw, which decreased to undetectable levels by 1 dpw for the earliest steps, phytoene synthase (12.1-12.2) and phytoene desaturase (13.1). Lycopene β -cyclase catalyzes the final step of β -carotene biosynthesis, and its encoding genes (14.1-14.2) demonstrated lower \log_2 FPKM levels than earlier steps, but remained consistent over the time course, and increased slightly by 3 dpw.

Transcripts associated with at least one functionally annotated version of each ABA biosynthesis gene (steps 15-20) were detected at 0 dpw, albeit at lower levels than most isoprenoid biosynthetic genes (**Figure 3.5B**). Steps involved in the initial conversion of β -carotene were down-regulated after 0 dpw. In contrast to carotenoid and early ABA biosynthetic steps, genes encoding later steps (17-20) were up-regulated over time,

especially xanthoxin dehydrogenase (19.1) and abscisic aldehyde oxidase (20.1), which encode the two final steps for ABA production. For both of these steps, different patterns of expression were observed over the time course for multiple genes with the same annotated function (e.g. 19.1, 19.2 and 19.3 do not share the same patterns, nor do 20.1, 20.2 and 20.3), but together, represent some level of expression for that gene at every time point during wound-healing. Additionally, at least one gene per annotated function demonstrated expression into 3 dpw, which was not observed for all carotenoid biosynthetic genes.

ABA catabolism involves inactivation by hydroxylation and/or glucosylation, whereas β -glucosidase returns catabolized products back to active ABA. ABA-8'-hydroxylase (CYP707A)-encoding genes (1.1-1.3) decreased in transcript levels between 0-0.5 dpw, where one annotated version maintained detectable transcript levels throughout the time course, but the other two were close to undetectable from 0.5-3 dpw (**Figure 3.5C, Table C8**). Genes encoding ABA-glucosyltransferase (2.1-2.3) were expressed in differential patterns, with at least one version expressed at each time point. β -Glucosidases (3.1-3.3) also displayed varied patterns of expression. At 3 dpw, one β -glucosidase (3.1) exhibited the highest \log_2 FPKM level across ABA catabolism genes.

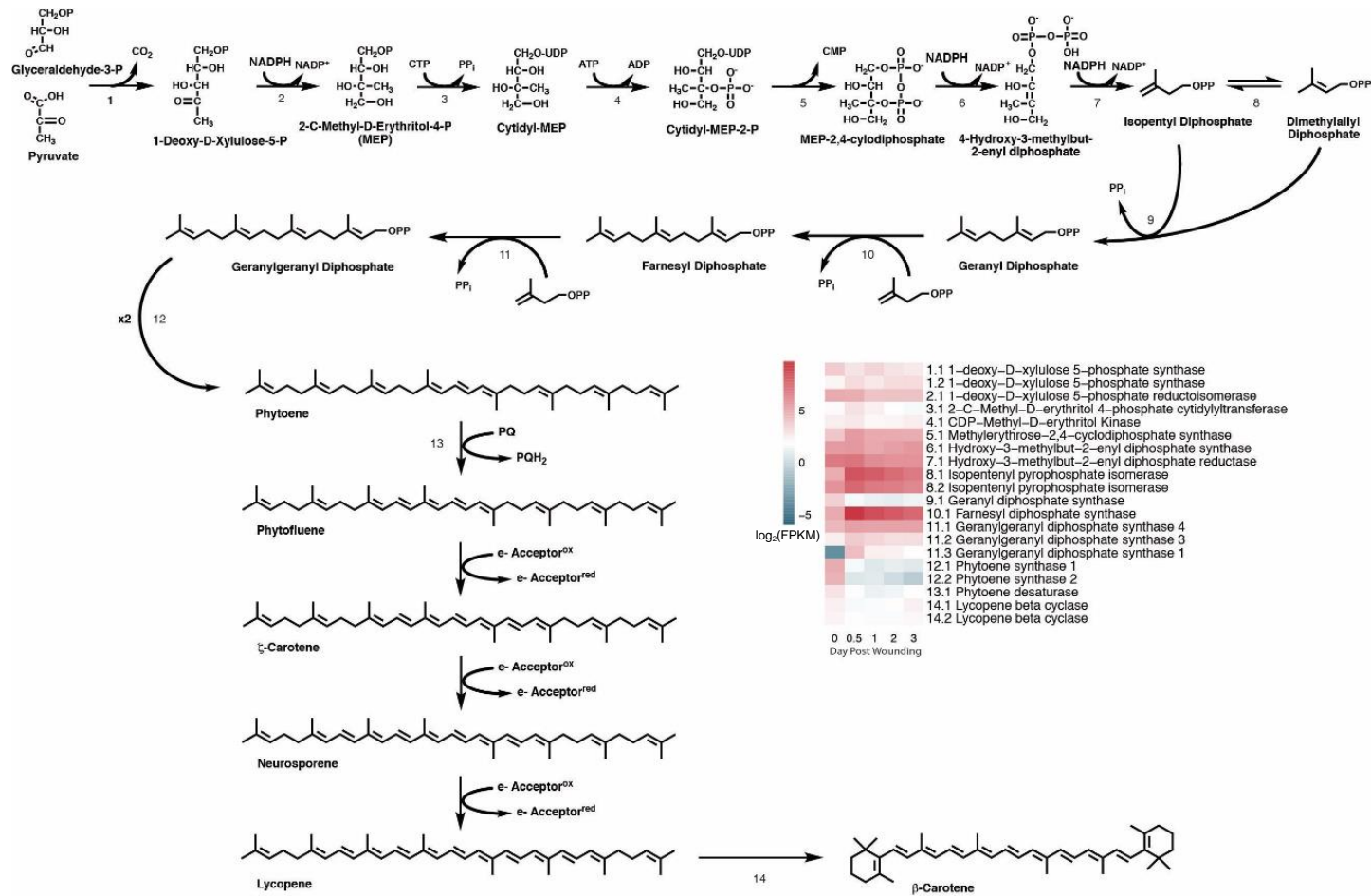
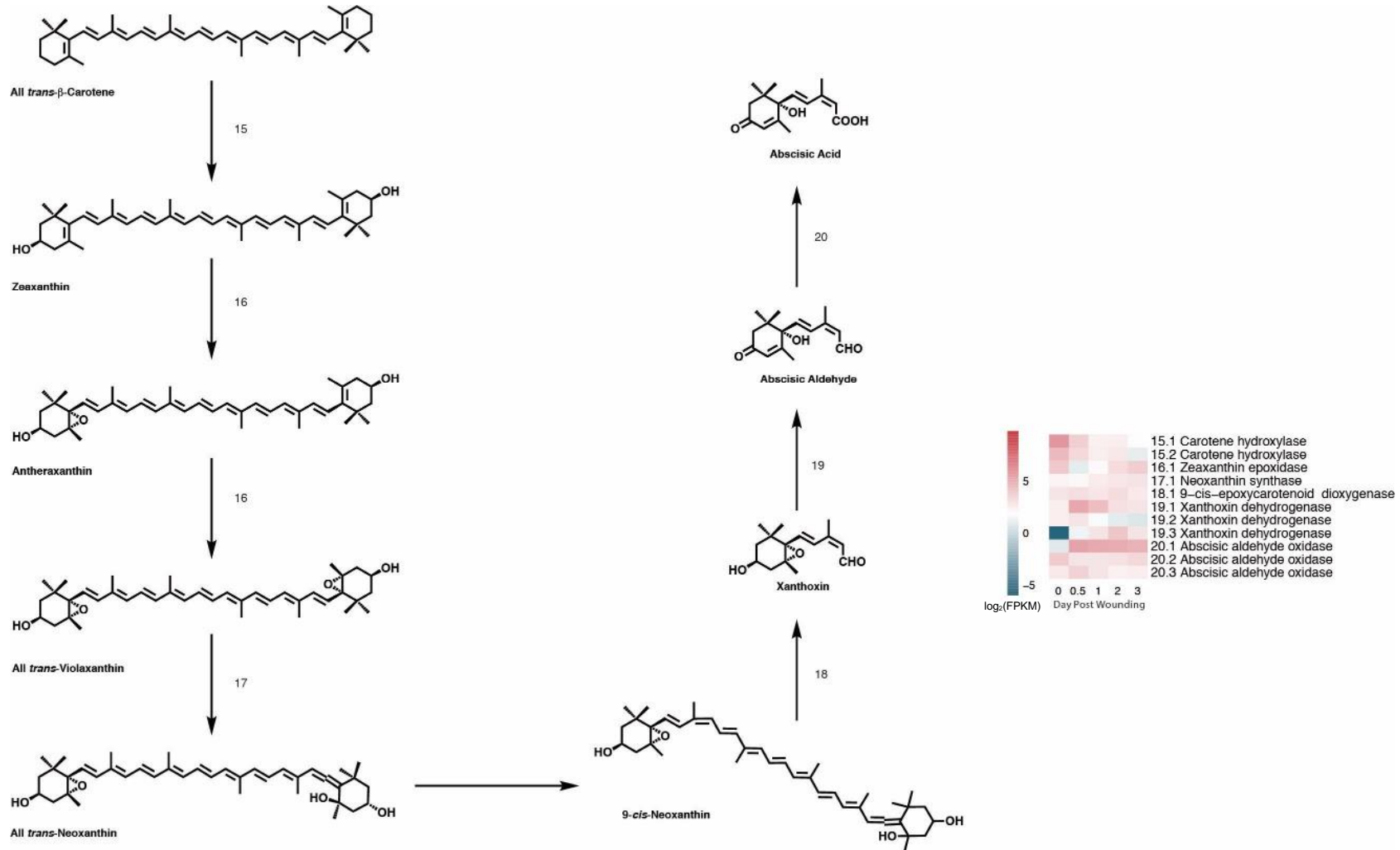
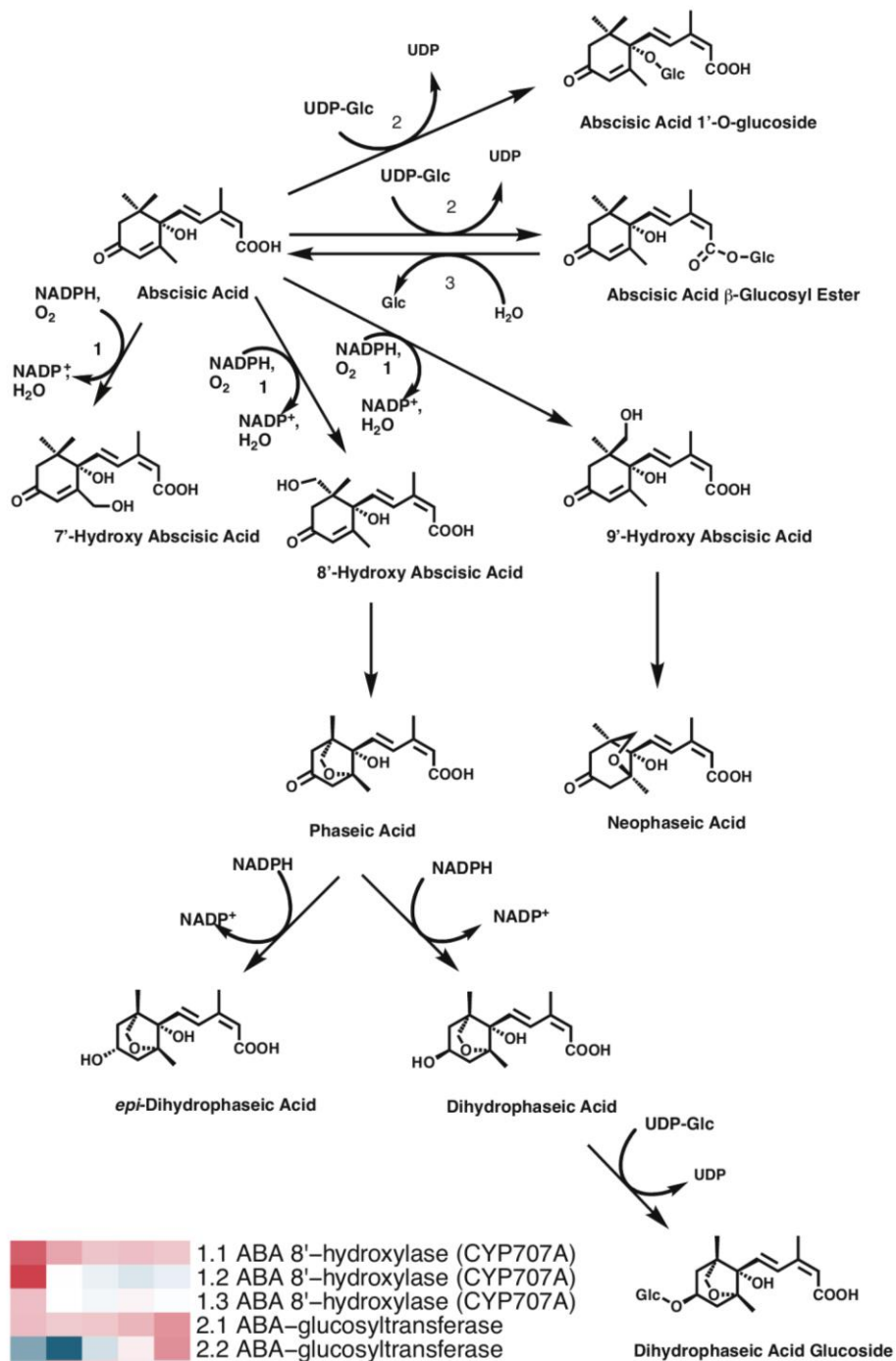


Figure 3.5. Transcriptional changes in abscisic acid (ABA)-related metabolism during wound-healing. A. Isoprenoid and β -carotene biosynthesis. **B.** Abscisic acid biosynthesis. **C.** ABA catabolism. $\log_2\text{FPKM}$ means for $n=3$ biological replicates are presented for each time point. Numbered pathway steps correspond to gene information provided in **Tables C7** and **C8**.

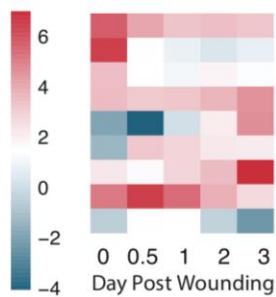


B



C

log₂(FPKM)



3.3.8 Temporal gene expression patterns of transcription factor candidates

As transcription factors (TFs) often function as the link between hormones and target gene expression, a set of putative TF candidates were identified using known TFs as a guide (**Table C9**). Transcription factors with known roles in suberin pathway-related metabolism (e.g. suberin regulators AtMYB41 and StNAC103, and phenylpropanoid pathway regulator StWRKY1) were used to find putative potato homologs that might regulate suberization during tuber wound-healing. The amino acid sequences of known suberin-associated TFs were queried by BLAST to find the top 10 protein matches in the potato PGSC database. Only those displaying some level of expression (i.e., 21 of 23 original candidates, data not shown) in the time course were used further analysis. Expression profiles for these candidate TFs were analyzed within the RNA-seq data using hierarchical clustering analysis with genes encoding known TFs, to formulate hypotheses about their likely roles (**Figure C5, Table C9**).

At the amino acid sequence level, MYB3 (TF.1) and MYB39 (TF.2) had the highest hit scores to AtMYB41, WRKY19/WRKY56 (TF.16) was most similar to the phenylpropanoid regulator WRKY1, and NAC58 (TF.9) was the most similar candidate to the characterized repressor NAC103 (**Table C9**). Their encoding genes all clustered together in this analysis. These genes showed no expression at 0 dpw and were up-regulated by 0.5 dpw. *NAC103* (TF.8) clustered closely with *MYB102* (TF.5) and *MYBODOI* (TF.7), along with two NACs that were not expressed until 2 dpw. WRKY1 clustered with two other highly and consistently expressed TFs from MYB and WRKY families. A group of candidates representing MYB, WRKY, and NAC-type TFs demonstrated lower expression levels than other known and candidate TFs, and either exhibited a gradual increase (TF.6, TF.13, TF.12, TF.20) or a gradual decrease (TF.4, TF.17, TF.19) in expression over time (**Figure C5**).

Further analysis involved clustering the known and putative TFs with targeted suberin-related pathway genes to determine where similar temporal patterns occurred on a broader scale (**Figure 3.6A-D**). *NAC103* (TF.8) clustered with several other transcription factors such as *MYB102* (TF.5), MYB39 (TF.2), NAC58 (TF.9) and other MYB and

NAC-encoding genes (**Figure 3.6A**). These TF genes mostly grouped with aliphatic biosynthetic genes that were not detectably expressed until 1 or 2 dpw. Genes that are thought to be regulated by NAC103 (*KAR*, *CYP86A33*, *ABCG11*) demonstrated similar expression patterns as *NAC103*, but were in the adjacent major cluster, with candidates including *MYB3*, and *WRK19/WRKY56* along with other hydroxylases and reductases responsible for key aliphatic modification steps. These genes had no initial detectable expression at 0 dpw and were mostly up-regulated by 0.5 or 1 dpw. Several TF candidates that demonstrated low, consistent levels of expression such as *MYB ODORANTI* (TF.4) and *NAC21/22* (TF.13) clustered with primary metabolism genes, or phenylpropanoid genes, such as *MYBI* (TF.6) and cinnamoyl-CoA reductase (*CCR*, 49.1) (**Figure 3.6B**). *WRKY1* (TF.15), *WRKY4* (TF.18) and *MYB34* (TF.3) clustered with mostly primary metabolism pathway genes, as well as phenylalanine ammonia-lyase (*PAL1*, 40.3), the first committed step towards phenylpropanoid metabolism (**Figure 3.6C**). *WRKY1* did not cluster closely with genes it is known to regulate in aerial tissues, 4-coumarate:CoA ligase (*4CL*, 42.1, **Figure 3.6C**) and tyramine hydroxycinnamoyl transferase (*THT*, 51.1, **Figure 3.6B**). These genes demonstrated similarly consistent temporal profiles as *WRKY1*, but at varied levels of expression, and appeared in visibly separate clusters. There were no transcription factors in the clusters presented in **Figure 3.6D**, which mostly consists of primary metabolism genes.

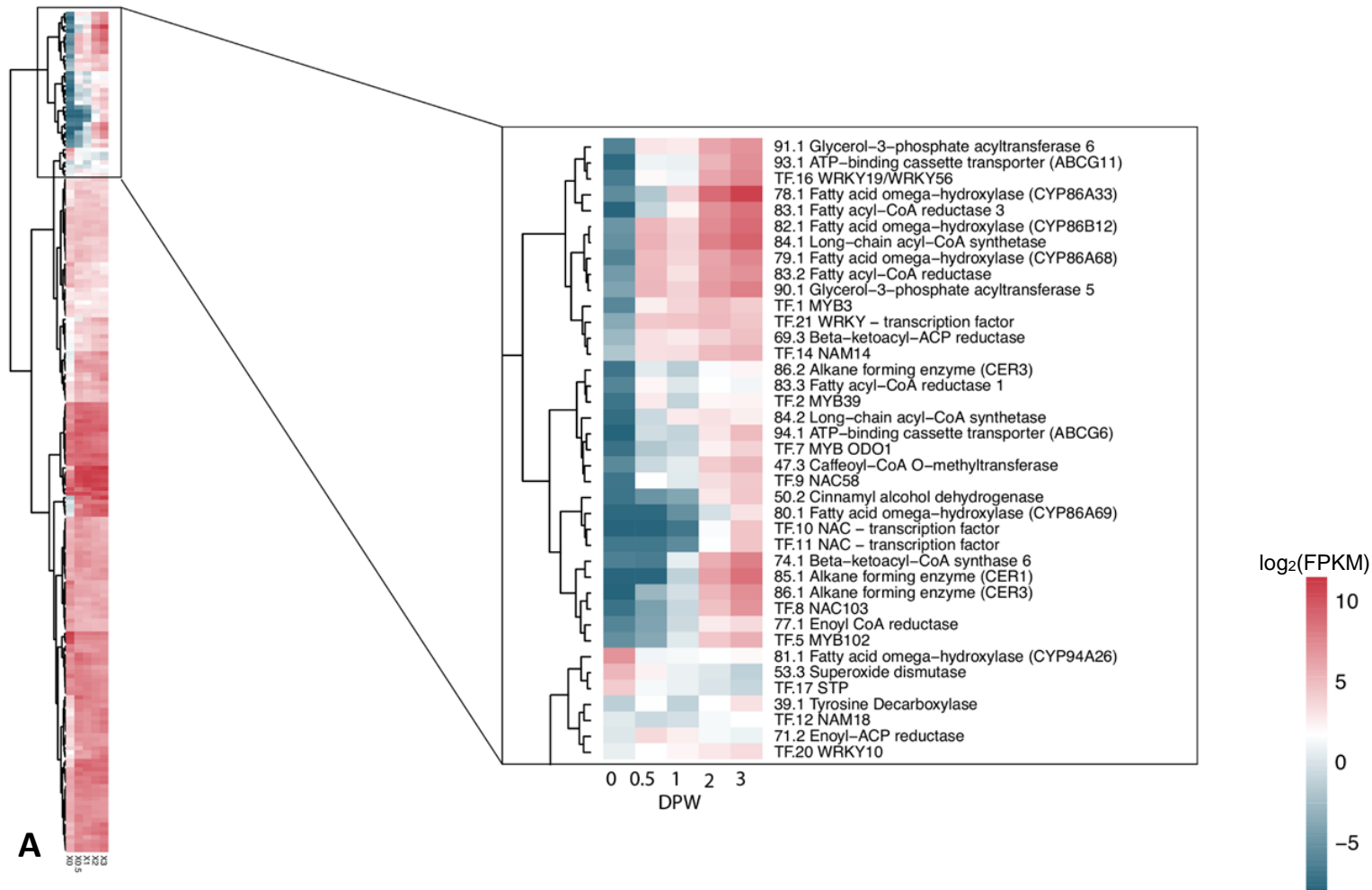
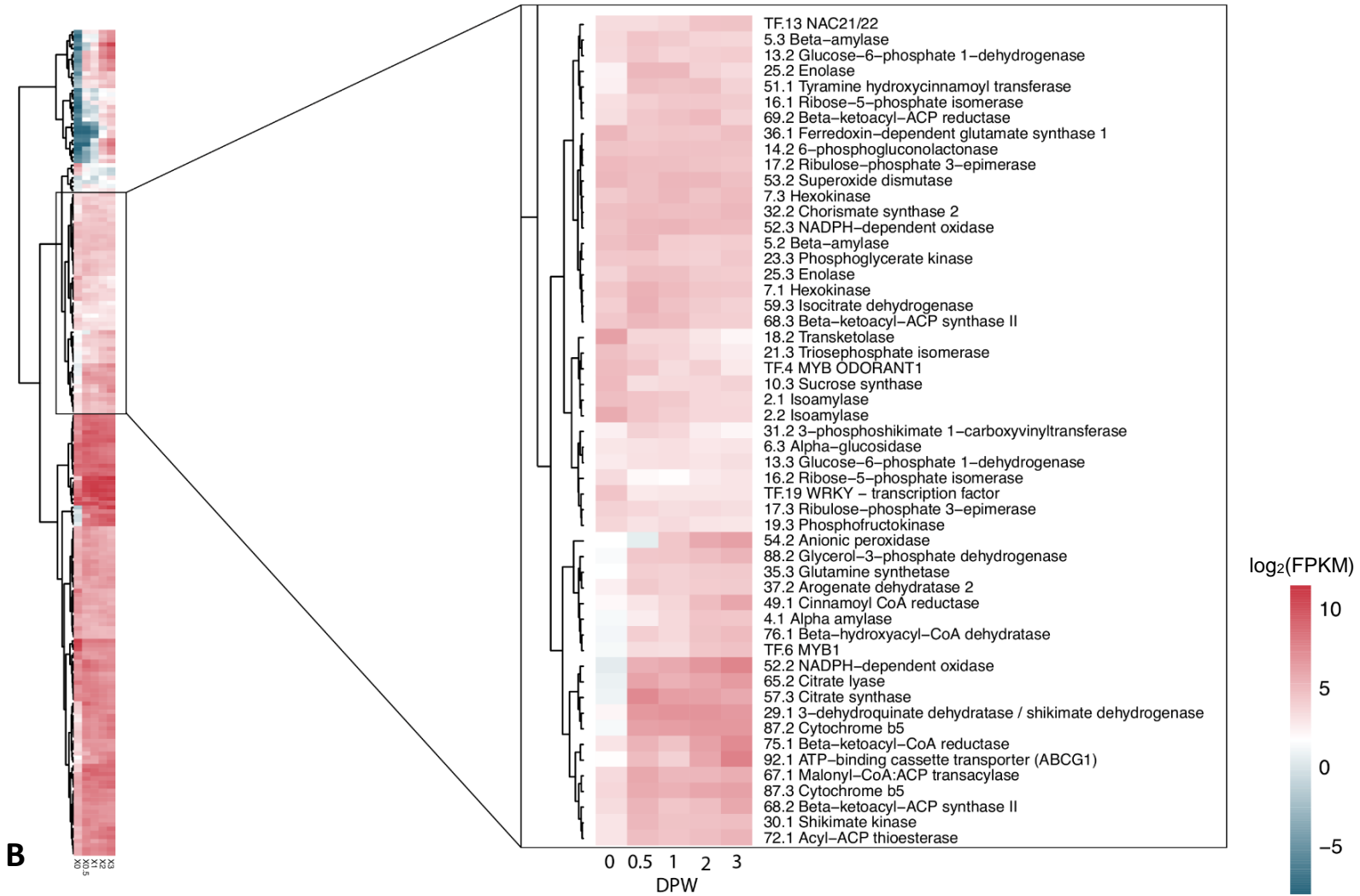
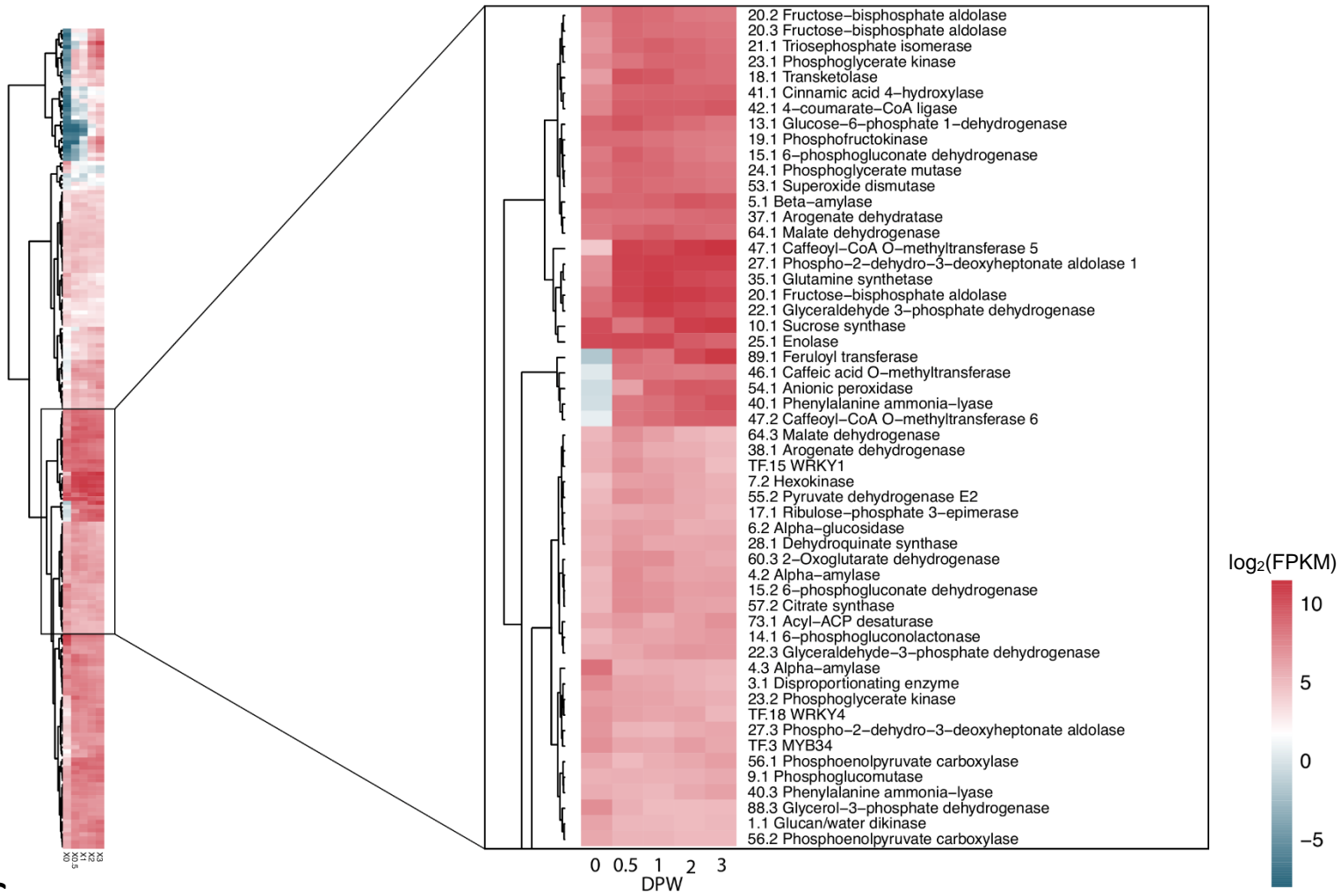
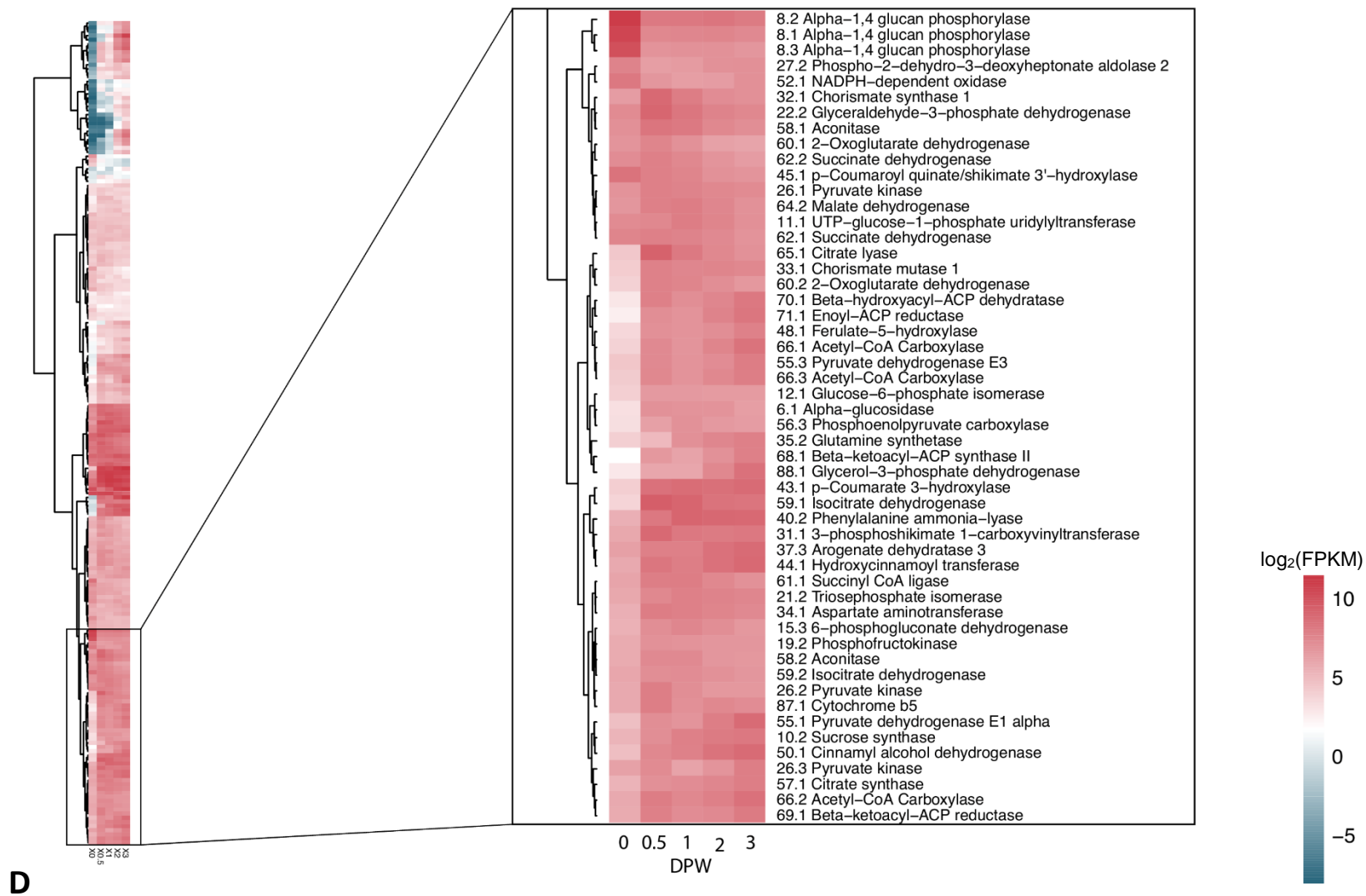


Figure 3.6. Hierarchical clustering analysis of transcription factor candidates with suberin-related biosynthetic and assembly genes across the tuber wound-healing time course. Panels A-D provide a detailed view of sub-clusters within the overall heatmap. Transcription factors are numbered as TFs; other targeted genes are numbered as in Figure 3.3A-I heatmaps. Log₂FPKM means for n=3 biological replicates are presented for each time point. Numbered pathway steps correspond to Table C9 TF gene information.







3.3.9 Validation of RNA-seq quantification by gene-specific RT-qPCR expression analysis

RT-qPCR was used to validate wound-healing time course transcript levels observed in RNA-seq counts. cDNA was generated from RNA used for RNA-seq as well as from separate experiments outlined in Woolfson et al. (2018) to encompass technical and biological validation. Pearson correlations were performed for 14 selected genes, where each data point represents the X,Y coordinate of expression values ($\log_2(\text{fold change})$ from 0 dpw) for one gene at one time point across both experimental methods (**Figure 3.7**). Genes encompass key known and putative suberin biosynthetic genes (*PAL*, *C4H*, *THT*, *CCR*, *CYP86A33*, *CYP86B12*, *KCS6*, *GPAT5*, *GPAT6*, *FHT*, *ABCG1*) and transcription factor candidates (*MYB34*, *MYB3*, *ODORANT1*; **Table C10**) that could be normalized to their respective 0 dpw expression level (i.e. four selected genes were excluded from the correlation analysis due to no detectable expression at 0 dpw and inability to perform normalization). The overall Pearson correlation co-efficient of $\log_2(\text{fold change})$ gene expression values from RNA-seq (CPM) and RT-qPCR ($\Delta\Delta Cq$) revealed a significantly positive ($p < 0.0001$) r -value of 0.8598 (n=45) (**Table C11**). These findings demonstrate that overall, gene expression values correlate between two methods of quantification.

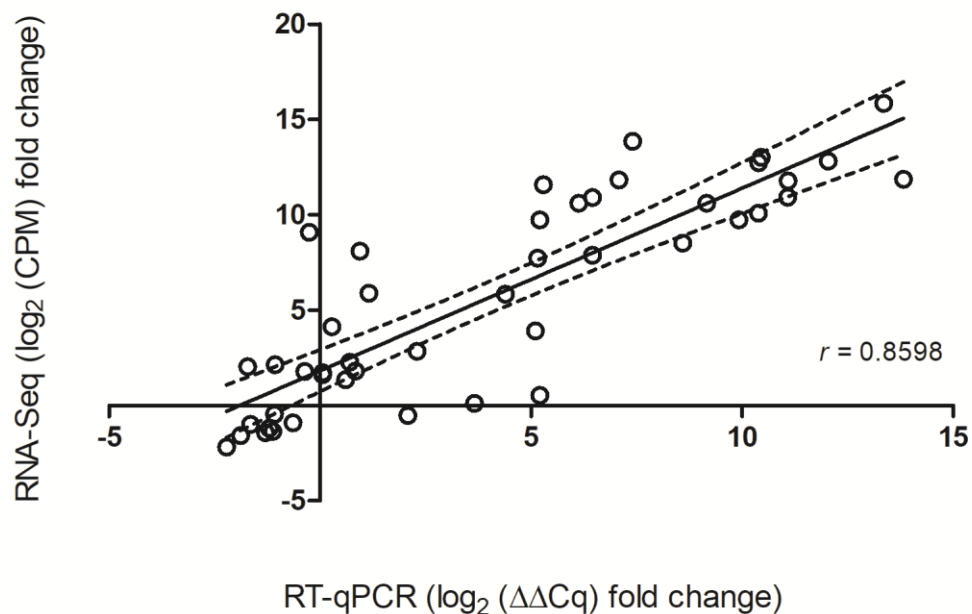


Figure 3.7. Validation of gene expression by Pearson correlation of RNA-seq with RT-qPCR expression values. Data points represent coordinates of expression values between the two experimental approaches for 14 genes over time, in which 3 genes encompass 4 time points and 11 genes include 3 time points (n=45). Mean expression values from biological triplicates for each experimental method were log₂-transformed and normalized to 0 dpw for all presented data points to represent the log₂ (fold change) from the control time point. Pearson's correlation coefficient (r) is shown at the bottom right. The regression line is plotted with 95% confidence interval bands. RT-qPCR expression values were normalized to *EF1-α* (3 genes) and also to *APRT* (11 genes). Gene and primer information can be found in **Table C10** and the statistical output is provided in **Table C11**.

3.4 Discussion

Wounding of potato tubers induces a multitude of responses in order to heal and seal over damaged cells to prevent water loss and infection (Kolattukudy, 1987; Lyon 1989; Lulai and Orr, 1994; Lulai and Corsini, 1998). One major induced process is the formation of suberin in cells immediately below the wound surface. Suberization requires the biosynthesis of monomers from both phenylpropanoid and fatty acid metabolic pathways, including the biosynthesis of precursor molecules (phenylalanine and fatty acids) from available carbohydrate resources. Wound-induced suberin production requires initial signals and coordinated regulatory oversight to ensure all required metabolic pathways have been appropriately engaged. While some aspects of the regulation of wound-induced suberization have been elucidated in *Arabidopsis* and potato, including transcription factors (e.g. AtMYB41, Kosma et al., 2014; StNAC103, Verdaguer et al., 2016) and the role of ABA (Soliday et al., 1978; Lulai et al., 2008; Kumar et al., 2010; Suttle et al., 2013; Woolfson et al., 2018), and the differential temporal patterns of suberin-related metabolism have been established to some degree (Lulai and Corsini, 1998; Kumar et al., 2010; Lulai and Neubauer, 2014; Woolfson et al., 2018), many steps of suberization remain uncharacterized. Additionally, the overall potato wound-healing response that includes necessary primary metabolism has been less well described at the molecular level, relative to suberin-specific studies (Neubauer et al., 2012; Lulai and Neubauer, 2014).

In this study, RNA-seq was employed to uncover transcriptional changes that occur during the course of induced wound-healing in order to further our understanding of processes that relate to suberization in potato tubers. Taken together, unbiased and targeted gene expression analyses revealed a rapid, large-magnitude transcriptional re-configuration followed by fine scale temporal changes that occur after wounding across individual genes independently, and as components of diverse metabolic pathway branches, whether predetermined or identified through gene ontology (GO) analysis. This approach allowed for the generation of an updated and novel framework for suberin-related metabolism and facilitated the identification and validation of novel components

of induced wound-healing. An improved understanding of the mechanisms involved in wound-healing in an agricultural crop species may have important implications for future crop improvement efforts.

3.4.1 Wound-healing is a dynamic process that leads to differential temporal patterns of transcription

The generation of a wound-healing potato tuber transcriptome time series allowed for the investigation of overall changes that drive significant differential gene expression as well as targeted suberin-specific analyses. On a global level, findings from differential expression and GO analyses support the hypothesis that wound-induced suberization in the dormant potato tuber requires an initial re-organization of biological processes at the transcriptional level that are re-routed and focused towards more specialized activities that relate to suberin biosynthesis and physical wound-healing. These findings were corroborated by the temporal expression patterns revealed by targeted investigation of suberin-related metabolic pathways and associated regulatory components. The targeted approach included genes that were not necessarily differentially expressed, but rather provided a detailed investigation through the suberization lens. This comprehensive overview of the broad suberin biosynthetic pathway supports observed patterns for gene sets organized by GO term, providing further evidence towards the hypothesis regarding a shift from more general primary metabolism to specialized suberin-associated metabolism. Targeted analysis results demonstrate that overall, different pathway branches are expressed at different times after wounding, of which similar temporal expression patterns are shared across genes that constitute entire pathways involved in precursor and suberin-specific monomer biosynthesis, as well as polymer assembly. However, some distinct profiles exist at the individual gene level and among sub-groups of genes within pathways. This time course transcriptome provides evidence for the differential temporal induction of genes and their overarching pathways, and highlights the likeliness of various levels of regulatory oversight to coordinate their expression.

After harvest and curing, potato tubers maintain a limited set of physiological activities during the ensuing dormancy, such as respiration, accumulation of reducing sugars,

synthesis of RNA, DNA and proteins, and subcellular compartmentation (as reviewed in Wiltshire and Cobb, 1996). Many of these processes were initially altered by the wounding event as seen by changes in differentially expressed genes (DEGs) reflected by enriched gene set terms for primary metabolic pathways like “carbohydrate metabolic process” and “tricarboxylic acid cycle”, amino acid biosynthesis including “aromatic amino acid family biosynthetic process” and “L-phenylalanine biosynthetic process”, and synthetic events like “DNA replication” and “translation” (**Figure 3.2, Table 3.1**).

Targeted analysis of genes involved in the enriched metabolic pathways also demonstrated that the majority were expressed at 0 dpw, and their levels changed substantially within 12 hours of wounding (**Figure 3.3A-F**). The highest proportion of DEGs occurred within this initial 12 hour timeframe and coincided with the observed substantial shift in maintenance metabolism. In both global DEG and targeted pathway-specific analyses, these aspects of primary metabolism generally achieved a new steady state of expression that remained consistent throughout the rest of the wound-healing time course, which highlights the importance of ongoing primary metabolism to fuel downstream reactions during wound-healing through the provision of precursor and energy molecules. As the wound-healing time course went on, new terms became enriched and genes from different pathway branches became up- or down-regulated, reflecting a more focused set of responses. Overall, the observed switch in the quantity and biological role of enriched terms over the time course marked a shift from broad and precursor-synthesizing metabolism to more healing and suberization-specific processes.

While the response of these preliminary metabolic pathway steps have not been well-characterized in a wound-healing tuber system, Strehmel et al. (2010) took a metabolomics approach to investigate the biochemical changes in tuber tissue primary metabolism within 48 hours of mechanical impact that leads to blackspot bruising. While metabolism associated with blackspot may be involved in the formation of melanin as a visible bruise, this type of mechanical injury can be considered a wound-related defect (Lulai, 2007). Key metabolites identified in this early stress response were intermediates of primary and carbon metabolism. These findings were also consistent with a metabolite profiling study (Yang and Bernards, 2007) that demonstrated an induced shift in primary

metabolites (e.g. sugars, organic acids and amino acids) during early tuber wound-healing. Proteomic analysis of wound-healing tubers also demonstrated early (0-2 dpw) induction of processes related to primary metabolism and generalized defense responses, including storage glycoproteins like patatins and general protective protease inhibitors (Chaves et al., 2009). The transcriptomic approach described herein further illustrates the wound-induced changes within these primary pathways.

Gene expression and metabolite analyses have previously revealed that the suberin poly(phenolic) domain is synthesized and deposited prior to the poly(aliphatic) domain in wound-healing potato tubers (Lulai and Corsini, 1998; Lulai et al., 2008), where ABA only regulates the latter (Woolfson et al., 2018). Our RNA-seq analysis included twelve genes representing phenolic, aliphatic and assembly genes that were studied in these previous wound-healing tuber experiments (e.g. Lulai and Neubauer, 2014; Woolfson et al., 2018), and displayed conserved patterns of gene expression. The shared expression patterns between our RNA-seq data and those observed in previous studies validates our findings and provides confidence in the conclusions that can be drawn from the RNA-seq data. In unbiased analyses, GSEA also indicated that primary and polar metabolism-related GO terms were up-regulated earlier, followed by response to ABA, and finally terms involved in fatty acid metabolism (e.g. “fatty acid biosynthetic process”, “oxidation-reduction process” and “lipid metabolic process”; nodes 1, 5, and 9; **Figure 3.2**). The fatty acid-related terms include key genes involved in aliphatic suberin modification, such as *CYP86A33* (Serra et al., 2009b, Bjelica et al., 2016), *KCS6* (Serra et al., 2009a), *FAR3* (Domergue et al., 2010) and *KAR* (Beaudoin et al., 2009). These enriched terms demonstrate the importance of suberization as a specialized process within the overall wound response and subsequent healing, and changes in expression are congruent with the differential timing demonstrated in the targeted expression analysis (**Figure 3.3H**).

Gene set enrichment analysis was performed with genes grouped by ontology term, where the determination of directional regulation for an enriched term depended on the significance and magnitude of change for all genes within the term. Genes were grouped

by metabolic pathway branches for targeted analysis, and entire branches shared similar patterns over time with relevant GSEA terms. Differential temporal patterns were also observed between individual genes and/or gene subsets within overarching pathway branches. For example, phenylpropanoid metabolism yields hydroxycinnamic acid-derived products specifically for the poly(phenolic) suberin assembly pathway, but also wound-associated tyramine-derived hydroxycinnamic acid amides and monolignols involved in both phenolic suberin and cell wall-associated lignin production (**Figure 3.3D**). Expression patterns differed between these different subgroups within the phenylpropanoid branch, where *THT* transcripts remained at consistent, albeit lower levels than other genes (as previously observed in Woolfson et al., 2018). *THT* encodes the only committed step towards tyramine-derived hydroxycinnamic acid amide (HCAA) biosynthesis, and while it yields cell wall- and phenolic suberin-associated products, it represents a distinct branch point of polar suberin metabolism (reviewed by Facchini et al., 2002). *CCR* transcripts accumulate at lower quantities and more gradually over time, which is consistent with minimal induction of *CCR* enzyme activity (Bernards et al., 2000) and lower accumulation of monolignols relative to other phenolic monomers (Bernards et al., 1995). Cinnamoyl CoA reductase (*CCR*) commits hydroxycinnamic acid carbon skeletons into monolignol formation and controls the flux of metabolites towards monolignol biosynthesis as the first committed step for this sub-branch of the phenylpropanoid pathway. This may explain why the subsequent *CAD*-encoded step exhibited higher \log_2 FPKM levels; i.e., it is present at high levels to ensure complete reduction of hydroxycinnamic acids to monolignols, as has been previously suggested (Bernards et al., 2000).

Within the phenolic suberin assembly branch, oxidases and dismutases were generally active early on and consistently throughout the time course, whereas peroxidase genes were expressed at higher levels later in the time course than biosynthetic genes (**Figure 3.3E**). This timing is consistent with previous studies on wound responses and phenolic polymerization (reviewed in Bernards et al., 2004). NADPH-dependent oxidases are known to be activated rapidly after wounding during the respiratory burst to generate superoxide, which is involved in plant signaling. Dismutases then convert superoxide into

hydrogen peroxide, which is used for peroxidase-mediated polymerization of polar suberin monomers (as reviewed by Bernards et al., 2004). Overall, these patterns reflect the difference in genes encoding enzymes for production of metabolites destined solely for suberin via two metabolic routes, or towards production of monolignols that can be incorporated into suberin or lignin, or HCAAs incorporated into the cell wall whether in association with suberin (e.g. feruloyl tyramine) or not, as well as steps involved in the initial wound response and of final polymerization of monomers.

Genes involved in aliphatic suberin production also demonstrate differences in their temporal expression patterns that reflect varying levels of suberin-related specialization. Preliminary fatty acid modification steps such as chain elongation, and genes encoding cytochrome *b₅* proteins that act as electron donors for a multitude of fatty acid modification reactions including fatty acid desaturation and hydroxylation (Kumar et al., 2006), had consistent transcript abundance, which contrasts other modification steps that gradually increase in expression. Modification and assembly genes shared similar patterns of later onset up-regulated expression. These patterns of expression are supported by the enzymatic progression of aliphatic suberin biosynthesis and assembly – acetyl-CoA is produced first from products of the tricarboxylic acid cycle to feed into fatty acid biosynthesis. Once fatty acids have been generated, they can be modified, where elongation steps occur initially, and downstream modifications (e.g hydroxylation, reduction and decarboxylation) use long to very long chain fatty acids as substrates (e.g. AtCYP86B1, Compagnon et al., 2009 and its putative potato homolog StCYP86B12, Bjelica et al., 2016) in some cases (**Figure 3.3H**). These products must be formed before final linkage and assembly steps are possible, and expression patterns of genes encoding the final assembly steps are similar to those of the later modification steps. Feruloyl transferase (*FHT*, step 89 **Figure 3.3I**) is an exception as it is expressed prior to the fatty acid modification genes and other aliphatic assembly genes. The early gene expression observed could represent the ability of *FHT* to catalyze acyltransferase reactions as soon as both its phenylpropanoid-derived feruloyl-CoA and aliphatic monomer substrates are available, or this could allude to its possible generic transferase activity that may involve other reactions and substrates (Molina et al., 2009; Serra et al., 2010). Landgraf et al.

(2014) characterized the ATP-binding cassette transporter ABCG1 as the main exporter of aliphatic suberin components in potato. ABCG1 and putative homologs of Arabidopsis aliphatic suberin transporters, ABCG6 (Yadav et al., 2014) and ABCG11 (Bird et al., 2007), exhibited slightly different gene expression patterns over time. This suggests they may transport different products, or could coordinately function to transport products as they become available.

The timing of cell wall and membrane related GO terms appear to match the respective timing of phenolic and aliphatic suberin deposition, and offers insight into the spatial locations of these gene expression events. Cell wall biogenesis appears to be up-regulated early in the time course, from 0.5 to 1 dpw, around the same time as GO terms related to, and genes involved in, phenolic suberin biosynthesis and assembly of the polar poly(phenolic) suberin domain. Over the 2-3 dpw time period, Golgi apparatus, membrane, and integral membrane cellular component GO terms were enriched with overall up-regulation of the genes within these terms, where membrane and integral membrane terms include many overlapping genes (**Figure C2**). Genes encoding ABC transporters with involvement in aliphatic suberin deposition, ABCG1, ABCG6 and ABCG11, were included in the “integral component of membrane” term, along with suberin assembly genes *FHT*, *GPAT5*, and *GPAT6* (Beisson et al., 2007; Serra et al., 2010). The CASP candidates *CASP8* (C.12) and *CASP9* (C.13) that were predicted to be involved in the wound-induced suberization process due to their previously observed expression in potato periderm (Vulavala et al., 2017), also came up in the up-regulated enriched membrane GO terms. CASPs involved in Casparian strip assembly in Arabidopsis roots are four-transmembrane proteins associated with the plasma membrane (Roppolo et al., 2011). Interestingly, transcriptome analysis by Massa et al. (2011), which is available on the PGSC database, demonstrated that *CASP9* FPKM levels are higher in tubers than in roots, and *CASP8* is present at comparable transcript levels between these two tissues. Coincidentally, targeted clustering analysis of assembly candidates and known genes demonstrated shared temporal expression profiles of *CASP8* and *CASP9* with the aforementioned linkage and deposition genes, along with an anionic peroxidase linked to phenolic polymerization (Bernards et al., 1999), where these two CASPs were

the most highly expressed candidates to cluster with known suberin assembly genes (**Figure 3.4**). The poly(aliphatic) domain of suberin is thought to exist between the plasma membrane and the primary cell wall, where it links to the cell wall-anchored poly(phenolic) suberin domain (Bernards, 2002; Graça, 2015). The up-regulation of key assembly genes and newly identified wound-induced suberization *CASP* candidates within the cellular component integral membrane GO term reflects the activities of these genes occurring at this site, and likely represents the localization of components involved in the regulatory oversight and organization of suberin assembly and deposition.

Taken together, the GO and clustering analyses, the timing of up-regulation and the lack of root-specific localization point to a potential role for *CASP8* and *CASP9* in wound-induced tuber suberization. *CASP8* and *CASP9* likely function in recruiting polymerization machinery and localizing cell wall modifications as described for root-specific *CASP* family proteins involved in Casparian strip assembly (Roppolo et al., 2011; Roppolo et al., 2014), which in this case might involve mediating linkage of aliphatic monomers to build the SPAD, organizing the correct pattern of SPAD deposition by directing localization, as well as promoting linkage between the two spatially distinct suberin domains (Bernards, 2002; Graça, 2015). Many *CASP* candidates expressed in this time course displayed temporal profiles more consistent with those of genes required for phenolic polymerization, and could therefore possess similar mediator roles for SPPD assembly, and coordination of cell wall modifications associated with SPPD deposition.

Cutin synthase homologs (GDSLs) were incorporated into this analysis as candidates for aliphatic linkage. Since the only two expressed candidates (G.6, G.7) clustered closely with *CASP8* (C.12), *CASP9* (C.13) and known aliphatic assembly genes (**Figure 3.4**), it is possible that these are also involved in the process of SPAD monomer polymerization, although they could also be involved in other biosynthetic activities. Multi-species transcriptome comparisons of suberizing tissues demonstrated the up-regulation of several GDSL-motif esterase/acyltransferase/lipase genes, along with many known suberin biosynthesis genes (Lashbrooke et al., 2016). GDSL G.7 identified in this study

was also highlighted by Lashbrooke et al. (2016) as a putative “suberin synthase” with hypothesized extracellular polymerization function. Transcriptomic analysis of *Nicotiana benthamiana* leaves transiently over-expressing MdMYB93, a regulator of suberin deposition in russeted apple skin, demonstrated the enhanced expression of suberin-related biosynthetic genes along with several genes encoding GDSL-esterase/lipases, and provides further support for the potential role of GDSLs in aliphatic suberin assembly (Legay et al., 2016).

Lulai et al. (2016) described two stages of tuber wound-healing – closing layer formation during the first five to seven days post wounding, followed by wound periderm formation. There are marked differences in biological processes that occur during these two phases of suberization-associated healing. Closing layer formation involves DNA synthesis and nuclear division (Lulai et al., 2014), but not cell division; the latter occurs during the later healing stage of wound periderm formation (Lulai et al., 2016). Our findings were consistent with this timeline regarding DNA synthesis, as several mitosis-related cell cycle GO terms became up-regulated early during wound-healing, then were significantly enriched as down-regulated for most other time points captured within our time course. As cell cycle-related genes decreased over the duration of the time course, cell wall organization and cell wall biogenesis GO terms became up-regulated. Considering that cell division does not occur during this early stage of wound-healing, up-regulated genes within cell wall-related GO terms must not be involved in cell wall synthesis for newly generated cells, but rather for the reinforcement of existing cells, as expected during closing layer formation (Thomson et al., 1995; Lulai, 2007). In this case, the enrichment of these GO terms offers lists of mainly cell wall modification genes that are likely relevant to the physical aspects of wound-healing (see below), like the production of the closing layer in cells surrounding the wound site.

The phenylpropanoid pathway and phenolic suberin assembly steps are expressed early in the time course and around when the first cell wall GO terms demonstrate enrichment. Suberin SPPD components, guaiacyl acid and sinapyl acid, are thought to covalently bond with cellulosic cell wall components (Yan and Stark, 2000). These cell wall-related

changes may signify that the healing process is occurring in cells adjacent to wounded cells and could reflect processes that allow for required SPPD components to be embedded into the cell wall. Several genes in the cell wall organization and biogenesis GO terms code for xyloglucan endotransglucosylase/hydrolases, which are involved in primary cell wall structural modifications, and typically associated with cell wall loosening, through the cleavage of xyloglucan chains and subsequent joining of new ends with xyloglucan or oligosaccharide acceptors (Fry et al., 1992; Rose et al., 2002). Pectin esterases, cellulose synthases, and glycosyltransferases were also represented in the up-regulated cell wall terms. To our knowledge, no wound-induced tuber suberization studies have quantified changes in cell wall polysaccharides. However, it is possible that the differentially expressed cell wall organization genes and biogenesis are involved in cell wall remodeling that promotes correct deposition of phenolic suberin components.

Notably, genes in the plant-type secondary cell wall biogenesis term are only significantly up-regulated later in the time course, between 2-3 days post-wounding. This could reflect the final steps of closing layer formation, since secondary cell walls are only formed after completion of primary cell wall formation and cell expansion has ceased.

The dynamic set of temporal patterns over the wound-healing period reflects an initial largescale set of changes that subsequently achieve a new steady state, followed by fine-tuning of specialized responses. Wounding can be linked to both biotic and abiotic stress since injury can occur as a product of herbivory, infection, or environmental stress, and physical damage alone can introduce the potential for infection and water loss. Since this type of damage can occur as a component of different threats, the initial upheaval of metabolism could prime the tuber to respond accordingly, as observed in the case of wounding herbivory (e.g. Schwachtje and Baldwin, 2008). In the present experiment, tubers were kept in a sterile, high humidity environment, and therefore the later processes that reflect fine-tuning of responses appear to largely reflect suberization and cell wall related processes required for initial formation of the closing layer.

Overall, these findings establish a detailed view of the differential timing and patterns of suberin-related metabolic pathway activities, both between and within pathway branches.

Many genes within a pathway branch share temporal patterns of expression, which could imply that these sets of genes are concomitantly regulated by the same signal molecules and/or proteins like transcription factors. In contrast, those with further differentiation in temporal expression within pathways are likely regulated by different or additional components to coordinate their activities on a finer scale.

3.4.2 Regulatory components of wound-healing and suberization

The differential timing of suberin-related processes has been established through histochemical investigations (Lulai and Morgan, 1992; Lulai and Corsini, 1998) and time course metabolite profiling (Yang and Bernards, 2007) of suberin accumulation, that are further supported by studies integrating histochemistry-based suberin ratings with analysis of suberin biosynthetic gene expression (Lulai and Neubauer, 2014), and by combining a molecular approach with metabolite analyses (Woolfson et al., 2018). Proteomic analysis of the wound-healing tuber has provided further evidence of a temporal difference in suberization events at the protein expression level (Chaves et al., 2009). The observation that suberin-related events occur in two major phases directed our previous investigation towards how the various pathways required for suberin biosynthesis are coordinately regulated and activated at different points in time (Woolfson et al., 2018). Given the dynamic temporal patterns of transcript accumulation between and within pathway branches, there are likely multiple levels of regulation at play, and within each level, several individual constituents. Regulatory components can control the plant stress response at RNA, DNA and/or protein levels. Based on previous knowledge in combination with findings from this RNA-seq time course, regulation of the potato wound response likely includes phytohormones and transcription factors (e.g. Kosma et al., 2014; Verdaguer et al., 2016), as well as epigenetic, post-transcriptional and post-translational modifications.

The regulation of phenolic and aliphatic suberin biosynthesis and deposition is largely uncharacterized, especially in the potato tuber model. A role for ABA has been established in the regulation of aliphatic suberin production, and in part explains the differential timing of phenolic and aliphatic suberin related metabolism, since it impacts

aliphatic biosynthesis and linkage genes that are expressed later into wound-healing, but not phenolic pathway steps (Woolfson et al., 2018). However, there is evidence for enhanced PAL activity when ABA is added exogenously to wounded tubers (Lulai et al., 2008; Kumar et al., 2010).

The synthesis and catabolism of phytohormones that regulate normal growth and development as well as stress responses, such as ABA and JA, occurs during dormancy (Koda and Kikuta, 1994; De Stefano-Beltrán et al., 2006). The expression profiles for genes involved in ABA biosynthesis are consistent with this knowledge, as they are already expressed at some level in the 0 dpw libraries. In previous wound-healing studies, endogenous levels of ABA present in resting tubers prior to wounding dropped to very low levels within 1 dpw. This was followed by *de novo* synthesis of ABA within 2 dpw, reaching a maximum, sustained level by 3 dpw (Woolfson et al., 2018) or 4 dpw (Lulai et al., 2008). The importance of *de novo* ABA synthesis has been further demonstrated via application of the inhibitor fluridone (e.g. Lulai et al., 2008; Woolfson et al., 2018), which specifically led to delayed expression of aliphatic biosynthetic and assembly genes and their corresponding metabolite products, whereas exogenous ABA treatment resulted in their earlier induction (Woolfson et al., 2018). Abscisic acid biosynthetic reactions are not necessarily up-regulated by wounding, but rather, some degradation genes drop in log₂FPKM level over time, likely to maintain circulation of active forms of ABA as needed (**Figure 3.5**). These gene expression changes are consistent with the observed decrease in ABA concentration immediately after wounding followed by gradual increase (Lulai et al., 2008; Woolfson et al., 2018), and support the hypothesis that changes in ABA content can be attributed to shifts in degradation and synthesis activities during wound-healing (Lulai et al., 2008). It is likely that the initial wound-induced drop in existing ABA content reflects the use of ABA as an early wound-responsive signal, and subsequently, the concomitant *de novo* synthesis and attenuated degradation of ABA results in its accumulation at levels that induce SPAD metabolism by 2-3 dpw.

In the BP GSEA, the GO term “response to ABA” was the only enriched, up-regulated term pertaining to hormone signaling (**Figure 3.2, Table 3.1**), and the timing of its up-

regulation between 1-2 dpw followed by no further significant change over 2-3 dpw is congruent with previously established timelines for ABA accumulation. Transcription factors implicated in aliphatic suberin production, namely *AtMYB41* and *StNAC103*, are both regulated by ABA, offering further support for a regulatory role for this phytohormone (Kosma et al., 2014; Verdaguer et al., 2016). Although these genes were not present in the “response to ABA” GO term, the transcription factor candidate *MYB102* was included along with other uncharacterized MYB family TFs, and it was up-regulated between 1-2 dpw. *MYB102* was previously identified as *StMYB93* by Lashbrooke et al. (2016) as a member of a multi-species MYB transcription factor clade linked to suberin biosynthesis. *Asg1* was another gene up-regulated in the “response to ABA” term, which has been described as an ABA-induced positive regulator of the potato osmotic stress response (Batelli et al., 2012).

The delayed pattern of expression for genes involved in aliphatic metabolism appears to match the profile of ABA accumulation after wounding. That is, after an initial depletion of the pre-wounding levels of ABA, it begins to accumulate by 2 dpw, and reaches maximum, sustained levels as of 3 dpw, coinciding with the time at which aliphatic metabolism and assembly genes are up-regulated (Woolfson et al., 2018). Identification of ABA-responsive promoter regions of genes involved in SPAD-destined monomer production, such as cytochrome P450s (Bjelica et al., 2016) and *feruloyl transferase (FHT)* (Boher et al., 2013), offer evidence for the direct regulation of aliphatic metabolism genes by ABA. The timing of the induced accumulation of ABA is supported by the expression of ABA biosynthetic genes and lower expression of catabolic genes (**Figure 3.5A-C**). Notably, the “response to ABA” term increased in expression at the time post-wounding when up-regulation of fatty acid metabolism-related GO terms that include key aliphatic suberin genes also increased. This suggests that the perception of ABA for suberin-specific metabolism occurs when ABA accumulates, just prior to aliphatic gene expression, and, consistent with our previous work (Woolfson et al., 2018), does not support a role for ABA in phenolic suberin production.

In contrast to ABA-related processes during wound-healing, a BP term reflecting genes involved in the JA-mediated response was down-regulated in the GSEA. This further supports the hypothesis that JA has little role in suberization (Lulai et al., 2011). However, it does not preclude involvement of an initial JA burst, as observed by Lulai and Suttle (2009), which may be involved in early wound signaling. There is also no evidence for the requirement of ethylene in wound-induced potato suberization (Lulai and Suttle, 2004; Lulai and Suttle, 2009). JA has demonstrated involvement in the general wound response in different potato organs (Dammann et al., 2002; Koda and Kikuta, 1994), and both JA and ethylene play a role in tomato and Arabidopsis wound signaling and responses, (e.g. O'Donnell et al., 1996; Reymond et al., 2000; Wasternack et al., 2006). More specifically, JA is involved in Arabidopsis cell wall damage-induced lignin biosynthesis (Denness et al, 2011).

Two transcription factors were recently characterized as regulators of suberin deposition. The Arabidopsis AtMYB41 has root-localized, ABA- and salt stress-induced gene expression, and acts as positive regulator of aliphatic suberin production, and less definitively, phenylpropanoid and lignin biosynthesis (Kosma et al., 2014). The potato StNAC103 is a negative regulator of aliphatic suberin production, induced by wounding in tuber parenchyma and ABA treatment in tuber periderm and roots (Verdaguer et al., 2016). In spite of recent advances towards understanding the regulation of aliphatic suberin production in the context of ABA and the TFs it impacts, mechanisms that control phenolic suberin metabolism have yet to be elucidated. StWRKY1 was recently characterized as a regulator of pathogen-induced phenylpropanoid metabolism in potato leaves that binds promoter regions of *4-coumarate:CoA ligase (4CL)* and *tyramine hydroxycinnamoyl transferase (THT)* to mediate deposition of hydroxycinnamic acid amides into secondary cell walls for reinforcement. Its potential role in the regulation of SPPD-related metabolism had not been addressed prior to this study.

While *AtMYB41* heterologous overexpression in *Nicotiana benthamiana* leaves promoted suberization by enhancing transcripts of suberin genes, including those with characterized potato homologs (e.g. *AtCYP86A1*, *AtCYP86B1*, *AtGPAT5*, *AtFAR5*, *AtFAR4*, *AtFAR1*,

AtASFT, *AtKCS2* *AtPAL1*, *AtCCoAMT*, *AtCAD5*, *AtC4H*), *StNAC103*-RNAi experiments highlight the genes under suppressive control of *StNAC103*. Potato *StNAC103* silencing by Verdaguer et al. (2016) led to the induction of key fatty acid modification and aliphatic suberin biosynthesis and assembly genes (*StKAR*, *StCYP86A33*, *StFHT*, *StACBG11*). The repressive activity of *StNAC103* suggests that it is responsible for fine-tuning aliphatic suberin production and deposition, both temporally and spatially (Verdaguer et al., 2016). Interestingly, *StNAC103* displayed similar transcript accumulation patterns in our RNA-seq transcriptome to other TF candidates identified as putative homologs of positive suberin-related gene regulators (e.g. *MYB39*, *MYB3*, *MYB102*, *WRKY45* and *WRKY56*; based on Kosma et al., 2014; Lashbrooke et al., 2016; Yogendra et al., 2015) and clusters with many aliphatic suberin-related genes, although it did not cluster with its targets *KAR* and *CYP86A33*, despite similar temporal profiles (**Figure 3.5**). As a specific example, *MYB102* is the current PGSC-annotated name for *StMYB93*, the potato homolog of Arabidopsis *AtMYB9* and tomato *SlMYB93* (Lashbrooke et al., 2016), which has a role in positively regulating both phenolic and aliphatic related suberin biosynthesis and assembly in Arabidopsis seed coats. In the wound-healing tuber, *MYB102* expression followed a typical pattern for aliphatic genes as well as the characterized suberin regulator *NAC103*, with which it clustered very closely. The similar expression profiles observed between putative positive regulators and a known negative regulator emphasize the fine level of control that must be in place to allow for the correct temporal-spatial production and deposition of the highly organized, two-domain polymer, suberin. This observation also provides further support for the notion that multiple transcription factors are likely involved.

StWRKY1 is a TF that has not been characterized in the context of suberization, but was included in this study along with highly similar genes (*WRKY4*, *WRKY45*, *WRKY56*) due to its known regulation of phenylpropanoid genes, some of which are involved in suberin biosynthesis, and because it is stress-induced (Yogendra et al., 2015). *WRKY1* did not cluster with the genes it is known to regulate, though it did share highly similar expression patterns with them, and a likely reason for separation during clustering is the difference in 0 dpw log₂FKPM levels. That is, expression levels of *WRKY1* were much

lower at 0 dpw compared with phenolic genes such as *phenylalanine ammonia lyase* (*PAL*, step 40). Nevertheless, *PAL* genes were the closest suberin-related biosynthetic gene to cluster with *WRKY1*, along with other transcription factor candidates *WRKY4* and *MYB34* (**Figure 3.6C**).

MYB34 is highly similar to *MYB103*. In *Arabidopsis* stems, the homolog *AtMYB103* regulates *ferulate-5-hydroxylase* (*F5H*) transcription that is required for syringyl lignin biosynthesis (Öhman et al., 2013). *StMYB103* expression was not observed in our RNA-seq experiment, which could be due to organ localization, or reflective of developmental rather than stress-induced phenolic gene regulation. Since the highly similar TF candidate *MYB34* was expressed and clustered with the known phenolic regulator, *WRKY1*, and some key biosynthetic genes, it is a good candidate for a TF with a role in phenylpropanoid pathway regulation during induced suberization. *WRKY4* (TF.18) clusters closely with *MYB34*, and would also be a justifiable candidate for further pursuit.

Transcription factors were generally predicted to demonstrate onset of expression prior to induction of their putative targets. However, we also considered that initial TF induction may not have been captured within the sampled time points, and thus TFs and targets could exhibit what appear to be shared, or co-expressed, temporal profiles. The characterized TFs *WRKY1* and *NAC103* did not cluster closely with their targets, indicating that regulatory components are not necessarily expressed in the exact pattern or to the same degree as biosynthetic genes, but rather follow similar temporal transcript accumulation profiles that are reflective of typical phenolic or aliphatic suberin biosynthetic genes (**Figure 3.6A-D**). *NAC103* expression was evident later into wound-healing than all of its described targets (*KAR*, *CYP86A33*, *FHT* and *ABCG1*), but this is likely explained by its role as a transcriptional repressor (Verdaguer et al., 2016). The lack of clustering between TF and target genes renders the precise identification of most likely TF candidates and their putative downstream targets more challenging, but if TF expression follows a wound-induction pattern characteristic of some aspect of suberization, this can guide appropriate hypothesis generation for future work.

Additionally, similarities in expression between TFs were considered when assigning proposed roles to candidate TFs.

Other regulatory processes identified as enriched GO terms throughout time course include “histone phosphorylation”, “histone H3-K9 methylation”, “post-translational modifications”, “DNA-methylation”, “gene silencing”, and “chromatin silencing” (**Figure 3.2, Table 3.1**). These GO terms are not specific to suberization, but are also involved in general wound-healing process and other pathways, and provide insight into the many levels of regulation that allow for the coordination of a broad response to a major stress (i.e., wounding). For example, methylation of histone H3 at lysine 9 (H3-K9) is generally associated with transcriptional repression. The “H3-K9 methylation” GO term was significantly up-regulated between the two earlier time point comparisons, but significantly down-regulated between 1-2 and 2-3 dpw, along with the “DNA methylation” and “gene silencing” terms. The GO term “RNA methylation” was also enriched with mostly up-regulated genes initially, but significantly down-regulated at the later three time point comparisons. RNA methylation can enhance or silence mRNA production and impact other types of nuclear RNA (Fu et al., 2014), while DNA methylation also typically represses transcription, and can interplay with H3-K9 histone methylation (reviewed in Rose and Klose, 2014; Zhang et al., 2018). Fu et al. (2014) posit that reversible RNA methylation evolved as a regulatory mechanism to control processes that require rapid changes in expression of large groups of genes and proteins. These dynamic epigenetic, post-transcriptional and post-translational modification mechanisms could be responsible for the observed switch in metabolism from primary and phenolic suberin-related pathways at early time points to those required for later aliphatic suberin production and assembly.

Many regulatory aspects of wound-induced suberization have yet to be elucidated, but our RNA-seq transcriptome-based study emphasizes the vast complexity of the wound-healing process and points towards a dynamic regulatory network capable of fine-tuning events both temporally and spatially. A high degree of control would ensure expression

of required genes within and among pathway branches for appropriate metabolite accumulation, linkage and deposition during suberization.

3.4.3 Targeting putative suberin biosynthesis and regulation genes in the wound-healing tuber transcriptome provides support for uncharacterized steps

The generation of a transcriptome time series that tracked the wound-healing process in potato tubers was used to study nuances in temporal changes and gain support for putative steps of suberin-associated biosynthetic pathways. Many uncharacterized gene-encoded steps now have associated temporal expression profiles that provide evidence for their involvement based on wound-induction patterns and similar expression profiles to known biosynthetic genes in the same pathways. A number of additional steps were also placed in primary metabolic pathways such as starch degradation, and the TCA cycle was incorporated into this scheme.

In some cases, pathways were revised based on the identification and expression of candidate genes. For example, a previous biosynthetic scheme for suberin (Bernards, 2002) proposed roles for two CYP98A enzymes, *p*-coumaric acid 3-hydroxylase and *p*-coumaroyltyramine-3-hydroxylase, that catalyze hydroxylations prior to methylations performed by three hypothesized *O*-methyltransferases thought to be responsible for five enzymatic steps with caffeoyl conjugates as substrates: caffeic acid *O*-methyltransferase (COMT), caffeoyl-CoA-3-*O*-methyltransferase (CCoAOMT), and caffeoyltyramine-*O*-methyltransferase (CTOMT). It was initially hypothesized that one of the aforementioned CYP98As acted on *p*-coumaroyl-tyramine to yield caffeoyltyramine, followed by CTOMT-mediated methylation to produce feruloyltyramine. The hydroxylase and subsequent *O*-methyltransferase enzyme-catalyzed steps are analogous to the conversion of *p*-coumaroyl-CoA to caffeoyl-CoA and subsequently to feruloyl-CoA. This pathway also uses similar coumaroyl conjugates followed by caffeoyl conjugates as substrates. Investigation of the annotated potato genome, however, did not lead to the identification of the specific CYP98A-type hydroxylases by predicted functional name, but revealed several *p*-coumaroyl quinate/shikimate 3'-hydroxylases. CTOMT did not come up in a

functional annotation search, but COMT and CCoAOMT queries yielded several candidates. The targeted expression analysis included these genes in the phenylpropanoid metabolism pathway, where several demonstrate similar temporal profiles to characterized phenolic biosynthetic genes. This analysis provided support for the role of one recently characterized *p*-coumaroyl quinate/shikimate 3'-hydroxylase (Knollenberg et al., 2018), with the possibility of a second also being involved (steps 45.1-45.2), and could potentially map it to the alternate hypothetical *p*-coumaroyl-tyramine sub-branch. There is also good evidence for the role of one COMT, which is in agreement with the proposed progression from caffeic acid through to sinapic acid, where two methyltransferase steps are catalyzed by one enzyme (**Figure 3.3D**). There are also clear induction patterns followed by sustained expression for two CCoAOMTs, with another two demonstrating similar profiles, but at lower levels of expression (steps 47.1-47.54). It is possible that one of these highly expressed genes could encode an enzyme hypothesized to convert caffeoyl tyramine to feruloyl tyramine, or perhaps suggests that the 5'-OH-feruloyl-CoA conversion to sinapoyl-CoA is catalyzed by a secondary enzyme to the first *O*-methyltransferase activity on caffeoyl-CoA. These findings allowed for an update to the phenylpropanoid portion of the suberin roadmap by removing the unsupported CTOMT step, while also offering candidates for future analysis to determine whether one or several enzymes in these families are involved.

Pathways leading to aliphatic suberin production were also updated at the level of precursor formation in the TCA cycle and fatty acid biosynthesis branch (**Figure 3.3F-3.3G**), and a rearrangement of the aliphatic metabolism pathway that emphasizes the split between desaturation (steps 72-73, **Figure 3.3G**) and elongation (steps 68-71, **Figure 3.3G**; 74-77, **Figure 3.3H**). Putative hydroxylases investigated by Bjelica et al. (2016) were included (**Figure 3.3H**) along with many genes definitively characterized or implicated in suberin biosynthesis since 2002, e.g. specifically in potato, *FHT* by Serra et al. (2010) and *ABCG1* by Landgraf et al. (2014).

In addition, this targeted investigative approach provided evidence for the role of putative assembly genes and regulatory transcription factors that encourages further pursuit

(**Figure 3.4, Figure 3.6A-C**). Candidates with expression patterns that align with both phenolic and aliphatic suberin-related genes warrant future investigation and characterization to better elucidate the regulation of pathways that are differentially expressed both temporally and spatially, and the assembly of their metabolite products into the organized suberin heteropolymer. Both RNAi and overexpression studies have been used recently to characterize transcription factors StNAC103 (Verdaguer et al., 2016) and AtMYB41 (Kosma et al., 2014) that control aspects of suberin biosynthesis. Further investigation of shared motifs in promoter regions of genes that behave similarly on a temporal scale could reveal transcription factor binding domains and lead to discovery of transcription factors common to groups or subsets of genes.

This work highlights the fine level of regulation and discrete differences between genes in their expression over time, even within a metabolic pathway. While a 0.5 dpw time point was included in this study to capture different regulatory and biosynthetic events, future studies could focus on even shorter time intervals to fill any gaps that may have been missed in this study.

3.4.4 Comparison of transcriptome findings with metabolite and protein based studies

The generation of an mRNA-based transcriptome time course highlights the transcriptional response as a proxy for gene expression, but not all steps involved in this process are necessarily regulated at the transcriptional level, and the accumulation of mRNA does not necessarily reflect rates of translation or quantities of active proteins. However, prior studies have demonstrated the importance of transcription in the activation of suberization and our past work has matched temporal gene expression patterns to metabolite accumulation (e.g. Woolfson et al., 2018). Enzyme activities, protein accumulation, and metabolite levels have been used to corroborate RNA-seq generated transcript abundances over time where possible. For example, Chaves et al. (2009) conducted a time course based proteomic evaluation of wound-healing in potato tubers, where groups of enzymes clustered into two major groups, determined by sampling dates. These findings were congruent with changes in metabolite composition

over time determined by Yang and Bernards (2006), which also matched timing of gene expression and suberin metabolite accumulation over time by Woolfson et al. (2018).

Yang and Bernards (2007) performed principle component analysis (PCA) of polar and non-polar metabolite profiles to characterize global changes in the wound-healing tuber metabolome. Overall, cluster analysis of polar and non-polar metabolite profiles revealed a large-scale, temporal reorganization of metabolism comparable with the magnitude of transcriptional reconfiguration observed in my RNA-seq time course (**Figures 3.1-3.3**). In the Yang and Bernards (2007) metabolome study, 0 dpw polar profiles were mostly influenced by primary metabolites such as sugars, amino acids and organic acids, consistent with primary metabolic pathway gene expression profiles (**Figure 3.3A-C, F**). The appearance of suberin-associated phenolic compounds such as ferulic acid distinguished 1 and 2 dpw polar metabolite profiles from the 0 dpw profiles. Transcripts of hydroxycinnamic acid biosynthesis genes also accumulated soon after wounding, as evidenced by up-regulation between 0-0.5 dpw (steps 40-47, **Figure 3.3D**). Non-polar metabolite profile PCAs formed three clusters mostly separated by time – 0-2 dpw, 3-4 dpw and 5-7 dpw. The first cluster included profiles dominated by aliphatic products of primary metabolism and membrane components, then the appearance of suberin-associated aliphatics such as 18:1 ω -hydroxy fatty acids increased from 3-4 dpw, followed by an accumulation of wax components from 5-7 dpw (Yang and Bernards, 2007). These findings are consistent with the observed up-regulation of aliphatic suberin genes that typically occurred later into the 3-day time course than all other targeted genes, from 1-2 or 2-3 dpw (**Figure 3.3H**).

Generally, differential temporal metabolite profile patterns matched those of the observed transcriptome time course, through targeted (**Figure 3.3A-I**) and GO-based gene set analyses (**Figure 3.2**). The similarity in temporal profiles between transcriptome and metabolome results suggests that changes at the protein level, which act to bridge gene expression and downstream metabolism, may also follow similar patterns.

Chaves et al. (2009) highlighted that their wound-healing tuber proteome observations were consistent with the timing of metabolome-based findings by Yang and Bernards

(2007). In the wound-healing tuber proteome, the first two days after wounding were dominated by proteins involved in energy production and primary metabolism, along with changes in defensive and secondary metabolism proteins that are not necessarily related to suberization (e.g. high molecular weight patatins). Notably, superoxide dismutases and several peroxidase isoenzymes, including a known suberization-associated anionic peroxidase, were either detected immediately, or their levels were up-regulated within the first two days after wounding, and quantities were generally sustained throughout an 8-day time course. These observations are largely consistent with temporal changes of phenolic suberin assembly genes in the wound-healing transcriptome, including superoxide dismutases and anionic peroxidases (**Figure 3.3E**).

CCoAOMT, which has a predicted role in the production of feruloyl-CoA found in both the SPPD and SPAD, was up-regulated between 1 dpw and 4 dpw (Chaves et al., 2009). Two of the most strongly up-regulated *CCoAOMT* genes were highly expressed by 0.5 dpw (**Figure 3.3D**), and continued to increase throughout my 3-day time course. The Chaves et al. (2009) proteomic study did not detect significant changes in proteins required for SPAD-specific metabolism, or explain the lack thereof, but used microscopy to demonstrate accumulation of aliphatic suberin by 4 dpw.

Some enzymes involved in suberin biosynthesis and assembly have been studied in the context of tuber wound-healing, and the timing of up-regulation of enzyme activities and/or accumulation of protein is also similar to observed RNA-seq based gene expression profiles. For example, phenylalanine ammonia lyase (PAL) activity is induced within the first 6-12 hours of wounding (Borchert, 1978; Bernards et al., 2000), 4-coumaroyl CoA ligase (4CL) activity is detectable within 12 hours of wounding (Bernards et al., 2000), and tyramine hydroxycinnamoyl transferase (THT) activity is detectable within 3-4 hours after wounding (Negrel et al., 1993). All of the genes that encode these enzymes follow similar expression profiles in my wound-healing transcriptome (**Figure 3.3D**).

Monolignol biosynthesis enzymes cinnamoyl CoA reductase (CCR) and cinnamyl alcohol dehydrogenase (CAD) demonstrate minimal induction during suberization

(Bernards et al., 2000), and the activity of the latter is greater than that of the former. These findings are echoed in my transcriptome analysis (**Figure 3.3D**), as described in **§3.4.1**.

Feruloyl transferase (FHT) conjugates feruloyl-CoA, a phenylpropanoid pathway derived product, with aliphatic chains (Serra et al., 2010). Boher et al. (2013) demonstrated that FHT accumulates in wounded tubers within 1 dpw, and continues to increase during wound-healing time course. This timing is similar to the observed up-regulation of *FHT* from 0-0.5 dpw, followed by further increased transcript accumulation, in my wound-healing transcriptome (**Figure 3.3I**)

Studies by Agrawal and Kolattukudy (1977, 1978a, 1978b) used cell-free extracts obtained from wound-healing tubers to characterize the accumulation and activity of a putative ω -hydroxyacid dehydrogenase involved in the formation of α,ω -dioic acids found in the SPAD. The described ω -hydroxyacid dehydrogenase was transcribed within 3 dpw, translated into active protein before 4 dpw (Agrawal and Kolattukudy, 1977), and remained active at 5 dpw (Agrawal and Kolattukudy, 1978a), overall matching the timing of aliphatic suberin accumulation. Genes encoding putative oxidoreductases involved in aliphatic suberin metabolism were typically expressed by 2-3 dpw in the wound-healing transcriptome (steps 78-80, 82, **Figure 3.3H**; Woolfson et al., 2018).

Since the majority of the protein and metabolite focused studies noted above did not include analysis between 0-1 dpw, it is possible that proteins also accumulated within 12 hours of wounding, as observed for many genes. It is also feasible that transcription precedes detectable protein accumulation by half a day or more for many possible reasons. Some considerations include the time lag between transcription and translation, transcript and protein turnover, and factors such as post-translational modifications or substrate availability that may be required for enzyme activation. Regardless of slight differences, the overall temporal patterns observed in my wound-healing transcriptome were consistent with other studies that track suberization-related metabolite and protein accumulation over time. Specifically, all analyses to date point to an activation of

primary metabolism followed by induced phenolic metabolism, in advance of induced aliphatic metabolism.

3.4.5 Final considerations and conclusions

In this work, I sequenced the first transcriptome time series investigating wound-healing in potato and has improved our current state of knowledge on suberization. The data generated by this RNA-seq project was used to better establish the nuances of transcriptional changes throughout the wound-healing time course through both global and targeted approaches. These findings provided support for novel, and in some cases wound-induced, candidate genes involved in different metabolic branches required for suberization, and new information was integrated into an updated and comprehensive hypothetical framework for suberin biosynthesis in the wound-healing potato tuber.

Suberin biosynthesis is one aspect of wound-healing, which also includes primary metabolism and secondary metabolism that can be considered responsive to both abiotic and biotic stress. Certain biological processes are critical for physical healing and formation of the closing layer initially, and a new wound periderm later into wound-healing. This study provides a more complete overview of the early processes that occur during the first three days after wounding and include events involved in closing layer formation.

Wounding leads to transcriptional changes that follow distinctive temporal patterns – primary metabolic pathways were already expressed, or up-regulated immediately, and maintained at levels that would allow for precursor carbon skeletons and energy to feed into downstream metabolic processes. Genes involved in pathways for phenolic and aliphatic suberin production generally followed previously established differential temporal patterns, while also revealing a finer level of within-pathway changes. Evaluation of putative Casparian band membrane and cutin synthase-like genes pinpointed wound-responsive candidates that may mediate polymerization and deposition processes, and oversee the high level of organization required for appropriate suberin assembly. Analyses of regulatory components further investigated the steps involved in

the known aliphatic suberin regulating hormone ABA to better establish timing of events, and highlighted the potential role of candidate transcription factors.

The roadmap towards suberin biosynthesis was updated to include steps characterized since its first publication (Bernards, 2002), with corresponding changes in gene expression at each pathway step incorporated to provide a comprehensive overview of the metabolism required for suberin biosynthesis and assembly.

My study has yielded a dataset that will offer a valuable resource for continued exploration of the tuber wound response, including screening transcriptional changes in genes of interest during wound-healing, for comparison and/or use with other potato transcriptome datasets, and for future hypothesis generation. Future work could utilize this information towards crop improvement applications, in potato specifically, and in other species, if novel characterized biosynthetic genes and regulatory components are conserved in roots, fruit skins and cork.

3.5 References

- Agrawal, V.P. and Kolattukudy, P.E.** (1977). ω -Hydroxyacid oxidation in enzyme preparations from suberizing potato tuber disks. *Plant Physiology* **59**, 667-672.
- Agrawal, V.P. and Kolattukudy, P.E.** (1978a). Purification and characterization of a wound-induced omega-hydroxy fatty acid:NADP oxidoreductase from potato tuber disks (*Solanum tuberosum* L.). *Archives of Biochemistry and Biophysics* **191**, 452-465.
- Agrawal, V.P. and Kolattukudy, P.E.** (1978b). Mechanism of action of a wound-induced ω -hydroxy fatty acid:NADP oxidoreductase isolated from potato tubers (*Solanum tuberosum* L.) *Archives of Biochemistry and Biophysics* **191**, 466-478.
- Anders, S., Pyl, P.T. and Huber, W.** (2015). HTSeq—a Python framework to work with high-throughput sequencing data. *Bioinformatics* **31**(2), 166-169.
- Andrews, S.** (2010). FastQC: a quality control tool for high throughput sequence data. Available online at: <http://www.bioinformatics.babraham.ac.uk/projects/fastqc>
- Alexa, A., and Rahnenfuhrer, J.** (2016). topGO: Enrichment Analysis for Gene Ontology. R package version 2.32.0.
- Batelli, G., Massarelli, I., Van Oosten, M., Nurcato, R., Vannini, C., Raimondi, G., Leone, A., Zhu, J.-K., Maggio, A. and Grillo, S.** (2012). *Asg1* is a stress-inducible gene which increases stomatal resistance in salt stressed potato. *Journal of Plant Physiology* **169**, 1849-1857.
- Beaudoin, F., Wu, X., Li, F., Haslam, R.P., Markham, J.E., Zheng, H., Napier, J.A., and Kunst, L.** (2009). Functional characterization of the *Arabidopsis* B-ketoacyl-coenzyme A reductase candidates of the fatty acid elongase. *Plant Physiology* **150**, 1174-1191.
- Beisson, F., Li-Beisson, Y., Pollard, M.** (2012). Solving the puzzles of cutin and suberin polymer biosynthesis. *Current Opinion in Plant Biology* **15**, 1-9.
- Beisson, F., Li, Y., Bonaventure, G., Pollard, M. and Ohlrogge, J.B.** (2007). The acyltransferase GPAT5 is required for the synthesis of suberin in seed coat and root of *Arabidopsis*. *The Plant Cell*, **19**(1), 351-368.
- Benjamini, Y. and Hochberg, Y.** (1995). Controlling the false discovery rate: a practical and powerful approach to multiple testing. *Journal of the Royal Statistical Society B* **57**, 289-300.
- Berardini, T.Z., Reiser, L., Li, D., Mezheritsky, Y., Muller, R., Strait, E. and Huala, E.** (2015). The *Arabidopsis* Information Resource: Making and mining the "gold standard" annotated reference plant genome. *Genesis* **53**, 474-485.

- Bernards, M.A., Susag, L.M., Bedgar, D.L., Anterola, A.M. and Lewis, N.G.** (2000). Induced phenylpropanoid metabolism during suberization and lignification: a comparative analysis. *Journal of Plant Physiology* **157**(6), 601-607.
- Bernards, M.A.** (2002). Demystifying suberin. *Canadian Journal of Botany* **80**, 227-240.
- Bernards, M.A., Lopez, M.L., Zajicek, J., and Lewis, N.G.** (1995). Hydroxycinnamic acid-derived polymers constitute the polyaromatic domain of suberin. *Journal of Biological Chemistry* **270**, 7382-7386.
- Bernards, M.A., Summerhurst, D.K., and Razem, F.A.** (2004). Oxidases, peroxidases and hydrogen peroxide: The suberin connection. *Phytochemistry Reviews* **3**, 113-126.
- Bernards, M.A., Fleming, W.D., Llewellyn, D.B., Priefer, R., Yang, X., Sabatino, A., and Plourde, G.L.** (1999). Biochemical characterization of the suberization-associated anionic peroxidase of potato. *Plant Physiology* **121**, 135-145.
- Bird, D., Beisson, F., Brigham, A., Shin, J., Greer, S., Jetter, R., Kunst, L., Wu, X., Yephremov, A. and Samuels, L.** (2007). Characterization of *Arabidopsis* ABCG11/WBC11, an ATP binding cassette (ABC) transporter that is required for cuticular lipid secretion. *The Plant Journal* **52**(3), 485-498.
- Bjelica, A., Haggitt, M.L., Woolfson, K.N., Lee, D.P., Makhzoum, A.B. and Bernards, M.A.** (2016). Fatty acid ω -hydroxylases from *Solanum tuberosum*. *Plant Cell Reports* **35**(12), 2435-2448.
- Boher, P., Serra, O., Soler, M., Molinas, M. and Figueras, M.** (2013). The potato suberin feruloyl transferase FHT which accumulates in the phellogen is induced by wounding and regulated by abscisic and salicylic acids. *Journal of Experimental Botany* **64**(11), 3225-3236.
- Bolger, A.M., Lohse, M. and Usadel, B.** (2014). Trimmomatic: a flexible trimmer for Illumina sequence data. *Bioinformatics* **30**(15), 2114-20.
- Borchert, R.** (1978). Time course and spatial distribution of phenylalanine ammonia-lyase and peroxidase activity in wounded potato tuber tissue. *Plant Physiology* **62**, 789-793.
- Carlson, M.** (2018). GO.db: A set of annotation maps describing the entire Gene Ontology. R package version 3.6.0.
- Chang, S., Puryear, J. and Cairney, J.** (1993). A simple and efficient method for isolating RNA from pine trees. *Plant Molecular Biology Reporter* **11**, 113-116.
- Chaves, I., Pinheiro, C., Paiva, J.A., Planchon, S., Sergeant, K., Renaut, J., Graça, J.A., Costa, G., Coelho, A.V. and Ricardo, C.P.P.** (2009). Proteomic evaluation of wound-healing processes in potato (*Solanum tuberosum* L.) tuber tissue. *Proteomics* **9**(17), 4154-4175.
- Compagnon, V., Diehl, P., Benveniste, I., Meyer, D., Schaller, H., Schreiber, L., Franke, R., and Pinot, F.** (2009). CYP86B1 is required for very long chain ω -

hydroxyacid and α , ω -dicarboxylic acid synthesis in root and seed suberin polyester. *Plant Physiology* **150**, 1831-1843.

- Dammann, C., Rojo, E. and Sanchez-Serrano, J.J.** (2002). Abscisic acid and jasmonic acid activate wound-inducible genes in potato through separate, organ-specific signal transduction pathways. *The Plant Journal* **11**(4), 773-782.
- Denness, L., McKenna, J.F., Segonzac, C., Wormit, A., Madhou, P., Bennett, M., Mansfield, J., Zipfel, C., and Hamann, T.** (2011). Cell wall damage-induced lignin biosynthesis is regulated by a reactive oxygen species- and jasmonic acid-dependent process in *Arabidopsis*. *Plant Physiology* **156**(3), 1364-1374.
- De Stefano-Beltrán, L., Knauber, D., Huckle, L., and Suttle, J.C.** (2006). Effects of postharvest storage and dormancy status on ABA content, metabolism, and expression of genes involved in ABA biosynthesis and metabolism in potato tuber tissues. *Plant Molecular Biology* **61**, 687-697.
- Domergue, F., Vishwanath, S. J., Joubès, J., Ono, J., Lee, J. A., Bourdon, M., Alhattab, R., Lowe, C., Pascal, S., Lessire, R. and Rowland, O.** (2010). Three *Arabidopsis* fatty acyl-coenzyme A reductases, FAR1, FAR4, and FAR5, generate primary fatty alcohols associated with suberin deposition. *Plant Physiology* **153**, 1539-1554.
- Esau, K.** (1977). *Anatomy of Seed Plants*, 2nd Edition (pp. 183-197). New York, NY: Wiley & Sons.
- Facchini, P.J., Hagel, J., and Zulak, K.G.** (2002). Hydroxycinnamic acid amide metabolism: physiology and biochemistry. *Canadian Journal of Botany* **80**, 577-589.
- Fernandez-Pozo, N., Menda, N., Edwards, J.D., Saha, S., Teclé, I.Y., Strickler, S.R., Bombarely, A., Fisher-York, T., Pujar, A., Foerster, H., Yan, A. and Mueller, L.A.** (2015). The Sol Genomics Network (SGN): from genotype to phenotype to breeding. *Nucleic Acids Research* **43**, D1036-41.
- Fry, S.C., Smith, R.C., Renwick, K.F., Martin, D.J., Hodge, S.K., and Matthews, K.J.** (1992). Xyloglucan endotransglycosylase, a new wall-loosening enzyme activity from plants. *Biochemical Journal* **282**, 821-828.
- Fu, Y., Dominissini, D., Rechavi, G., and He, C.** (2014). Gene expression regulation mediated through reversible m⁶A RNA methylation. *Nature Reviews Genetics* **15**, 293-306.
- Gálvez, J.H., Tai, H.H., Lagüe, M., Zebarth, B.J. and Strömviik, M.V.** (2016). The nitrogen responsive transcriptome in potato (*Solanum tuberosum* L.) reveals significant gene regulatory motifs. *Scientific Reports* **6**, p.26090.
- Gao, L., Tu, Z.J., Millett, B.P. and Bradeen, J.M.** (2013). Insights into organ-specific pathogen defense responses in plants: RNA-seq analysis of potato tuber-*Phytophthora infestans* interactions. *BMC Genomics* **14**, 340-352.

- Gong, L., Zhang, H., Gan, X., Zhang, L., Chen, Y., Nie, F., Shi, L., Li, M., Guo, Z., Zhang, G. and Song, Y.** (2015). Transcriptome profiling of the potato (*Solanum tuberosum* L.) plant under drought stress and water-stimulus conditions. *PLoS One* **10**(5), p.e0128041.
- Goyer, A., Hamlin, L., Crosslin, J.M., Buchanan, A. and Chang, J.H.** (2015). RNA-Seq analysis of resistant and susceptible potato varieties during the early stages of potato virus Y infection. *BMC Genomics* **16**(1), 472-485.
- Graça, J.** (2015). Suberin: the biopolyester at the frontier of plants. *Frontiers in Chemistry* **3**(62), doi:10.3389/fchem.2015.00062.
- Graça, J. and Pereira, H.** (2000a). Methanolysis of bark suberins: analysis of glycerol and acid monomers. *Phytochem. Anal.* **11**, 45-51.
- Graça, J. and Pereira, H.** (2000b). Diglycerol alkendioates in suberin: building units of a poly(acylglycerol) polyester. *Biomacromolecules* **1**, 519-522.
- Graça, J. and Pereira, H.** (2000c). Suberin structure in potato periderm: glycerol, longchain monomers, and glyceryl and feruloyl dimers. *Journal of Agricultural and Food Chemistry* **48**, 5476- 5483.
- Graça, J. and Santos, S.** (2007). Suberin: a biopolyester of plants' skin. *Macromolecular Bioscience* **7**, 128-135.
- Guenther, J.F.** (1995). Economics of potato storage. *American Potato Journal* **72**(8), 493-502.
- Guenther, J.F., Michael, K.C. and Nolte, P.** (2001). The economic impact of potato late blight on US growers. *Potato Research* **44**(2), 121-125.
- Holloway, P.J.** (1983). Some variations in the composition of suberin from the cork layers of higher-plants. *Phytochemistry* **22**, 495-502.
- Kim, S.-Y., and Volsky D. J.** (2005). PAGE: Parametric Analysis of Gene Set Enrichment. *BMC Bioinformatics* **6**, 144-156.
- Kinsella, R.J., Kahari, A., Haider, S., Zamora, J., Proctor, G., Spudich, G., Almeida-King, J., Staines, D., Derwent, P., Kernhornou, A., Kersey, P., and Flicek, P.** (2011). Ensembl BioMarts: a hub for data retrieval across taxonomic space. *Database (Oxford)*, bar030.
- Knollenberg, B.J., Liu, J., Yu, S., Lin, H. and Tian, L.** (2018). Cloning and functional characterization of a p-coumaroyl quinate/shikimate 3'-hydroxylase from potato (*Solanum tuberosum*). *Biochemical and Biophysical Research Communications* **496**(2), 462-467.
- Koda, Y. and Kikuta, Y.** (1994). Wound-induced accumulation of jasmonic acid in tissues of potato tubers. *Plant and Cell Physiology* **35**, 751-756.
- Kolattukudy, P.E.** (1987). Lipid-derived defensive polymers and waxes and their role in plant-microbe interaction. In *Lipids: Structure and Function* (pp. 291-314).
- Kolde, R.** (2012). Pheatmap: pretty heatmaps. R package version, 61.

- Kosma, D.K., Murmu, J., Razeq, F.M., Santos, P., Bourgault, R., Molina, I. and Rowland, O.** (2014). AtMYB41 activates ectopic suberin synthesis and assembly in multiple plant species and cell types. *The Plant Journal* **80**(2), 216-229.
- Kumar, G.N.M., Lulai, E.C., Suttle, J.C. and Knowles, N.R.** (2010). Age-induced loss of wound-healing ability in potato tubers is partly regulated by ABA. *Planta* **232**, 1433-1445.
- Kumar, R., Wallis, J.G., Skidmore, C. and Browse, J.** (2006). A mutation in *Arabidopsis* cytochrome b5 reductase identified by high-throughput screening differentially affects hydroxylation and desaturation. *The Plant Journal* **48**, 920-932.
- Lashbrooke, J.G., Cohen, H., Levy-Samocho, D., Tzfadia, O., Panizel, I., Zeisler, V., Massalha, H., Stern, A., Trainotti, L., Schreiber, L. and Costa, F.** (2016). MYB107 and MYB9 homologs regulate suberin deposition in angiosperms. *The Plant Cell* **28**, 2097-2116.
- Law, C.W., Chen, Y., Shi, W. and Smyth, G.K.** (2014). voom: Precision weights unlock linear model analysis tools for RNA-seq read counts. *Genome Biology* **15**(2), R29.
- Landgraf, R., Smolka, U., Altmann, S., Eschen-Lippold, L., Senning, M., Sonnewald, S., Weigel, B., Frolova, N., Strehmel, N., Hause, G. and Scheel, D.** (2014). The ABC transporter ABCG1 is required for suberin formation in potato tuber periderm. *The Plant Cell* **26**, 3403-3415.
- Legay, S., Guerriero, G., Andre, C., Guignard, C., Cocco, E., Charton, S., Boutry, M., Rowland, O., Hausman, J.-F.** (2016). MdMyb93 is a regulator of suberin deposition in russeted apple fruit skins. *New Phytologist* **212**(4), 977-991.
- Li, Y., Beisson, F., Koo, A.J., Molina, I., Pollard, M. and Ohlrogge, J.** (2007). Identification of acyltransferases required for cutin biosynthesis and production of cutin with suberin-like monomers. *Proceedings of the National Academy of Sciences of the United States of America* **104**(46), 18339-18344.
- Lulai, E.C.** (2007). The canon of potato science: 43. Skin-set and wound-healing/suberization. *Potato Research* **50**, 387-390.
- Lulai, E.C. and Corsini, D.L.** (1998). Differential deposition of suberin phenolic and aliphatic domains and their roles in resistance to infection during potato tuber (*Solanum tuberosum* L.) wound-healing. *Physiological and Molecular Plant Pathology* **53**(4), 209-222.
- Lulai, E.C. and Freeman, T.P.** (2001). The importance of phellogen cells and their structural characteristics in susceptibility and resistance to excoriation in immature and mature potato tuber (*Solanum tuberosum* L.) periderm. *Annals of Botany* **88**, 555-561.
- Lulai, E.C., Huckle, L., Neubauer, J.D. and Suttle, J.C.** (2011) Coordinate expression of AOS genes and JA accumulation: JA is not required for initiation of closing layer in wound healing tubers. *Journal of Plant Physiology* **168**, 976-982.

- Lulai, E.C. and Morgan, W.C.** (1992). Histochemical probing of potato periderm with neutral red: a sensitive cytofluorochrome for the hydrophobic domain of suberin. *Biotechnic & Histochemistry* **67**, 185-195.
- Lulai, E.C. and Neubauer, J.D.** (2014). Wound-induced suberization genes are differentially expressed, spatially and temporally, during closing layer and wound periderm formation. *Postharvest Biology and Technology* **90**, 24-33.
- Lulai, E.C., Neubauer, J.D. and Suttle, J.C.** (2014). Kinetics and localization of wound-induced DNA biosynthesis in potato tuber. *Journal of plant physiology*, **171**(17), 1571-1575.
- Lulai, E.C. and Orr, P.H.** (1994). Techniques for detecting and measuring developmental and maturational changes in tuber native periderm. *American Potato Journal* **71**, 489-505.
- Lulai, E.C. and Suttle, J.C.** (2004). The involvement of ethylene in wound-induced suberization of potato tuber (*Solanum tuberosum* L.): a critical assessment. *Postharvest Biology and Technology* **34**(1), 105-112.
- Lulai, E.C. and Suttle, J.C.** (2009). Signals involved in tuber wound-healing. *Plant Signaling and Behavior* **4**(7), 620-622.
- Lulai, E.C., Suttle, J.C., and Pederson, S.M.** (2008). Regulatory involvement of abscisic acid in potato tuber wound-healing. *Journal of Experimental Botany*, **59**(6), 1175-1186.
- Lulai, E.C., Campbell, L.G., Fugate, K.K. and McCue, K.F.** (2016). Biological differences that distinguish the 2 major stages of wound healing in potato tubers. *Plant Signaling & Behavior* **11**(12), e1256531.
- Lyon, G. D.** (1989). The biochemical basis of resistance of potatoes to soft rot *Erwinia* *supp.*—a review. *Plant Pathology* **38**, 313-339.
- Martel, C., Zhurov, V., Navarro, M., Martinez, M., Cazaux, M., Auger, P., Migeon, A., Santamaria, M.E., Wybouw, N., Diaz, I. and Van Leeuwen, T.** (2015). Tomato whole genome transcriptional response to *Tetranychus urticae* identifies divergence of spider mite-induced responses between tomato and *Arabidopsis*. *Molecular Plant-Microbe Interactions* **28**(3), 343-361.
- Massa, A.N., Childs, K.L., Lin, H., Bryan, G.J., Giuliano, G. and Buell, C.R.** (2011). The transcriptome of the reference potato genome *Solanum tuberosum* Group Phureja Clone DM1-3 516R44. *PLoS ONE* **6**(10): e26801.
- Molina, I., Li-Beisson, Y., Beisson, F., Ohlrogge, J.B. and Pollard, M.** (2009). Identification of an *Arabidopsis* feruloyl-coenzyme A transferase required for suberin synthesis. *Plant Physiology*, **151**(3), 1317-1328.
- Murtagh, F., and Legendre, P.** (2014). Ward's hierarchical agglomerative clustering method: Which algorithms implement Ward's criterion? *Journal of Classification* **31**(3), 274-295.

- Negrel, J., Javelle, F. and Paynot, M.** (1993) Wound-induced tyramine hydroxycinnamoyl transferase in potato (*Solanum tuberosum*) tuber discs. *Journal of Plant Physiology* **142**(5), 518-524.
- Negrel, J., Pollet, B. and Lapierre, C.** (1996). Ether-linked ferulic acid amides in natural and wound periderms of potato tuber. *Phytochemistry* **43**, 1195-1199.
- Neubauer, J.D., Lulai, E.C., Thompson, A.L., Suttle, J.C. and Bolton, M.D.** (2012). Wounding coordinately induces cell wall protein, cell cycle and pectin methyl esterase genes involved in tuber closing layer and wound periderm development. *Journal of Plant Physiology* **169**(6), 586-595.
- Nicot, N., Hausman, J.-F., Hoffmann, L. and Evers, D.** (2005). Housekeeping gene selection for real-time RT-PCR normalization in potato during biotic and abiotic stress. *Journal of Experimental Biology* **56**, 2907-2914.
- O'Donnell, P.J., Calvert, C., Atzorn, R., Wasternack, C., Leyser, H.M.O., and Bowles, D.J.** (1996). Ethylene as a signal mediating the wound responses of tomato plants. *Science* **274**(5294), 1914-1917.
- Öhman, D., Demedts, B., Kumar, M., Gerber, L., Gorzsás, A., Goeminne, G., Hedenström, M., Ellis, B., Boerjan, W. and Sundberg, B.** (2013). MYB103 is required for *FERULATE-5-HYDROXYLASE* expression and syringyl lignin biosynthesis in *Arabidopsis* stems. *The Plant Journal* **73**(1), 63-76.
- Pagès, H., Carlson, M., Falcon, S. and Li, N.** (2018). AnnotationDbi: Annotation Database Interface. R package version 1.42.1.
- Pfaffl, M.W.** (2001). A new mathematical model for relative quantification in real-time RT-PCR. *Nucleic Acids Research* **29**, 2002-2007.
- Potato Genome Sequencing Consortium (PGSC)** (2011). Genome sequence and analysis of the tuber crop potato. *Nature* **475**, 189–195.
- R Core Team** (2018). R: A language and environment for statistical computing. R Foundation for Statistical Computing, Vienna, Austria. ISBN 3-900051-07-0, URL <http://www.R-project.org>.
- Ranathunge, K., Schreiber, L. and Franke, R.** (2011). Suberin research in the genomics era – New interest for an old polymer. *Plant Science* **180**, 399-413.
- Reymond, P., Weber, H., Damond, M. and Farmer, E.E.** (2000). Differential gene expression in response to mechanical wounding and insect feeding in *Arabidopsis*. *Plant Cell* **12**, 707-719.
- Ritchie, M.E., Phipson, B., Wu, D., Hu, Y., Law, C.W., Shi, W. and Smyth, G.K.** (2015). limma powers differential expression analyses for RNA-sequencing and microarray studies. *Nucleic Acids Research* **43**(7), e47.
- Robinson, M.D., McCarthy, D.J. and Smyth, G.K.** (2010). edgeR: a Bioconductor package for differential expression analysis of digital gene expression data. *Bioinformatics* **26**(1), 139-140.

- Roppolo, D., De Rybel, B., Tendon, V.D., Pfister, A., Alassimone, J., Vermeer, J.E., Yamazaki, M., Stierhof, Y.D., Beeckman, T. and Geldner, N.** (2011) A novel protein family mediates Casparian strip formation in the endodermis. *Nature* **473**(7347), 380-383.
- Roppolo, D., Boeckmann, B., Pfister, A., Boutet, E., Rubio, M.C., Dénervaud-Tendon, V., Vermeer, J.E., Gheyselinck, J., Xenarios, I. and Geldner, N.** (2014). Functional and evolutionary analysis of the CASPARIAN STRIP MEMBRANE DOMAIN PROTEIN family. *Plant Physiology* **165**(4), 1709-1722.
- Rose, J.K.C., Braam, J., Fry, S.C. and Nishitani, K.** (2002). The XTH family of enzymes involved in xyloglucan endotransglucosylation and endohydrolysis: current perspectives and a new unifying nomenclature, *Plant and Cell Physiology* **43**, 1421-1435.
- Rose, N.R. and Klose, R.J.** (2014). Understanding the relationship between DNA methylation and histone lysine methylation. *Biochimica et Biophysica Acta* **1839**(12), 1362-1372.
- Schwachtje, J. and Baldwin, I.T.** (2008). Why does herbivore attack reconfigure primary metabolism? *Plant Physiology* **146**(3), 845-851.
- Serra, O., Soler, M., Hohn, C., Sauveplane, V., Pinot, F., Franke, R., Schreiber, L., Prat, S., Molinas, M. and Figueras, M.** (2009a). *CYP86A33*-targeted gene silencing in potato tuber alters suberin composition, distorts suberin lamellae, and impairs the periderm's water barrier function. *Plant Physiology* **149**, 1050-1060.
- Serra, O., Soler, M., Hohn, C., Franke, R., Schreiber, L., Prat, S., Molinas, M. and Figueras, M.** (2009b). Silencing of *StKCS6* in potato periderm leads to reduced chain lengths of suberin and wax compounds and increased peridermal transpiration. *Journal of Experimental Botany* **60**, 697-707.
- Serra, O., Hohn, C., Franke, R., Prat, S., Molinas, M. and Figueras, M.** (2010). A feruloyl transferase involved in the biosynthesis of suberin and suberin-associated wax is required for maturation and sealing properties of potato periderm. *The Plant Journal* **62**, 277-290.
- Sharma, S. K., Bolser, D., de Boer, J., Sønderkær, M., Amoros, W., Carboni, M. F., D'Ambrosio, J. M., de la Cruz, G., Di Genova, A., Douches, D. S., Eguiluz, M., Guo, X., Guzman, F., Hackett, C. A., Hamilton, J. P., Li, G., Li, Y., Lozano, R., Maass, A., Marshall, D., Martinez, D., McLean, K., Mejía, N., Milne, L., Munive, S., Nagy, I., Ponce, O., Ramirez, M., Simon, R., Thomson, S. J., Torres, Y., Waugh, R., Zhang, Z., Huang, S., Visser, R. G. F., Bachem, C. W. B., Sagredo, B., Feingold, S. E., Orjeda, G., Veilleux, R. E., Bonierbale, M., Jacobs, J. M. E., Milbourne, D., Martin, D. M. A. and Bryan, G. J.** (2013). Construction of reference chromosome-scale pseudomolecules for potato: Integrating the potato genome with genetic and physical maps. *G3: Genes/Genomes/Genetics* **3**, 2031-2047.

- Smyth, G.K.** (2005). Limma: linear models for microarray data. In *Bioinformatics and computational biology solutions using R and Bioconductor* (pp. 397-420). New York, NY: Springer.
- Soliday, C.L., Dean, B.B. and Kolattukudy, P.E.** (1978). Suberization: inhibition by washing and stimulation by abscisic acid in potato disks and tissue culture. *Plant Physiology* **61**(2), 170-174.
- Strehmel, N., Praeger, U., König, C., Fehrle, I., Erban, A., Geyer, M., Kopka, J. and van Dongen, J.T.** (2010). Time course effects on primary metabolism of potato (*Solanum tuberosum*) tuber tissue after mechanical impact. *Postharvest Biology and Technology* **56**(2), 109-116.
- Suttle, J.C., Lulai, E.C., Huckle, L.L. and Neubauer, J.C.** (2013). Wounding of potato tubers induces increases in ABA biosynthesis and catabolism and alters expression of ABA metabolic genes. *Journal of Plant Physiology* **170**, 560-566.
- Thomson, N., Evert, R.F. and Kelman, A.** (1995). Wound healing in whole potato tubers: a cytochemical, fluorescence, and ultrastructural analysis of cut and bruise wounds. *Canadian Journal of Botany* **73**(9), 1436-1450.
- Trapnell, C., Roberts, A., Goff, L., Pertea, G., Kim, D., Kelley, D.R., Pimentel, H., Salzberg, S.L., Rinn, J.L. and Pachter, L.** (2012). Differential gene and transcript expression analysis of RNA-seq experiments with TopHat and Cufflinks. *Nature Protocols* **7**(3), 562-578.
- Vandesompele, J., De Preter, K., Pattyn, F., Poppe, B., Van Roy, N., De Paepe, A. and Speleman, F.** (2002). Accurate normalization of real-time quantitative RT-PCR data by geometric averaging of multiple internal control genes. *Genome Biology* **3**(7), research0034.1-research003411.
- Väremo, L., Nielsen, J., and Nookaew, I.** (2013). Enriching the gene set analysis of genome-wide data by incorporating directionality of gene expression and combining statistical hypotheses and methods. *Nucleic Acids Research* **41**(8), 4378-4391.
- Verdaguer, R., Soler, M., Serra, O., Garrote, A., Fernández, S., Company-Arumí, D., Anticó, E., Molinas, M. and Figueras, M.** (2016). Silencing of the potato *StNAC103* gene enhances the accumulation of suberin polyester and associated wax in tuber skin. *Journal of Experimental Botany* **67**(18), 5415-5427.
- Vishwanath, S.J., Delude, C., Domergue, F. and Rowland, O.** (2015). Suberin: biosynthesis, regulation, and polymer assembly of a protective extracellular barrier. *Plant Cell Reports* **34**, 573-586.
- Vulavala, V.K., Fogelman, E., Rozental, L., Faigenboim, A., Tanami, Z., Shoseyov, O. and Ginzberg, I.** (2017). Identification of genes related to skin development in potato. *Plant Molecular Biology* **94**(4-5), 481-494.
- Ward, J.H. Jr.** (1963). Hierarchical grouping to optimize an objective function. *Journal of the American Statistical Association* **58**(301), 236-244.

- Wasternack, C., Stenzel, I., Hause, B., Hause, G., Kutter, C., Maucher, H., Neumerkel, J., Feussner, I., and Miersch, O.** (2006). The wound response in tomato – Role of jasmonic acid. *Journal of Plant Physiology* **163**(3), 297-306.
- Wiltshire, J.J.J., and Cobb, A.H.** (1996). A review of the physiology of potato tuber dormancy. *Annals of Applied Biology* **129**, 553-569.
- Woolfson, K.N., Haggitt, M.L., Zhang, Y., Kachura, A., Bjelica, A., Rey Rincon, M.A., Kaberi, K.M. and Bernard, M.A.** (2018). Differential induction of polar and non-polar metabolism during wound-induced suberization in potato (*Solanum tuberosum* L.) tubers. *The Plant Journal* **93**(5), 931-942.
- Yadav, V., Molina, I., Ranathunge, K., Castillo, I.Q., Rothstein, S.J. and Reed, J.W.** (2014). ABCG transporters are required for suberin and pollen wall extracellular barriers in *Arabidopsis*. *The Plant Cell* **26**(9), 3569-3588.
- Yang, W.L. and Bernard, M.A.** (2006). Wound-induced metabolism in potato (*Solanum tuberosum*) tubers: biosynthesis of aliphatic domain monomers. *Plant Signaling & Behavior* **1**(2), 59-66.
- Yang, W.L. and Bernard, M.A.** (2007). Metabolite profiling of potato (*Solanum tuberosum* L.) tubers during wound-induced suberization. *Metabolomics* **3**(2), 147-159.
- Yan, B. and Stark, R.E.** (2000) Biosynthesis, molecular structure, and domain architecture of potato suberin: A ¹³C NMR study using isotopically labelled precursors. *Journal of Agricultural and Food Chemistry* **48**, 3298-3304.
- Yogendra, K.N., Kumar, A., Sarkar, K., Li, Y., Pushpa, D., Mosa, K.A., Duggavathi, R., and Kusalappa, A.C.** (2015). Transcription factor *StWRKY1* regulates phenylpropanoid metabolites conferring late blight resistance in potato. *Journal of Experimental Botany* **66**(22), 7377-7389.
- Zhang, H., Lang, Z., and Zhu, J.-K.** (2018). Dynamics and function of DNA methylation in plants. *Nature Reviews Molecular Cell Biology* **19**, 489-506.

Chapter 4

4 General discussion

4.1 Thesis summary

I used a wounded potato tuber model system to study the progression of suberization and other wound-healing related processes over time. The wound-induced suberization process is complex on both temporal and spatial scales, and must involve a high level of coordination and regulation to result in the synthesis of the large, precisely organized macromolecular biopolymer suberin.

4.1.1 The role of ABA in the differential temporal regulation of suberin-associated metabolism

To better understand the regulatory mechanisms underlying the differential temporal induction of suberin-related metabolic pathways, I used a 6-day wound-healing potato tuber time course experiment to test the hypothesis that abscisic acid (ABA) is involved in the differential regulation of a select sub-set of suberin biosynthetic, linkage and deposition genes as they relate to the production and assembly of suberin phenolic and aliphatic monomers (**Chapter 2**). The application of the ABA biosynthesis inhibitor, fluridone (FD) to cut tuber slices led to the delayed induction of aliphatic and convergent (i.e. linkage and deposition) gene expression, whereas the exogenous application of ABA or ABA together with FD resulted in earlier up-regulation of these genes. In contrast, genes involved in phenolic suberin biosynthesis were not affected by different ABA-related treatments. Chemical analyses demonstrated a shift in polar metabolite (i.e. phenolic compound) profiles over time, of which some differences between treatments were evident by later time points during wound-healing. At the individual metabolite level, an early drop in aromatic amino acids that feed into later phenylpropanoid metabolism for the synthesis of different polar suberin products preceded an observed increase in several phenolic products. Non-polar, aliphatic metabolites accumulated in soluble pools of control tubers by 3 dpw, coinciding with the time at which ABA reached its peak level. This change was followed by an increase in deposited, insoluble (i.e.

polymerized) aliphatic monomers between 4-6 dpw. Fluridone-treated tubers demonstrated both suppression of, and a lag in, soluble aliphatic accumulation, but the same impact was not observed at the level of insoluble non-polar compounds. Taken together, these findings suggest that ABA is involved in the regulation of aliphatic and convergent metabolism at the transcriptional level, but not phenolic metabolism. This regulatory oversight of aliphatic suberin-associated gene expression has important implications for the synthesis of soluble aliphatic monomers, but also suggests that ABA is not solely responsible for coordinating polymerization and/or deposition of these monomers. These findings also suggest that one or more mechanisms of regulation must control phenylpropanoid metabolism, which have yet to be elucidated in the context of tuber suberization.

4.1.2 The wound-healing tuber transcriptome

The study described in **Chapter 2**, along with the recent characterization of suberin-associated transcription factors, led to the generation of new hypotheses about additional regulatory mechanisms involved in this process. More specifically, these findings led to the hypothesis that regulatory components, such as transcription factors, must be in place to control phenolic suberin metabolism, and others likely interplay with ABA to oversee aliphatic suberin production. To expand upon the list of previously studied genes and incorporate novel candidates (e.g. transcription factors and assembly genes) into targeted investigations as well as global overviews, I took an RNA-seq approach to studying the wound-healing potato tuber during the first three days of closing layer formation, including a 0.5 dpw time point to capture putative regulatory gene activation (**Chapter 3**). This transcriptomic analysis was used to gain insight into changes that occur after wounding that include suberization, but also encompass additional requirements for wound-healing, such as primary metabolism, and the transcription of genes involved in physical healing and cell wall modification. By exploring the wound-healing tuber transcriptome during the early stages of closing layer formation, I was able to identify new targets with potential involvement in the regulation of biosynthesis and assembly of both phenolic and aliphatic suberin components. This largescale investigation outlined temporal shifts of groups of genes (organized by GO term or by pre-determined

biosynthetic pathway), while also highlighting the nuances in gene expression that exist within pathways to offer insight into the timing of suberization and wound-healing events. On a global scale, I observed an initial reconfiguration of biological processes, followed by fewer changes that reflected more specialized activities related to suberization and wound-healing. Additionally, the transcriptome data were used to generate an updated, comprehensive framework for suberin biosynthesis that incorporates new transcriptomic data from this study, and also up-to-date information from the literature. My findings from both global and targeted analyses provide support for the role of previously uncharacterized genes involved in wound-healing that can be targeted in future work.

4.1.3 Summary

My work has helped to update the current knowledge of ABA regulation of suberin production at the transcriptional level and in connection to the biosynthesis of soluble and cross-linked metabolites incorporated into the insoluble suberin polymer. I generated data to further define the transcriptional changes that occur at different times after wounding that relate to suberin biosynthesis and deposition, primary metabolism that provides energetic fuel and precursors for suberin production, components for regulatory oversight of suberin-associated processes, and physical healing during closing layer formation. By exploring this new set of information, I was able to contribute to the construction of largescale overviews of the wound-healing process that includes, but is not limited to, suberization (**Figure 3.3, Figures 4.1-4.2**).

4.2 Wound-healing events during induced suberization and closing layer formation

I generated an overview of transcriptional and metabolic changes over the course of wound-healing during closing layer formation. These highlight the differential temporal induction and steady states of different branches of metabolism that relate to the synthesis of primary precursors, phenolic and aliphatic suberin-related biosynthesis and assembly, and regulatory components including the phytohormone abscisic acid (ABA), as well as changes in gene expression of putative transcription factors and of genes involved in sub-

cellular processes (**Figure 4.1**). A synthesis of established and putative wound-healing events described in this thesis, including hypothetical mechanisms related to the regulatory oversight and assembly of suberin components, is presented in **Figure 4.2**.

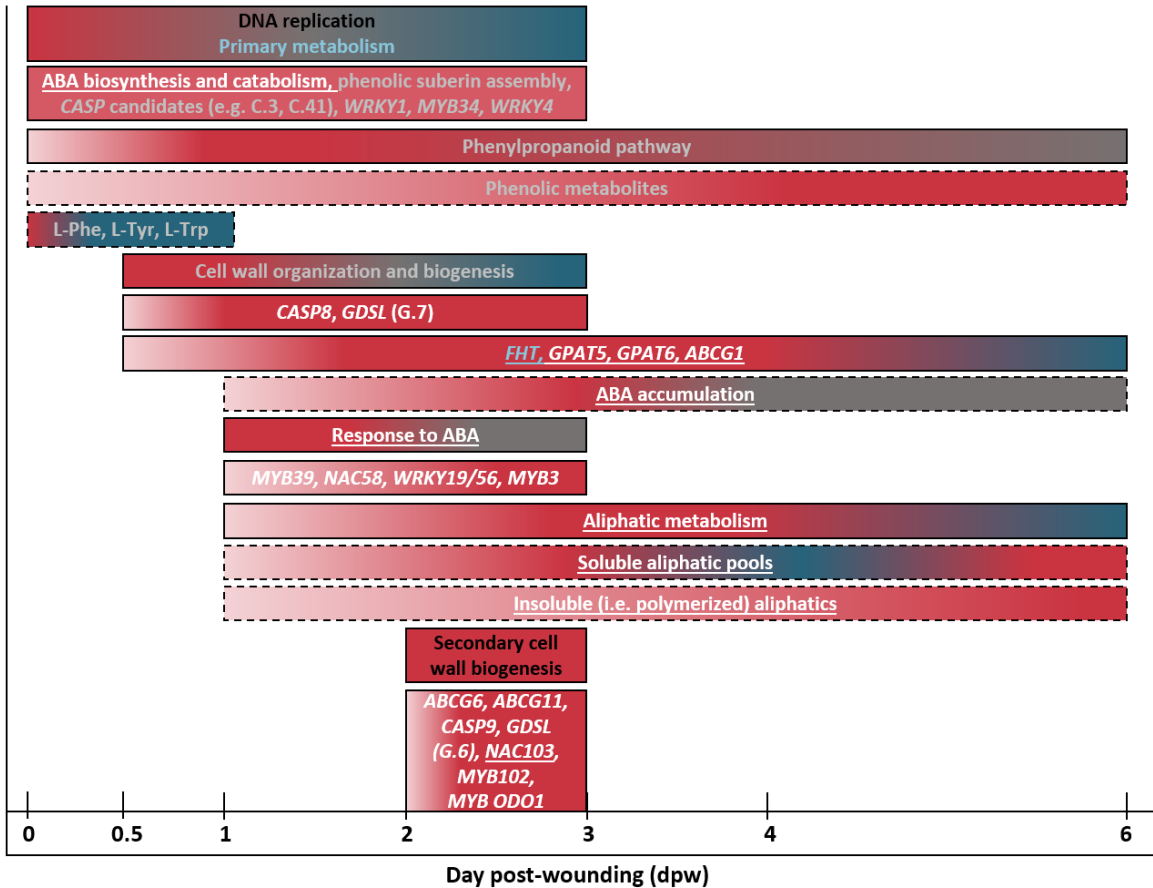


Figure 4.1. Temporal summary of biosynthetic and regulatory events during wound-healing and associated suberization. Observations from gene expression and metabolite analysis in a six day wound-healing time course that involved manipulation of wound-induced *de novo* ABA biosynthesis (**Chapter 2**) are integrated with findings from both targeted and unbiased analyses from a three day wound-healing tuber transcriptomic study (**Chapter 3**). Solid lines represent gene expression results, and dashed lines signify findings from metabolite analyses. Bar colours represent gene expression (from targeted or GO term enrichment analysis) or metabolite accumulation as follows: red symbolizes high levels, while blue represents low levels, with differing intensity showing gradual change over time, and grey denotes a time period with no observed further change. White text is used to show processes with known or hypothesized involvement in aliphatic suberin metabolism, grey text represents phenolic suberin-associated metabolism, blue text signifies convergent processes (i.e. pertaining to both phenolic and aliphatic suberin metabolism), black text represents other wound-healing processes that are not necessarily directly related to suberization, and text is underlined if is impacted by ABA.

4.2.1 Primary metabolism

In the three-day RNA-seq transcriptome time course, targeted metabolic pathways involved in the production of suberin precursors were generally expressed throughout the time course, although gene set enrichment analysis highlighted several primary metabolic pathway GO terms as initially up-regulated, then down-regulated ca. 2-3 dpw. These findings suggest the reconfiguration of primary metabolic processes is tailored towards the up-regulation of those that are required for this specific response, i.e. channeling of energy and metabolism towards producing precursors for suberin biosynthesis, and followed by down-regulation of processes that are not necessary or worth the resource investment. Although most primary metabolites were not analyzed in the **Chapter 2** time course, Yang and Bernards (2007) noted the timing of primary metabolite accumulation in their polar metabolite analysis. Polar metabolite profiles included sugars, amino acids and organic acids as major components detected at 0 dpw. The metabolite profile at this time point was distinguished from 1 and 2 dpw profiles by the appearance of newly synthesized suberin phenolic compounds such as ferulic acid (Yang and Bernards 2007).

4.2.2 Phenylpropanoid metabolism

Phenylpropanoid biosynthetic genes were studied in both time course experiments, while phenolic suberin assembly gene expression was analyzed in the three-day wound-healing study. Overall, phenylpropanoid metabolism genes were expressed to some degree prior to wounding, and then up-regulated and maintained at a steady level of expression early into wound-healing. Associated metabolites were shown to accumulate over time, whereas aromatic amino acids phenylalanine, tyrosine and tryptophan used as precursors for the biosynthesis of hydroxycinnamates and their CoA-esters, hydroxycinnamic acid amides, and monolignols, decreased quickly after wounding. GSEA showed that GO terms for biosynthesis of these amino acids persisted throughout the time course. At the metabolism level, this suggests that these compounds are continuously synthesized to support suberization, and then quickly utilized, since their levels did not appear to increase over 14 days of wound-healing (**Chapter 2, Figure B5**), but SPPD-destined products were shown to accumulate over time.

Phenylpropanoids such as chlorogenic acid (i.e. caffeoyl quinic acid) and coumaroyl quinic acids have been demonstrated to accumulate in tubers and may act as pools for remobilization of phenolic carbon skeletons, depending on plant needs, such as suberin biosynthesis (Valiñas et al., 2015), although not incorporated into the SPPD directly. This may help to explain the prompt induction of phenylpropanoid metabolism after wounding. For example, Payyavula et al. (2015) used *hydroxycinnamoyl CoA:quinic acid hydroxycinnamoyl transferase (HQT)*-silenced potato plants to study the synthesis and regulation of chlorogenic acid, a product of *HQT* and major potato phenolic compound, and determined the likely existence of a regulatory loop between chlorogenic acid levels and *phenylalanine ammonia-lyase (PAL)* gene expression and enzyme activity, which is required for the first committed step of phenylpropanoid biosynthesis. The reduction of total phenolic levels was not as strong as the decrease in chlorogenic acid, which demonstrated the likely re-routing towards the flux of other phenylpropanoids (Payyavula et al., 2015). Valiñas et al. (2015) observed a negative correlation between chlorogenic acid levels and genes involved in downstream suberin biosynthetic activities such as *hydroxycinnamoyl-transferase (HCT)* and *caffeoyl-CoA O-methyltransferase (CCoAOMT)*, suggesting that chlorogenic acid is channeled towards suberin and lignin biosynthesis. Sucrose feeding induces chlorogenic acid biosynthesis, and was also shown to up-regulate the expression of *PAL*, *HCT* and *p-coumarate 3' hydroxylase (C3H)* in potato tubers with purple flesh (Payyavula et al., 2015). It is possible that a similar signaling system could function to activate phenylpropanoid synthesis in the context of suberin production in non-purple potatoes.

4.2.3 Aliphatic metabolism

Induction of genes involved in aliphatic suberin production generally occurs later into wound-healing relative to phenylpropanoid metabolism genes. The onset of aliphatic gene expression appears to track the time at which ABA accumulates (**Chapter 2**) and coincides with the up-regulation of the enriched “response to ABA” GO term (**Chapter 3**), which includes transcription factors of interest. Key aliphatic suberin-associated genes like *KCS6* (Serra et al., 2009a), *FAR3* (Domergue et al., 2010), and *CYP86A33* (Serra et al., 2009b), and their respective VLC aliphatic, 1-alkanol, and 18:1 ω -hydroxy and α,ω -

dioic acid biosynthetic products were impacted by altered ABA levels. RNA-seq analysis demonstrated similar temporal patterns for targeted suberin-specific fatty acid modification genes, although within the larger sub-set of genes, some demonstrated expression immediately after wounding, and others did not have detectable transcripts until 3 dpw. It is likely that the majority of the genes that follow similar patterns as those assessed in **Chapter 2** are influenced by ABA accumulation, but others may be subjected to additional regulatory control, or have higher sensitivity to lower ABA quantities. These between-gene differences within the pathway point to the likelihood of finer levels of regulation that allow for biosynthetic steps to be carried out in the correct sequential order, such as elongation steps that occur prior to further modification of VLCFAs.

4.2.4 SPPD and SPAD assembly

4.2.4.1 Genes previously implicated in suberin assembly

Genes with known involvement in SPPD assembly, such as NADPH-dependent oxidases and superoxide dismutases, were expressed throughout the three-day wound-healing time course, whereas anionic peroxidases were expressed by 0.5 or 1 dpw (**Chapter 3**).

Linkage and assembly steps that reflect the convergence points of different biosynthetic pathways via esterification of aliphatics to feruloyl-CoA (*FHT*, Serra et al., 2010) or glycerol (*GPAT5* and *GPAT6*, Beisson et al., 2007; Li et al., 2007), and transport of SPAD-affiliated esterified monomers (*ABCG1*, Landgraf et al., 2014) were demonstrably impacted by attenuated or enhanced ABA levels at the gene expression level, similarly to aliphatic genes (**Chapter 2; Figure 4.2**). The finer RNA-seq based temporal investigation revealed that these four genes are up-regulated prior to those encoding aliphatic modification genes for SPAD monomer biosynthesis. These findings suggest that either another regulator is involved in addition to ABA, that these genes are more sensitive to lower ABA levels during initial accumulation, or, at least for *FHT* and the *GPATs*, that they are somewhat induced by the presence of one of their substrates.

Bacterial operons (i.e. gene clusters) are induced by the presence of their substrates. In the classical example of the lac operon, *lac* genes are transcriptionally activated in the presence of the substrate lactose (Jacob and Monod, 1961). Gene clusters comparable to

operons have also been described in plants, of which many are involved in secondary metabolite biosynthesis (reviewed by Boycheva et al., 2014). At the protein level, metabolons are complexes that transiently form between enzymes catalyzing sequential metabolic steps. Metabolon formation and activity might also be metabolite-induced (e.g. Norris et al., 1999). This type of multi-enzyme complex has been established for tricarboxylic acid cycle enzymes in potato (Zhang et al., 2017) and proposed for the phenylpropanoid pathway towards the biosynthesis of phenolic metabolites and lignin (Stafford, 1974; reviewed by Laursen et al., 2015). Payyavula et al. (2015) demonstrated that *PAL* expression is induced by chlorogenic acid accumulation. *PAL* does not use chlorogenic acid directly as a substrate, but catalyzes the first step of phenylpropanoid biosynthesis towards synthesis of chlorogenic acid and its derivatives (Payyavula et al., 2015). It is possible that genes encoding enzymatic steps towards suberin production are activated by the presence of their substrates. Glycerol-3-phosphate is synthesized via dehydrogenation of the glycolysis-derived dihydroacetone-phosphate. Genes involved in the glycolytic pathway are active in dormant tubers and after wounding (steps 7, 12, 19-26, **Figure 3.3B**), with the glycerol-3-phosphate dehydrogenase gene also consistently expressed throughout wound-healing (step 88, **Figure 3.3H**). Feruloyl-CoA is synthesized via the phenylpropanoid pathway that is expressed during the wound-healing time course. Therefore, it is possible that genes encoding enzymes involved in esterification of modified fatty acids to these metabolites that are synthesized earlier into wound-healing are induced by their presence. This would ensure that their protein products are poised to catalyze linkage steps once aliphatic components become available later into wound-healing, and may highlight a further method of control and organization over this process. *ABCG1* expression also occurs earlier than expected, if it is primarily a transporter of SPAD components. Landgraf et al. (2014) used RNAi to silence *ABCG1*, then evaluated the build-up of suberin monomers and the concomitant decrease in quantities of certain polymerized components in tuber periderm to characterize *ABCG1* and generate hypotheses about its putative substrates. An observed reduction in \geq C24 chains, including major C18:1 ω -hydroxy and α,ω -dioic acid monomers deposited in tuber periderm suggests they are exported by *ABCG1* (Landgraf et al., 2014). The increase in ω -feruloyloxy fatty acid glycerol esters in RNAi-*ABCG1* potato also provides

evidence for monoacylglycerol derivatives as ABCG1 substrates (Landgraf et al., 2014, **Figure 4.2**). *CYP86A33*-silencing led to a drop in 18:1 ω -hydroxy fatty acids, but also of glycerol, therefore ω -hydroxylation is thought to occur before export of esterified aliphatics (Serra et al., 2009b). *FHT*-RNAi potatoes showed decreased C18:1 ω -hydroxy acid levels, highlighting the additional importance of conjugation to ferulic acid prior to export of these aliphatic components (Serra et al., 2010).

ABCG1 is induced by 12 hours after tuber wounding and is sensitive to changes in ABA levels, similarly to *FHT* and *GPATs*, which utilize substrates derived from more than one biosynthetic pathway. This provides further support for the likelihood that ABCG1 transports SPAD-destined esterified products, and also suggests that *ABCG1* could be co-regulated with *FHT* and *GPATs* involved in the synthesis of its esterified substrates. The fact that the timing of *ABCG1* transcript accumulation precedes that of aliphatic metabolism genes and peak ABA levels indicates that these genes are likely regulated by mechanisms in addition to ABA-mediated control, such as transcription factors (**Figure 4.2**). ABCG6 and ABCG11 are putative potato suberin transporters with high amino acid-level similarity to characterized transporters from Arabidopsis (e.g. AtABCG11/AtWBC11, Bird et al., 2007; AtABCG6, Yadav et al., 2014) that follow the temporal profile of aliphatic gene expression, and therefore may be more important for the export of non-esterified aliphatic products that will either undergo polymerization, or remain in the SPAD as soluble associated wax components (**Figure 4.2**). The timing of expression of genes involved in the synthesis and transport of esterified products precedes the observed accumulation of soluble (3 dpw) and insoluble (4-6 dpw) SPAD components. This is especially evident for wound-induced *FHT*, which synthesizes ferulate esters that are incorporated in the SPAD ca. 3-4 dpw, but also yields alkyl ferulates that do not accumulate until ca. 14 days after wounding (**Chapter 2**). Together, the observed differences in expression of genes within pathways toward SPAD production and disparity between gene expression and metabolite accumulation suggest that additional regulation is involved in the coordination of these linkage and transport processes.

Future studies could focus on comparative promoter analyses including these convergent metabolism genes that have been shown to be under some level of ABA control, but also are likely regulated by one or more additional mechanisms. Further exploration of regulatory elements in promoter regions of *FHT* (Boher et al., 2013) or analysis of the *ABCG1* promoter in comparison with phenolic or aliphatic metabolism-specific genes could offer insight into both major suberin pathways and their coordination. For example, regulatory motifs shared across the promoters of *FHT* and aliphatic genes may not also be present in phenolic biosynthetic gene promoters, and vice versa, and allow for identification of pathway-specific motifs.

4.2.4.2 Novel candidates and proposed mechanism for suberin assembly and its coordination

The key genes for linkage and deposition of SPAD monomers (*FHT*, *GPAT5*, *GPAT6*, *ABCG1*) demonstrate gene expression early into wound-healing and are impacted by ABA. Despite the enhanced synthesis of soluble aliphatic components by exogenous ABA application and diminished and delayed accumulation by FD treatment, the temporal patterns of insoluble aliphatic deposition did not differ between ABA-related treatments (**Chapter 2**). This inconsistency in ABA effect suggests an additional level of regulation aside from ABA, or some other limiting factor that prevents the assembly of soluble monomers into the SPAD. It is possible that beyond the likely role of regulatory components such as transcription factors or phytohormone interactions, mediators of deposition may be involved. The Casparian strip membrane domain protein (CASP) candidate *CASP8* that was previously identified as expressed during tuber periderm maturation (Vulavala et al., 2017), was expressed over time in a highly similar pattern to the convergent metabolism genes required for SPAD assembly, along with a candidate cutin synthase-like GDSL lipase/esterase (*G.7*). The timing of *CASP8* and *GDSL* (*G.7*) appeared to overlap with the expression of aliphatic metabolism genes, and *CASP9* and *GDSL* (*G.6*), although aliphatic genes share more similar temporal profiles with *CASP9* and *GDSL* (*G.6*) (**Chapter 3, Figure 4.1**). It is feasible that, if involved in the process, the *CASP* genes expressed in this transcriptome encode proteins that recruit machinery for organization and deposition of the polymeric domains of suberin, similarly to those

involved in Casparian strip assembly (Roppolo et al., 2014). While CASPs have been characterized as mediators of lignin-like polymerization by coordinating necessary enzymes and forming transmembrane scaffolds (Roppolo et al., 2014), the fact that there are actively expressed *CASP* genes that appear to be wound-induced and co-expressed with linkage and aliphatic suberin-related genes could indicate that they have involvement in mediating aliphatic component polymerization, possibly via GDSLs or similar polyester-forming enzymes. The temporal overlap in induction of these putative mediators of assembly and polymerization could point to a mechanism that coordinates the deposition of different suberin components, and possibly the linkage of the SPPD and SPAD (**Figure 4.2**).

Some *CASP* and *GDSL* assembly candidates were expressed in patterns similar to either phenylpropanoid or aliphatic-specific metabolism, but *CASP8* and *GDSL* (G.7) were most similar to convergent metabolism genes. Thus it is possible that *CASP8* and *GDSL* (G.7) specifically target esterified products and act to regulate their incorporation into the SPAD at a later time than when genes are first expressed and soluble monomers accumulate. Additionally, *CASP8* could act as a mediator between SPPD and SPAD assembly activities, possibly by orchestrating the linkage of the two domains. (**Figure 4.2**). *CASP9* and *GDSL* (G.6) followed temporal expression patterns similar to aliphatic metabolism genes, and are therefore hypothesized to primarily have involvement in SPAD assembly.

The hypothesis that CASPs mediate suberin assembly fits within the context of an additional level of regulation of deposition beyond ABA control, since characterized CASPs to date do not appear to be under ABA-mediated regulation, or at least not directly. For example, in *Arabidopsis* roots, MYB36 (Kamiya et al., 2015) directs Casparian strip organization and deposition via control over *CASP1* and its recruitment of the respiratory burst oxidase homolog *PER64* and *ESB1*. Potato homologs of MYB36 and ESB1 were not detected at the transcriptional level in this RNA-seq study (**Chapter 3**), consistent with publicly available transcriptome data that demonstrates FPKM levels are equal to or close to 0 in tubers (Massa et al., 2011). A family of peptide hormones are signals that must specifically bind to Casparian strip-associated receptor kinases for the

correct localization of *CASP* expression and deposition of the Casparian strip (Nakayama et al., 2017), but a role for ABA has not been described for the developmental deposition of the Casparian strip. Casparian strip deposition has been observed in response to salt stress (e.g. Karahara et al., 2004), and although ABA-mediated signaling is often linked to salt and drought stress responses, the role of ABA has not been specifically established in the context of stress-induced Casparian strip development.

GO terms encompassing cell wall organization and biogenesis were up-regulated from 0.5-1 dpw, around the time that the phenylpropanoid pathway genes increase in expression and phenolic metabolites begin to accumulate (**Chapter 2**), and also the time at which *CASP8* and *GDSL* (G.7) transcript levels rose (**Figure 4.1**). *CASP* and *CASP*-like proteins have speculative involvement in forming membrane scaffolds for Casparian strip deposition, and/or in the recruitment of cell wall modification machinery (Roppolo et al., 2014). Since cell division does not occur during closing layer formation (Lulai et al., 2016), it is likely that the up-regulation of cell wall modification genes reflects cell wall reinforcement in cells surrounding the wound site. It is feasible that cell wall remodeling in wound-healing tubers may promote the anchoring of the SPPD into the primary cell wall during closing layer formation. Since *CASPs* can influence the localization of cell wall modifying activities (Lee et al., 2013), the differentially expressed cell wall modification genes highlighted in this study along with SPPD oxidative coupling machinery could be targets of recruitment by active *CASPs* (**Figure 4.2**).

The term “secondary cell wall biogenesis” was significantly up-regulated between 2-3 dpw (**Chapter 3**), at the same time that aliphatic monomer levels increase to their peak levels at 3 dpw, and just prior to the time when insoluble aliphatics begin to accumulate by 4 dpw (**Chapter 2**). The RNA-seq experiment measured transcriptomic changes up to 3 dpw, so it is not clear whether these secondary cell wall changes would continue to undergo up-regulation beyond this time point. It is possible that the implicated genes within this term are important for the organization, correct spatial localization and deposition of aliphatic monomers prior to the formation of the secondary cell wall. In periderm, secondary cell wall synthesis occurs after suberin aliphatics have been

deposited between the primary cell wall and the plasma membrane, and the secondary cell wall itself is also deposited in this sub-cellular location, meaning the final suberin polymer is found between the primary and secondary cell walls in tissues that undergo secondary thickening (Esau, 1977; Schmidt and Schönherr, 1982). *ABCG6* and *ABCG11* may be involved in the export of SPAD monomers, and the latter appears to be regulated by *NAC103* (Verdaguer et al., 2016). These genes co-expressed with *CASP9*, *GDSL* (G.6), *NAC103*, *MYB102* and *MYBODO1*, offering further support for the possibility that aliphatic suberin organization and assembly is overseen by *CASP9*-mediated recruitment of cell wall modifying genes in this distinct spatial location where the SPAD is deposited, analogous to the predicted SPPD assembly process described above (**Figure 4.2**).

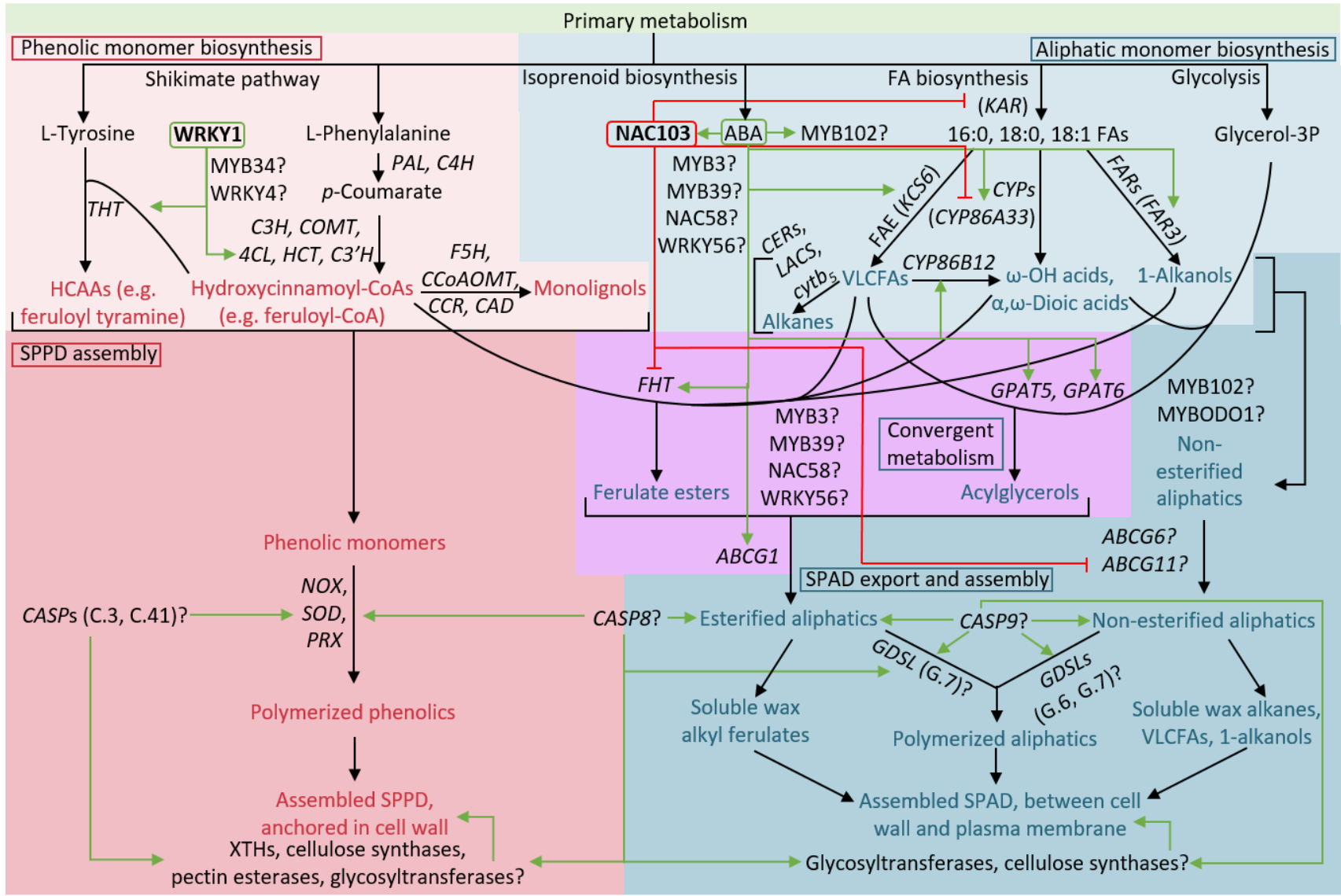


Figure 4.2. Proposed mechanism for the suberization process in wound-healing tubers. This overview offers a synthesis of findings from **Chapter 2** and **Chapter 3**, and offers novel hypothetical aspects of regulation at the levels of monomer biosynthesis, deposition, polymerization and assembly established in this thesis. Primary metabolic pathways (shaded green) yield precursors and energy molecules that feed into specialized suberin-related metabolic branches. Carbohydrate metabolism yields pyruvate used towards shikimate pathway production of aromatic amino acids used as precursors for phenolic suberin biosynthesis. Pyruvate is also used along with glycolysis-derived glyceraldehyde-3-phosphate for isoprenoid metabolism that yields the phytohormone abscisic acid (ABA) via the carotenoid pathway, and as a substrate for the tricarboxylic acid cycle that yields acetyl-CoA for fatty acid biosynthesis, which results in the generation of 16:0, 18:0 and 18:1 fatty acids that undergo various modifications for aliphatic suberin monomer production. Glycerol-3-phosphate is synthesized from the dehydrogenation of dihydroxyacetone phosphate produced during glycolysis. The biosynthesis of suberin poly(phenolic) domain monomers (dark red) may be regulated by WRKY1, which regulates *THT* and *4CL* in relation to phenylpropanoid metabolism in pathogen-infected aerial potato organs (Yogendra et al., 2015). Transcription factors like *WRKY4* and *MYB34* that demonstrate similar temporal expression profiles and cluster with known phenolic suberin-associated genes are also included as candidate regulators of this metabolic pathway branch. ABA regulates the biosynthesis of several key suberin poly(aliphatic) domain monomers (blue) by positively impacting genes involved in their production. NAC103 acts as a transcriptional suppressor of fatty acid and aliphatic suberin-related genes, and is induced by ABA (Verdaguer et al., 2016). Several candidate transcription factors (*MYB3*, *MYB39*, *NAC58*, *WRKY56*) co-expressed with aliphatic metabolism genes and are presented as putative regulators of aliphatic suberin production. *MYB102* was significantly up-regulated under the “response to ABA” GO term between 1-2 dpw, and offers a potential regulator of aliphatic suberin biosynthesis. Most phenolic monomers are solely polymerized and incorporated into the SPPD. Feruloyl-CoA can also be conjugated to very long chain fatty acids (VLCFAs), ω -hydroxy and α,ω -dioic acids, and 1-alkanols to yield ferulate esters, including alkyl ferulates as SPAD-associated soluble wax components. Modified fatty acids can also be esterified to glycerol via the glycerol-3-phosphate acyltransferases (GPATs). Esterified aliphatic constituents are exported by ABCG1 (Landgraf et al., 2014). These steps are referred to as “convergent metabolism” (shaded purple). *MYB3*, *MYB39*, *NAC58* and *WRKY56* expression coincided with peak levels of convergent metabolism genes, and are also considered putative regulators of these genes. Since convergent metabolism steps require substrates derived from pathways activated at different times after wounding, there is likely a high level of regulation and coordination between different pathway branches. Oligomer and polymer formation are thought to occur after monomers and esterified building blocks are transported. The translocation of aliphatic monomers (alkanes, VLCFAs, modified fatty acids, 1-alkanols) that are not esterified to glycerol or feruloyl-CoA (i.e. soluble components destined for polymerization, or that remain non-polymerized as associated wax) has not been established in potato, but ABCG6 and ABCG11 have predicted involvement. Phenolic monomers are thought to undergo a NADPH-dependent oxidase (NOX), superoxide dismutase (SOD), and anionic peroxidase (PRX)-mediated polymerization, whereas SPAD polymerization activities remain uncharacterized. The coordination and organization of SPPD and SPAD assembly and linkage is not currently

established, but novel candidates and mechanisms are presented based on findings from RNA-seq analysis (**Chapter 3**). *CASP* candidates were expressed at different times during wound-healing, along with *GDSL* candidates for SPAD polymerization. *CASPs* expressed early in the time course (C.3, C.41) may recruit *NOX*, *SOD*, *PRX* for polymerization, and influence enzymes involved in the organization of cell wall polysaccharides in a process that may be associated with SPPD deposition via localization of cell wall modifying activities. *CASP8* co-expresses with *GDSL* (G.7), and their expression profiles overlap with those of phenylpropanoid and convergent metabolism genes. These could regulate the linkage between two domains, their spatial organization, and/or the polymerization and deposition of esterified aliphatics that act as building blocks for SPAD assembly. *CASP9* co-expresses with *GDSL* (G.6), *ABCG6*, *ABCG11*, *MYB102*, *MYBODO1*, and *NAC103*, which negatively regulates *ABCG11* (Verdaguer et al., 2016). Based on their temporal expression profiles and co-expression with *NAC103*, these genes are proposed to be involved in the export, deposition and polymerization of non-esterified aliphatics, as well as the organization of non-polymerized, soluble waxes. Up-regulated secondary cell wall biogenesis glycosyltransferases and cellulose synthases may be regulated by *CASP9* to organize the deposition of polymerized aliphatics between the cell wall and plasma membrane, prior to secondary cell wall formation.

Abbreviations: *4CL*, 4-coumarate-CoA ligase; ABA, abscisic acid; *ABCG1*, ATP-binding cassette (ABC) subfamily G transporter 1; *ABCG11*, ATP-binding cassette (ABC) subfamily G transporter 11; *ABCG6*, ATP-binding cassette (ABC) subfamily G transporter 6; *C3H*, *p*-coumarate 3-hydroxylase; *C3'H*, *p*-coumaroyl quinate/shikimate 3'-hydroxylase; *C4H*, cinnamic acid 4-hydroxylase; *CAD*, cinnamyl alcohol dehydrogenase; *CASP8*, Casparian strip membrane domain protein 8; *CASP9*, Casparian strip membrane domain protein 9; *CCoAOMT*, caffeoyl-CoA O-methyltransferase; *CCR*, cinnamoyl CoA reductase; *CER*, *ECERIFERUM*; *COMT*, caffeic acid O-methyltransferase; *CYP*, cytochrome P450; *CYP86A33*, cytochrome P450 subfamily 86A 33; *CYP86B12*, cytochrome P450 subfamily 86B 12; *CYTB5*, cytochrome P450 b5; *F5H*, ferulate 5-hydroxylase; FA, fatty acid; FAE, fatty acid elongase; *GDSL*, *GDSL* domain esterase/lipase; Glycerol-3P, glycerol-3-phosphate; *GPAT5*, glycerol-3-phosphate acyltransferase 5; *GPAT6*, glycerol-3-phosphate acyltransferase 6; HCAA, hydroxycinnamic acid amide; *HCT*, hydroxycinnamate transferase; *KAR*, β -ketoacyl-ACP reductase; *KCS6*, β -ketoacyl-CoA reductase 6; *LACS*, long-chain acyl-CoA synthetase; *MYB*, MYB family transcription factor; *NAC*, NAC domain transcription factor (NAM, no apical meristem, ATAF, Arabidopsis transcription activation factor, and CUC, cup-shaped cotyledon); *NOX*, NADPH-dependent oxidase; *PAL*, phenylalanine ammonia lyase; *PRX*, anionic peroxidase; *SOD*, superoxide dismutase; SPAD, suberin poly(aliphatic) domain; SPPD, suberin poly(phenolic) domain; *THT*, tyramine hydroxycinnamoyl transferase; VLCFA, very long chain fatty acid; *WRKY*, WRKY domain family transcription factor; *XTH*, xyloglucan endotransglucosylase/hydrolase

4.2.5 Regulators of differential induction of suberization processes

The evidence supporting the differential induction of various processes during suberization suggests a role for different mechanisms of control that differentially regulate biosynthetic activities and events. **Chapter 2** aimed to further address the role of ABA as a regulator of certain suberin-associated pathways, while **Chapter 3** targeted ABA biosynthesis and catabolism and captured the time point at which several transcription factor (TF) candidates underwent changes in gene expression after wounding. ABA contributes to part of this differential temporal regulation, but does not account for nuances within aliphatic suberin-related pathways or the regulation of phenylpropanoid biosynthesis, and factors controlling the initial wound-induced up-regulation of primary metabolism are also not known.

AtMYB41 was previously demonstrated as an ABA-induced regulator of aliphatic, and possibly phenolic, suberin production (Kosma et al., 2014), and genes encoding its putative potato homologs were included in this analysis, including *MYB3* and *MYB39*. *NAC103* was demonstrated to be an ABA-responsive negative regulator of aliphatic suberin biosynthesis and deposition (Verdaguer et al., 2016), whereas *WRKY1* has been shown to regulate hydroxycinnamic acid amide deposition in pathogen-infected potato leaves. Therefore genes encoding highly similar proteins to *NAC103* and *WRKY1* were incorporated into targeted RNA-seq investigations. Of the candidate genes included in this analysis, *NAC58*, *WRKY19/56* and *MYB102* (previously called *StMYB93*) were highlighted as part of the suberization signature described across species by Lashbrooke et al. (2016). Two Arabidopsis homologs of *MYB102*, *AtMYB107* and *AtMYB9*, are thought to coordinately and positively regulate phenylpropanoid and aliphatic suberin metabolism in Arabidopsis seed coats (Lashbrooke et al., 2016). The closest Arabidopsis homolog of potato *NAC58* is *ANAC058*, which is the putative ortholog of *StNAC103* (Verdaguer et al., 2016), and is also implicated in the regulation of suberin production (Markus, 2018). **Chapter 3** demonstrated that different transcription factor candidates clustered with genes involved in different suberin-related metabolic pathways, or with known TFs, and therefore offer several good candidates for further pursuit (**Figure 3.6**).

Hypotheses were generated about the putative roles of these TFs based on their temporal patterns of transcript accumulation with respect to typical profiles for suberization genes, or if they clustered closely with characterized TFs (**Figure 3.6**). For example, *WRKY1*, *MYB34* and *WRKY4* cluster together, and are predicted to have involvement in phenolic biosynthesis, since *WRKY1* regulates phenylpropanoid genes *THT* and *4CL* (Yogendra et al., 2015), and they demonstrate similar temporal expression profiles as phenylpropanoid pathway and phenolic assembly genes. *MYB39*, *NAC58*, *WRKY19/56* and *MYB3* mostly cluster with fatty acid modification, deposition and glycerol-esterification genes. They could be involved in coordination between phenolic and aliphatic suberin production since they are all up-regulated between 0-0.5 dpw, or in aliphatic-specific regulation due to peak expression later into wound-healing. *MYB102* and *MYB ODO1* are encoded by genes that follow the same temporal expression profile as *NAC103*, and may be co-regulators of *NAC103* targets, and could therefore participate in the fine-tuning of aliphatic suberin metabolism and/or assembly by countering the suppressive control exerted by *NAC103* (Verdaguer et al., 2016) (**Figure 4.2**). *MYB102* is also a good candidate for regulation of SPAD production due to its inclusion in the “response to ABA” GO term, since aliphatic genes (**Chapter 2**) and characterized SPAD regulators are ABA-responsive (e.g. *AtMYB41*, Kosma et al., 2014; *StNAC103*, Verdaguer et al., 2016). If CASPs are involved in orchestrating suberin assembly in tubers, they could be regulated by candidate TFs that demonstrate patterns of expression similar to *CASPs*, biosynthesis and assembly genes (**Figure 4.2**).

The regulatory control of ABA over aliphatic suberin-associated TFs suggests that a similar mechanism could be in place for indirect regulation of phenolic metabolism through other signal compounds. Other hormones do not have any established impact on any of the suberization process except for the inhibitory effect of salicylic acid on *FHT* expression (Boher et al., 2013). Jasmonic acid and ethylene levels change in response to wounding, but are not required for suberin production (Lulai and Suttle, 2004; Lulai and Suttle, 2009; Lulai et al., 2011). Sucrose enhances chlorogenic acid pools in potato plants and leads to *PAL* expression, but a role for sucrose signaling has not been defined in the suberization context. GO term enrichment analysis of the wound-healing transcriptome

also identified points at which terms including genes involved in non-transcriptional levels of regulation were differentially regulated. In cases where most genes followed similar temporal profiles for changes in transcript levels within pathways for suberin metabolite production, there were always exceptions to the general pattern, suggesting the likely existence of factors that control entire pathways as well as individual gene-level regulation and fine-tuning. Taken together, the coordination of different pathways required for suberization in the wound-healing tuber is a highly complex process, and likely involves many levels and types of regulation. This thesis presents some new insights into the regulatory oversight and coordination of biosynthesis and assembly events, while providing targets for further analysis. The generation of a wound-healing transcriptome also offers a large scale dataset that can be further mined during future investigations of genes of interest.

4.2.6 Other wound-healing processes involved in closing layer formation

Many enriched GO terms identified as differentially regulated were relevant to suberization, and also to cell-level changes that occur during closing layer formation (**Chapter 3**). Several GO terms relating to cell cycle processes like DNA replication were up-regulated early in the wound-healing time course then decreased, which was consistent with a previously established timeline for the *S*-phase of mitosis in wound-healing tubers that occurs between 18-48 hours after wounding (Lulai et al., 2014). DNA synthesis occurs prior to the second phase of wound-healing, during which time the meristematic phellogen tissues develop and give rise to suberized phellem cells to generate the wound periderm (Lulai et al., 2016).

In tubers monitored for 6 days after wounding (**Chapter 2**), genes involved in aliphatic and convergent metabolism decreased around 4-6 dpw, which matched previous observations by Lulai and Neubauer (2014). In time course experiments that extend into wound periderm formation, it appears that this drop in gene expression marks the time at which closing layer formation has reached completion, and is followed by a second wave of up-regulation related to suberization of phellem cells during wound periderm formation (Lulai and Neubauer; 2014; Lulai et al., 2016). Between the studies outlined in

Chapter 2 and **Chapter 3**, transcriptional and metabolic aspects of closing layer formation were captured and integrated to better understand aspects of wound-healing that include signaling, regulation, suberization and physical healing (i.e. cell wall-related changes that may be implicated in suberin deposition and organization during closing layer formation).

4.3 Applications for crop improvement

Suberin acts as a barrier to abiotic (e.g. Schreiber et al., 2005; Baxter et al., 2009) and biotic threats (e.g. Lulai and Corsini, 1998; Thomas et al., 2007) in underground plant organs, and is responsible for the characteristics that make cork commercially important (Marques and Pereira, 1987), making it a good target for crop improvement applications that rely on existing plant defenses. The recent characterization of the AtMYB41 transcription factor from *Arabidopsis* by Kosma et al. (2014) highlights the possibility of identifying a “master regulator” capable of activating the suberization process in a model species. However, similar studies have not been conducted in underground organs of crop species, therefore this fundamental discovery has not yet been translated into a functional application. Further understanding of the overall suberization process and its regulation in an economically important crop species such as potato could lead to the identification of gene targets for enhancement efforts, and could also be relevant to other crops in the Solanaceae family.

The importance of appropriate suberization to prevent water loss and infection in the context of potato tuber skin set and maturation, as well as healing wounds incurred during harvest, has been well-described (reviewed by Lulai, 2007). Additionally, the deposition of suberin in roots of important crop species, such as soybean, has been shown to correlate with resistance to soil borne pathogen infection (Thomas et al., 2007). Loss-of-function mutant (e.g. Yadav et al., 2014) and knockdown (e.g. Serra et al., 2010) studies have demonstrated that the correct assembly and organization of suberin is critical in its ability to function as a protective chemical and exhibit its characteristic properties, such as water impermeability.

ABA-related treatments altered soluble aliphatic pool accumulation, but not the timing of insoluble, polymerized aliphatic metabolite accumulation, suggesting additional mechanisms regulate SPAD assembly (**Chapter 2**). This finding further emphasizes the importance of addressing genes involved in the coordination of suberin deposition and assembly in addition to enhancing monomer production. Each domain of the suberin macromolecule is also important for exhibiting the different characteristic protective qualities of suberin. The characterization of genes involved in the coordinated regulation of both SPPD and SPAD-related metabolism could have important implications. For example, MYB102 (previously identified as StMYB93) is a putative ortholog of an Arabidopsis TF involved in the regulation of both phenolic and aliphatic suberin metabolism (Lashbrooke et al., 2016) and would therefore be an ideal target for enhancing suberin biosynthesis. Since organized and coordinated assembly and deposition are important for the production of functional suberin, the roles of CASP and GDSL candidates highlighted in **Chapter 3** should be elucidated. Crop improvement via enhanced suberization should address regulators of suberin biosynthetic genes and/or entire pathways in concert with genes involved in polymerization and assembly. This would more likely lead to increased accumulation of polymerized, correctly deposited suberin that would exhibit all of its characteristic protective properties in plant organs including roots, wounded tubers, tuber periderm, and cork.

4.4 Concluding remarks

This thesis presents a detailed overview of the wound-healing process that integrates information pertaining to suberin biosynthesis and assembly at the levels of gene expression and metabolism, and control of these processes by hormone-mediated and transcriptional regulation. I helped define the role of ABA as a regulator of aliphatic and convergent metabolism genes and factor in the differential induction of suberin biosynthetic pathways, while acknowledging that ABA cannot be the sole regulator of these pathways. I generated the first wound-healing tuber transcriptome data set that was used to revise a broad “roadmap” to suberin assembly that incorporated many more components than previously, and matched transcriptome derived gene expression profiles

for each known or candidate gene involved in wound-healing suberization, including primary metabolic pathway genes.

This provides not only an overview of suberization, but also support for the involvement of previously unexplored candidate genes with putative involvement in many aspects of suberin production. I carried out global analyses that corroborated targeted analyses and provided further information about other wound-healing events. By integrating findings pertaining to gene expression, metabolite accumulation, and ABA impact, I was able to identify novel candidate genes and describe putative mechanisms for the regulation and coordination of suberin biosynthesis and assembly involving putative CASP mediators and polyester-forming GDSLs, as well as transcription factors. I synthesized this information and provided insight into the wound-healing process by exploring a complex transcriptional and regulatory network underlying suberization. I have contributed to the current state of knowledge in this field and generated new hypotheses regarding wound-healing and suberization in the potato tuber, which is a valuable suberin model system and an important crop species.

4.5 References

- Baxter, I., Hosmani, P.S., Rus, A., Lahner, B., Borevitz, J.O., Muthukumar, B., Mickelbart, M.V., Schreiber, L., Franke, R.B. and Salt, D.E.** (2009). Root suberin forms an extracellular barrier that affects water relations and mineral nutrition in *Arabidopsis*. *PLoS Genetics* **5**(5), p.e1000492.
- Beisson, F., Li, Y., Bonaventure, G., Pollard, M. and Ohlrogge, J.B.** (2007) The acyltransferase GPAT5 is required for the synthesis of suberin in seed coat and root of *Arabidopsis*. *The Plant Cell* **19**, 351-368.
- Bird, D., Beisson, F., Brigham, A., Shin, J., Greer, S., Jetter, R., Kunst, L., Wu, X., Yephremov, A. and Samuels, L.** (2007). Characterization of *Arabidopsis* ABCG11/WBC11, an ATP binding cassette (ABC) transporter that is required for cuticular lipid secretion. *The Plant Journal* **52**(3), 485-498.
- Boher, P., Serra, O., Soler, M., Molinas, M. and Figueras, M.** (2013). The potato suberin feruloyl transferase FHT which accumulates in the phellogen is induced by wounding and regulated by abscisic and salicylic acids. *Journal of Experimental Botany* **64**(11), 3225-3236.
- Boycheva, S., Daviet, L., Wolfender, J.L. and Fitzpatrick, T.B.** (2014). The rise of operon-like gene clusters in plants. *Trends in Plant Science*, **19**(7), pp.447-459.
- Domergue, F., Vishwanath, S. J., Joubès, J., Ono, J., Lee, J. A., Bourdon, M., Alhattab, R., Lowe, C., Pascal, S., Lessire, R. and Rowland, O.** (2010). Three *Arabidopsis* fatty acyl-coenzyme A reductases, FAR1, FAR4, and FAR5, generate primary fatty alcohols associated with suberin deposition. *Plant Physiology* **153**, 1539-1554.
- Esau, K.** (1977). *Anatomy of Seed Plants*, 2nd Edition (pp. 183-197). New York, NY: Wiley & Sons.
- Kamiya, T., Borghi, M., Wang, P., Danku, J.M., Kalmbach, L., Hosmani, P.S., Naseer, S., Fujiwara, T., Geldner, N. and Salt, D.E.** (2015). The MYB36 transcription factor orchestrates Casparian strip formation. *Proceedings of the National Academy of Sciences of the United States of America* **112**(33), 10533-10538.
- Karahara, I., Ikeda, A., Kondo, T. and Uetake, Y.** (2004) Development of the Casparian strip in primary roots of maize under salt stress. *Planta* **219**(1), 41-47.
- Kosma, D.K., Murmu, J., Razeq, F.M., Santos, P., Bourgault, R., Molina, I. and Rowland, O.** (2014). AtMYB41 activates ectopic suberin synthesis and assembly in multiple plant species and cell types. *The Plant Journal* **80**(2), 216-229.
- Jacob, F. and Monod, J.** (1961) Genetic regulatory mechanisms in the synthesis of proteins. *Journal of Molecular Biology* **3**, 318-356.
- Landgraf, R., Smolka, U., Altmann, S., Eschen-Lippold, L., Senning, M., Sonnwald, S., Weigel, B., Frolova, N., Strehmel, N., Hause, G. and Scheel,**

- D.** (2014). The ABC transporter ABCG1 is required for suberin formation in potato tuber periderm. *The Plant Cell* **26**, 3403-3415.
- Lashbrooke, J.G., Cohen, H., Levy-Samocho, D., Tzfadia, O., Panizel, I., Zeisler, V., Massalha, H., Stern, A., Trainotti, L., Schreiber, L. and Costa, F.** (2016) MYB107 and MYB9 homologs regulate suberin deposition in angiosperms. *The Plant Cell* **28**, 2097–2116.
- Laursen, T., Møller, B.L. and Bassard, J.E.** (2015). Plasticity of specialized metabolism as mediated by dynamic metabolons. *Trends in Plant Science* **20**(1), 20-32.
- Lee, Y., Rubio, M.C., Alassimone, J. and Geldner, N.** (2013). A mechanism for localized lignin deposition in the endodermis. *Cell* **153**(2), 402-412.
- Li, Y., Beisson, F., Koo, A.J., Molina, I., Pollard, M. and Ohlrogge, J.** (2007) Identification of acyltransferases required for cutin biosynthesis and production of cutin with suberin-like monomers. *Proceedings of the National Academy of Sciences of the United States of America* **104**(46), 18339-18344.
- Lulai, E.C.** (2007). Skin-set, wound healing, and related defects. In D. Vreugenhill (Ed.), *Potato Biology and Biotechnology* (pp. 471-500). Oxford, UK: Elsevier.
- Lulai, E.C., Campbell, L.G., Fugate, K.K. and McCue, K.F.** (2016). Biological differences that distinguish the 2 major stages of wound healing in potato tubers. *Plant Signaling & Behavior* **11**(12), p.e1256531.
- Lulai, E.C. and Corsini, D.L.** (1998). Differential deposition of suberin phenolic and aliphatic domains and their roles in resistance to infection during potato tuber (*Solanum tuberosum* L.) wound-healing. *Physiological and Molecular Plant Pathology* **53**(4), 209-222.
- Lulai, E.C. and Neubauer, J.D.** (2014). Wound-induced suberization genes are differentially expressed, spatially and temporally, during closing layer and wound periderm formation. *Postharvest Biology and Technology* **90**, 24-33.
- Lulai, E.C., Neubauer, J.D. and Suttle, J.C.** (2014). Kinetics and localization of wound-induced DNA biosynthesis in potato tuber. *Journal of plant physiology*, **171**(17), 1571-1575.
- Lulai, E.C. and Suttle, J.C.** (2004). The involvement of ethylene in wound induced suberization of potato tuber (*Solanum tuberosum* L.): a critical assessment. *Postharvest Biology and Technology* **34**, 105-112.
- Lulai, E.C. and Suttle, J.C.** (2009). Signals involved in tuber wound-healing. *Plant Signaling & Behavior* **4**(7), 620-622.
- Lulai, E.C., Huckle, L., Neubauer, J.D. and Suttle, J.C.** (2011) Coordinate expression of AOS genes and JA accumulation: JA is not required for initiation of closing layer in wound healing tubers. *Journal of Plant Physiology* **168**, 976-982.
- Marques, A. and Pereira, H.** (1987) On the determination of suberin and other structural components in cork from *Quercus suber* L. *Anais do Instituto Superior de Agronomia* **42**, 321-335.

- Markus, K.** (2018). Characterization of the transcription factor ANAC058 and its role in suberin regulation. *PhD Dissertation* (<http://hss.ulb.uni-bonn.de/2018/5175/5175.htm>), University of Bonn, Germany.
- Massa, A.N., Childs, K.L., Lin, H., Bryan, G.J., Giuliano, G., and Buell, C.R.** (2011). The transcriptome of the reference potato genome *Solanum tuberosum* Group Phureja Clone DM1-3 516R44. *PLoS ONE* **6**(10): e26801.
- Nakayama, T., Shinohara, H., Tanaka, M., Baba, K., Ogawa-Ohnishi, M. and Matsubayashi, Y.** (2017). A peptide hormone required for Casparian strip diffusion barrier formation in *Arabidopsis* roots. *Science* **355**(6322), 284-286.
- Norris, V., Gascuel, P., Guespin-Michel, J., Ripoll, C. and Saier Jr, M.H.** (1999). Metabolite-induced metabolons: the activation of transporter–enzyme complexes by substrate binding. *Molecular Microbiology* **31**(5), 1592-1595.
- Payyavula, R.S., Shakya, R., Sengoda, V.G., Munyaneza, J.E., Swamy, P. and Navarre, D.A.** (2015). Synthesis and regulation of chlorogenic acid in potato: Rerouting phenylpropanoid flux in HQT-silenced lines. *Plant Biotechnology Journal* **13**(4), 551-564.
- Roppolo, D., Boeckmann, B., Pfister, A., Boutet, E., Rubio, M.C., Dénervaud-Tendon, V., Vermeer, J.E., Gheyselinck, J., Xenarios, I. and Geldner, N.** (2014). Functional and evolutionary analysis of the CASPARIAN STRIP MEMBRANE DOMAIN PROTEIN family. *Plant Physiology* **165**(4), 1709-1722.
- Serra, O., Soler, M., Hohn, C., Franke, R., Schreiber, L., Prat, S., Molinas, M. and Figueras, M.** (2009a). Silencing of *StKCS6* in potato periderm leads to reduced chain lengths of suberin and wax compounds and increased peridermal transpiration. *Journal of Experimental Botany* **60**, 697-707.
- Serra, O., Soler, M., Hohn, C., Sauveplane, V., Pinot, F., Franke, R., Schreiber, L., Prat, S., Molinas, M. and Figueras, M.** (2009b) *CYP86A33*-targeted gene silencing in potato tuber alters suberin composition, distorts suberin lamellae, and impairs the periderm's water barrier function. *Plant Physiology* **149**, 1050-1060.
- Serra, O., Hohn, C., Franke, R., Prat, S., Molinas, M. and Figueras, M.** (2010). A feruloyl transferase involved in the biosynthesis of suberin and suberin-associated wax is required for maturation and sealing properties of potato periderm. *The Plant Journal* **62**, 277-290.
- Schmidt, H.W. and Schönherr, J.** (1982). Fine structure of isolated and non-isolated potato tuber periderm. *Planta* **154**(1), 76-80.
- Schreiber, L., Franke, R., and Hartmann, K.** (2005) Effects of NO₃ deficiency and NaCl stress on suberin deposition in rhizo- and hypodermal (RHCW) and endodermal cell walls (ECW) of castor bean (*Ricinus communis* L.) roots. *Plant Soil* **269**, 333-339.
- Stafford, H.A.** (1974). Possible multienzyme complexes regulating the formation of C6-C3 phenolic compounds and lignins in higher plants. *Recent Advances in Phytochemistry* **8**, 53-79.

- Thomas, R., Fang, X., Ranathunge, K., Anderson, T.R., Peterson, C.A. and Bernard, M.A.** (2007). Soybean root suberin: Anatomical distribution, chemical composition and relationship to partial resistance to *Phytophthora sojae*. *Plant Physiology* **144**(1), 299-311.
- Valiñas, M.A., Lanteri, M.L., Ten Have, A., and Andreu, A.B.** (2015) Chlorogenic acid biosynthesis appears linked with suberin production in potato tuber (*Solanum tuberosum*). *Journal of Agricultural and Food Chemistry* **63**, 4902-4913.
- Verdaguer, R., Soler, M., Serra, O., Garrote, A., Fernández, S., Company-Arumí, D., Anticó, E., Molinas, M. and Figueras, M.** (2016) Silencing of the potato *StNAC103* gene enhances the accumulation of suberin polyester and associated wax in tuber skin. *Journal of Experimental Botany* **67**(18), 5415-5427.
- Vulavala, V.K., Fogelman, E., Rozenal, L., Faigenboim, A., Tanami, Z., Shoseyov, O. and Ginzberg, I.** (2017) Identification of genes related to skin development in potato. *Plant Molecular Biology* **94**(4-5), 481-494.
- Yadav, V., Molina, I., Ranathunge, K., Castillo, I.Q., Rothstein, S.J. and Reed, J.W.** (2014). ABCG transporters are required for suberin and pollen wall extracellular barriers in *Arabidopsis*. *The Plant Cell* **26**(9), 3569-3588.
- Yang, W.-L., and Bernard, M.A.** (2007) Metabolite profiling of potato (*Solanum tuberosum* L.) tubers during wound-induced suberization. *Metabolomics* **3**(2), 147-159.
- Yogendra, K.N., Kumar, A., Sarkar, K., Li, Y., Pushpa, D., Mosa, K.A., Duggavathi, R., and Kushalappa, A.C.** (2015) Transcription factor *StWRKY1* regulates phenylpropanoid metabolites conferring late blight resistance in potato. *Journal of Experimental Botany* **66**(22), 7377-7389.
- Zhang, Y., Beard, K.F., Swart, C., Bergmann, S., Krahnert, I., Nikoloski, Z., Graf, A., Ratcliffe, R.G., Sweetlove, L.J., Fernie, A.R. and Obata, T.** (2017) Protein-protein interactions and metabolite channelling in the plant tricarboxylic acid cycle. *Nature Communications* **8**, 15212-15232.

Appendix A: Reprint permission for Chapter 1

ELSEVIER LICENSE TERMS AND CONDITIONS

Sep 19, 2018

This Agreement between Western University -- Kathlyn Woolfson ("You") and Elsevier ("Elsevier") consists of your license details and the terms and conditions provided by Elsevier and Copyright Clearance Center.

License Number	4432681142619
License date	Sep 19, 2018
Licensed Content Publisher	Elsevier
Licensed Content Publication	Postharvest Biology and Technology
Licensed Content Title	Wound-induced suberization genes are differentially expressed, spatially and temporally, during closing layer and wound periderm formation
Licensed Content Author	Edward C. Lulai, Jonathan D. Neubauer
Licensed Content Date	Apr 1, 2014
Licensed Content Volume	90
Licensed Content Issue	n/a
Licensed Content Pages	10
Start Page	24
End Page	33
Type of Use	reuse in a thesis/dissertation
Portion	figures/tables/illustrations
Number of figures/tables/illustrations	1
Format	both print and electronic
Are you the author of this Elsevier article?	No
Will you be translating?	No
Original figure numbers	Figure 2
Title of your thesis/dissertation	SUBERIN BIOSYNTHESIS AND DEPOSITION IN THE WOUND-HEALING POTATO (SOLANUM TUBEROSUM L.) TUBER MODEL
Expected completion date	Dec 2018
Estimated size (number of pages)	250
Requestor Location	Western University 1151 Richmond Street

London, ON N6A3K7
Canada
Attn: Western University
GB 494 6272 12
0.00 CAD

Publisher Tax ID
Total



Mail Address:

AOCS, P.O. Box 17190, Urbana, IL 61803-7190 USA

Street Address:

AOCS, 2710 S. Boulder Drive,

Urbana, IL 61802-6996 USA

Phone: +1-217-359-2344 • **Fax:** +1-217-351-8091

E-Mail: general@aocs.org • **Web:** www.aocs.org

October 19, 2018

Kathlyn Woolfson
Department of Biology
University of Western Ontario
1151 Richmond St, London
ON N6A 3K7, Canada

Dear Katie,

On behalf of the AOCS Lipid Library, we grant you permission to reprint Figure 3 from the online Open Access article, Biosynthesis of Plant Lipid Polyesters, found at:

<https://lipidlibrary.aocs.org/Biochemistry/content.cfm?ItemNumber=40311>

When citing, please use the above URL and include "AOCS Lipid Library."

Congratulations on your achievement and AOCS looks forward to your contributions to our journals, books and more.

Regards,

Janet S. Brown
Director, AOCS Membership and Publications

www.aocs.org

Appendix B: Chapter 2 supplementary material

Table B1. Statistical analysis for gene expression data of four month old tubers. A. Treatment comparisons at each time point.

B. Time comparisons within each treatment. Significant differences between water and each ABA-related treatment were denoted in figures, all additional treatment and sequential time point comparisons are also provided in this table. After initial two-way ANOVAs, one-way ANOVAs were performed for treatment (if significant, using Tukey's honest significance difference post-hoc test) and/or for time (if significant, using contrasts that only made pairwise time comparisons between sequential time points within the series, and the Benjamini-Hochberg test), to isolate the effects of each factor. In the two-way ANOVA, *THT* was the only gene to show no significant interaction, no treatment effect and solely a time effect, so statistical analysis for treatment effect on *THT* expression was not performed. Statistically significant differences are denoted by * for both $|\log_2(\text{fold change})| \geq 1$ and $p \leq 0.05$. Note: There is no treatment comparison for *THT* because two-way ANOVA revealed no treatment:time interaction or treatment effect for *THT* expression data.

Table B1-A. Treatment comparisons at each time point.

Day post-wounding	Treatment comparison	<i>PAL1</i>	<i>C4H</i>	<i>CCR</i>	<i>CYP86A33</i>	<i>CYP86B12</i>	<i>FAR3</i>	<i>KCS6</i>	<i>GPAT5</i>	<i>GPAT6</i>	<i>FHT</i>	<i>ABCG1</i>
0	Water-FD											
1	Water-FD								*	*		
2	Water-FD											
3	Water-FD				*	*	*	*	*	*	*	*
4	Water-FD				*	*	*	*	*	*		*
6	Water-FD									*		
0	Water-ABA				*	*			*			
1	Water-ABA			*	*	*	*		*	*		*
2	Water-ABA									*		*
3	Water-ABA											
4	Water-ABA											
6	Water-ABA											
0	Water-FD+ABA	*				*			*			

1	Water-FD+ABA	*	*	*	*	*	*	*	*	*
2	Water-FD+ABA	*						*		
3	Water-FD+ABA									
4	Water-FD+ABA									
6	Water-FD+ABA							*		
0	FD-ABA		*	*			*			
1	FD-ABA	*	*	*	*	*	*	*	*	*
2	FD-ABA		*	*	*	*	*	*	*	*
3	FD-ABA		*	*	*	*	*	*	*	*
4	FD-ABA	*	*				*		*	*
6	FD-ABA									
0	FD+ABA-FD			*			*			
1	FD+ABA-FD	*	*	*	*	*	*	*	*	*
2	FD+ABA-FD	*	*	*	*	*	*	*	*	*
3	FD+ABA-FD		*	*	*	*	*	*	*	*
4	FD+ABA-FD	*	*	*			*	*	*	*
6	FD+ABA-FD									
0	FD+ABA-ABA									
1	FD+ABA-ABA									
2	FD+ABA-ABA									
3	FD+ABA-ABA									
4	FD+ABA-ABA									
6	FD+ABA-ABA									

Table B1-B. Time comparisons within each treatment.

Treatment	Time comparison	<i>PAL1</i>	<i>C4H</i>	<i>CCR</i>	<i>THT</i>	<i>CYP86A33</i>	<i>CYP86B12</i>	<i>FAR3</i>	<i>KCS6</i>	<i>GPAT5</i>	<i>GPAT6</i>	<i>FHT</i>	<i>ABCG1</i>
Water	1d-0d	*						*		*	*	*	*
	2d-1d	*		*	*	*	*	*	*	*			*
	3d-2d	*		*		*	*	*	*	*	*	*	*
	4d-3d								*		*		*
	6d-4d									*	*		
FD	1d-0d	*						*		*	*	*	*
	2d-1d	*		*	*	*	*	*	*	*		*	
	3d-2d	*		*		*	*	*	*	*	*	*	
	4d-3d					*	*	*	*	*	*	*	*
	6d-4d								*				
ABA	1d-0d	*		*		*			*	*	*	*	*
	2d-1d	*		*		*	*	*	*	*	*		*
	3d-2d			*		*	*	*	*	*	*		*
	4d-3d												
	6d-4d	*								*	*		
FD+ABA	1d-0d	*		*		*			*	*	*	*	*
	2d-1d					*	*	*	*	*	*		*
	3d-2d			*		*	*	*	*	*	*		*
	4d-3d						*		*				*
	6d-4d						*			*	*		

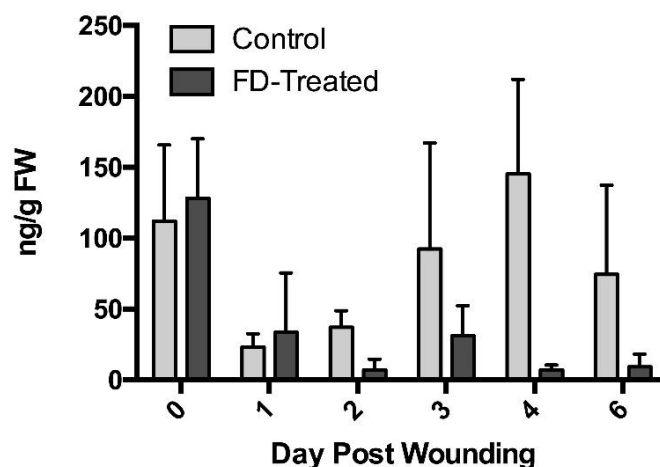


Figure B1. ABA verification by isotope dilution. ABA was measured in un-treated, wound-healing tubers using a targeted, isotope dilution method. Frozen tissue was ground to a fine powder under liquid N₂ with a mortar and pestle and weighed into 1 g subsamples. To each sample, 5 mL ice-cold 90% v/v/ methanol (MeOH) containing 0.1% v/v acetic acid was added, along with 20 μ L ABA-d₄ standard (2.5 μ g/mL; National Research Council-Plant Biotechnology Institute, Saskatchewan, Canada). Tissue was incubated with occasional stirring for 5 minutes, and then transferred to a 15 mL centrifuge tube. The mortar and pestle were washed three times with 3 mL ice cold 90% v/v MeOH (containing 0.1% v/v acetic acid), and the washes added to the initial 5 mL extraction. Samples were centrifuged at 12 000 x g for 10 minutes, and the supernatant transferred to 25 mL round-bottom flasks and the solvent volume reduced under vacuum at 40°C using a roto-evaporator (Buchi, Switzerland). When less than 1.5 mL liquid extract remained, samples were transferred to 1.5 mL microcentrifuge tubes and centrifuged at 15 000 x g for 5 minutes. The supernatant was transferred to a LC vial containing a micro-volume insert (Agilent Technologies, USA). For LC-MS analysis, 100 μ L samples were injected onto a Zorbax C-18 column (3.0 x 50 mm, 1.8 μ m; Agilent Technologies, USA) attached to an Agilent 1260 LC system and eluted with the following solvent gradient (solvent A = 0.1% v/v formic acid in Milli-Q H₂O; solvent B = 0.1% v/v formic acid in 90% v/v acetonitrile-10% Milli-Q H₂O): Start condition, 20% v/v B in A, followed by a three step gradient to 60% v/v B in A over 4.5 minutes, 80% v/v B in A over 3 minutes and finally 100% B over 2.5 minutes. After 2 minutes at 100% B, the initial conditions were restored over 1 minute, followed by a 7 minute equilibration before the next sample was injected. Solvent flow rate was 0.3 mL/min. Compounds were detected by UV absorbance (240 nm) and ESI-TOF-MS (Agilent Technologies model 6230) in negative ion mode. ESI-TOF parameters: drying gas at 350°C, 10 mL/min; nebulizer at 45 PSI; Vcap at 4000 V; Fragmentor at 150 V. Spectra were collected at 1.03/sec (9729 transients/spectrum) in the 100-1700 m/z range. Reference mass solution (112.985587 m/z and 1033.988109 m/z) was infused constantly via a second nebulizer at 15 psi. ABA ([M-H]⁻ = 263.1289 m/z) was quantified using the ABA-d₄ ([M-H]⁻ = 267.1540 m/z) peak area as an internal calibration standard, using Agilent Mass Hunter Qualitative Analysis software (VB05) (Agilent Technologies, USA).

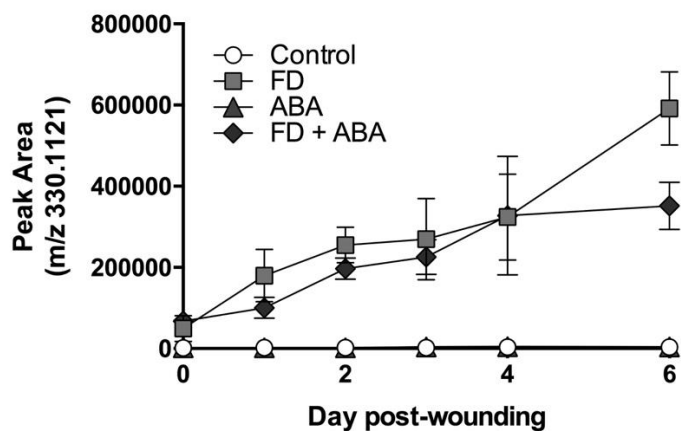


Figure B2. Persistence of fluridone in potato tubers. Fluridone (m/z 330.1121) signals were extracted from the MS-data collected for polar metabolite extracts prepared from wound-induced potato tuber discs after treatment with water, FD, ABA or FD+ABA. Data are from four-month old tubers and correspond to the gene expression data in **Figure 2.2**.

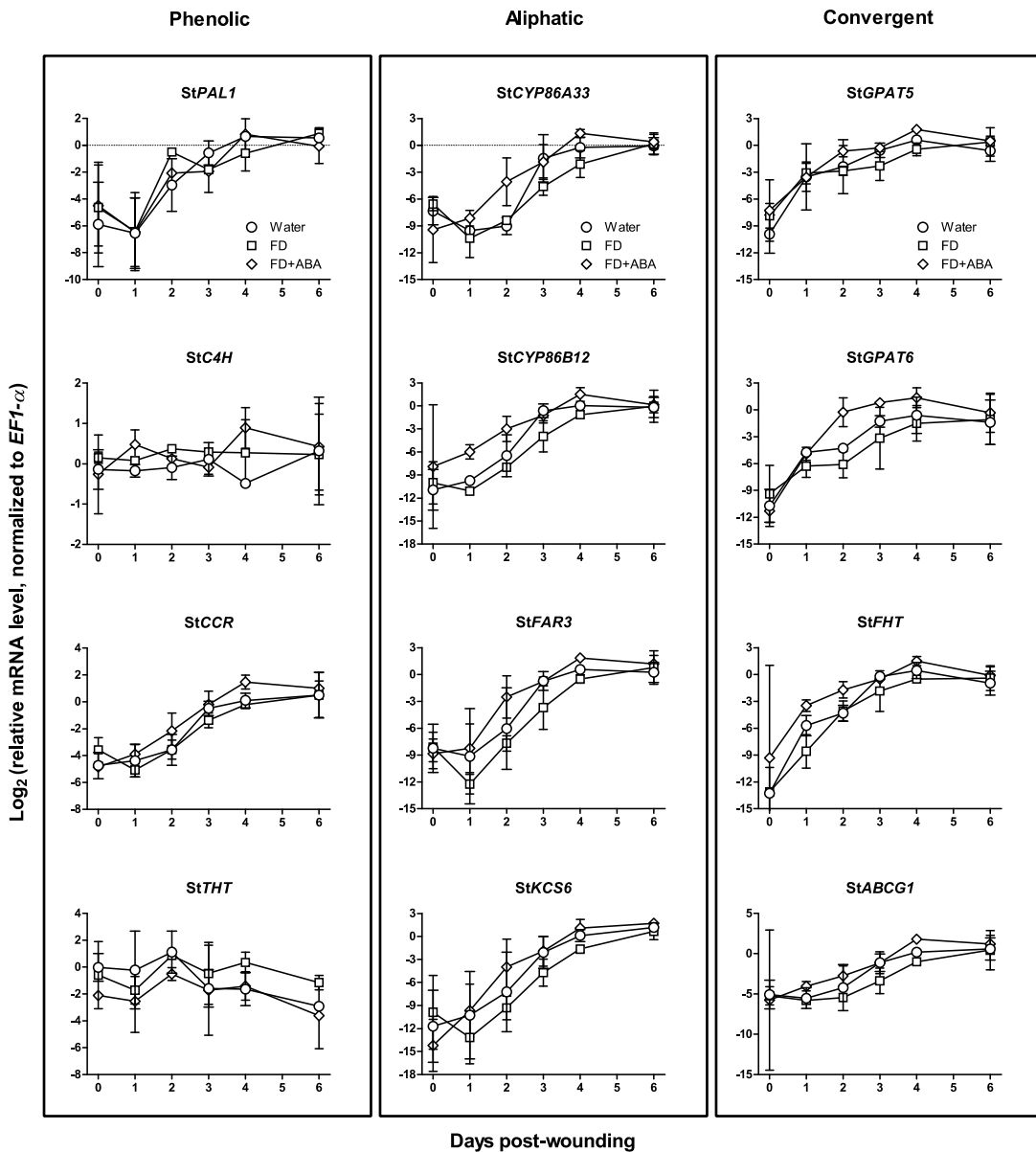


Figure B3. Expression of suberin biosynthesis genes after wounding of eight month old tubers. Expression of phenolic suberin biosynthetic genes (*StPAL1*, *StC4H*, *StCCR* and *StTHT*), aliphatic suberin biosynthetic genes (*StCYP86A33*, *StKCS6*, *StCYP86B12* and *StFAR3*) and genes involved in linkage and deposition (Convergent; *StGPAT5*, *StGPAT6*, *StFHT* and *StABCG1*) was measured using RT-qPCR. RNA was extracted from tuber tissue previously treated with water, FD or FD + ABA. Gene expression values were normalized to the endogenous reference gene *StEF1-α*. Data points represent the sample mean \pm SD (n = 3 technical replicates).

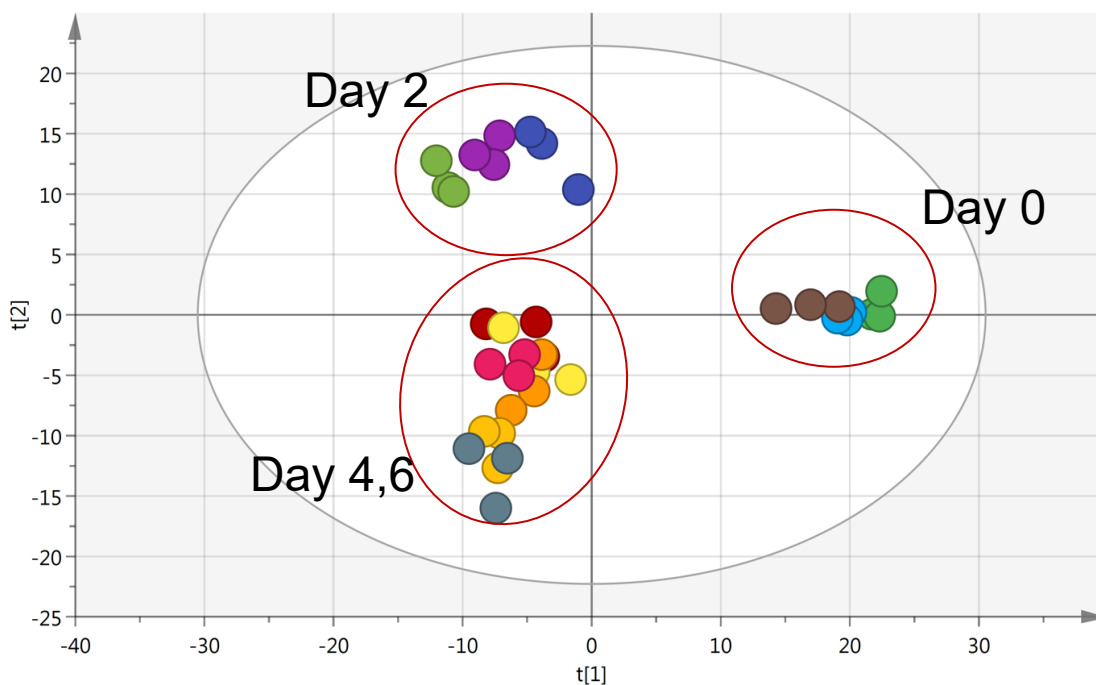


Figure B4. PLS-DA analysis of polar metabolites isolated from eight month old tubers. Polar metabolites were extracted from wound-induced potato tuber discs after treatment with water, FD or FD + ABA and analyzed by LC-MS. After molecular feature extraction, alignment and normalization, the data were analyzed using SIMCA-P (Umetrics) software. The PLS-DA plot was generated using treatment and time groupings as discriminant factors to help maximize separation between treatments and time points. Each symbol represents a single polar metabolite profile.

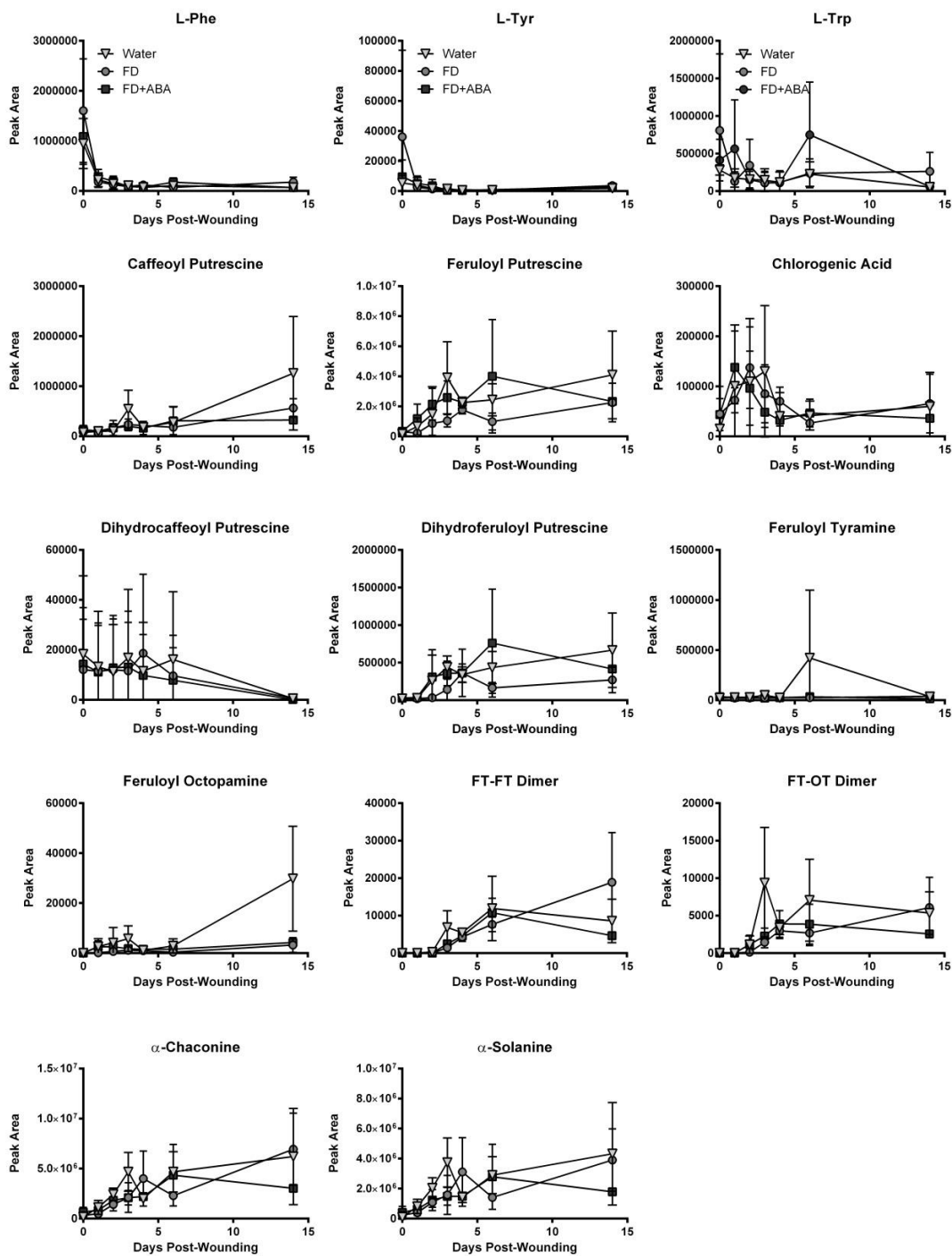


Figure B5. Accumulation of polar compounds in wound-healing tubers. Polar metabolites were extracted from wound-induced potato tuber discs treated with water, FD or FD+ABA, and analyzed by LC-MS. MS data was mined for known compounds based on their exact mass ($[M+H]^+$), according to Landgraf et al. (2014).

Figure B6-9 (below). Aliphatic suberin monomer analysis. Detailed chain length distribution of aliphatic monomers. Data for individual monomers are presented for both solubles extracted from suberizing tissues and the monomers released from the polymer after methanolic HCl transesterification (i.e., insolubles). Monomers were analysed as their methyl esters/TMS-ethers. Four month old tuber tissue was treated with water, FD, ABA or FD+ABA. Data points represent the sample mean \pm standard deviation ($n = 3$).

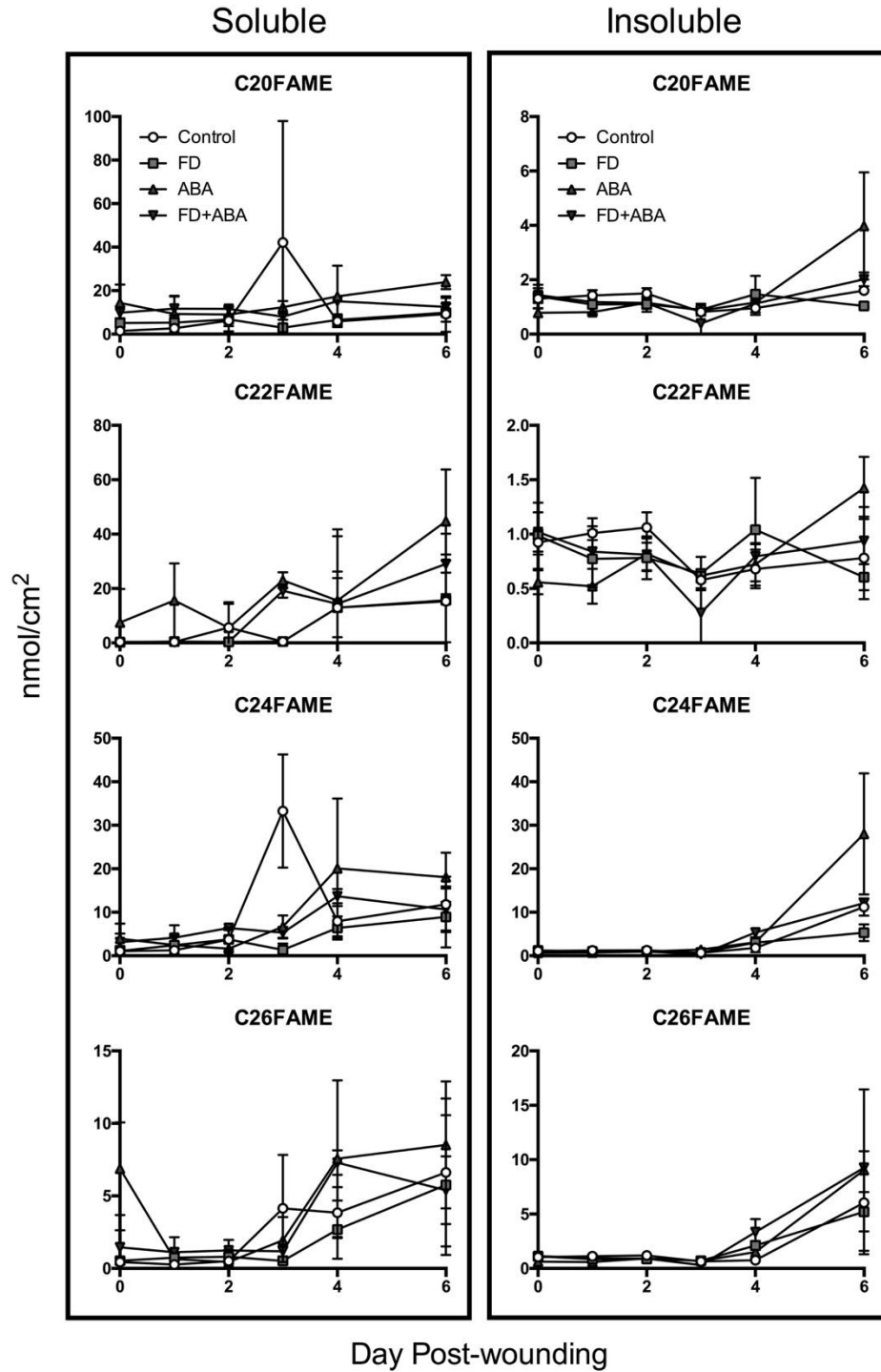


Figure B6. Chain length distribution of fatty acids isolated from suberizing potato tubers.

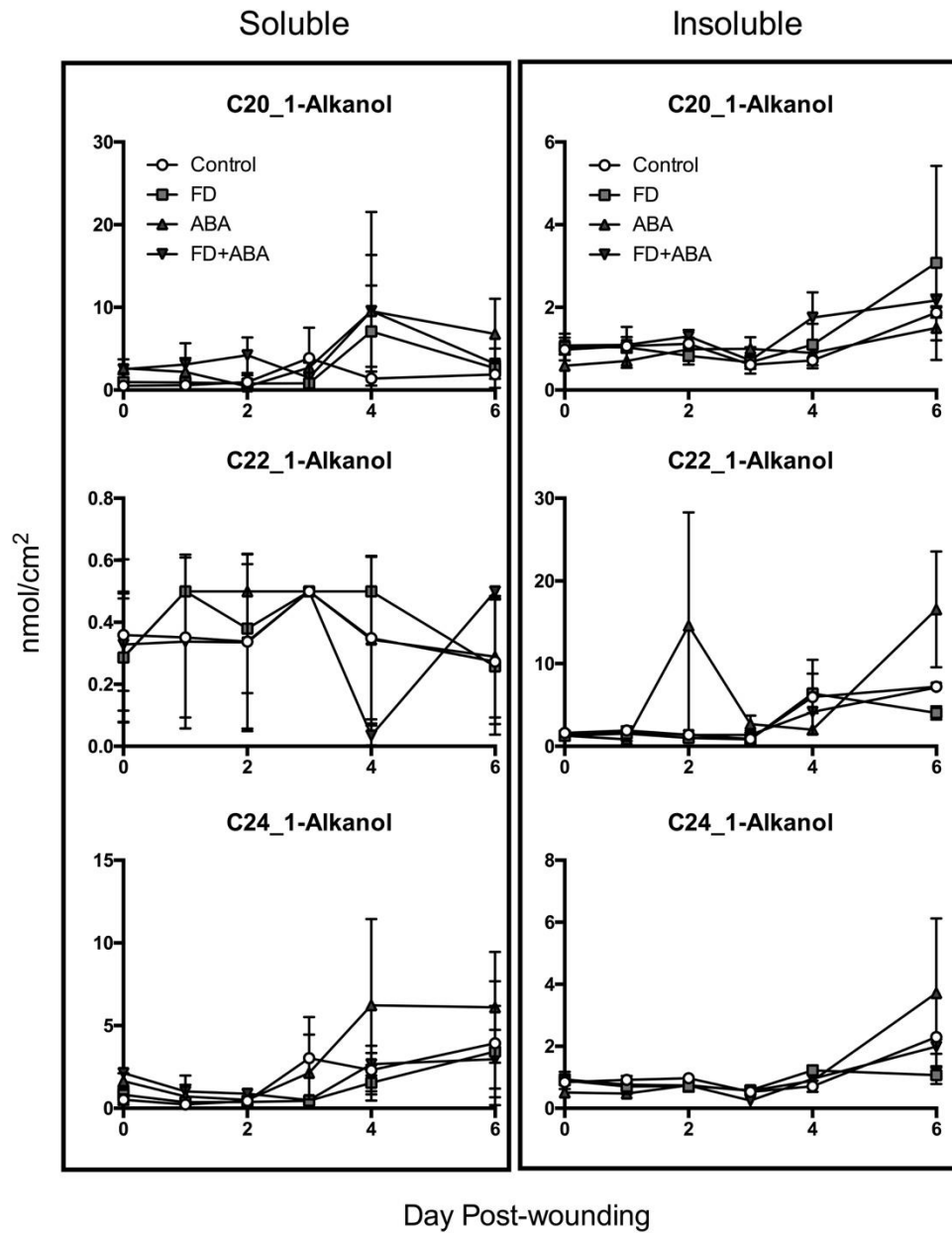


Figure B7. Chain length distribution of 1-alkanols isolated from suberizing potato tubers.

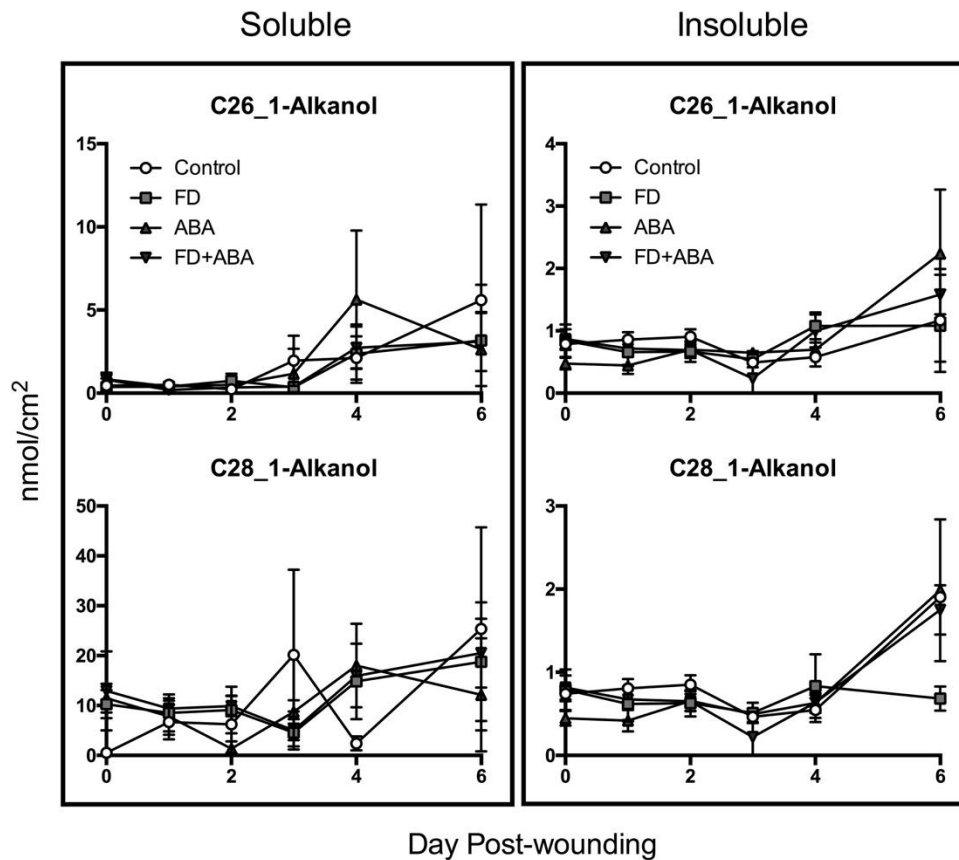


Figure B7 (continued). Chain length distribution of 1-alkanols isolated from suberizing potato tubers.

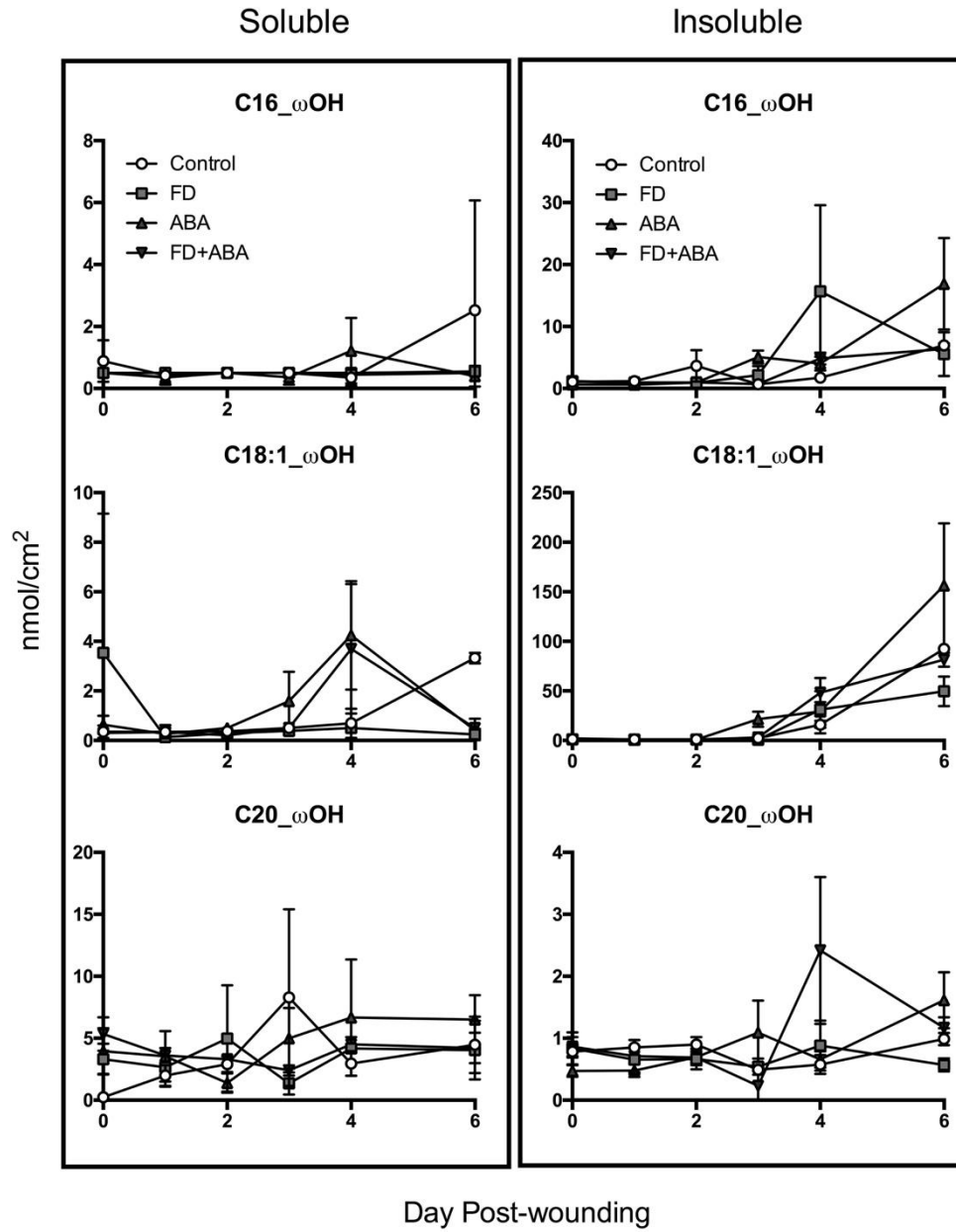


Figure B8. Chain length distribution of ω -hydroxy fatty acids isolated from suberizing potato tubers.

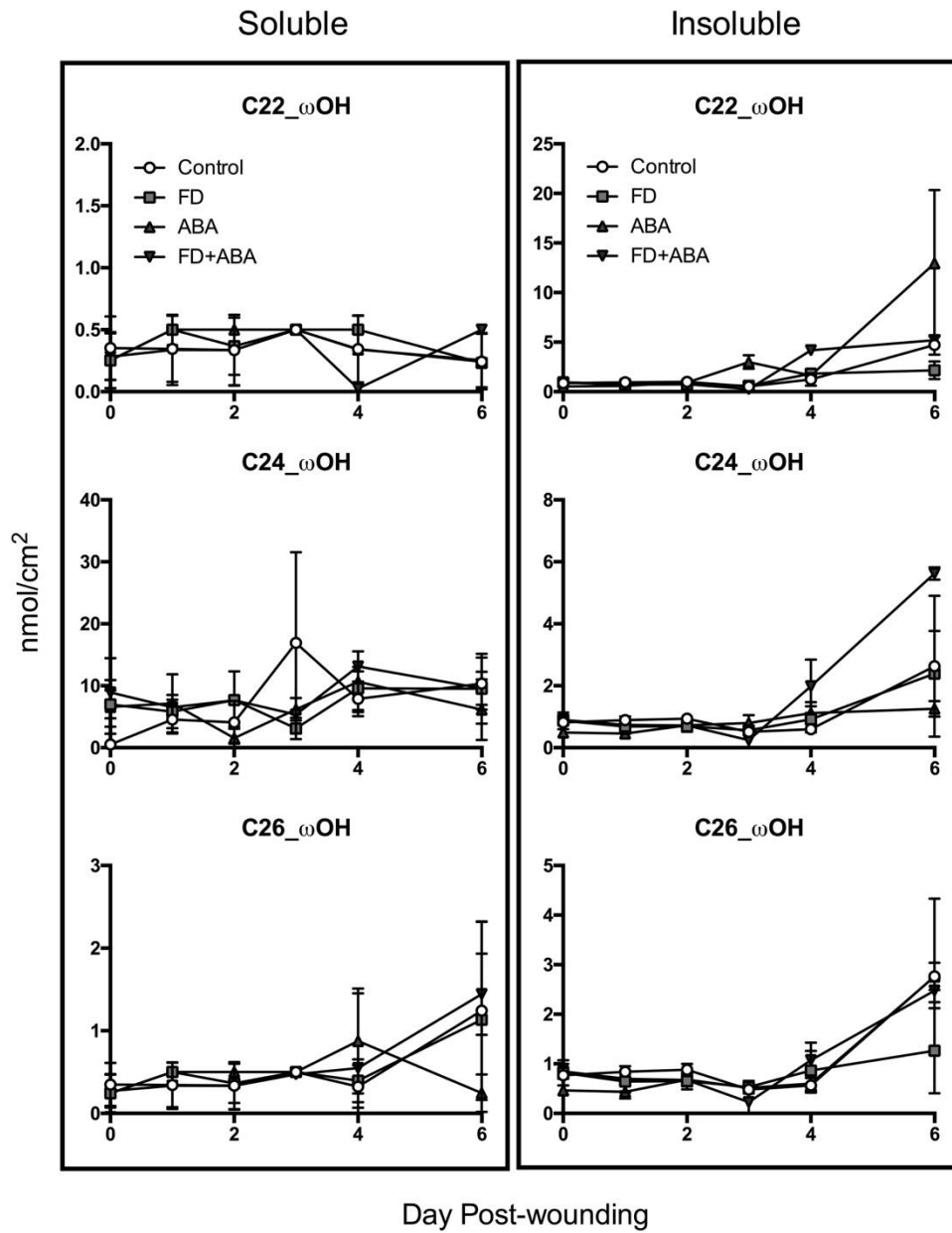


Figure B8 (continued). Chain length distribution of ω-hydroxy fatty acids isolated from suberizing potato tubers.

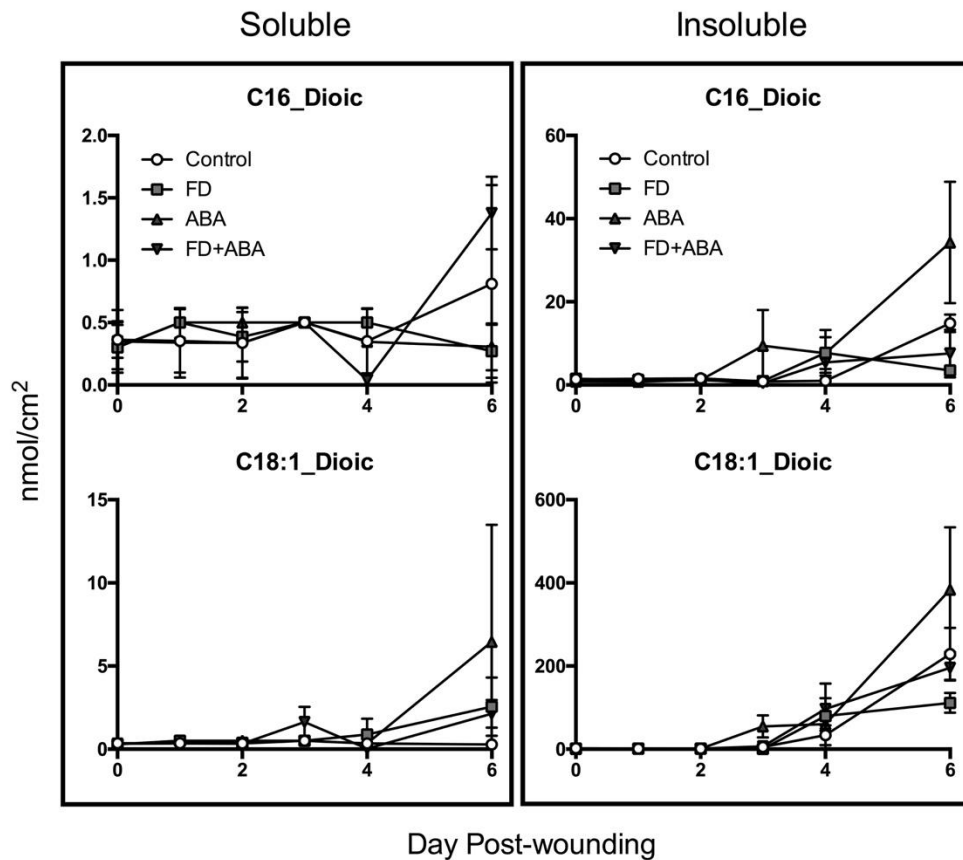


Figure B9. Chain length distribution of α,ω -dioic acids (as methyl esters) isolated from suberizing potato tubers.

Appendix C: Chapter 3 supplementary material

Table C1. TopGO analysis of top 50 gene ontology terms enriched within 5441 differentially expressed genes identified from the wound-healing tuber time course.

GO.ID	Term	Annotated	Significant	Expected	Weighted Fisher
GO:0007018	microtubule-based movement	58	36	11.5	2.30E-12
GO:0010411	xyloglucan metabolic process	32	21	6.35	2.20E-08
GO:0006270	DNA replication initiation	22	15	4.36	1.10E-06
GO:0009765	photosynthesis, light harvesting	48	24	9.52	4.40E-06
GO:0042546	cell wall biogenesis	158	56	31.33	5.50E-06
GO:0018298	protein-chromophore linkage	48	23	9.52	1.10E-05
GO:0006629	lipid metabolic process	1010	225	200.29	1.40E-05
GO:0006950	response to stress	2272	473	450.56	1.50E-05
GO:0055114	oxidation-reduction process	2194	499	435.1	1.90E-05
GO:0006334	nucleosome assembly	47	22	9.32	2.70E-05
GO:0008283	cell proliferation	75	24	14.87	3.00E-05
GO:0006260	DNA replication	143	58	28.36	9.20E-05
GO:0006275	regulation of DNA replication	34	16	6.74	0.0002
GO:0009219	pyrimidine deoxyribonucleotide metabolic process	5	5	0.99	0.00031
GO:0016572	histone phosphorylation	14	9	2.78	0.00035
GO:0010951	negative regulation of endopeptidase activity	84	30	16.66	0.00049
GO:0080167	response to karrikin	66	25	13.09	0.00052
GO:0008299	isoprenoid biosynthetic process	196	34	38.87	0.00057
GO:0009408	response to heat	137	43	27.17	0.00076
GO:0015979	photosynthesis	241	66	47.79	0.00126
GO:0048827	phyllome development	259	49	51.36	0.0015
GO:0009070	serine family amino acid biosynthetic process	62	18	12.3	0.00154
GO:0010075	regulation of meristem growth	60	22	11.9	0.00179

GO:0006569	tryptophan catabolic process	11	7	2.18	0.00186
GO:0016126	sterol biosynthetic process	39	16	7.73	0.00195
GO:0046274	lignin catabolic process	20	10	3.97	0.00241
GO:0006974	cellular response to DNA damage stimulus	238	57	47.2	0.0029
GO:0009607	response to biotic stimulus	497	125	98.56	0.00297
GO:0016998	cell wall macromolecule catabolic process	34	14	6.74	0.00352
GO:0010389	regulation of G2/M transition of mitotic cell cycle	12	7	2.38	0.0037
GO:0051726	regulation of cell cycle	132	41	26.18	0.00391
GO:0048438	floral whorl development	126	31	24.99	0.00399
GO:0051225	spindle assembly	15	8	2.97	0.004
GO:0016132	brassinosteroid biosynthetic process	31	13	6.15	0.00403
GO:0000226	microtubule cytoskeleton organization	106	41	21.02	0.00593
GO:0030245	cellulose catabolic process	19	9	3.77	0.00625
GO:0009157	deoxyribonucleoside monophosphate biosynthetic process	5	4	0.99	0.0065
GO:0042814	monopolar cell growth	5	4	0.99	0.0065
GO:0048544	recognition of pollen	66	22	13.09	0.00681
GO:0009147	pyrimidine nucleoside triphosphate metabolic process	14	5	2.78	0.00779
GO:0016311	dephosphorylation	293	53	58.11	0.00904
GO:0006545	glycine biosynthetic process	8	5	1.59	0.01001
GO:0009664	plant-type cell wall organization	144	37	28.56	0.01011
GO:0006032	chitin catabolic process	14	7	2.78	0.01105
GO:0009684	indoleacetic acid biosynthetic process	11	6	2.18	0.01115
GO:0009617	response to bacterium	141	36	27.96	0.01177
GO:0009834	plant-type secondary cell wall biogenesis	24	10	4.76	0.01184
GO:0005975	carbohydrate metabolic process	1101	271	218.34	0.01201
GO:0000911	cytokinesis by cell plate formation	55	19	10.91	0.01315
GO:0006084	acetyl-CoA metabolic process	34	14	6.74	0.01353

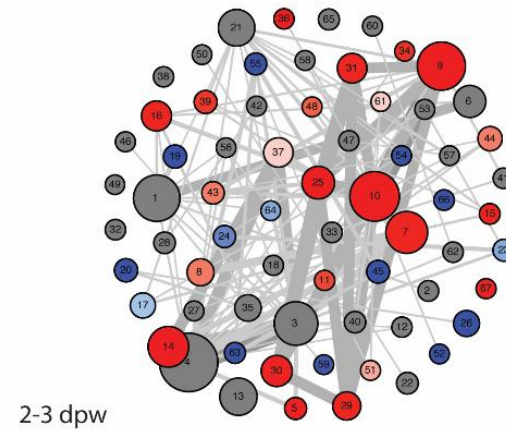
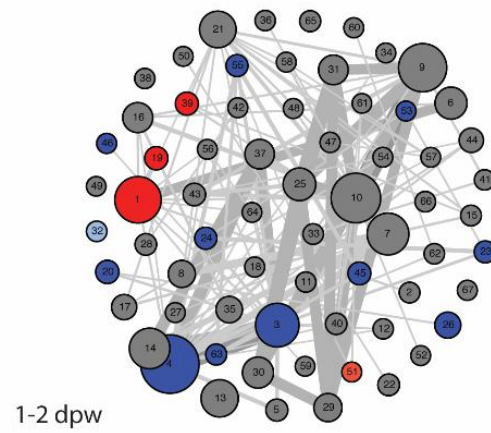
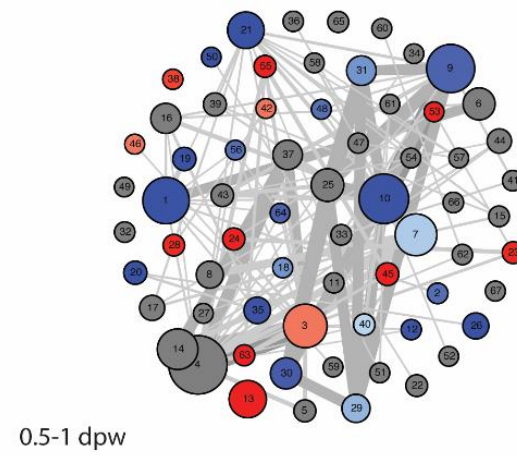
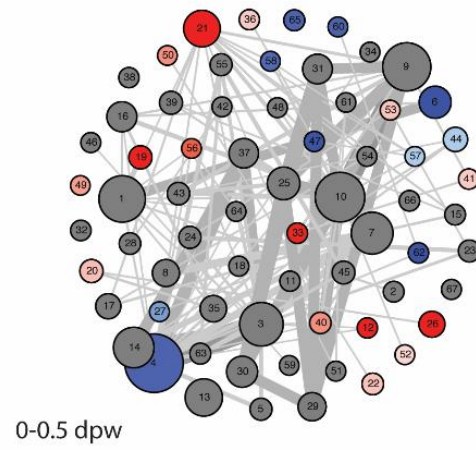
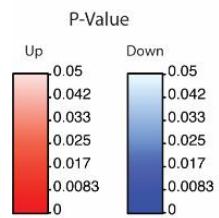


Figure C1. Gene set enrichment analysis (GSEA) of molecular function across differentially expressed genes (DEGs) identified in sequential wound-healing time point comparisons. Together, time point comparison panels represent a union parametric analysis of gene set enrichment (PAGE) of molecular function (MF) categorized gene ontology (GO) terms. Nodes represent gene sets and size represent ranges from 5-495 genes, and edges show overlapping genes between sets, with width representing ranges from 5-269 genes. Blue sets are down-regulated, red are up-regulated, and grey node denote terms that were not detected as significantly differentially regulated (i.e. enriched) at that time point comparison. Labels denote assigned node numbers that correspond to **Table C2** with associated GO ID, GO term and regulation overview.

Table C2. Summary of gene ontology information represented in molecular function gene set enrichment analysis plot and change in terms over time.

Node	GO ID	GO Term	Time point comparison (days post-wounding)			
			0-0.5	0.5-1	1-2	2-3
1	GO:0003677	DNA binding	-	↓	↑	-
2	GO:0003682	chromatin binding	-	↓	-	-
3	GO:0000166	nucleotide binding	-	↑	↓	-
4	GO:0005524	ATP binding	↓	-	↓	-
5	GO:0016887	ATPase activity	-	-	-	↑
6	GO:0003700	transcription factor activity, sequence-specific DNA binding	↓	-	-	-
7	GO:0016740	transferase activity	-	↓	-	↑
8	GO:0016757	transferase activity, transferring glycosyl groups	-	-	-	↑
9	GO:0016491	oxidoreductase activity	-	↓	-	↑
10	GO:0046872	metal ion binding	-	↓	-	↑
11	GO:0045735	nutrient reservoir activity	-	-	-	↑
12	GO:0016874	ligase activity	↑	↓	-	-
13	GO:0003674	molecular_function	-	↑	-	-
14	GO:0004672	protein kinase activity	-	-	-	↑
15	GO:0016746	transferase activity, transferring acyl groups	-	-	-	↑
16	GO:0008270	zinc ion binding	-	-	-	↑
17	GO:0016798	hydrolase activity, acting on glycosyl bonds	-	-	-	↓
18	GO:0042803	protein homodimerization activity	-	↓	-	-
19	GO:0046982	protein heterodimerization activity	↑	↓	↑	↓
20	GO:0003723	RNA binding	↑	↓	↓	↓
21	GO:0003824	catalytic activity	↑	↓	-	-
22	GO:0016853	isomerase activity	↑	-	-	-
23	GO:0003924	GTPase activity	-	↑	↓	↓
24	GO:0005525	GTP binding	-	↑	↓	↓
25	GO:0020037	heme binding	-	-	-	↑
26	GO:0003735	structural constituent of ribosome	↑	↓	↓	↓
27	GO:0016779	nucleotidyltransferase activity	↓	-	-	-
28	GO:0009055	electron carrier activity	-	↑	-	-
29	GO:0004497	monooxygenase activity	-	↓	-	↑
30	GO:0005506	iron ion binding	-	↓	-	↑
31	GO:0016705	oxidoreductase activity, acting on paired donors, with incorporation or reduction of molecular oxygen	-	↓	-	↑
32	GO:0003779	actin binding	-	-	↓	-
33	GO:0051287	NAD binding	↑	-	-	-
34	GO:0016772	transferase activity, transferring phosphorus-containing groups	-	-	-	↑
35	GO:0003676	nucleic acid binding	-	↓	-	-

36	GO:0008171	O-methyltransferase activity	↑	-	-	↑
37	GO:0004674	protein serine/threonine kinase activity	-	-	-	↑
38	GO:0005199	structural constituent of cell wall	-	↑	-	-
39	GO:0016747	transferase activity, transferring acyl groups other than amino-acyl groups	-	-	↑	↑
40	GO:0000287	magnesium ion binding	↑	↓	-	-
41	GO:0016616	oxidoreductase activity, acting on the CH-OH group of donors, NAD or NADP as acceptor	↑	-	-	-
42	GO:0015035	protein disulfide oxidoreductase activity	-	↑	-	-
43	GO:0004601	peroxidase activity	-	-	-	↑
44	GO:0005509	calcium ion binding	↓	-	-	↑
45	GO:0008017	microtubule binding	-	↑	↓	↓
46	GO:0008061	chitin binding	-	↑	↓	-
47	GO:0004722	protein serine/threonine phosphatase activity	↓	-	-	-
48	GO:0052716	hydroquinone:oxygen oxidoreductase activity	-	↓	-	↑
49	GO:0008308	voltage-gated anion channel activity	↑	-	-	-
50	GO:0003755	peptidyl-prolyl cis-trans isomerase activity	↑	↓	-	-
51	GO:0030145	manganese ion binding	-	-	↑	↑
52	GO:0030570	pectate lyase activity	↑	-	-	↓
53	GO:0005200	structural constituent of cytoskeleton	↑	↑	↓	-
54	GO:0008810	cellulase activity	-	-	-	↓
55	GO:0003777	microtubule motor activity	-	↑	↓	↓
56	GO:0004386	helicase activity	↑	↓	-	-
57	GO:0004721	phosphoprotein phosphatase activity	↓	-	-	-
58	GO:0043169	cation binding	↓	-	-	-
59	GO:0004568	chitinase activity	-	-	-	↓
60	GO:0031072	heat shock protein binding	↓	-	-	-
61	GO:0010333	terpene synthase activity	-	-	-	↑
62	GO:0051082	unfolded protein binding	↓	-	-	-
63	GO:0003774	motor activity	-	↑	↓	↓
64	GO:0003678	DNA helicase activity	-	↓	-	↓
65	GO:0016168	chlorophyll binding	↓	-	-	-
66	GO:0004866	endopeptidase inhibitor activity	-	-	-	↓
67	GO:0008970	phosphatidylcholine 1-acylhydrolase activity	-	-	-	↑

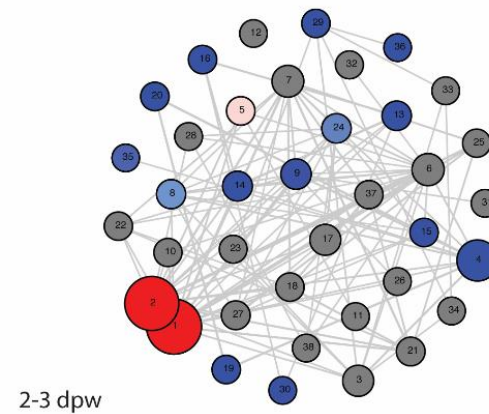
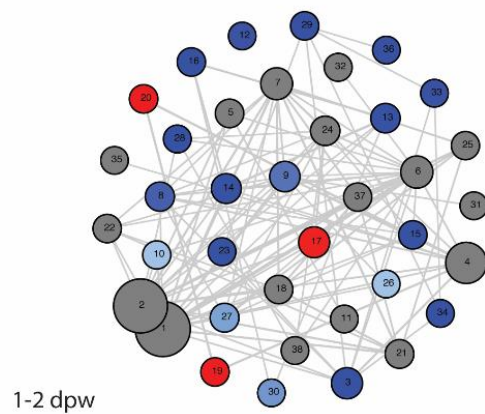
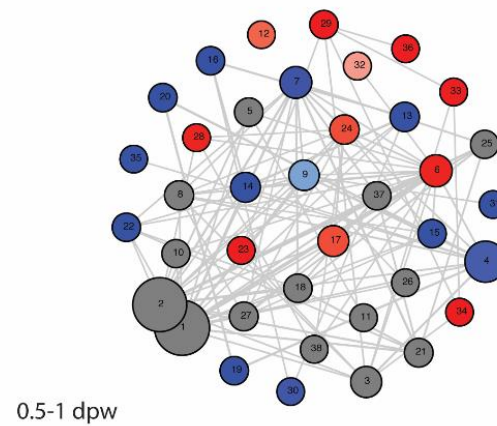
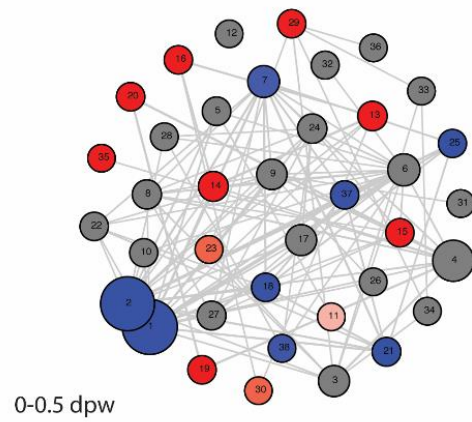
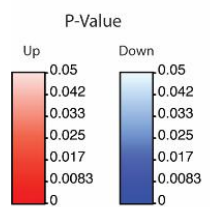


Figure C2. Gene set enrichment analysis (GSEA) of cellular components across differentially expressed genes (DEGs) identified in sequential wound-healing time point comparisons. Together, time point comparison panels represent a union parametric analysis of gene set enrichment (PAGE) of cellular component (CC) categorized gene ontology (GO) terms. Nodes represent gene sets and size represent ranges from 5-1220 genes, and edges show overlapping genes between sets, with width representing ranges from 5-1150 genes. Blue sets are down-regulated, red are up-regulated, and grey node denote terms that were not detected as significantly differentially regulated (i.e. enriched) at that time point comparison. Labels denote assigned node numbers that correspond to Table C3 with associated GO ID, GO term and regulation overview.

Table C3. Summary of gene ontology information represented in cellular component gene set enrichment analysis plot and change in terms over time.

Node	GO ID	GO Term	Time point comparison (days post-wounding)			
			0-0.5	0.5-1	1-2	2-3
1	GO:0016020	membrane	↓	-	-	↑
2	GO:0016021	integral component of membrane	↓	-	-	↑
3	GO:0005737	cytoplasm	-	-	↓	-
4	GO:0005634	nucleus	-	↓	-	↓
5	GO:0005794	Golgi apparatus	-	-	-	↑
6	GO:0005886	plasma membrane	-	↑	-	-
7	GO:0009507	chloroplast	↓	↓	-	-
8	GO:0005829	cytosol	-	-	↓	↓
9	GO:0005739	mitochondrion	-	↓	↓	↓
10	GO:0005773	vacuole	-	-	↓	-
11	GO:0005802	trans-Golgi network	↑	-	-	-
12	GO:0009504	cell plate	-	↑	↓	-
13	GO:0005840	ribosome	↑	↓	↓	↓
14	GO:0005622	intracellular	↑	↓	↓	↓
15	GO:0005730	nucleolus	↑	↓	↓	↓
16	GO:0030529	intracellular ribonucleoprotein complex	↑	↓	↓	↓
17	GO:0005576	extracellular region	-	↑	↑	-
18	GO:0009579	thylakoid	↓	-	-	-
19	GO:0000786	nucleosome	↑	↓	↑	↓
20	GO:0005694	chromosome	↑	↓	↑	↓
21	GO:0009535	chloroplast thylakoid membrane	↓	-	-	-
22	GO:0009941	chloroplast envelope	-	↓	-	-
23	GO:0005856	cytoskeleton	↑	↑	↓	-
24	GO:0005618	cell wall	-	↑	-	↓
25	GO:0009523	photosystem II	↓	-	-	-
26	GO:0005743	mitochondrial inner membrane	-	-	↓	-
27	GO:0009506	plasmodesma	-	-	↓	-
28	GO:0009524	phragmoplast	-	↑	↓	-
29	GO:0005874	microtubule	↑	↑	↓	↓
30	GO:0015935	small ribosomal subunit	↑	↓	↓	↓
31	GO:0005759	mitochondrial matrix	-	↓	-	-
32	GO:0031225	anchored component of membrane	-	↑	-	-
33	GO:0005871	kinesin complex	-	↑	↓	-
34	GO:0045298	tubulin complex	-	↑	↓	-
35	GO:0042555	MCM complex	↑	↓	-	↓
36	GO:0005819	spindle	-	↑	↓	↓
37	GO:0009522	photosystem I	↓	-	-	-
38	GO:0005884	actin filament	↓	-	-	-

Starch/Sucrose Degradation

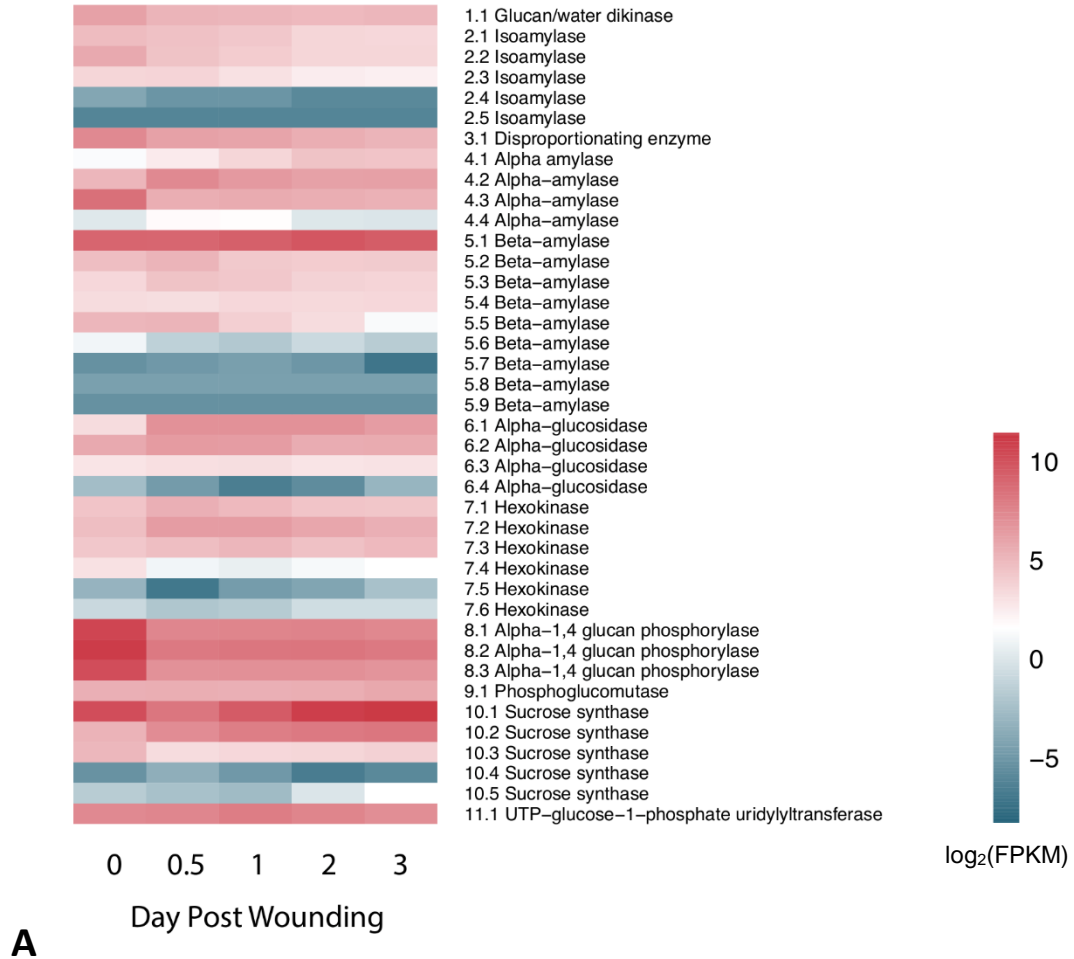
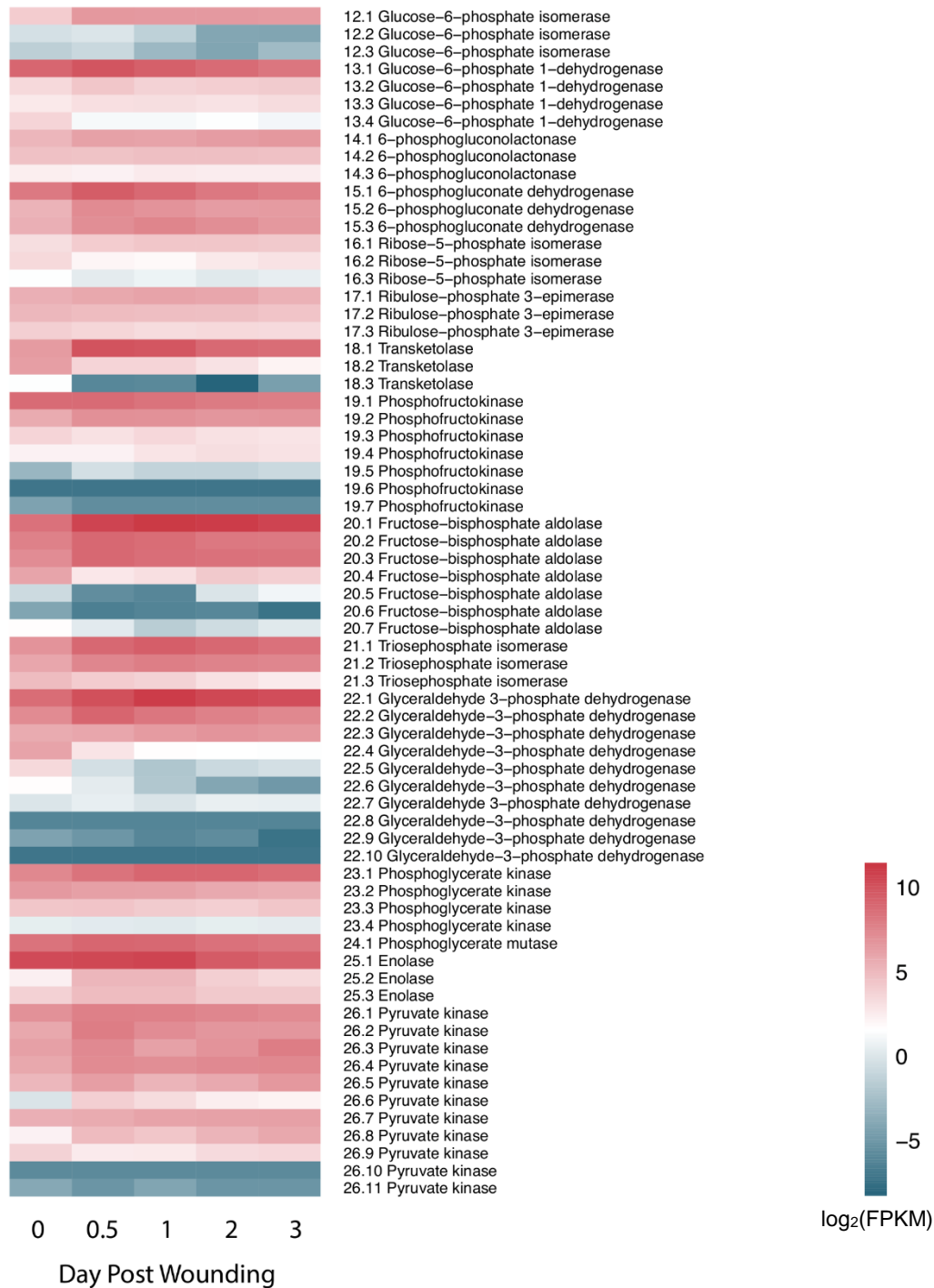
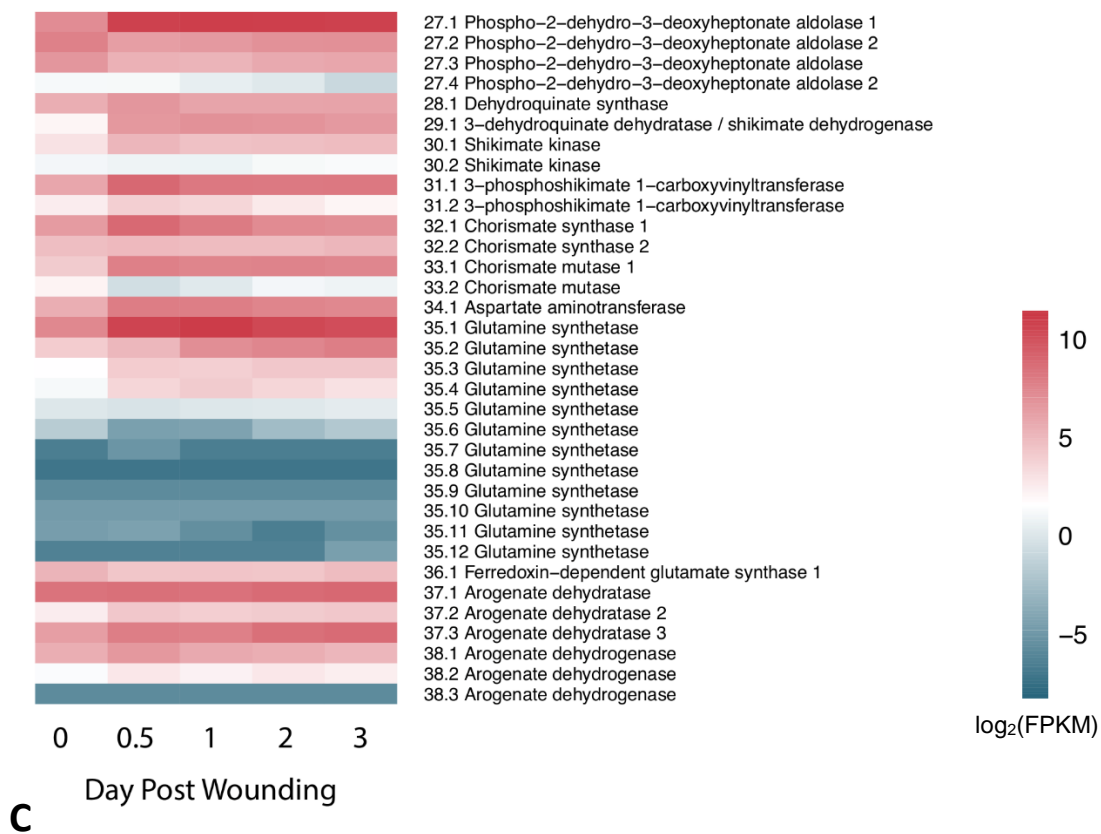


Figure C3. Transcriptional changes of known and putative genes encoding enzymes for suberin production over the wound-healing time course. **A.** Starch and sucrose degradation. **B.** Carbohydrate metabolism. **C.** Shikimate pathway. **D.** Phenylpropanoid pathway and SPPD assembly. **E.** Tricarboxylic acid cycle. **F.** Fatty acid biosynthesis. **G.** Aliphatic metabolism and SPAD assembly. Mean \log_2 FPKM values of $n=3$ biological replicates are presented for each time point. This extensive list of genes was used to screen candidates for further targeted analysis (**Figure 3.3**). A maximum of three genes demonstrating the highest expression levels and/or wound-induction profiles were selected, where possible. Numbers correspond to pathway steps and further gene information that is available in **Table C4**.

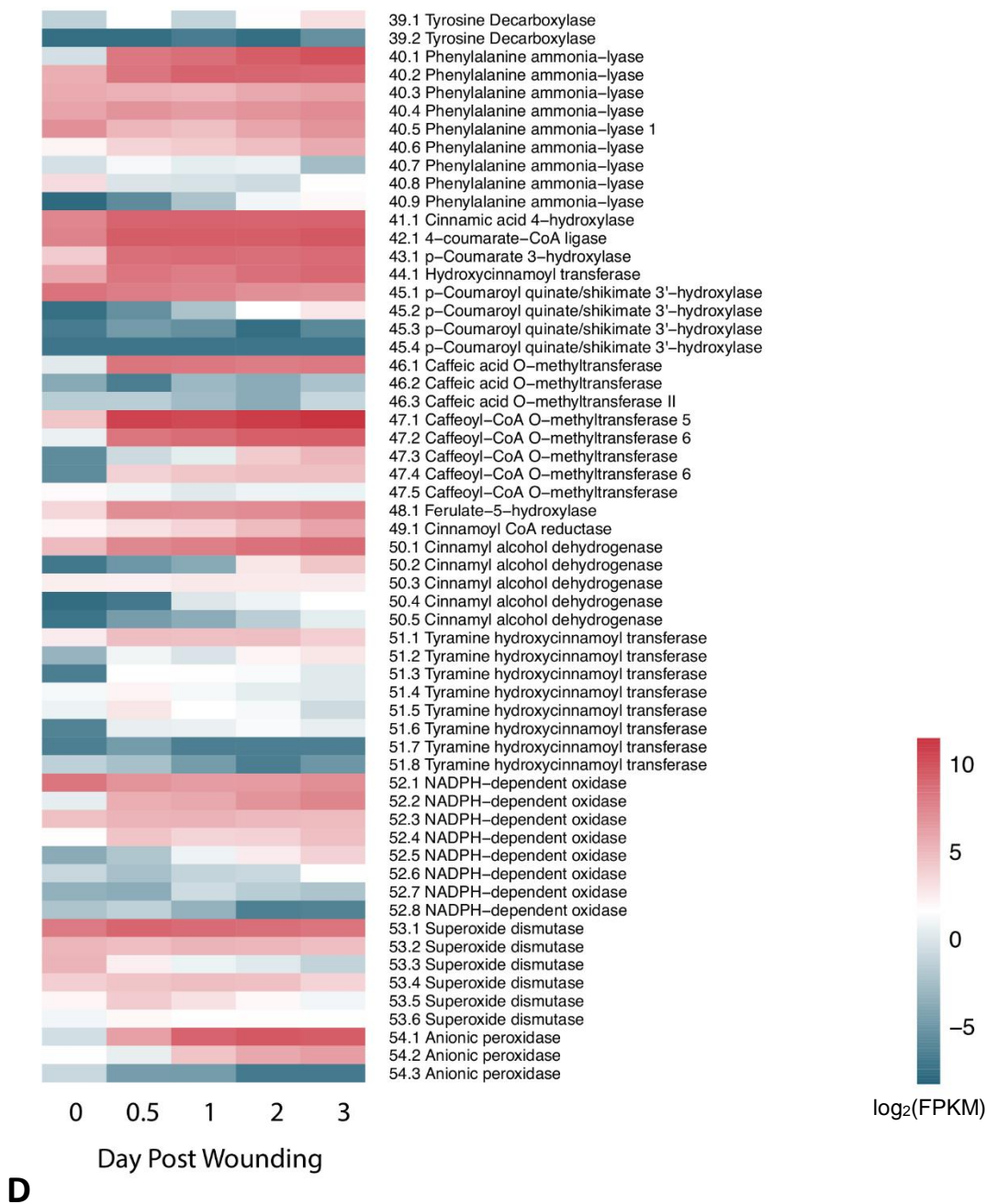
Carbohydrate Metabolism



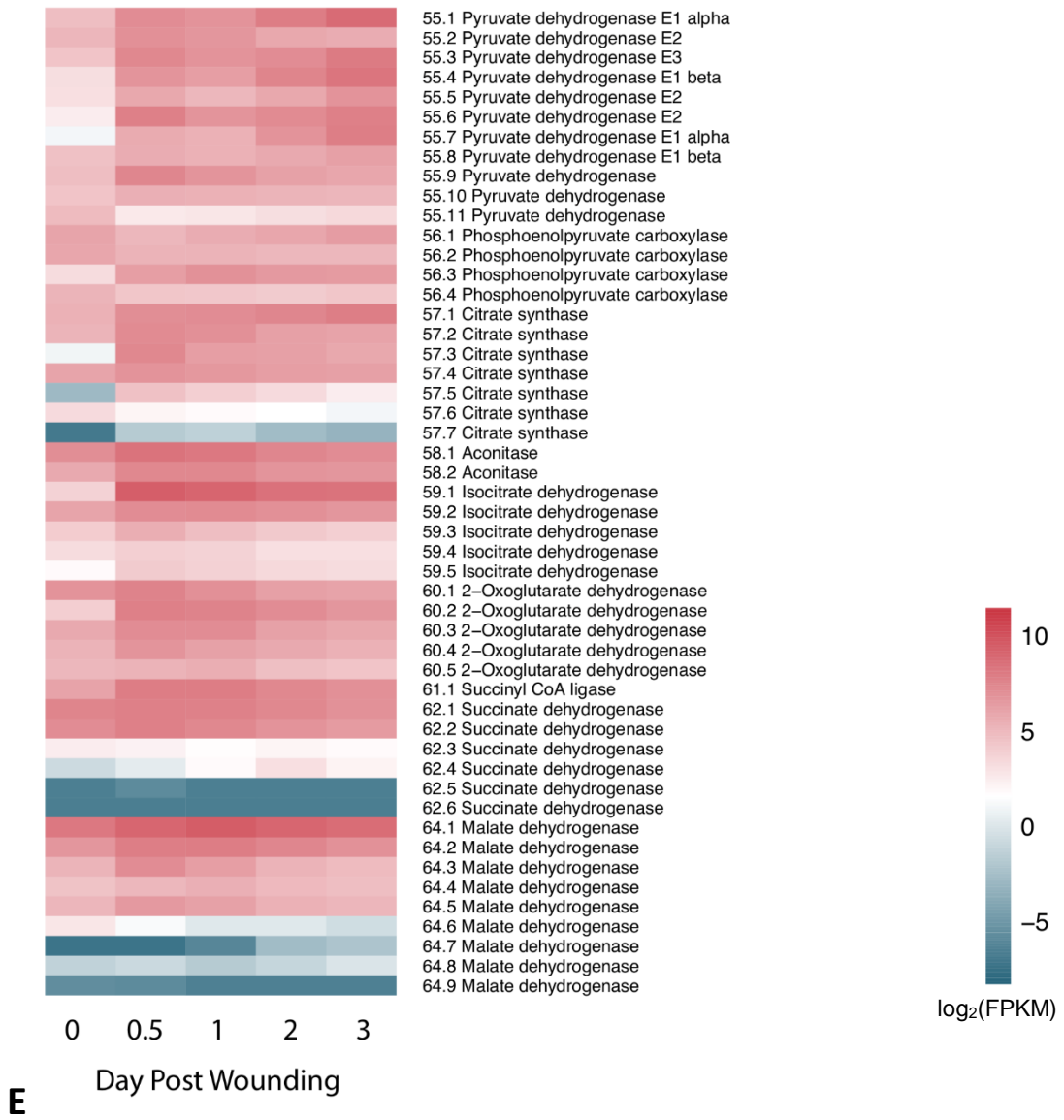
Shikimate Pathway



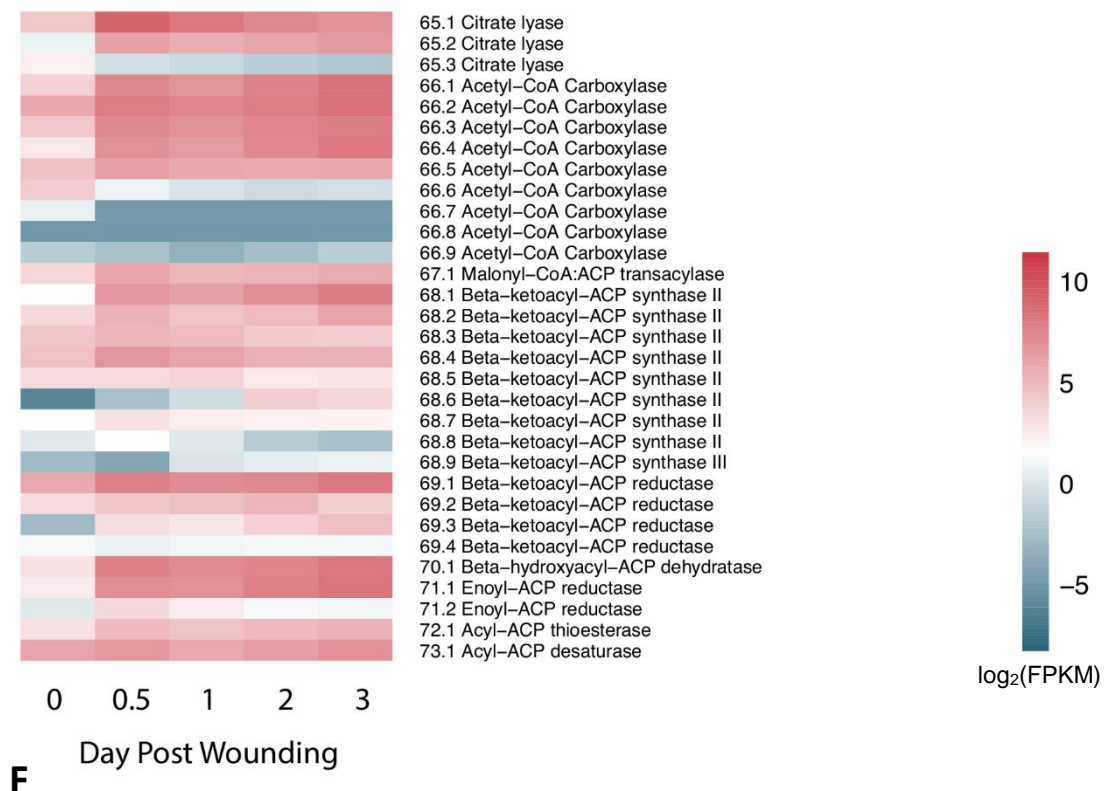
Phenylpropanoid Metabolism & Phenolic Suberin Assembly



Tricarboxylic Acid Cycle

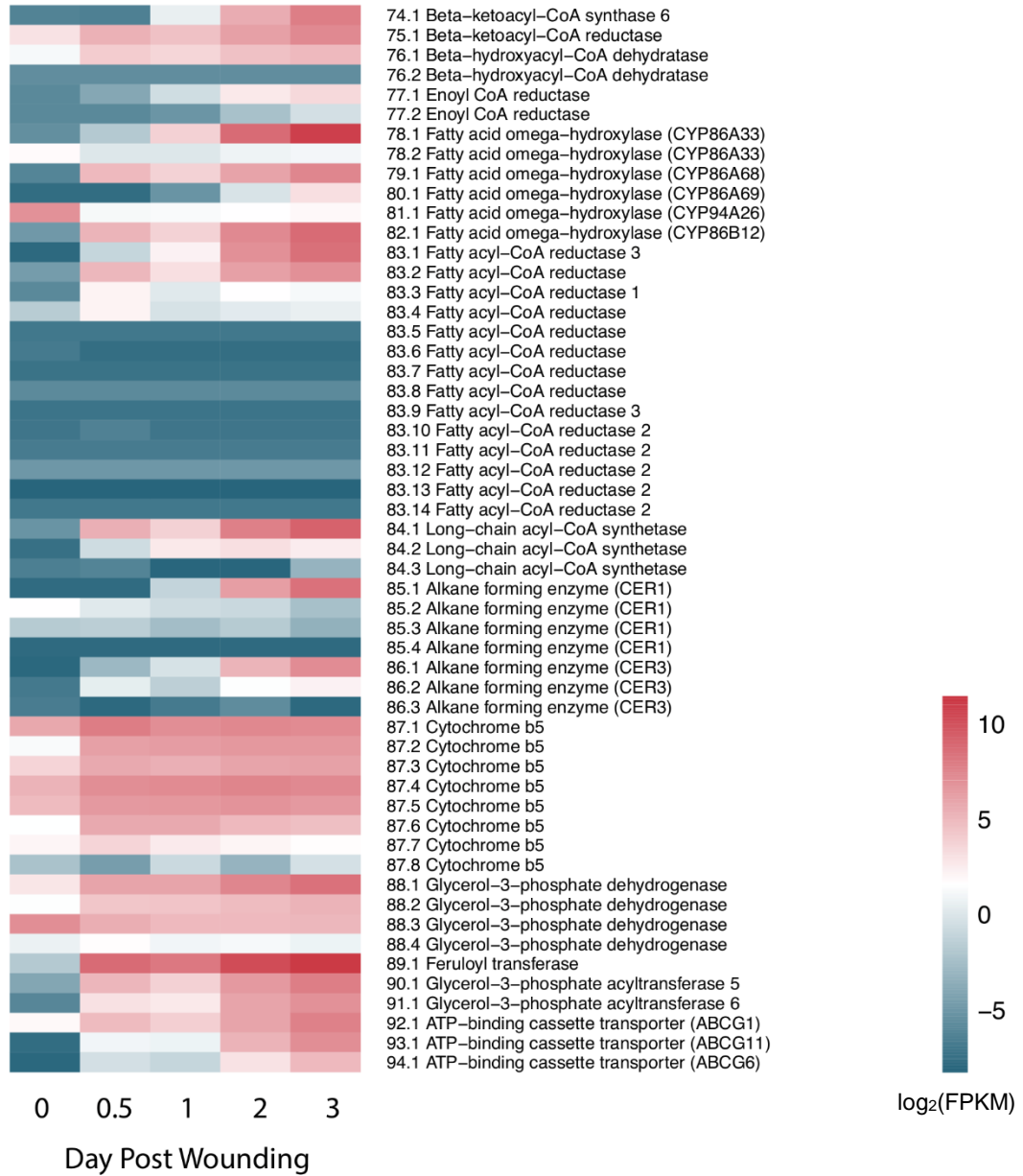


Fatty Acid Biosynthesis



F

Aliphatic Metabolism & Aliphatic Assembly



G

Table C4. Suberin-related biosynthetic and assembly gene and encoded enzyme list. Numbers, PGSC gene IDs and annotated functional names are associated with **Figure 3.3** and **Figure C3**. Bolded numbers correspond to up to three selected gene IDs per functional name used to generate heatmaps for main pathway branch figures (**Figure 3.3A-I**). Known or predicted functional names were used for consistency and simplicity relative to given PGSC annotations. *Note: fumarase (step 63) is included as a step in the pathway, but its sequence did not have a corresponding PGSC gene ID.

Group Name	Number	Known or predicted enzyme functional name	PGSC gene ID	PGSC annotated functional name
Starch and sucrose degradation				
	1.1	Glucan/water dikinase	PGSC0003DMG400016613	Glucan/water dikinase
	2.1	Isoamylase	PGSC0003DMG400000954	Isoamylase isoform 2
	2.2	Isoamylase	PGSC0003DMG402007274	Isoamylase isoform 3
	2.3	Isoamylase	PGSC0003DMG400020699	Isoamylase isoform 1
	2.4	Isoamylase	PGSC0003DMG400030253	Isoamylase isoform 1
	2.5	Isoamylase	PGSC0003DMG401007274	Isoamylase isoform 3
	3.1	Disproportionating enzyme	PGSC0003DMG400016589	Glucosyl transferase (4-alpha-glucanotransferase)
	4.1	Alpha amylase	PGSC0003DMG400020603	Alpha amylase
	4.2	Alpha-amylase	PGSC0003DMG401017626	Alpha-amylase
	4.3	Alpha-amylase	PGSC0003DMG400009891	Alpha-amylase
	4.4	Alpha-amylase	PGSC0003DMG400007974	Alpha-amylase
	5.1	Beta-amylase	PGSC0003DMG400001549	Beta-amylase
	5.2	Beta-amylase	PGSC0003DMG400000169	Beta-amylase
	5.3	Beta-amylase	PGSC0003DMG400012129	Beta-amylase PCT-BMYI
	5.4	Beta-amylase	PGSC0003DMG400024145	Beta-amylase
	5.5	Beta-amylase	PGSC0003DMG400001855	Beta-amylase PCT-BMYI
	5.6	Beta-amylase	PGSC0003DMG402020509	Beta-amylase PCT-BMYI
	5.7	Beta-amylase	PGSC0003DMG400026199	Beta-amylase

5.8	Beta-amylase	PGSC0003DMG400026198	Beta-amylase
5.9	Beta-amylase	PGSC0003DMG400026166	Beta-amylase
6.1	Alpha-glucosidase	PGSC0003DMG400014540	Alpha-glucosidase
6.2	Alpha-glucosidase	PGSC0003DMG400005353	Alpha-glucosidase
6.3	Alpha-glucosidase	PGSC0003DMG400016018	Alpha-glucosidase
6.4	Alpha-glucosidase	PGSC0003DMG400015881	Alpha-glucosidase
7.1	Hexokinase	PGSC0003DMG400016521	Hexokinase
7.2	Hexokinase	PGSC0003DMG400002525	Hexokinase 7
7.3	Hexokinase	PGSC0003DMG400009861	Plastidic hexokinase
7.4	Hexokinase	PGSC0003DMG400013187	Hexokinase 6
7.5	Hexokinase	PGSC0003DMG400030624	Hexokinase
7.6	Hexokinase	PGSC0003DMG400000295	Hexokinase 5
8.1	Alpha-1,4 glucan phosphorylase	PGSC0003DMG400007782	Alpha-1,4 glucan phosphorylase L-1 isozyme, chloroplastic/amyloplastic
8.2	Alpha-1,4 glucan phosphorylase	PGSC0003DMG400002479	Alpha-1,4 glucan phosphorylase L-1 isozyme, chloroplastic/amyloplastic
8.3	Alpha-1,4 glucan phosphorylase	PGSC0003DMG400003495	Alpha-1,4 glucan phosphorylase L-1 isozyme, chloroplastic/amyloplastic
9.1	Phosphoglucomutase	PGSC0003DMG400001912	Phosphoglucomutase
10.1	Sucrose synthase	PGSC0003DMG400002895	Sucrose synthase
10.2	Sucrose synthase	PGSC0003DMG400013546	Sucrose synthase 2
10.3	Sucrose synthase	PGSC0003DMG400006672	Sucrose synthase
10.4	Sucrose synthase	PGSC0003DMG400031046	Sucrose synthase
10.5	Sucrose synthase	PGSC0003DMG400016730	Sucrose synthase
11.1	UTP-glucose-1-phosphate uridylyltransferase	PGSC0003DMG401013333	UTP-glucose-1-phosphate uridylyltransferase
Carbohydrate Metabolism			
12.1	Glucose-6-phosphate	PGSC0003DMG400012910	Glucose-6-phosphate isomerase

	isomerase		
12.2	Glucose-6-phosphate isomerase	PGSC0003DMG400030128	Glucose-6-phosphate isomerase
12.3	Glucose-6-phosphate isomerase	PGSC0003DMG400009848	Glucose-6-phosphate isomerase
13.1	Glucose-6-phosphate 1-dehydrogenase	PGSC0003DMG400020269	Glucose-6-phosphate 1-dehydrogenase, cytoplasmic isoform
13.2	Glucose-6-phosphate 1-dehydrogenase	PGSC0003DMG400010802	Glucose-6-phosphate 1-dehydrogenase
13.3	Glucose-6-phosphate 1-dehydrogenase	PGSC0003DMG400002750	Glucose-6-phosphate 1-dehydrogenase
13.4	Glucose-6-phosphate 1-dehydrogenase	PGSC0003DMG400017394	Glucose-6-phosphate 1-dehydrogenase, chloroplastic
14.1	6-phosphogluconolactonase	PGSC0003DMG400018511	6-phosphogluconolactonase
14.2	6-phosphogluconolactonase	PGSC0003DMG402026150	6-phosphogluconolactonase
14.3	6-phosphogluconolactonase	PGSC0003DMG401026150	6-phosphogluconolactonase
15.1	6-phosphogluconate dehydrogenase	PGSC0003DMG400001932	6-phosphogluconate dehydrogenase, decarboxylating
15.2	6-phosphogluconate dehydrogenase	PGSC0003DMG400043373	6-phosphogluconate dehydrogenase, decarboxylating
15.3	6-phosphogluconate dehydrogenase	PGSC0003DMG400025121	6-phosphogluconate dehydrogenase, decarboxylating
16.1	Ribose-5-phosphate isomerase	PGSC0003DMG400019448	Ribose-5-phosphate isomerase
16.2	Ribose-5-phosphate isomerase	PGSC0003DMG400030509	Ribose-5-phosphate isomerase
16.3	Ribose-5-phosphate isomerase	PGSC0003DMG400005961	Ribose-5-phosphate isomerase
17.1	Ribulose-phosphate 3-epimerase	PGSC0003DMG400023059	Ribulose-phosphate 3-epimerase, cytoplasmic isoform

17.2	Ribulose-phosphate 3-epimerase	PGSC0003DMG400019521	Ribulose-phosphate 3-epimerase, chloroplastic
17.3	Ribulose-phosphate 3-epimerase	PGSC0003DMG400023318	Conserved gene of unknown function
18.1	Transketolase	PGSC0003DMG400007019	Transketolase 1
18.2	Transketolase	PGSC0003DMG400022088	Transketolase, chloroplastic
18.3	Transketolase	PGSC0003DMG400014756	Transketolase
19.1	Phosphofructokinase	PGSC0003DMG400016726	Pyrophosphate--fructose 6-phosphate 1-phosphotransferase subunit beta
19.2	Phosphofructokinase	PGSC0003DMG400010007	Pyrophosphate--fructose 6-phosphate 1-phosphotransferase subunit alpha
19.3	Phosphofructokinase	PGSC0003DMG400025455	Phosphofructokinase
19.4	Phosphofructokinase	PGSC0003DMG400017413	Phosphofructokinase
19.5	Phosphofructokinase	PGSC0003DMG400019734	Phosphofructokinase
19.6	Phosphofructokinase	PGSC0003DMG400027554	Phosphofructokinase
19.7	Phosphofructokinase	PGSC0003DMG400045386	Phosphofructokinase
20.1	Fructose-bisphosphate aldolase	PGSC0003DMG400002675	Fructose-bisphosphate aldolase
20.2	Fructose-bisphosphate aldolase	PGSC0003DMG400030565	Fructose-bisphosphate aldolase
20.3	Fructose-bisphosphate aldolase	PGSC0003DMG400028261	Fructose-bisphosphate aldolase
20.4	Fructose-bisphosphate aldolase	PGSC0003DMG400003548	Fructose-bisphosphate aldolase
20.5	Fructose-bisphosphate aldolase	PGSC0003DMG400012012	Fructose-bisphosphate aldolase
20.6	Fructose-bisphosphate aldolase	PGSC0003DMG400022263	Fructose-bisphosphate aldolase
20.7	Fructose-bisphosphate aldolase	PGSC0003DMG400003123	Fructose-bisphosphate aldolase

21.1	Triosephosphate isomerase	PGSC0003DMG400027745	Triosephosphate isomerase
21.2	Triosephosphate isomerase	PGSC0003DMG400001595	Triosephosphate isomerase, chloroplastic
21.3	Triosephosphate isomerase	PGSC0003DMG400004436	Triosephosphate isomerase, chloroplastic
22.1	Glyceraldehyde 3-phosphate dehydrogenase	PGSC0003DMG400017433	Glyceraldehyde 3-phosphate dehydrogenase
22.2	Glyceraldehyde-3-phosphate dehydrogenase	PGSC0003DMG400011246	Glyceraldehyde-3-phosphate dehydrogenase
22.3	Glyceraldehyde-3-phosphate dehydrogenase	PGSC0003DMG400015253	Glyceraldehyde-3-phosphate dehydrogenase
22.4	Glyceraldehyde-3-phosphate dehydrogenase	PGSC0003DMG400011132	NADP-dependent glyceraldehyde-3-phosphate dehydrogenase
22.5	Glyceraldehyde-3-phosphate dehydrogenase	PGSC0003DMG400009992	Glyceraldehyde-3-phosphate dehydrogenase B subunit
22.6	Glyceraldehyde-3-phosphate dehydrogenase	PGSC0003DMG400011530	Glyceraldehyde-3-phosphate dehydrogenase A, chloroplastic
22.7	Glyceraldehyde 3-phosphate dehydrogenase	PGSC0003DMG400017434	Glyceraldehyde 3-phosphate dehydrogenase
22.8	Glyceraldehyde-3-phosphate dehydrogenase	PGSC0003DMG400036713	Glyceraldehyde-3-phosphate dehydrogenase
22.9	Glyceraldehyde-3-phosphate dehydrogenase	PGSC0003DMG400029406	Glyceraldehyde-3-phosphate dehydrogenase B subunit
22.10	Glyceraldehyde-3-phosphate dehydrogenase	PGSC0003DMG400004130	Glyceraldehyde-3-phosphate dehydrogenase C subunit
23.1	Phosphoglycerate kinase	PGSC0003DMG400022119	Phosphoglycerate kinase
23.2	Phosphoglycerate kinase	PGSC0003DMG400022118	Phosphoglycerate kinase
23.3	Phosphoglycerate kinase	PGSC0003DMG400001147	Conserved gene of unknown function
23.4	Phosphoglycerate kinase	PGSC0003DMG400003882	Phosphoglycerate kinase
24.1	Phosphoglycerate mutase	PGSC0003DMG400000935	Phosphoglycerate mutase
25.1	Enolase	PGSC0003DMG402002721	Enolase

25.2	Enolase	PGSC0003DMG400011044	Enolase
25.3	Enolase	PGSC0003DMG400030344	Enolase
26.1	Pyruvate kinase	PGSC0003DMG400025298	Pyruvate kinase, cytosolic isozyme
26.2	Pyruvate kinase	PGSC0003DMG400028177	Pyruvate kinase
26.3	Pyruvate kinase	PGSC0003DMG400006590	Pyruvate kinase
26.4	Pyruvate kinase	PGSC0003DMG400010913	Pyruvate kinase, cytosolic isozyme
26.5	Pyruvate kinase	PGSC0003DMG400024220	Pyruvate kinase isozyme G, chloroplastic
26.6	Pyruvate kinase	PGSC0003DMG400002690	Pyruvate kinase
26.7	Pyruvate kinase	PGSC0003DMG400027321	Pyruvate kinase
26.8	Pyruvate kinase	PGSC0003DMG400025734	Pyruvate kinase
26.9	Pyruvate kinase	PGSC0003DMG400019605	Pyruvate kinase family protein
26.10	Pyruvate kinase	PGSC0003DMG400027347	Pyruvate kinase
26.11	Pyruvate kinase	PGSC0003DMG400027346	Pyruvate kinase

Shikimate Pathway

27.1	Phospho-2-dehydro-3-deoxyheptonate aldolase 1	PGSC0003DMG400030812	Phospho-2-dehydro-3-deoxyheptonate aldolase 1, chloroplastic
27.2	Phospho-2-dehydro-3-deoxyheptonate aldolase 2	PGSC0003DMG402016226	Phospho-2-dehydro-3-deoxyheptonate aldolase 2, chloroplastic
27.3	Phospho-2-dehydro-3-deoxyheptonate aldolase	PGSC0003DMG400012549	2-dehydro-3-deoxyphosphoheptonate aldolase/ 3-deoxy-d-arabino-heptulosonate 7-phosphate synthetase
27.4	Phospho-2-dehydro-3-deoxyheptonate aldolase 2	PGSC0003DMG401016226	Phospho-2-dehydro-3-deoxyheptonate aldolase 2, chloroplastic
28.1	Dehydroquinate synthase	PGSC0003DMG400003582	Dehydroquinate synthase
29.1	3-dehydroquinate dehydratase / shikimate dehydrogenase	PGSC0003DMG400005284	3-dehydroquinate dehydratase / shikimate dehydrogenase isoform 2
30.1	Shikimate kinase	PGSC0003DMG400016553	Shikimate kinase, chloroplastic
30.2	Shikimate kinase	PGSC0003DMG401020240	Shikimate kinase

31.1	3-phosphoshikimate 1-carboxyvinyltransferase	PGSC0003DMG400026006	3-phosphoshikimate 1-carboxyvinyltransferase, chloroplastic
31.2	3-phosphoshikimate 1-carboxyvinyltransferase	PGSC0003DMG400007018	3-phosphoshikimate 1-carboxyvinyltransferase, chloroplastic
32.1	Chorismate synthase 1	PGSC0003DMG400024392	Chorismate synthase 1, chloroplastic
32.2	Chorismate synthase 2	PGSC0003DMG400016016	Chorismate synthase 2, chloroplastic
33.1	Chorismate mutase 1	PGSC0003DMG400001438	Chorismate mutase 1
33.2	Chorismate mutase	PGSC0003DMG400009237	Chorimate mutase
34.1	Aspartate aminotransferase	PGSC0003DMG400027919	Aspartate aminotransferase
35.1	Glutamine synthetase	PGSC0003DMG400013235	Glutamine synthetase
35.2	Glutamine synthetase	PGSC0003DMG400023620	Glutamine synthetase
35.3	Glutamine synthetase	PGSC0003DMG400028276	Glutamate-ammonia ligase
35.4	Glutamine synthetase	PGSC0003DMG400014592	Glutamine synthetase
35.5	Glutamine synthetase	PGSC0003DMG400004355	Glutamine synthetase
35.6	Glutamine synthetase	PGSC0003DMG400033059	Glutamine-dependent NAD(+) synthetase
35.7	Glutamine synthetase	PGSC0003DMG403009595	Glutamate-ammonia ligase
35.8	Glutamine synthetase	PGSC0003DMG400028171	Glutamate-ammonia ligase
35.9	Glutamine synthetase	PGSC0003DMG401019012	Glutamate-ammonia ligase
35.10	Glutamine synthetase	PGSC0003DMG400014115	Glutamine synthetase
35.11	Glutamine synthetase	PGSC0003DMG400014454	Glutamine synthetase
35.12	Glutamine synthetase	PGSC0003DMG400017703	Glutamine synthetase
36.1	Ferredoxin-dependent glutamate synthase 1	PGSC0003DMG400009698	Ferredoxin-dependent glutamate synthase 1
37.1	Arogenate dehydratase	PGSC0003DMG400007122	Arogenate dehydratase
37.2	Arogenate dehydratase 2	PGSC0003DMG400025374	Arogenate dehydratase 2
37.3	Arogenate dehydratase 3	PGSC0003DMG400026536	Arogenate dehydratase 3
38.1	Arogenate dehydrogenase	PGSC0003DMG400030683	Arogenate dehydrogenase
38.2	Arogenate dehydrogenase	PGSC0003DMG400020334	Prephenate dehydrogenase

	38.3	Arogenate dehydrogenase	PGSC0003DMG400042196	Prephenate dehydrogenase
Phenylpropanoid Metabolism				
	39.1	Tyrosine Decarboxylase	PGSC0003DMG400024278	Phenylacetaldehyde synthase
	39.2	Tyrosine Decarboxylase	PGSC0003DMG400014863	Phenylacetaldehyde synthase
	40.1	Phenylalanine ammonia-lyase	PGSC0003DMG400023458	Phenylalanine ammonia-lyase
	40.2	Phenylalanine ammonia-lyase	PGSC0003DMG400031365	Phenylalanine ammonia-lyase
	40.3	Phenylalanine ammonia-lyase	PGSC0003DMG402021564	Phenylalanine ammonia-lyase
	40.4	Phenylalanine ammonia-lyase	PGSC0003DMG401021549	Phenylalanine ammonia-lyase
	40.5	Phenylalanine ammonia-lyase 1	PGSC0003DMG400031457	Phenylalanine ammonia-lyase 1
	40.6	Phenylalanine ammonia-lyase	PGSC0003DMG402021549	Phenylalanine ammonia-lyase
	40.7	Phenylalanine ammonia-lyase	PGSC0003DMG401021564	Phenylalanine ammonia-lyase
	40.8	Phenylalanine ammonia-lyase	PGSC0003DMG400019386	Phenylalanine ammonia-lyase
	40.9	Phenylalanine ammonia-lyase	PGSC0003DMG400005492	Phenylalanine ammonia-lyase
	41.1	Cinnamic acid 4-hydroxylase	PGSC0003DMG401030469	Cinnamic acid 4-hydroxylase
	42.1	4-coumarate-CoA ligase	PGSC0003DMG400014223	4-coumarate-CoA ligase 2
	43.1	p-Coumarate 3-hydroxylase	PGSC0003DMG400003289	P-coumarate 3-hydroxylase
	44.1	Hydroxycinnamoyl transferase	PGSC0003DMG400014152	Hydroxycinnamoyl transferase
	45.1	p-Coumaroyl quinate/shikimate 3'-hydroxylase	PGSC0003DMG400007178	P-coumaroyl quinate/shikimate 3'-hydroxylase

45.2	p-Coumaroyl quinate/shikimate 3'-hydroxylase	PGSC0003DMG401014734	P-coumaroyl quinate/shikimate 3'-hydroxylase
45.3	p-Coumaroyl quinate/shikimate 3'-hydroxylase	PGSC0003DMG400007180	P-coumaroyl quinate/shikimate 3'-hydroxylase
45.4	p-Coumaroyl quinate/shikimate 3'-hydroxylase	PGSC0003DMG400029243	P-coumaroyl quinate/shikimate 3'-hydroxylase
46.1	Caffeic acid O-methyltransferase	PGSC0003DMG400000560	Catechol O-methyltransferase
46.2	Caffeic acid O-methyltransferase	PGSC0003DMG400007863	Caffeic acid 3-O-methyltransferase
46.3	Caffeic acid O-methyltransferase II	PGSC0003DMG400017552	Caffeic acid O-methyltransferase II
47.1	Caffeoyl-CoA O-methyltransferase 5	PGSC0003DMG400006214	Caffeoyl-CoA O-methyltransferase 5
47.2	Caffeoyl-CoA O-methyltransferase 6	PGSC0003DMG400025882	Caffeoyl-CoA O-methyltransferase 6
47.3	Caffeoyl-CoA O-methyltransferase	PGSC0003DMG400018688	O-methyltransferase
47.4	Caffeoyl-CoA O-methyltransferase 6	PGSC0003DMG400030131	Caffeoyl-CoA O-methyltransferase 6
47.5	Caffeoyl-CoA O-methyltransferase	PGSC0003DMG401026272	O-methyltransferase family 3 protein
48.1	Ferulate-5-hydroxylase	PGSC0003DMG400003546	Ferulate-5-hydroxylase
49.1	Cinnamoyl CoA reductase	PGSC0003DMG400019825	Cinnamoyl CoA reductase
50.1	Cinnamyl alcohol dehydrogenase	PGSC0003DMG401025767	Cinnamyl alcohol dehydrogenase
50.2	Cinnamyl alcohol	PGSC0003DMG400012919	Cinnamyl alcohol dehydrogenase

	dehydrogenase			
50.3	Cinnamyl alcohol dehydrogenase	PGSC0003DMG400005001	Alcohol dehydrogenase	
50.4	Cinnamyl alcohol dehydrogenase	PGSC0003DMG400010305	Cinnamyl alcohol dehydrogenase	
50.5	Cinnamyl alcohol dehydrogenase	PGSC0003DMG400018446	Cinnamyl alcohol dehydrogenase	
51.1	Tyramine hydroxycinnamoyl transferase	PGSC0003DMG400014778	Tyramine hydroxycinnamoyl transferase	
51.2	Tyramine hydroxycinnamoyl transferase	PGSC0003DMG400014770	N-hydroxycinnamoyl-CoA:tyramine N-hydroxycinnamoyl transferase THT7-8	
51.3	Tyramine hydroxycinnamoyl transferase	PGSC0003DMG400014772	Tyramine hydroxycinnamoyl transferase	
51.4	Tyramine hydroxycinnamoyl transferase	PGSC0003DMG400014774	N-hydroxycinnamoyl-CoA:tyramine N-hydroxycinnamoyl transferase THT7-1	
51.5	Tyramine hydroxycinnamoyl transferase	PGSC0003DMG400014776	Tyramine hydroxycinnamoyl transferase	
51.6	Tyramine hydroxycinnamoyl transferase	PGSC0003DMG400014777	Tyramine hydroxycinnamoyl transferase	
51.7	Tyramine hydroxycinnamoyl transferase	PGSC0003DMG400037933	N-hydroxycinnamoyl-CoA:tyramine N-hydroxycinnamoyl transferase THT1-3	
51.8	Tyramine hydroxycinnamoyl transferase	PGSC0003DMG400014771	Tyramine hydroxycinnamoyl transferase	
Phenolic Suberin Assembly				
52.1	NADPH-dependent oxidase	PGSC0003DMG400014168	Respiratory burst oxidase homolog protein C	
52.2	NADPH-dependent oxidase	PGSC0003DMG400012316	Respiratory burst oxidase homolog protein A	
52.3	NADPH-dependent oxidase	PGSC0003DMG400025890	NADPH oxidoreductase	
52.4	NADPH-dependent oxidase	PGSC0003DMG400024754	Respiratory burst oxidase homolog protein B	
52.5	NADPH-dependent oxidase	PGSC0003DMG400013550	Respiratory burst oxidase	
52.6	NADPH-dependent oxidase	PGSC0003DMG400025701	Respiratory burst oxidase	

	52.7	NADPH-dependent oxidase	PGSC0003DMG400030390	NOX1
	52.8	NADPH-dependent oxidase	PGSC0003DMG400015543	NOX1
	53.1	Superoxide dismutase	PGSC0003DMG400010660	Superoxide dismutase [Cu-Zn] 2
	53.2	Superoxide dismutase	PGSC0003DMG400023086	Superoxide dismutase [Cu-Zn]
	53.3	Superoxide dismutase	PGSC0003DMG400027577	Superoxide dismutase
	53.4	Superoxide dismutase	PGSC0003DMG400000417	Superoxide dismutase [Cu-Zn]
	53.5	Superoxide dismutase	PGSC0003DMG400005247	Superoxide dismutase
	53.6	Superoxide dismutase	PGSC0003DMG400017948	Superoxide dismutase
	54.1	Anionic peroxidase	PGSC0003DMG400022342	Suberization-associated anionic peroxidase
	54.2	Anionic peroxidase	PGSC0003DMG400022341	Suberization-associated anionic peroxidase 2
	54.3	Anionic peroxidase	PGSC0003DMG400030430	Anionic peroxidase swpa7
TCA Cycle				
	55.1	Pyruvate dehydrogenase E1 alpha	PGSC0003DMG402013561	Pyruvate dehydrogenase E1 alpha subunit
	55.2	Pyruvate dehydrogenase E2	PGSC0003DMG400018735	Dihydrolipoamide acetyltransferase component of pyruvate dehydrogenase
	55.3	Pyruvate dehydrogenase E3	PGSC0003DMG400002777	Dihydrolipoyl dehydrogenase
	55.4	Pyruvate dehydrogenase E1 beta	PGSC0003DMG400031370	Pyruvate dehydrogenase E1 beta subunit
	55.5	Pyruvate dehydrogenase E2	PGSC0003DMG400009219	Pyruvate dehydrogenase E2 subunit
	55.6	Pyruvate dehydrogenase E2	PGSC0003DMG400012966	Dihydrolipoyllysine-residue acetyltransferase component of pyruvate dehydrogenase
	55.7	Pyruvate dehydrogenase E1 alpha	PGSC0003DMG400002921	Pyruvate dehydrogenase E1 alpha subunit
	55.8	Pyruvate dehydrogenase E1 beta	PGSC0003DMG400007488	Pyruvate dehydrogenase E1 beta subunit
	55.9	Pyruvate dehydrogenase	PGSC0003DMG401004334	Pyruvate dehydrogenase
	55.10	Pyruvate dehydrogenase	PGSC0003DMG400026943	Pyruvate dehydrogenase
	55.11	Pyruvate dehydrogenase	PGSC0003DMG400025407	Pyruvate dehydrogenase

56.1	Phosphoenolpyruvate carboxylase	PGSC0003DMG400007466	Phosphoenolpyruvate carboxylase
56.2	Phosphoenolpyruvate carboxylase	PGSC0003DMG400020422	Phosphoenolpyruvate carboxylase
56.3	Phosphoenolpyruvate carboxylase	PGSC0003DMG400021264	Phosphoenolpyruvate carboxylase
56.4	Phosphoenolpyruvate carboxylase	PGSC0003DMG400015385	Phosphoenolpyruvate carboxylase
57.1	Citrate synthase	PGSC0003DMG403018293	ATP-citrate synthase
57.2	Citrate synthase	PGSC0003DMG400028982	Citrate synthase (mitochondrial)
57.3	Citrate synthase	PGSC0003DMG400013485	ATP-citrate synthase
57.4	Citrate synthase	PGSC0003DMG400007797	Citrate synthase (peroxisomal)
57.5	Citrate synthase	PGSC0003DMG400025587	ATP-citrate synthase
57.6	Citrate synthase	PGSC0003DMG400017338	Citrate synthase (peroxisomal)
57.7	Citrate synthase	PGSC0003DMG400029179	Gene of unknown function
58.1	Aconitase	PGSC0003DMG400028951	Aconitase
58.2	Aconitase	PGSC0003DMG400008740	Aconitase
59.1	Isocitrate dehydrogenase	PGSC0003DMG400032124	Isocitrate dehydrogenase [NADP]
59.2	Isocitrate dehydrogenase	PGSC0003DMG400016826	NAD-dependent isocitrate dehydrogenase
59.3	Isocitrate dehydrogenase	PGSC0003DMG400000481	Isocitrate dehydrogenase [NADP]
59.4	Isocitrate dehydrogenase	PGSC0003DMG400001525	NAD-dependent isocitrate dehydrogenase
59.5	Isocitrate dehydrogenase	PGSC0003DMG400013332	Isocitrate dehydrogenase [NADP]
60.1	2-Oxoglutarate dehydrogenase	PGSC0003DMG400023519	2-oxoglutarate dehydrogenase
60.2	2-Oxoglutarate dehydrogenase	PGSC0003DMG401010423	2-oxo acid dehydrogenase, lipoyl-binding site
60.3	2-Oxoglutarate dehydrogenase	PGSC0003DMG400022308	Dihydrolipoamide succinyltransferase component of 2-oxoglutarate dehydrogenase
60.4	2-Oxoglutarate	PGSC0003DMG400027873	Dihydrolipoamide succinyltransferase

	dehydrogenase		component of 2-oxoglutarate dehydrogenase
60.5	2-Oxoglutarate dehydrogenase	PGSC0003DMG400027739	2-oxoglutarate dehydrogenase
61.1	Succinyl CoA ligase	PGSC0003DMG400020149	Succinyl CoA ligase beta subunit
62.1	Succinate dehydrogenase	PGSC0003DMG400012624	Mitochondrial succinate dehydrogenase iron sulfur subunit
62.2	Succinate dehydrogenase	PGSC0003DMG400014901	Succinate dehydrogenase
62.3	Succinate dehydrogenase	PGSC0003DMG400024973	Mitochondrial succinate dehydrogenase iron sulfur subunit
62.4	Succinate dehydrogenase	PGSC0003DMG402008334	Succinate dehydrogenase subunit 3
62.5	Succinate dehydrogenase	PGSC0003DMG400036514	Succinate dehydrogenase
62.6	Succinate dehydrogenase	PGSC0003DMG400020612	Succinate dehydrogenase
63.1	Fumarase*		
64.1	Malate dehydrogenase	PGSC0003DMG400017170	Malate dehydrogenase
64.2	Malate dehydrogenase	PGSC0003DMG400012395	Malate dehydrogenase
64.3	Malate dehydrogenase	PGSC0003DMG400019511	NAD-malate dehydrogenase
64.4	Malate dehydrogenase	PGSC0003DMG400010386	Malate dehydrogenase
64.5	Malate dehydrogenase	PGSC0003DMG400015379	Malate dehydrogenase
64.6	Malate dehydrogenase	PGSC0003DMG400031063	Malate dehydrogenase
64.7	Malate dehydrogenase	PGSC0003DMG400026029	Malate dehydrogenase
64.8	Malate dehydrogenase	PGSC0003DMG400011570	NAD-malate dehydrogenase
64.9	Malate dehydrogenase	PGSC0003DMG402025430	NAD-malate dehydrogenase
Fatty Acid Biosynthesis			
65.1	Citrate lyase	PGSC0003DMG400004696	ATP:citrate lyase
65.2	Citrate lyase	PGSC0003DMG400024016	ATP:citrate lyase
65.3	Citrate lyase	PGSC0003DMG400027212	ATP:citrate lyase
66.1	Acetyl-CoA Carboxylase	PGSC0003DMG400016395	Acetyl co-enzyme A carboxylase biotin carboxylase subunit

66.2	Acetyl-CoA Carboxylase	PGSC0003DMG400020325	Acetyl co-enzyme A carboxylase carboxyltransferase alpha subunit
66.3	Acetyl-CoA Carboxylase	PGSC0003DMG400023955	Biotin carboxyl carrier protein of acetyl-CoA carboxylase
66.4	Acetyl-CoA Carboxylase	PGSC0003DMG400033054	Biotin carboxyl carrier protein subunit
66.5	Acetyl-CoA Carboxylase	PGSC0003DMG401023454	Biotin carboxylase carrier protein
66.6	Acetyl-CoA Carboxylase	PGSC0003DMG400000025	Acetyl-coenzyme A carboxylase carboxyl transferase alpha
66.7	Acetyl-CoA Carboxylase	PGSC0003DMG400010806	Acetyl-coenzyme A carboxylase carboxyl transferase alpha
66.8	Acetyl-CoA Carboxylase	PGSC0003DMG400011755	Acetyl-coenzyme A carboxylase carboxyl transferase alpha
66.9	Acetyl-CoA Carboxylase	PGSC0003DMG400016327	Acetyl-coenzyme A carboxylase carboxyl transferase alpha
67.1	Malonyl-CoA:ACP transacylase	PGSC0003DMG400021362	Acyl-carrier-protein S-malonyltransferase/transferase
68.1	Beta-ketoacyl-ACP synthase II	PGSC0003DMG400008311	50 kDa ketoavyl-ACP synthase
68.2	Beta-ketoacyl-ACP synthase II	PGSC0003DMG400013579	Beta-ketoacyl-ACP synthase II
68.3	Beta-ketoacyl-ACP synthase II	PGSC0003DMG400027322	3-oxoacyl-[acyl-carrier-protein] synthase
68.4	Beta-ketoacyl-ACP synthase II	PGSC0003DMG400030158	50 kDa ketoavyl-ACP synthase
68.5	Beta-ketoacyl-ACP synthase II	PGSC0003DMG400022891	Beta-ketoacyl-ACP synthase II
68.6	Beta-ketoacyl-ACP synthase II	PGSC0003DMG400012262	3-oxoacyl-[acyl-carrier-protein] synthase
68.7	Beta-ketoacyl-ACP synthase II	PGSC0003DMG400006426	3-oxoacyl-[acyl-carrier-protein] synthase
68.8	Beta-ketoacyl-ACP synthase II	PGSC0003DMG400002927	Beta-ketoacyl-ACP synthase II-1
68.9	Beta-ketoacyl-ACP synthase III	PGSC0003DMG400026308	3-oxoacyl-(Acyl-carrier-protein) synthase III
69.1	Beta-ketoacyl-ACP reductase	PGSC0003DMG401026981	3-oxoacyl-(Acyl-carrier protein) reductase
69.2	Beta-ketoacyl-ACP reductase	PGSC0003DMG400014095	2,4-dienoyl-CoA reductase
69.3	Beta-ketoacyl-ACP reductase	PGSC0003DMG400017459	Ketoacyl-ACP Reductase (KAR)

69.4	Beta-ketoacyl-ACP reductase	PGSC0003DMG400015249	3-oxoacyl-(Acyl-carrier protein) reductase
70.1	Beta-hydroxyacyl-ACP dehydratase	PGSC0003DMG400012564	DH putative beta-hydroxyacyl-ACP dehydratase
71.1	Enoyl-ACP reductase	PGSC0003DMG400011436	Enoyl-acyl-carrier-protein reductase
71.2	Enoyl-ACP reductase	PGSC0003DMG400032152	Enoyl-acyl-carrier-protein reductase
72.1	Acyl-ACP thioesterase	PGSC0003DMG400020163	Acyl-ACP thioesterase
73.1	Acyl-ACP desaturase	PGSC0003DMG400000978	Acyl-[acyl-carrier-protein] desaturase, chloroplastic
Fatty Acid Modification			
74.1	Beta-ketoacyl-CoA synthase 6	PGSC0003DMG400012670	3-ketoacyl-CoA synthase
75.1	Beta-ketoacyl-CoA reductase	PGSC0003DMG400012642	3-ketoacyl-CoA reductase 1
76.1	Beta-hydroxyacyl-CoA dehydratase	PGSC0003DMG400023576	PASTICCINO 2
76.2	Beta-hydroxyacyl-CoA dehydratase	PGSC0003DMG400016135	3-hydroxyacyl-CoA dehydratase PASTICCINO 2
77.1	Enoyl CoA reductase	PGSC0003DMG400029352	Trans-2-enoyl CoA reductase
77.2	Enoyl CoA reductase	PGSC0003DMG402029257	Trans-2-enoyl CoA reductase
78.1	Fatty acid omega-hydroxylase (CYP86A33)	PGSC0003DMG400030349	CYP86A33 fatty acid omega-hydroxylase
78.2	Fatty acid omega-hydroxylase (CYP86A33)	PGSC0003DMG400002111	CYP86A33 fatty acid omega-hydroxylase
79.1	Fatty acid omega-hydroxylase (CYP86A68)	PGSC0003DMG400046813	Cytochrome P450
80.1	Fatty acid omega-hydroxylase (CYP86A69)	PGSC0003DMG400012202	Cytochrome P450 fatty acid omega-hydroxylase
81.1	Fatty acid omega-hydroxylase (CYP94A26)	PGSC0003DMG400018744	Cytochrome P450-dependent fatty acid hydroxylase
82.1	Fatty acid omega-hydroxylase (CYP86B12)	PGSC0003DMG400010578	Cytochrome P450

83.1	Fatty acyl-CoA reductase 3	PGSC0003DMG400007113	Fatty acyl-CoA reductase 3
83.2	Fatty acyl-CoA reductase	PGSC0003DMG400007405	Acyl CoA reductase
83.3	Fatty acyl-CoA reductase 1	PGSC0003DMG401007406	Fatty acyl-CoA reductase 1
83.4	Fatty acyl-CoA reductase	PGSC0003DMG402007406	Male sterility protein
83.5	Fatty acyl-CoA reductase	PGSC0003DMG400007115	Male sterility protein
83.6	Fatty acyl-CoA reductase	PGSC0003DMG400023759	Male sterility protein
83.7	Fatty acyl-CoA reductase	PGSC0003DMG400023916	Male sterility protein
83.8	Fatty acyl-CoA reductase	PGSC0003DMG400045792	Male sterility protein
83.9	Fatty acyl-CoA reductase 3	PGSC0003DMG400007114	Fatty acyl-CoA reductase 3
83.10	Fatty acyl-CoA reductase 2	PGSC0003DMG400008885	Fatty acyl-CoA reductase 2
83.11	Fatty acyl-CoA reductase 2	PGSC0003DMG400008886	Fatty acyl-CoA reductase 2
83.12	Fatty acyl-CoA reductase 2	PGSC0003DMG400041559	Fatty acyl-CoA reductase 2
83.13	Fatty acyl-CoA reductase 2	PGSC0003DMG401002698	Fatty acyl-CoA reductase 2
83.14	Fatty acyl-CoA reductase 2	PGSC0003DMG402002698	Fatty acyl-CoA reductase 2
84.1	Long-chain acyl-CoA synthetase	PGSC0003DMG402000216	Long-chain acyl-CoA synthetase 4
84.2	Long-chain acyl-CoA synthetase	PGSC0003DMG400009052	Long-chain-fatty-acid CoA ligase
84.3	Long-chain acyl-CoA synthetase	PGSC0003DMG400025174	Acyl CoA synthetase
85.1	Alkane forming enzyme (CER1)	PGSC0003DMG400028022	Sterol desaturase
85.2	Alkane forming enzyme (CER1)	PGSC0003DMG400005436	Sterol desaturase
85.3	Alkane forming enzyme (CER1)	PGSC0003DMG400033650	Sterol desaturase
85.4	Alkane forming enzyme (CER1)	PGSC0003DMG400001676	Sterol desaturase
86.1	Alkane forming enzyme	PGSC0003DMG400007879	Protein WAX2

	(CER3)		
86.2	Alkane forming enzyme (CER3)	PGSC0003DMG401014160	Protein WAX2
86.3	Alkane forming enzyme (CER3)	PGSC0003DMG400011170	Protein WAX2
87.1	Cytochrome b5	PGSC0003DMG400018534	Cytochrome b5
87.2	Cytochrome b5	PGSC0003DMG400020160	Cytochrome b5
87.3	Cytochrome b5	PGSC0003DMG400017661	Cytochrome b5
87.4	Cytochrome b5	PGSC0003DMG400000127	Cytochrome b5 isoform Cb5-A
87.5	Cytochrome b5	PGSC0003DMG400005465	Cytochrome b5
87.6	Cytochrome b5	PGSC0003DMG400001228	Cytochrome b5
87.7	Cytochrome b5	PGSC0003DMG400028310	Cytochrome b5 isoform Cb5-D
87.8	Cytochrome b5	PGSC0003DMG400007706	Cytochrome b5
88.1	Glycerol-3-phosphate dehydrogenase	PGSC0003DMG400012712	Glycerol-3-phosphate dehydrogenase
88.2	Glycerol-3-phosphate dehydrogenase	PGSC0003DMG400006965	Glycerol-3-phosphate dehydrogenase
88.3	Glycerol-3-phosphate dehydrogenase	PGSC0003DMG400006765	Glycerol-3-phosphate dehydrogenase
88.4	Glycerol-3-phosphate dehydrogenase	PGSC0003DMG400016644	Glycerol-3-phosphate dehydrogenase

Aliphatic Suberin Assembly

89.1	Feruloyl transferase	PGSC0003DMG400031731	Feruloyl transferase
90.1	Glycerol-3-phosphate acyltransferase 5	PGSC0003DMG400006342	ER glycerol-phosphate acyltransferase
91.1	Glycerol-3-phosphate acyltransferase 6	PGSC0003DMG400020315	Glycerol-3-phosphate acyltransferase 6
92.1	ATP-binding cassette transporter (ABCG1)	PGSC0003DMG400023506	ATP-binding cassette transporter

93.1	ATP-binding cassette transporter (ABCG11)	PGSC0003DMG400016225	ATP-binding cassette transporter
94.1	ATP-binding cassette transporter (ABCG6)	PGSC0003DMG400011482	Stigma/style ABC transporter (ABCG6)



Figure C4. Hierarchical clustering analysis of genes encoding putative Casparian membrane strip protein (CASP) and cutin esterase-like (GDSL) proteins to screen for candidate novel assembly genes. Biological triplicate means of $\log_2\text{FPKM}$ are presented at each time point. CASPs are denoted by numbering with C, and GDSLs are denoted with G. Both groups of genes correspond to information in Table C5 and Table C6.

Table C5. Casparian strip membrane protein (CASP) family in *Solanum tuberosum*. Putative Arabidopsis homolog information is provided for all PGSC gene IDs that had this associated information, as accessed through the PGSC database.

Number	PGSC name	PGSC gene ID	Arabidopsis homolog accession	Arabidopsis homolog name	% ID	% Query	E-value
C.1	CASP	PGSC0003DMG400027047	AT2G39530.1	CASPL4D1	56.6	94	1.00E-19
C.2	CASP	PGSC0003DMG400011859	AT2G38480.1	CASPL4B1	72	85	7.70E-45
C.3	CASP	PGSC0003DMG400008080	AT2G28370.1	CASPL5A2	85.5	99	2.90E-68
C.4	CASP	PGSC0003DMG400017235	AT3G23200.1	CASPL5B3	78.1	99	8.10E-50
C.5	CASP	PGSC0003DMG400024498	AT2G36330.1	CASPL43A	54.2	76	2.50E-30
C.6	CASP	PGSC0003DMG400027092	AT2G36330.1	CASPL43A	63.9	81	5.60E-58
C.7	CASP	PGSC0003DMG400027136	AT5G02060.1	CASPL5B1	78	97	1.00E-49
C.8	CASP	PGSC0003DMG400011620	AT2G38480.1	CASPL4B1	67.4	89	2.90E-45
C.9	CASP	PGSC0003DMG400017586	AT2G28370.1	CASPL5A2	76.8	99	3.00E-59
C.10	CASP	PGSC0003DMG400019144	AT3G53850.1	CASPL5B2	83.1	90	1.50E-57
C.11	CASP	PGSC0003DMG403000524	AT2G36330.1	CASPL43A	64.5	70	4.70E-54
C.12	CASP 8	PGSC0003DMG400022659	AT4G15610.1	CASPL1D1	71.6	86	2.20E-40
C.13	CASP 9	PGSC0003DMG400021195	AT4G20390.1	CASPL1B2	75.1	85	1.10E-50
C.14	CASP GSVIVT00013434001	PGSC0003DMG400029690	AT4G03540.1	CASPL1C1	74.2	98	5.40E-44
C.15	CASP GSVIVT00013502001	PGSC0003DMG400013293	AT2G35760.1	CASPL2B2	82.9	71	8.80E-60
C.16	CASP GSVIVT00013502001	PGSC0003DMG400008455	AT2G35760.1	CASPL2B2	79.1	100	7.20E-65
C.17	CASP GSVIVT00034332001	PGSC0003DMG400002535	AT3G16300.1	CASPL3A1	65.1	85	1.40E-38
C.18	CASP PIMP1	PGSC0003DMG400027748	AT2G39518.1	CASPL4D2	60.6	99	7.70E-29
C.19	CASP PIMP1	PGSC0003DMG400035890	AT2G39530.1	CASPL4D1	62	97	2.50E-23
C.20	CASP PIMP1	PGSC0003DMG400027749	AT2G39518.1	CASPL4D2	59.2	99	6.30E-27
C.21	CASP POPTRDRAFT_822486	PGSC0003DMG400023526	AT3G55390.1	CASPL4C1	71.9	99	2.90E-61
C.22	CASP POPTRDRAFT_822486	PGSC0003DMG400027734	AT3G55390.1	CASPL4C1	76.4	98	2.50E-62
C.23	CASP POPTRDRAFT_823430	PGSC0003DMG400012025	AT4G25040.1	CASPL1F1	53.5	85	6.90E-21

C.24	CASP RCOM_0680180	PGSC0003DMG400011355	AT4G15620.1	CASPL1E2	63.8	87	1.50E-34
C.25	CASP RCOM_0680180	PGSC0003DMG400022677	AT4G15630.1	CASPL1E1	70.9	96	9.60E-47
C.26	CASP RCOM_1206790	PGSC0003DMG400037321	AT2G39530.1	CASPL4D1	58	88	1.10E-20
C.27	CASP RCOM_1206790	PGSC0003DMG400001986	AT2G39530.1	CASPL4D1	57	98	1.40E-15
C.28	CASP RCOM_1302390	PGSC0003DMG400027868	AT5G54980.1	CASPL2D1	72.1	93	2.60E-44
C.29	CASP SDM1_58t00016	PGSC0003DMG400002855	AT5G15290.1	CASP5	69.4	99	2.20E-47
C.30	CASP SDM1_58t00016	PGSC0003DMG400018410	AT5G15290.1	CASP5	72.6	99	9.30E-49
C.31	CASP VIT_01s0010g01870	PGSC0003DMG400031087	AT1G17200.1	CASPL2A1	82.3	83	2.70E-58
C.32	CASP VIT_01s0010g01870	PGSC0003DMG400021246	AT1G17200.1	CASPL2A1	80.1	98	1.60E-53
C.33	CASP VIT_17s0000g00560	PGSC0003DMG400026945	AT4G25040.1	CASPL1F1	62.4	84	1.70E-26
C.34	CASP VIT_17s0000g00560	PGSC0003DMG400026944	AT4G25040.1	CASPL1F1	63.2	86	3.00E-27
C.35	CASP XL3	PGSC0003DMG400018742	AT4G25830.1	CASPL2C1	66.5	86	6.60E-39
C.36	Casparian strip membrane protein POPTRDRAFT_569472	PGSC0003DMG400001337	AT5G15290.1	CASP5	78.7	91	1.10E-52
C.37	Casparian strip membrane protein VIT_06s0080g00840	PGSC0003DMG400005887	AT5G06200.1	CASP4	72.3	97	1.00E-58
C.38	Casparian strip membrane protein 3	PGSC0003DMG400008859	AT5G06200.1	CASP4	71.8	98	1.20E-57
C.39	Casparian strip membrane protein POPTRDRAFT_569472	PGSC0003DMG400025146	AT5G15290.1	CASP5	79.6	97	1.40E-59
C.40	Casparian strip membrane protein RCOM_1282030	PGSC0003DMG400028249	AT3G11550.1	CASP2	72.6	99	2.60E-60
C.41	UPF0497 Integral membrane protein	PGSC0003DMG401008816	AT3G53850.1	CASPL5B2	83.8	99	2.40E-57
C.42	UPF0497, trans-membrane plant domain containing protein	PGSC0003DMG400022768	no hits	no hits	-	-	-

Table C6. List of cutin synthase-like candidates screened in the wound-healing tuber RNA-seq data. The amino acid sequence of the tomato cutin synthase, SICDS1, was queried by blastp against the PGSC database to yield similar proteins that could potentially be involved in aliphatic monomer polymerization.

Number	PGSC functional name	PGSC gene ID	Hit score	E value	Query %	ID %
G.1	Cutin-deficient 1 protein	PGSC0003DMG400000997	1741	0	100	91.48
G.2	Zinc finger protein	PGSC0003DMG400028701	1456	0	97.79	75.41
G.3	Tea geometrid larvae-inducible protein	PGSC0003DMG400028703	1411	0	100	70.99
G.4	Zinc finger protein	PGSC0003DMG400020084	1371	0	98.34	71.15
G.5	Zinc finger protein	PGSC0003DMG400018956	1226	1.00E-169	99.45	61.62
G.6	Lipolytic enzyme, G-D-S-L	PGSC0003DMG400015683	589	6.00E-73	92.82	37.65
G.7	Zinc finger protein	PGSC0003DMG400010076	588	9.00E-73	91.44	39.17
G.8	Zinc finger protein	PGSC0003DMG400005185	572	2.00E-70	94.75	35.9

Table C7. Abscisic acid-related biosynthetic gene information. Bolded numbers correspond to gene IDs used to generate heatmap figures.

Pathway branch	Number	Predicted or known enzyme name	PGSC gene ID
Isoprene Biosynthesis	1.1	1-deoxy-D-xylulose 5-phosphate synthase	PGSC0003DMG400022855
	1.2	1-deoxy-D-xylulose 5-phosphate synthase	PGSC0003DMG400029091
	1.3	1-deoxy-D-xylulose 5-phosphate synthase	PGSC0003DMG400016120
	2.1	1-deoxy-D-xylulose 5-phosphate reductoisomerase	PGSC0003DMG400024503
	3.1	2-C-Methyl-D-erythritol 4-phosphate cytidyltransferase	PGSC0003DMG401018218
	4.1	CDP-Methyl-D-erythritol Kinase	PGSC0003DMG400022703
	5.1	Methylerythrose-2,4-cyclodiphosphate synthase	PGSC0003DMG400012185
	6.1	Hydroxy-3-methylbut-2-enyl diphosphate synthase	PGSC0003DMG400008050
	7.1	Hydroxy-3-methylbut-2-enyl diphosphate reductase	PGSC0003DMG400025165
	8.1	Isopentenyl pyrophosphate isomerase	PGSC0003DMG400023359
	8.2	Isopentenyl pyrophosphate isomerase	PGSC0003DMG400007268
	8.3	Isopentenyl pyrophosphate isomerase	PGSC0003DMG400012082
	9.1	Geranyl diphosphate synthase	PGSC0003DMG400007081
	10.1	Farnesyl diphosphate synthase	PGSC0003DMG400029788
	10.2	Farnesyl diphosphate synthase	PGSC0003DMG400014369
	10.3	Farnesyl diphosphate synthase	PGSC0003DMG400008690
	11.1	Geranylgeranyl diphosphate synthase 4	PGSC0003DMG400002687
	11.2	Geranylgeranyl diphosphate synthase 3	PGSC0003DMG400047044
	11.3	Geranylgeranyl diphosphate synthase 1	PGSC0003DMG400015673
	11.4	Geranylgeranyl diphosphate synthase 2	PGSC0003DMG400027856
11.5	Geranylgeranyl diphosphate synthase	PGSC0003DMG400041508	
11.6	Geranylgeranyl diphosphate synthase	PGSC0003DMG400043267	
11.7	Geranylgeranyl diphosphate synthase	PGSC0003DMG400022214	
Carotenoid biosynthesis	12.1	Phytoene synthase 1	PGSC0003DMG400024063

	12.2	Phytoene synthase 2	PGSC0003DMG400016721
	12.3	Phytoene synthase 2	PGSC0003DMG400019372
	12.4	Phytoene synthase 2	PGSC0003DMG400029005
	12.5	Phytoene synthase 2	PGSC0003DMG400021926
	13.1	Phytoene desaturase	PGSC0003DMG400009156
	14.1	Lycopene beta cyclase	PGSC0003DMG400010637
	14.2	Lycopene beta cyclase	PGSC0003DMG400008159
ABA biosynthesis	15.1	Carotene hydroxylase	PGSC0003DMG400028897
	15.2	Carotene hydroxylase	PGSC0003DMG400010169
	15.3	Carotene hydroxylase	PGSC0003DMG400009501
	16.1	Zeaxanthin epoxidase	PGSC0003DMG400004020
	17.1	Neoxanthin synthase	PGSC0003DMG400014477
	17.2	Neoxanthin synthase	PGSC0003DMG401026407
	17.3	Neoxanthin synthase	PGSC0003DMG400024184
	17.4	Neoxanthin synthase	PGSC0003DMG402019589
	17.5	Neoxanthin synthase	PGSC0003DMG400005886
	18.1	9-cis-epoxycarotenoid dioxygenase	PGSC0003DMG400027633
	18.2	9-cis-epoxycarotenoid dioxygenase	PGSC0003DMG400019162
	18.3	9-cis-epoxycarotenoid dioxygenase	PGSC0003DMG400004311
	18.4	9-cis-epoxycarotenoid dioxygenase	PGSC0003DMG400004312
	19.1	Xanthoxin dehydrogenase	PGSC0003DMG400008389
	19.2	Xanthoxin dehydrogenase	PGSC0003DMG400025067
	19.3	Xanthoxin dehydrogenase	PGSC0003DMG400018801
	19.4	Xanthoxin dehydrogenase	PGSC0003DMG400011038
	19.5	Xanthoxin dehydrogenase	PGSC0003DMG400028245
	19.6	Xanthoxin dehydrogenase	PGSC0003DMG402025066
	19.7	Xanthoxin dehydrogenase	PGSC0003DMG400032163
19.8	Xanthoxin dehydrogenase	PGSC0003DMG400032162	
19.9	Xanthoxin dehydrogenase	PGSC0003DMG400008785	
20.1	Abscisic aldehyde oxidase	PGSC0003DMG403006826	
20.2	Abscisic aldehyde oxidase	PGSC0003DMG402018708	
20.3	Abscisic aldehyde oxidase	PGSC0003DMG400008710	
20.4	Abscisic aldehyde oxidase	PGSC0003DMG401006826	
20.5	Abscisic aldehyde oxidase	PGSC0003DMG401018708	
20.6	Abscisic aldehyde oxidase	PGSC0003DMG402006826	
20.7	Abscisic aldehyde oxidase	PGSC0003DMG402019668	

Table C8. Abscisic acid catabolism gene information. Bolded numbers correspond to gene IDs used to generate the associated heatmap figure.

Number	Predicted or known enzyme name	PGSC gene ID
1.1	ABA 8'-hydroxylase (CYP707A)	PGSC0003DMG400001960
1.2	ABA 8'-hydroxylase (CYP707A)	PGSC0003DMG402018475
1.3	ABA 8'-hydroxylase (CYP707A)	PGSC0003DMG400015100
1.4	ABA 8'-hydroxylase (CYP707A)	PGSC0003DMG400025795
1.5	ABA 8'-hydroxylase (CYP707A)	PGSC0003DMG400007972
2.1	ABA-glucosyltransferase	PGSC0003DMG400035666
2.2	ABA-glucosyltransferase	PGSC0003DMG400013559
2.3	ABA-glucosyltransferase	PGSC0003DMG400034632
2.4	ABA-glucosyltransferase	PGSC0003DMG400011971
2.5	ABA-glucosyltransferase	PGSC0003DMG400011973
2.6	ABA-glucosyltransferase	PGSC0003DMG400034882
2.7	ABA-glucosyltransferase	PGSC0003DMG400015327
2.8	ABA-glucosyltransferase	PGSC0003DMG400016611
2.9	ABA-glucosyltransferase	PGSC0003DMG400006737
2.10	ABA-glucosyltransferase	PGSC0003DMG400004573
2.11	ABA-glucosyltransferase	PGSC0003DMG400011972
3.1	β -glucosidase	PGSC0003DMG400006319
3.2	β -glucosidase	PGSC0003DMG400005656
3.3	β -glucosidase	PGSC0003DMG400028773
3.4	β -glucosidase	PGSC0003DMG400025239
3.5	β -glucosidase	PGSC0003DMG401016246
3.6	β -glucosidase	PGSC0003DMG400029676
3.7	β -glucosidase	PGSC0003DMG400019235
3.8	β -glucosidase	PGSC0003DMG400029974
3.9	β -glucosidase	PGSC0003DMG400019091

Table C9. Candidate transcription factors screened in the wound-healing transcriptome analysis. Three characterized transcription factors were used for blastp searches to query the PGSC database for putative potato homologs or similar regulatory proteins. Transcription factor names were given based on annotated PGSC or NCBI names, or previously published names where applicable.

Enzyme family	Number	Transcription factor name	PGSC gene ID	Hit from blastp against	Hit score	% Similarity	% Query	E-value
MYB	1	MYB3	PGSC0003DMG400011250	AtMYB41	729	53.61	94.33	6.00E-96
	2	MYB39	PGSC0003DMG400026628	AtMYB41	723	77.19	60.64	8.00E-95
	3	MYB34	PGSC0003DMG400022399	AtMYB41	724	70.18	74.11	2.00E-94
	4	MYB ODORANT1	PGSC0003DMG400018331	AtMYB41	714	80.57	62.06	2.00E-93
	5	MYB102	PGSC0003DMG400006408	AtMYB41	591	74.44	47.16	1.00E-74
	6	MYB1	PGSC0003DMG400031317	AtMYB41	542	71.88	45.39	4.00E-68
	7	MYB ODO1	PGSC0003DMG400004780	AtMYB41	538	72.66	45.39	1.00E-67
NAC	8	NAC103	PGSC0003DMG400005384	StNAC103	1797	100	100	1.70E-183
	9	NAC58	PGSC0003DMG400028779	StNAC103	920	99.7	59.82	1.00E-124
	10	NAC - transcription factor	PGSC0003DMG400014845	StNAC103	676	75.78	47.16	5.00E-87
	11	NAC - transcription factor	PGSC0003DMG400029593	StNAC103	667	73.65	49.25	2.00E-85
	12	NAM18	PGSC0003DMG400033047	StNAC103	646	74.21	46.27	2.00E-82
	13	NAC21/22	PGSC0003DMG400019523	StNAC103	628	71.7	46.27	1.00E-79
	14	NAM14	PGSC0003DMG400001338	StNAC103	607	69.14	47.16	1.00E-76
WRKY	15	WRKY1	PGSC0003DMG400021895	StWRKY1	928	100	100	1.00E-130
	16	WRKY19/WRKY 56	PGSC0003DMG400012317	StWRKY1	356	63.64	57.56	2.00E-42
	17	STP	PGSC0003DMG400031175	StWRKY1	313	57	57.56	8.00E-36
	18	WRKY4	PGSC0003DMG400009051	StWRKY1	316	67.95	45.35	1.00E-35

19	WRKY - transcription factor	PGSC0003DMG400028381	StWRKY1	310	64.63	47.67	1.00E-34
20	WRKY10	PGSC0003DMG400019706	StWRKY1	304	61.73	47.09	1.00E-34
21	WRKY - transcription factor	PGSC0003DMG400007788	StWRKY1	295	67.61	41.28	2.00E-32

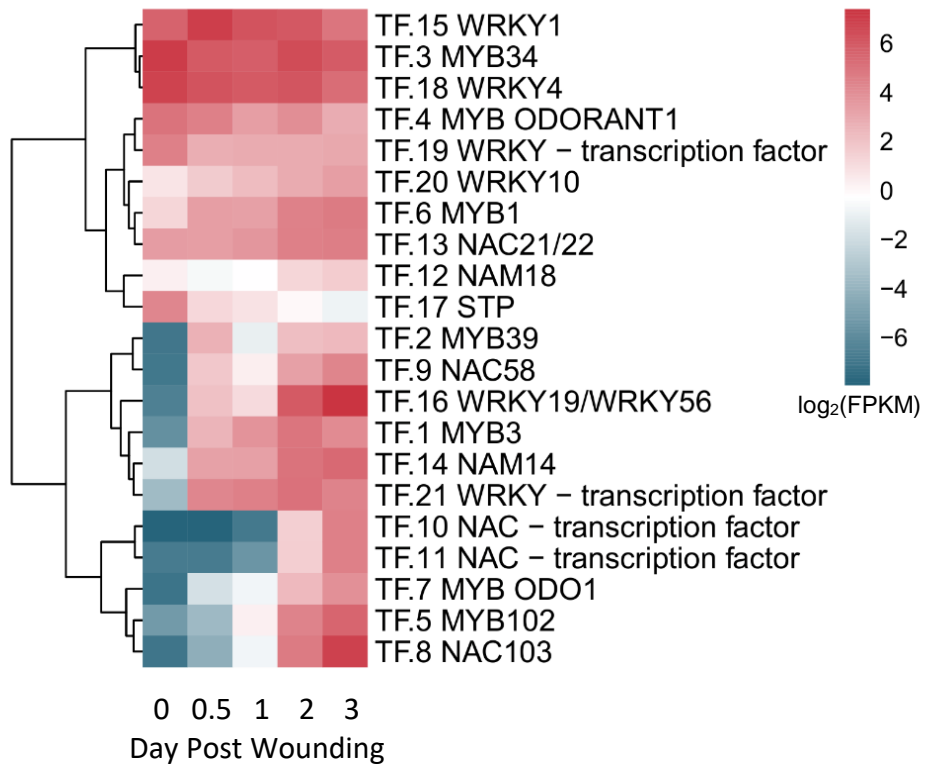


Figure C5. Hierarchical clustering analysis of transcription factor candidates with characterized potato transcription factors *NAC103* and *WRKY1*. Mean $\log_2\text{FPKM}$ values of n=3 biological replicates are presented.

Table C10. Gene information and primer sequences used for RT-qPCR validation of RNA-seq expression values.

Gene	PGSC ID	Primer sequences	Product length (bp)	Efficiency (%)
<i>MYB34</i>	PGSC0003DMG400022399	F:TGTTAGGCCATGTGCAACCT R:TGAGTTTTGGCGTTGGGATG	83	104.5
<i>MYB3</i>	PGSC0003DMG400011250	F:GTCTGCCTGGAAGGACTGAT R:CAAGAAGATCAAGACGAGGGCT	117	108.7
<i>ODORANT1</i>	PGSC0003DMG400018331	F:GGTCCTGAAAATTGGCGAAC R:CCACACCTTTGAAGTCCAGC	53	100.6
<i>PAL1</i>	PGSC0003DMG402021564	F:CAAATTGACGCTGATGAAGC R:ACAGGACAATTGATGCCATACC	131	107.6
<i>C4H</i>	PGSC0003DMG402030469	F:ACCAAGAGCATGGACAGCAA R:ATCCTCGTTGATCTCTCCCTTCT	84	104.6
<i>CCR</i>	PGSC0003DMG400019825	F:GAGCCAGCGGTTATAGGGAC R:TCCACAACCTTATCCGGGGC	131	113
<i>THT</i>	PGSC0003DMG400014778	F:AGGTATGGCAAATTGCATGGTG R:TGTCTCTTCTCAATTTTCCCCT	69	109.9
<i>KCS6</i>	PGSC0003DMG400012670	F:AACCGCACAAATCAAGACACCA R:TCTCTGGGATGAACACTGGGT	76	100.8
<i>CYP86A33</i>	PGSC0003DMG400030349	F:GACACGTGGCTCATGCAAAG R:TTGTCGTAGTGTCCGGGTTG	63	99.0
<i>CYP86B12</i>	PGSC0003DMG400010578	F:TCCACCCTCACTTACCCCAA R:CGTGGGAGTGACAAACCGTA	86	104.6
<i>GPAT5</i>	PGSC0003DMG400006342	F:ACCGAACCTACTTGACCCT R:GCGTCCACTTCTCGAATCCT	142	102.8
<i>GPAT6</i>	PGSC0003DMG400006342	F:TGGCCAACGTGGTGTACTTT R:CAGCAGTAACAACGGGGTCT	65	109.2
<i>FHT</i>	PGSC0003DMG400031731	F:TGTGAAGCAAGGAGTGCCAA R:ACCGGCACGGCTATATTCTG	99	107.7
<i>ABCG1</i>	PGSC0003DMG400022399	F:GCTGTAGGCCTTGTAGGTGG R:CCGGAGAGGAACGTGACAAA	101	108.1
<i>EF1-α*</i>	PGSC0003DMG400023272	F:TGGTCGTGTTGAGACTGGTG R:AACATTGTACCGGGGAGTG	133	101.5
<i>APRT*</i>	PGSC0003DMG400021527	F:GAACCGGAGCAGGTGAAGAA R:GAAGCAATCCCAGCGATACG	121	99.2

Table C11. Pearson correlation statistical output for RT-qPCR validation of RNA-seq transcript levels. 45 data pairs were used for this analysis that incorporated 14 genes across 3 or 4 time points. Input data were \log_2 (fold change) values normalized to the control 0 time point.

Number of XY Pairs	45
Pearson r	0.8598
95% confidence interval of Pearson r	0.7573 to 0.9209
P value (two-tailed)	< 0.0001
P value summary	***
Is the correlation significant? (alpha=0.05)	Yes
R squared	0.7392
95% confidence interval of R squared	Slope: 0.7824 to 1.132 Y-intercept when X=0.0: 0.7225 to 2.917 X-intercept when Y=0.0: -3.542 to -0.6717

Curriculum Vitae

Name: Kathlyn Woolfson

Post-secondary Education and Degrees: University of Ottawa
Ottawa, Ontario, Canada
2008-2012 Honours B.Sc. with specialization in Biology

Brock University
St. Catharines, Ontario, Canada
2012-2014 M.Sc. in Biology

Western University
London, Ontario, Canada
2014-2018 Ph.D. in Biology

Honours and Awards: QEII Ontario Graduate Scholarship in Science and Technology
2013-2014; 2016-2017

Best poster, PSNA annual meeting student competition
2016

Third place winner, SORA-CPS meeting student poster competition
2016

First place winner, SORA-CPS meeting student poster competition
2015

Distinguished Graduating Student Award
2015

Dean of Graduate Studies Excellence Scholarship
2013-2014

Dean of Graduate Studies Entrance Scholarship
2012

Related Work Experience: Teaching Assistant
Brock University and Western University
2012-2018 (taught six courses)

Publications:

- Woolfson, K.N.**, Haggitt, M.L., Zhang, Y., Kachura, A., Bjelica, A., Rey Rincon, M.A., Kaberi, K.M. and Bernard, M.A. (2018). Differential induction of polar and non-polar metabolism during wound-induced suberization in potato (*Solanum tuberosum* L.) tubers. *The Plant Journal* **93**(5), 931-942.
- Demessie, Z., **Woolfson, K.N.**, Yu, F., Qu, Y., and De Luca, V. (2017). The ATP binding cassette transporter, VmTPT2/VmABCG1, is involved in export of the monoterpenoid indole alkaloid, vincamine in *Vinca minor* leaves. *Phytochemistry*, **140**, 118-124.
- Bjelica, A., Haggitt, M.L., **Woolfson, K.N.**, Lee, D.P.N., Makhzoum, A.B., and Bernard, M.A. (2016) Fatty acid ω -hydroxylases from *Solanum tuberosum*. *Plant Cell Reports* **35**(12), 2435-2448.

Select conference presentations:

- Woolfson, K.N.** and Bernard, M.A. (2017). The wound-healing potato tuber: An RNA-seq approach. The International Symposium on Plant Apoplastic Diffusion Barriers: Biosynthesis and Functions (PADiBa), Oeiras, Portugal (oral).
- Woolfson, K.N.**, Kachura, A., Bjelica A., Haggitt, M., Zhang, Y., and Bernard, M.A. (2016). Regulation of suberin biosynthesis in a wound-healing potato (*Solanum tuberosum* L.) tuber model. Phytochemical Society of North America Annual Meeting, University of California at Davis, Davis, CA, USA (poster).
- Woolfson, K.N.**, Haggitt, M., Kachura, A., Abdali, T., Bjelica A., and Bernard, M.A. (2015). Abscisic acid regulation of suberin biosynthesis and deposition in potato. Southwestern Ontario Regional Association of the Canadian Phytopathological Society (SORA-CPS) Meeting, London, ON (poster).
- Woolfson, K.N.**, Yu, F., and De Luca, V. (2013). ATP-binding cassette transporter from *Vinca minor* is involved in alkaloid secretion. Canadian Society of Plant Biologists Eastern Regional Meeting, Mississauga, ON (oral).